THE
PHYSICAL REVIEW
A journal of experimental and theoretical physics established by E. L. Nichols in 1893

VOL. 62, NOS. 3 AND 4 AUGUST 1 AND 15, 1942 SECOND SERIES

The Pseudoscalar Meson Field with Strong Coupling

W. PAULI, *Institute for Advanced Study, Princeton, New Jersey*

AND

S. M. DANCOFF, *Institute for Advanced Study, Princeton, New Jersey and University of Illinois, Urbana, Illinois*

(Received June 23, 1942)

The present paper treats the symmetrical and charged pseudoscalar theories of the meson field, using the strong coupling approximation; it restricts itself to the case of a single source. The energy levels of the excited states of the heavy particle and the scattering cross section for free mesons are computed by wave mechanical methods. An expression is also obtained for the magnetic moment of the proton or neutron. While the scattering cross section can, with reasonable assumptions, be brought into agreement with experimental values, the results for the magnetic moment are qualitatively at variance with the known values in that equal and opposite moments are predicted for proton and neutron.

1. INTRODUCTION

THE perturbation theoretic treatment of the coupling of the meson field to the heavy particle, based on the assumption that the coupling is weak, encounters several fundamental difficulties in its application. The divergences which arise from the treatment of the heavy particle as an infinite point mass have been in some instances arbitrarily removed by cut-off methods, but it can be shown that such methods cannot be consistently formulated in such a way as to satisfy the criterion for weak coupling.[1] Moreover, calculations of the scattering cross section for mesons in this theory lead to values which are generally much too high to agree with cross sections observed for cosmic-ray mesons. The results vary somewhat depending on the particular type of meson field assumed. If we assume that the spin of the meson is zero[2] (charged or symmetrical pseudoscalar), perturbation theory leads to the following result[3] for the scattering of a meson by a nucleon.[4]

$$dq = g^4\kappa^{-2}(p/\kappa)^2(1+\cos\theta)d\Omega \quad \text{for} \quad hp \gg Mc,$$
$$dq = g^4\kappa^{-2}(p^2/\kappa E)^2 d\Omega \quad \text{for} \quad hp \ll Mc, \quad M\to\infty.$$

Here g is the dimensionless constant which expresses the magnitude of the coupling; $\kappa = \mu c/h$ where μ is the rest mass of the meson; p is the momentum of the incident meson divided by h; E the total energy divided by hc; M the rest mass of the nucleon; and θ the scattering angle. These cross sections refer to processes in which

[1] This point will be more fully discussed in a subsequent paper in which the two-source problem will be considered. We are indebted to Professor R. Serber for valuable discussions on this point as well as on several others considered in this paper.

[2] This is one of the two possibilities left open by a consideration of the electromagnetic radiation processes of the meson. See R. F. Christy and S. Kusaka, Phys. Rev. **59**, 405 and 414 (1941). The other possible value of the spin ($\frac{1}{2}$) will be discussed by J. R. Oppenheimer and E. Nelson in a forthcoming publication.

[3] H. Yukawa and Y. Tanikawa, Proc. Phys. Math. Soc. Japan **23**, 445 (1941).

[4] Nucleon is equivalent to "proton-neutron."

the meson is scattered with the original charge. In the case of the symmetrical theory there exists also a scattering process in which the meson changes its charge. If a negative (positive) meson collides with a proton (neutron) it can be scattered as a neutral meson, while the nucleon changes into a neutron (proton). According to computations of F. Adler, not yet published, the corresponding cross section is

$$dq = g^4\kappa^{-2}(p/\kappa)^2(1-\cos\theta/2)^2 d\Omega \quad \text{for} \quad hp \gg Mc,$$
$$dq = g^4\kappa^{-2}(p^2/\kappa E)^2 2\sin^2\theta d\Omega \quad \text{for} \quad hp \ll Mc, \; M\to\infty.$$

A numerical estimate of the total cross section depends upon an assignment of the magnitude of g. This is ordinarily done by considering the nuclear forces predicted by the theory and adjusting g to fit the properties of the deuteron. This involves a cut-off or other readjustment of the radial dependence of the interaction. As remarked above, such a procedure cannot be carried through in a manner consistent with the weak coupling hypothesis. Nevertheless, the value of g so determined ($g^2\sim 0.1$) will be used to give an order of magnitude estimate of the scattering cross section. We obtain a total cross section $\sim 2\times 10^{-26}$ cm^2, as compared with the upper limit of 5×10^{-28} cm^2 determined from experiments on cosmic-ray mesons.[5]

Two apparently different theories have been proposed to explain the smallness of the meson scattering cross section. Heisenberg pointed out that the reaction of the eigenfield of the nucleon to the motion of its spin—and particularly the terms proportional to $1/a$ which one can consider as an inertia of the spin—are considerable.[6] As an example, he computed by classical methods, the scattering in a neutral theory with spin 1 mesons; he found a scattering cross section proportional to $a^2(p/E)^4$ if $g^2 \gg \kappa a$.[7]

The second theory is due to Heitler[8] and Bhabha[9] and based on the assumption of the existence of excited states (isobars) of the nucleon with higher values of the charge (Bhabha) and of the spin (Heitler). In this theory the energy difference ΔE between consecutive isobaric states is not derived, but arbitrarily assumed. On the basis of these assumptions, one finds a considerably reduced value for the cross section for scattering of a meson by a nucleon (of infinite mass) at rest:

$$q_1 = q_0(\Delta E/E)^2.$$

E is the meson energy and q_0 is the total cross section (given above) for scattering as calculated by perturbation theory.

It was shown by Oppenheimer and Schwinger[10] that the two explanations are in reality one and the same. One can indeed derive from Heisenberg's assumptions the existence of excited states of the nucleon, corresponding to the degree of freedom associated with the reaction of the nucleon spin. It is easy to see that if we assume this excitation energy proportional to

$$\Delta E \sim \kappa^2 a/g^2$$

and combine this with Heisenberg's result

$$q_1 \sim a^2(p/E)^4$$

we obtain Heitler and Bhabha's formula for q_1/q_0. The above formula for ΔE, presumably valid for vector mesons, is identical with the corresponding formula that will be rigorously derived for the pseudoscalar case (see below).

2. RESULTS AND CONCLUSIONS

We give here the principal results of this investigation, including the excitation of the isobaric states, the cross section for meson scattering, and the resultant magnetic moments of the proton and neutron. As the condition for the validity of the strong coupling approximation we obtain $g \gg \kappa a$, in the case of small source size

[5] For instance, see R. P. Shutt, Phys. Rev. **61**, 6 (1942). Older literature is reviewed.

[6] The quantity a measures the radius of the nucleon. A precise definition is given by (4).

[7] W. Heisenberg, Zeits. f. Physik **113**, 61 (1939). The problem of interaction of a dipole with its own electromagnetic or meson field is treated in detail by H. J. Bhabha and H. C. Corben, Proc. Roy. Soc. **A178**, 273 (1941) and H. J. Bhabha, Proc. Roy. Soc. **A178**, 314 (1941). A classical but relativistically invariant method is used. The terms in the Hamiltonian proportional to $1/a$ are replaced by terms containing undetermined constants. Such a procedure may approximate an exact treatment more closely than the one used in this paper, but it is not suitable for a quantum-mechanical treatment of the problem.

[8] Compare the detailed paper of W. Heitler and S. T Ma, Proc. Roy. Soc. **A176**, 368 (1940).

[9] H. J. Bhabha, Phys. Rev. **59**, 100 (1941). We refer to this paper for the discussion of the influence of the Coulomb forces on the probability of the generation of a doubly charged proton.

[10] J. R. Oppenheimer and J. Schwinger, Phys. Rev. **60**, 150 (1941).

($\kappa a \ll 1$). For the energy of excitation of the isobars we find

$$\frac{\Delta E}{\mu c^2}=\frac{3}{2}\frac{\kappa a}{g^2}\left[j(j+1)-\frac{3}{4}\right] \text{ in the symmetrical theory,}$$

$$\frac{\Delta E}{\mu c^2}=\frac{3}{2}\frac{\kappa a}{g^2}\left[2j(j+1)-n^2-\frac{5}{4}\right] \text{ in the charged theory.}$$

Here the half-integer j is the total angular momentum, and the half-integer quantum number n is the electric charge (in units e) minus one-half. In both cases, the value of n is restricted to $-j \leqq n \leqq j$, otherwise the isobar energy in the first case is independent of n. The definition of the radius a of the nucleon is given by (4). The proton and neutron are identified as the two lowest states of this system, corresponding to $j=\frac{1}{2}$, $n=\pm\frac{1}{2}$. Higher states will be stable against "meson decay" to these ground states only if $\Delta E \ll \mu c^2$ or $g^2/\kappa a \gg 1$.

For the total scattering cross section (elastic plus inelastic scattering with and without change of the charge) we find under the conditions $g \gg \kappa a$, $\kappa a \ll 1$, $pa \ll 1$:

$$dq=\tfrac{3}{4}(p/E)^4a^2(1+\cos^2\theta)d\Omega,$$
$$q=4\pi(p/E)^4a^2 \text{ in the symmetrical theory;}$$
$$dq=\tfrac{3}{4}(p/E)^4a^2(1+3\cos^2\theta)d\Omega,$$
$$q=6\pi(p/E)^4a^2 \text{ in the charged theory.}$$

As has already been shown by Oppenheimer and Schwinger, one gets agreement with the experimental cross section for meson scattering, in the symmetrical theory for instance, by assuming $a \sim \hbar/Mc = 2\times10^{-14}$ cm which means $\kappa a \sim 0.1$. Referring to the condition for strong coupling, $g \gg \kappa a$, we see that values of $g^2 \gg 0.01$ satisfy this condition.

The magnetic moment of the system nucleon +meson field is found to be

$$\pm\left[\frac{10}{36}\frac{g^2}{\kappa a}+\frac{1}{6}\right] \text{ proton magnetons}$$

the $\pm$ symbol referring to proton and neutron, respectively. As regards order of magnitude, this is not inconsistent with the known magnitudes. A moment of 1.93 proton magnetons, such as has been observed for the neutron, can be obtained by taking $g^2/\kappa a = 6.3$; using $\kappa a = 0.1$ we find $g^2 = 0.63$, well into the strong coupling domain. However, the prediction that the neutron and proton moments are equal and opposite is in contradiction with experience. The second term in the bracket above represents the contribution of the nucleon itself. This contribution is somewhat uncertain because of our ignorance of the fundamental properties of the "bare" proton or neutron. Consequently the discrepancy cannot be taken as an unambiguous disproof of the strong coupling hypothesis. However, the hope that the anomalous moments would follow in a simple way from the theory has not been justified.

It is to be noted that the results obtained above are quantitatively different from the results of the application of semi-classical methods employed by Oppenheimer and Schwinger and described in detail by Schwinger.[11] The latter method treats the spin $\boldsymbol{\sigma}$ and the isotopic spin $\boldsymbol{\tau}$ as classical unit vectors. In the charged scalar and neutral pseudoscalar theories, it gave a quantitative agreement with the wave mechanical results in the limit of strong coupling. This is, however, not true in the present case; in particular the restriction $-j \leqq n \leqq j$ does not appear. The discrepancy cannot be considered surprising in view of the neglect, in the semi-classical method, of the commutation relations between the various components of $\boldsymbol{\tau}$ and $\boldsymbol{\sigma}$. One sees in the wave mechanical treatment that these relations play an essential part in determining the minimum eigenvalue of the interaction energy (see Section 4). Once this part of the problem has been solved, however, there is no difference between the two methods of treatment.

The remaining sections are devoted to the derivation of the results quoted above. In Sections 3 to 6 we introduce such new field variables for the symmetrical pseudoscalar field as to express the energy in terms of unbound mesons and mesons bound to the nucleon. In 6 we find the dependence of the energy on the charge and angular momentum of the bound meson cloud, and discuss in detail the conditions for validity of the various strong coupling approximations introduced. In 7 we calculate the scattering cross sections. Section 8 contains a

[11] J. Schwinger, publication in preparation.

specialization of all these calculations as applied to the charged pseudoscalar case. Section 9 consists of the magnetic moment computation and an appendix describes an alternate method for expanding field quantities, with the use of Euler angles.

3. SPLIT OF THE FIELD INTO A ZERO STATE AND UPPER STATES

In the symmetrical pseudoscalar theory it is convenient to describe the field by three *real* quantities $\varphi_\alpha(x)$, $\alpha=1, 2, 3$. The Hamiltonian H consists of the part H_0 of free particles and the interaction energy H_1. The first part is given by[12]

$$H_0=\sum_{\alpha=1}^{3}\tfrac{1}{2}\int[\pi_\alpha{}^2+(\nabla\varphi_\alpha)^2+\kappa^2\varphi_\alpha{}^2]dV$$
$$=\sum_{\alpha=1}^{3}\tfrac{1}{2}\int[\pi_\alpha{}^2+\varphi_\alpha(-\Delta+\kappa^2)\varphi_\alpha]dV, \quad (1)$$

where the π_α are the momenta conjugate to φ_α and fulfill, at a given instant of time, the commutation rules

$$i[\pi_\alpha(\mathbf{x}),\ \varphi_\beta(\mathbf{x}')]=\delta_{\alpha\beta}\delta(\mathbf{x}-\mathbf{x}'). \quad (2)$$

In the interaction energy we suppose the heavy particle, which we shall call nucleon, to be at rest and characterized by a spherically symmetrical source function $K(\mathbf{x})=K(|x|)$ which is normalized according to

$$\int K(x)dV=1 \quad (3)$$

and determines a radius a of the nucleon:

$$a^{-1}=\int\int K(x)(1/r)K(x')dVdV', \quad (4)$$

where here and in the following, r has the meaning

$$r=|\mathbf{x}-\mathbf{x}'|. \quad (5)$$

Furthermore, the nucleon is capable of existing in two states corresponding to proton and neutron, and moreover to two states corresponding to different directions of the spin. The first degree of freedom is described by the isotopic spin matrices τ_1, τ_2, τ_3, or τ_α with $\alpha=1, 2, 3$; the second by the spin matrices σ_x, σ_y, σ_z, or $\boldsymbol{\sigma}$. Both of them fulfill the same kind of relations

$$\tau_1\tau_2=i\tau_3, \ \cdots \quad \tau_1{}^2=1, \ \cdots, \quad (6)$$
$$\sigma_x\sigma_y=i\sigma_z, \ \cdots \quad \sigma_x{}^2=1, \ \cdots, \quad (7)$$

where the $\cdots$ denotes similar relations derived by cyclic permutations. The interaction energy is then given by

$$H=-(g/\kappa)(4\pi)^{\frac{1}{2}}/\sqrt{2}\sum_\alpha\int K(x)\tau_\alpha(\boldsymbol{\sigma}\cdot\nabla)\varphi_\alpha dV$$
$$=(g/\kappa)(4\pi)^{\frac{1}{2}}/\sqrt{2}\sum_\alpha\int\nabla K\tau_\alpha\cdot\boldsymbol{\sigma}\varphi_\alpha dV. \quad (8)$$

The factor $(4\pi)^{\frac{1}{2}}$ is introduced in order to measure g in ordinary units, not in Heaviside units; the factor $1/\sqrt{2}$ in order to bring it into accordance with the notation in the theories which introduce charged particles only; and the factor $1/\kappa$ in order to make g dimensionless.[13] The total charge of the system meson field+nucleon, measured in the unit e of the electron charge is given by

$$\epsilon=\int(\varphi_1\pi_2-\varphi_2\pi_1)dV+\tfrac{1}{2}(1+\tau_3). \quad (9)$$

The symmetrical theories are characterized by the fact that the charge is only one component of the isotopic spin $T_{\alpha\beta}=-T_{\beta\alpha}$ ($\alpha, \beta=1, 2, 3$) which is a more general integral of motion and given by

$$T_{\alpha\beta}=\int(\varphi_\alpha\pi_\beta-\varphi_\beta\pi_\alpha)dV+\tfrac{1}{2}\tau_{\alpha\beta} \quad (10)$$

with $\tau_{12}=-\tau_{21}=\tau_3, \ \cdots$. The charge is then the 12 component of the isotopic spin, $\epsilon=T_{12}+\frac{1}{2}$.

The form (8) of the interaction energy suggests the definition[14]

$$\overset{0}{\varphi}_{ak}=-(4\pi)^{\frac{1}{2}}\int K(x)\frac{\partial\varphi_\alpha}{\partial x_k}dV$$
$$=4\pi\int\frac{\partial K}{\partial x_k}\varphi_\alpha dV, \quad (11)$$

which gives

$$H_1=\frac{g}{\kappa\sqrt{2}}\sum_{\alpha,k}\tau_\alpha\sigma_k\overset{0}{\varphi}_{ak}. \quad (8')$$

Moreover, we split the field $\varphi_\alpha(x)$ into two parts

[12] We always use here natural units where $\hbar=c=1$ or, in other words, energies are divided by $\hbar c$, momenta by $\hbar$, angular momenta by $\hbar$, electric charges by $(\hbar c)^{\frac{1}{2}}$; κ is the rest mass μ of the free meson divided by $\hbar c$.

[13] The connection of our constant g with the constant g_γ introduced by Yukawa is
$$g=g_\gamma(\hbar c)^{-\frac{1}{2}}.$$

[14] Small roman indices i, k, $\cdots$ run from 1 to 3 and denote vector components in the ordinary space.

of which one, $\varphi_\alpha'(x)$, is orthogonal to the gradient of the source function

$$\int \varphi_\alpha' \nabla K dV = 0 \tag{12}$$

and the other proportional to the gradient of the potential $\mathrm{X}(x)$ which the source function generates according to

$$(-\Delta+\kappa^2)\mathrm{X} = 4\pi K,$$

$$\mathrm{X}(x) = \int K(x') e^{-\kappa r}/r dV'. \tag{13}$$

If we define

$$\delta_{ik} I = \int \frac{\partial \mathrm{X}}{\partial x_i}\frac{\partial K}{\partial x_k} dV = \int\int \frac{\partial K}{\partial x_i}\frac{e^{-\kappa r}}{r}\frac{\partial K}{\partial x_k} dV dV', \tag{14}$$

$$\xi(x) = \frac{\mathrm{X}(x)}{I}, \quad \delta_{ik} = \int \frac{\partial \xi}{\partial x_i}\frac{\partial K}{\partial x_k} dV, \tag{15}$$

then it follows from (11) and (12) that

$$\varphi_\alpha(x) = 1/(4\pi)^{\frac{1}{2}} \sum_k \overset{0}{\varphi}_{\alpha k}\frac{\partial \xi}{\partial x_k} + \varphi_\alpha'(x), \tag{16}$$

hence

$$\varphi_\alpha'(x) = \varphi_\alpha(x) - \nabla\xi \cdot \int \nabla K \varphi_\alpha dV. \tag{17}$$

The circumstance that we choose the first part of the field as a linear function of the $\partial \mathrm{X}/\partial x_k$ (and not of the $\partial K/\partial x_k$) has the consequence that in virtue of (12) no cross terms between $\overset{0}{\varphi}_{\alpha k}$ and $\varphi_\alpha'(x)$ occur in the potential energy H_0. Indeed, one has, using (13), (15),

$$\tfrac{1}{2}\sum_\alpha \int \varphi_\alpha(-\Delta+\kappa^2)\varphi_\alpha dV = \tfrac{1}{2}\sum_{\alpha,k}\frac{(\overset{0}{\varphi}_{\alpha k})^2}{I} + \tfrac{1}{2}\sum_\alpha \int \varphi_\alpha'(-\Delta+\kappa^2)\varphi_\alpha' dV. \tag{18}$$

The conjugate decomposition of the momentum $\pi(x)$ is given by

$$\pi_\alpha(x) = (4\pi)^{\frac{1}{2}} \sum_k \overset{0}{\pi}_{\alpha k}\frac{\partial K}{\partial x_k} + \pi_\alpha'(x), \tag{16'}$$

$$\int \pi_\alpha' \nabla\xi dV = 0, \tag{12'}$$

$$\overset{0}{\pi}_{\alpha k} = 1/(4\pi)^{\frac{1}{2}} \int (\partial\xi/\partial x_k)\pi_\alpha dV, \tag{11'}$$

$$\pi_\alpha' = \pi_\alpha(x) - \nabla K \cdot \int \nabla\xi \pi_\alpha dV, \tag{17'}$$

which leads, in accordance with (2), to the commutation rules

$$i[\overset{0}{\pi}_{\alpha i}, \overset{0}{\varphi}_{\beta k}] = \delta_{\alpha\beta}\delta_{ik}, \tag{19}$$

$$[\overset{0}{\pi}_{\alpha k}, \varphi_\beta'(x)] = [\pi_\alpha'(x), \overset{0}{\varphi}_{\beta k}] = 0, \tag{20}$$

$$i[\pi_\alpha'(\mathbf{x}_1), \varphi_\beta'(\mathbf{x}_2)] = \delta_{\alpha\beta}(\delta(\mathbf{x}_1-\mathbf{x}_2) - \nabla_1 K \cdot \nabla_2 \xi). \tag{21}$$

The latter relation is also in direct agreement with the orthogonality conditions (12), (12').

The isotopic spin (10) decomposes simply into

$$T_{\alpha\beta} = \int (\varphi_\alpha'\pi_\beta' - \varphi_\beta'\pi_\alpha')dV + \sum_k (\overset{0}{\varphi}_{\alpha k}\overset{0}{\pi}_{\beta k} - \overset{0}{\varphi}_{\beta k}\overset{0}{\pi}_{\alpha k}) + \tfrac{1}{2}\tau_{\alpha\beta}. \tag{22}$$

The kinetic energy however gets cross terms in $\overset{0}{\pi}_{\alpha i}$ and $\pi_\alpha'(x)$, and if we use the abbreviation

$$\delta_{ik} N = 4\pi \int \frac{\partial K}{\partial x_i}\frac{\partial K}{\partial x_k} dV$$

or

$$N = \frac{4\pi}{3}\int (\nabla K)^2 dV, \tag{23}$$

it is given by

$$\tfrac{1}{2}\sum_\alpha \int \pi_\alpha^2 dV = \tfrac{1}{2}N \sum_{\alpha,k} (\overset{0}{\pi}_{\alpha k})^2 + (4\pi)^{\frac{1}{2}} \sum_{\alpha,k} \overset{0}{\pi}_{\alpha k} \int \frac{\partial K}{\partial x_k}\pi_\alpha'(x) dV + \tfrac{1}{2}\sum_\alpha \int (\pi_\alpha')^2 dV. \tag{24}$$

One gets the total Hamiltonian by collecting (24), (18), (8'):

$$H = \tfrac{1}{2}N \sum_{\alpha,k} (\overset{0}{\pi}_{\alpha k})^2 + \tfrac{1}{2}\sum_{\alpha,k} (\overset{0}{\varphi}_{\alpha k})^2/I + g/\kappa\sqrt{2} \sum_{\alpha,k} \tau_\alpha \sigma_k \overset{0}{\varphi}_{\alpha k} + (4\pi)^{\frac{1}{2}} \sum_{\alpha,i} \overset{0}{\pi}_{\alpha i} \int (\partial K/\partial x_i)\pi_\alpha'(x) dV + \tfrac{1}{2}\sum_\alpha \int (\pi_\alpha')^2 dV + \tfrac{1}{2}\sum_\alpha \int \varphi_\alpha'(-\Delta+\kappa^2)\varphi_\alpha' dV. \tag{I}$$

Just as for the isotopic spin there exists in virtue of the spherical symmetry of the source function $K(x)$ the integral of the angular momentum $L_{ik} = -L_{ki}$ given by

$$L_{ik} = -\sum_\alpha \int \pi_\alpha \left(x_i\frac{\partial}{\partial x_k} - x_k\frac{\partial}{\partial x_i}\right)\varphi_\alpha dV + \tfrac{1}{2}\sigma_{ik}. \tag{10'}$$

It decomposes as follows:

$$L_{ik}=\tfrac{1}{2}\sigma_{ik}+\sum_\alpha(\overset{0}{\varphi}_{\alpha i}\overset{0}{\pi}_{\alpha k}-\overset{0}{\varphi}_{\alpha k}\overset{0}{\pi}_{\alpha i})$$
$$-(4\pi)^{\frac{1}{2}}\sum_{\alpha,l}\overset{0}{\pi}_{\alpha l}\int\frac{\partial K}{\partial x_l}\left(x_i\frac{\partial}{\partial x_k}-x_k\frac{\partial}{\partial x_i}\right)\varphi_\alpha' dV$$
$$-1/(4\pi)^{\frac{1}{2}}\sum_{\alpha,l}\overset{0}{\varphi}_{\alpha l}\int\pi_\alpha'\left(x_i\frac{\partial}{\partial x_k}-x_k\frac{\partial}{\partial x_i}\right)\frac{\partial\xi}{\partial x_l}dV$$
$$-\sum_\alpha\int\pi_\alpha'\left(x_i\frac{\partial}{\partial x_k}-x_k\frac{\partial}{\partial x_i}\right)\varphi_\alpha' dV. \quad (22')$$

The orthogonality relations (12), (12′) do not make the cross terms disappear in this case. We emphasize, however, the simple form of the angular momentum of the zero field, given by the first sum in (22′).

4. THE EIGENVALUES OF THE INTERACTION ENERGY. NEW VARIABLES FOR THE ZERO STATE

While in the usual treatment the interaction energy H_1 is considered as a small perturbation (weak coupling), we consider in this paper the opposite limit of strong coupling. In this case one has first to investigate the eigenvalues of the interaction energy H_1 given by (8′), and then to retain only the lowest of them under the assumption, whose validity will be investigated, that the next higher level of H_1 will not appreciably perturb a system in this lowest state.

In order to determine the four eigenvalues of the form

$$\sum_{\alpha,k}\tau_\alpha\sigma_k\overset{0}{\varphi}_{\alpha k}$$

in which the 9 coefficients $\overset{0}{\varphi}_{\alpha k}$ were real, we have to bear in mind that we are free to subject the τ's and σ's to independent real orthogonal transformations

$$\tau_\alpha=\sum_{r=1}^{3}\tau_r'B_{r\alpha},\quad \sigma_k=\sum_{s=1}^{3}A_{ks}\sigma_s', \quad (25)$$

where B and A fulfill orthogonality conditions which we can write in matrix notation

$$A\bar{A}=\bar{A}A=1,\quad B\bar{B}=\bar{B}B=1, \quad (26)$$

where $\bar{A}$ and $\bar{B}$ are the transposed matrices ($\bar{A}_{sk}=A_{ks}$, $\bar{B}_{\alpha r}=B_{r\alpha}$). The eigenvalues of our form are therefore the same as those of the other form

$$\sum_{r,s}\tau_r'(B\overset{0}{\varphi}A)_{rs}\sigma_s'. \quad (27)$$

We shall prove now that we can choose the orthogonal matrices A, B in such a way that the new matrix $B\overset{0}{\varphi}A$ becomes diagonal:

$$(B\overset{0}{\varphi}A)_{rs}=Q_r\delta_{rs} \quad (28)$$

or, according to (26),

$$\overset{0}{\varphi}_{\alpha k}=(\bar{B}Q\bar{A})_{\alpha k}=\sum_r B_{r\alpha}Q_rA_{kr}. \quad (29)$$

For this purpose we consider the two symmetrical forms

$$C=\bar{\varphi}\varphi \quad \text{or} \quad C_{ik}=C_{ki}=\sum_\alpha\overset{0}{\varphi}_{\alpha i}\overset{0}{\varphi}_{\alpha k}, \quad (30)$$

and

$$C'=\varphi\bar{\varphi} \quad \text{or} \quad C'_{\alpha\beta}=C'_{\beta\alpha}=\sum_k\overset{0}{\varphi}_{\alpha k}\overset{0}{\varphi}_{\beta k}. \quad (30')$$

We choose A as the orthogonal matrix which transforms C to principal axes (which is always possible because C is symmetric) and denote the eigenvalues of C by $(Q_r)^2$. These are certainly never negative because the form

$$\sum_{i,k}C_{ik}x_ix_k=\sum_\alpha(\sum_k\overset{0}{\varphi}_{\alpha k}x_k)^2$$

is definite. This means that we have

$$CA=AQ^2 \quad \text{or} \quad \bar{A}CA=Q^2. \quad (31)$$

We note that the matrix A is unique except for a sign, and except for the case where some of the Q_r's are zero or some of them are equal to each other. We now define the matrix B by

$$\varphi A=\bar{B}Q, \quad (32)$$

where Q_r is defined as the square root of the eigenvalue Q_r^2 of C, the sign of which we shall choose later. Multiplication by $\bar{\varphi}$ from the left gives, by virtue of (30), (31)

$$AQ^2=\bar{\varphi}\bar{B}Q,$$

or

$$AQ=\bar{\varphi}\bar{B},\quad \bar{A}AQ=Q=\bar{A}\bar{\varphi}\bar{B},$$

and by transposing the matrices, Q being diagonal

$$B\varphi A=Q$$

which proves Eq. (28). Now multiplying (32) by B from the left, we get

$$B\varphi A=Q=B\bar{B}Q.$$

Therefore $B\bar{B}=1$, which proves the orthogonality of B. (For the case of a multiple eigenvalue Q_r the orthogonality $B\bar{B}=1$ does not follow, but can easily be achieved.) Multiplying $AQ=\bar{\varphi}\bar{B}$

by $B\varphi$ from the left, we get

$$B\varphi AQ=Q^2=B\varphi\bar{\varphi}\bar{B}=BC'\bar{B},$$
$$BC'=Q^2B \quad \text{or} \quad BC'\bar{B}=Q^2, \tag{33}$$

which is analogous to (31) and shows that C' has the same eigenvalues as C.

If the eigenvalue Q_r is zero, the row $B_{r\alpha}$ of B is not defined by (32) and the preceding proof is incomplete. Let us assume first that there is a simple eigenvalue $Q_3=0$, $Q_1\neq 0$, $Q_2\neq 0$. From Eq. (32) we get for $r=3$

$$\sum_k \overset{0}{\varphi}_{ak}A_{k3}=0.$$

The equation $AQ=\bar{\varphi}\bar{B}$ is in this case not a consequence of the proved equation $AQ^2=\bar{\varphi}\bar{B}Q$ but can be used for $r=3$ as a definition of the third row of the matrix B, namely

$$\sum_\alpha \overset{0}{\varphi}_{ak}B_{3\alpha}=0.$$

This can always be fulfilled, the determinant of $\overset{0}{\varphi}_{ak}$ being zero in this case. There is still an arbitrary factor independent of α undetermined in $B_{3\alpha}$. This factor can be adjusted to satisfy the equation $Q=B\bar{B}Q$; it can simultaneously be made to satisfy the equation

$$\sum_\alpha B_{3\alpha}^2=1,$$

which does not follow directly from the above. Combining $Q=B\bar{B}Q$ and $\sum_\alpha B_{3\alpha}^2=1$, we obtain again $B\bar{B}=1$.

In Section 8 we shall meet the particular case

$$Q_3=0, \quad Q_1\neq 0, \quad Q_2\neq 0, \quad \overset{0}{\varphi}_{3k}=0.$$

In this case one has $B_{3\alpha}=0$ for $\alpha=1, 2$, which follows from

$$\sum_\alpha \overset{0}{\varphi}_{ak}B_{3\alpha}=0.$$

Moreover, (32) leads to $B_{\alpha 3}=0$ for $\alpha=1, 2$. Finally, B_{33} is fixed by $B\bar{B}=1$ and is equal to one. The latter condition also expresses the orthogonality of the two-row and two-column matrix $B_{r\alpha}$ ($r=1, 2$; $\alpha=1, 2$).

In a similar way the case of a multiple eigenvalue zero of C and C' can be treated by considering all equations in the preceding proof which cannot be directly derived as possible additional defining postulates.

In order to have the determinants of A and B both $+1$, which is essential for the validity of the correct algebraic relations for the τ_r', σ_s' we get from (32) the condition

$$\text{det. } \varphi=Q_1Q_2Q_3. \tag{34}$$

Apart from this condition, the signs of the Q_r's are arbitrary and can be fixed by definition. This means that to every combination of signs of the Q_r which fulfills (34) there exist, for a given $\overset{0}{\varphi}_{ak}$, matrices A and B which are orthogonal in the usual sense and which fulfill (28). We can for instance define all signs of the Q_r's as positive (negative) if det. φ is positive (negative).

Now inserting (28) in (27) we get

$$\sum_{\alpha,k} \tau_\alpha\sigma_k\overset{0}{\varphi}_{ak}=\sum_r Q_r\tau_r'\sigma_r'. \tag{35}$$

The eigenvalues of every τ_r', σ_r' are ± 1, but the product of the three matrices $\tau_r'\sigma_r'$ is always -1. Therefore, the eigenvalues of H_1 for a given field $\overset{0}{\varphi}_{ak}$ are

$$(g/\kappa\sqrt{2})\textstyle\sum_r Q_r\epsilon_r \quad \text{with} \quad \epsilon_1\epsilon_2\epsilon_3=-1 \tag{36}$$

or

$$\begin{aligned} E_1&=-(g/\kappa\sqrt{2})(Q_1+Q_2+Q_3),\\ E_2&=(g/\kappa\sqrt{2})(-Q_1+Q_2+Q_3),\\ E_3&=(g/\kappa\sqrt{2})(Q_1-Q_2+Q_3),\\ E_4&=(g/\kappa\sqrt{2})(Q_1+Q_2-Q_3). \end{aligned} \tag{36'}$$

The sum of all four E's is zero, but if E is an eigenvalue in general $-E$ is not an eigenvalue unless at least one of the three Q_r's is zero. We repeat that the Q_r's are the square roots of the eigenvalues of the symmetrical matrix C (or C'). From (31) we get immediately by evaluating the trace

$$\sum_{r=1}^{3} Q_r^2=\sum_k C_{kk}=\sum_{\alpha,k} (\overset{0}{\varphi}_{ak})^2. \tag{37}$$

The sum of the Q_r's themselves, however, cannot be expressed rationally by the field $\overset{0}{\varphi}_{ak}$.

We now introduce into the kinetic energy of the zero field the variables corresponding to Q_r, A_{kr}, $B_{r\alpha}$. Instead of expressing the latter variables by Euler angles and using their conjugate momenta, we can also use the components of the angular momentum

$$\overset{0}{L}_{ik}=\textstyle\sum_\alpha (\overset{0}{\varphi}_{\alpha i}\overset{0}{\pi}_{\alpha k}-\overset{0}{\varphi}_{\alpha k}\overset{0}{\pi}_{\alpha i}), \tag{22_0}$$

and the isotopic spin

$$\overset{0}{T}_{\alpha\beta}=\textstyle\sum_k (\overset{0}{\varphi}_{\alpha k}\overset{0}{\pi}_{\beta k}-\overset{0}{\varphi}_{\beta k}\overset{0}{\pi}_{\alpha k}). \tag{$22_0'$}$$

As operators they correspond to infinitesimal rotations of the ordinary space and of the isotopic spin space, and fulfill commutation relations with the A_{kr} and $B_{r\alpha}$ analogous to those with the $\overset{0}{\varphi}_{k\alpha}$, namely

$$i[\overset{0}{L}_{ik},\ A_{lr}]=\delta_{kl}A_{ir}-\delta_{il}A_{kr},$$
$$[\overset{0}{L}_{ik},\ B_{r\alpha}]=0, \quad (38)$$
$$i[\overset{0}{T}_{\alpha\beta},\ B_{\gamma r}]=\delta_{\beta\gamma}B_{\alpha r}-\delta_{\alpha\gamma}B_{\beta r},$$
$$[\overset{0}{T}_{\alpha\beta},\ A_{kr}]=0, \quad (38')$$

while the components of $\overset{0}{L}_{ik}$ or $\overset{0}{T}_{\alpha\beta}$ fulfill with each other the well-known commutation relations

$$i[\overset{0}{L}_{ik},\ \overset{0}{L}_{lm}]=\delta_{kl}\overset{0}{L}_{im}+\delta_{im}\overset{0}{L}_{kl}-\delta_{il}\overset{0}{L}_{km}-\delta_{km}\overset{0}{L}_{il}, \quad (39)$$

or, with the vector notation L_1^0, L_2^0, L_3^0 for $\overset{0}{L}_{23}$, $\overset{0}{L}_{31}$, $\overset{0}{L}_{12}$,

$$i[L_1^0,\ L_2^0]=-L_3^0,\ \cdots. \quad (39')$$

As scalars the Q_r's commute with both the $\overset{0}{L}_{ik}$ and the $\overset{0}{T}_{\alpha\beta}$,

$$[\overset{0}{L}_{ik},\ Q_r]=[\overset{0}{T}_{\alpha\beta},\ Q_r]=0. \quad (40)$$

In the same way we have

$$i[\overset{0}{T}_{\alpha\beta},\ \overset{0}{T}_{\gamma\delta}]=\delta_{\beta\gamma}\overset{0}{T}_{\alpha\delta}+\delta_{\alpha\delta}\overset{0}{T}_{\beta\gamma}-\delta_{\alpha\gamma}\overset{0}{T}_{\beta\delta}-\delta_{\beta\delta}\overset{0}{T}_{\alpha\gamma}, \quad (39'')$$

the $\overset{0}{T}_{\alpha\beta}$ and the $\overset{0}{L}_{ik}$ commute.

It is useful to introduce the components of (L^0), (T^0) with respect to the axes defined by (A_{kr}), $(B_{r\alpha})$ which we define by

$$L_0^{rs}=\sum_{i,k}A_{ir}A_{ks}\overset{0}{L}_{ik}=\sum_{i,k}\overset{0}{L}_{ik}A_{ir}A_{ks},$$
$$T_0^{rs}=\sum_{\alpha,\beta}B_{r\alpha}B_{s\beta}\overset{0}{T}_{\alpha\beta}=\sum_{\alpha,\beta}\overset{0}{T}_{\alpha\beta}B_{r\alpha}B_{s\beta}. \quad (41)$$

We note that in spite of the non-commutativity of $\overset{0}{L}_{ik}$ with the A_{lr} and of $\overset{0}{T}_{\alpha\beta}$ with the $B_{r\gamma}$ the L_0^{rs} and T_0^{rs} are Hermitian operators like the $\overset{0}{L}_{ik}$ and $\overset{0}{T}_{\alpha\beta}$ as a consequence of the equalities indicated in (41) which follow from (38), (38'). The total square of L_0 and T_0 is given by

$$L_0^2\equiv\sum_{i<k}(\overset{0}{L}_{ik})^2=\sum_{r<s}(L_0^{rs})^2, \quad (42)$$
$$T_0^2\equiv\sum_{\alpha<\beta}(\overset{0}{T}_{\alpha\beta})^2=\sum_{r<s}(T_0^{rs})^2. \quad (42')$$

The commutation relations of the L_0^{rs} with the A_{kr} and of T_0^{rs} with the $B_{r\alpha}$ are given by

$$i[L_0^{rs},\ A_{kt}]=\delta_{rt}A_{ks}-\delta_{st}A_{kr}, \quad (43)$$
$$i[T_0^{rs},\ B_{t\alpha}]=\delta_{rt}B_{s\alpha}-\delta_{st}B_{r\alpha}, \quad (43')$$

and of the L_0^{rs} or the T_0^{rs} with each other

$$i[L_0^{rs},\ L_0^{tu}]=\delta_{rt}L_0^{su}+\delta_{su}L_0^{rt}-\delta_{st}L_0^{ru}-\delta_{ru}L_0^{st}, \quad (44)$$
$$i[T_0^{rs},\ T_0^{tu}]=\delta_{rt}T_0^{su}+\delta_{su}T_0^{rt}-\delta_{st}T_0^{ru}-\delta_{ru}T_0^{st}. \quad (44')$$

The signs in the relations (43), (44) or (43'), (44') are just opposite to those in the relations (38), (39) or (38'), (39'').

Inserting (29), (22_0), and $(22_0')$ into (41) we get

$$L_0^{rs}=\sum_{k,\alpha}(Q_rA_{ks}B_{r\alpha}\overset{0}{\pi}_{\alpha k}-Q_sA_{kr}B_{s\alpha}\overset{0}{\pi}_{\alpha k}), \quad (45)$$
$$T_0^{rs}=\sum_{k,\alpha}(Q_rA_{kr}B_{s\alpha}\overset{0}{\pi}_{\alpha k}-Q_sA_{ks}B_{r\alpha}\overset{0}{\pi}_{\alpha k}). \quad (45')$$

From this we get the important expression

$$\sum_{k,\alpha}A_{kr}B_{s\alpha}\overset{0}{\pi}_{\alpha k}=\frac{1}{2}\left\{\frac{L_0^{rs}+T_0^{rs}}{Q_r-Q_s}-\frac{L_0^{rs}-T_0^{rs}}{Q_r+Q_s}\right\} \text{ for } r\neq s. \quad (46)$$

Finally, we get the variable canonically conjugate to Q_r, which we call P_r, by putting for $r=s$,

$$\sum_{k,\alpha}A_{kr}B_{r\alpha}\overset{0}{\pi}_{\alpha k}=P_r. \quad (47)$$

Therefore, we have finally

$$\overset{0}{\pi}_{\alpha k}=\sum_{r,s}A_{kr}B_{s\alpha}\times\left\{P_r\delta_{rs}+\frac{1}{2}\frac{L_0^{rs}+T_0^{rs}}{Q_r-Q_s}-\frac{1}{2}\frac{L_0^{rs}-T_0^{rs}}{Q_r+Q_s}\right\}, \quad (48)$$

where the second term is to be taken for $r\neq s$ only. Assuming

$$[P_r,\ A_{ks}]=[P_r,\ B_{s\alpha}]=[P_r,\ L_0^{st}]=[P_r,\ T_0^{st}]=0, \quad i[P_r,\ Q_s]=\delta_{rs}, \quad (49)$$

one can verify the canonical commutation relations (19) for the $\overset{0}{\pi}_{\alpha i}$ and $\overset{0}{\varphi}_{\beta k}$ with the help of (43) (44), (43'), (44'). It may be noted that the operator P_r defined by (47) is not Hermitian and that P_r in (48) has to be replaced by P_r^+ if the factor $A_{kr}B_{s\alpha}$ is put on the right side of the bracket. For the kinetic energy of the zero field (apart from the factor $N/2$) we get from (48), taking into account the anti-symmetry in r, s of

$(L_0^{rs}-T_0^{rs})/Q_r+Q_s$ and the symmetry in r, s of $(L_0^{rs}+T_0^{rs})/Q_r-Q_s$

$$\sum_{\alpha,k}(\overset{0}{\pi}_{\alpha,k})^2=\sum_r P_r^+P_r+\frac{1}{4}\sum_{r\neq s}\frac{(L_0^{rs}+T_0^{rs})^2}{(Q_r-Q_s)^2}+\frac{1}{4}\sum_{r,s}\frac{(L_0^{rs}-T_0^{rs})^2}{(Q_r+Q_s)^2}. \quad (50)$$

We conclude from (46) that if $Q_r=Q_s$ then it must also be true that $L_0^{rs}=-T_0^{rs}$. In view of the importance of this case it is sometimes convenient to use different coordinates. Indeed, if all three Q_r's are equal, which will be proved to be true in good approximation in the case of large coupling, according to (29) only the orthogonal matrix

$$e_{\alpha k}=\sum_r A_{kr}B_{r\alpha} \quad (51)$$

which fulfills

$$\sum_\alpha e_{\alpha i}e_{\alpha k}=\delta_{ik}, \quad \sum_k e_{\alpha k}e_{\beta k}=\delta_{\alpha\beta}, \quad (51a)$$

is uniquely determined by the field $\overset{0}{\varphi}_{\alpha k}$ and not the A_{kr} and $B_{r\alpha}$ themselves. Therefore, besides the three independent variables $e_{\alpha k}$, we can introduce the six symmetrical quantities

$$\overset{0}{q}_{\alpha\beta}=\sum_k \overset{0}{\varphi}_{\alpha k}e_{\beta k}=\sum_r B_{r\alpha}B_{r\beta}Q_r=\overset{0}{q}_{\beta\alpha} \quad (52)$$

to describe the field

$$\overset{0}{\varphi}_{\alpha k}=\sum_\beta e_{\beta k}\overset{0}{q}_{\alpha\beta}. \quad (53)$$

The components

$$L_0^{\alpha\beta}=\sum_{r,s}B_{r\alpha}B_{s\beta}L_0^{rs}=\sum_{i,k}e_{\alpha i}e_{\beta k}\overset{0}{L}_{ik} \quad (54)$$

commute with the $\overset{0}{q}_{\gamma\delta}$ and fulfill similar commutation relations with each other and with the $e_{\alpha i}$ as do the L_0^{rs} with each other and with the A_{kt},

$$i[L_0^{\alpha\beta}, e_{\gamma k}]=\delta_{\alpha\gamma}e_{\beta k}-\delta_{\beta\gamma}e_{\alpha k}, \quad (55)$$

$$i[L_0^{\alpha\beta}, L_0^{\gamma\delta}]=\delta_{\alpha\gamma}L_0^{\beta\delta}+\delta_{\beta\delta}L_0^{\alpha\gamma}-\delta_{\beta\gamma}L_0^{\alpha\delta}-\delta_{\alpha\delta}L_0^{\beta\gamma}. \quad (56)$$

Finally, we search for symmetrical quantities $\overset{0}{p}_{\alpha\beta}=\overset{0}{p}_{\beta\alpha}$ which are conjugate to the $\overset{0}{q}_{\alpha\beta}$ in the sense that they fulfill the commutation relations

$$i[\overset{0}{p}_{\alpha\beta}, \overset{0}{q}_{\gamma\delta}]=\tfrac{1}{2}(\delta_{\alpha\gamma}\delta_{\beta\delta}+\delta_{\alpha\delta}\delta_{\beta\gamma}). \quad (57)$$

(This means, for instance, that $i[p_{11}^0, q_{11}^0]=1$, $i[p_{12}^0, q_{12}^0]=\frac{1}{2}$; this is more convenient than to have the value 1 for the latter bracket.) This is just the case if, with the help of the first two terms in the bracket in (48), we put

$$\overset{0}{p}_{\alpha\beta}=\sum_r B_{r\alpha}B_{r\beta}P_r+\sum_{r\neq s}{}' B_{r\alpha}B_{s\beta}\frac{1}{2}\frac{L_0^{rs}+T_0^{rs}}{Q_r-Q_s}. \quad (58)$$

From (48) we find also

$$\overset{0}{p}_{\alpha\beta}=\tfrac{1}{2}\sum_k(e_{\alpha k}\overset{0}{\pi}_{\beta k}+e_{\beta k}\overset{0}{\pi}_{\alpha k}). \quad (59)$$

The remark made about the non-Hermitian character of the P_r in (47) applies also to the $\overset{0}{p}_{\alpha\beta}$ defined here. One can prove (57) with the help of (54), (43), (43′), and moreover

$$[\overset{0}{p}_{\alpha\beta}, L_0^{\gamma\delta}]=0. \quad (60)$$

We have therefore three kinds of variables for the zero field:

(1) $\overset{0}{\varphi}_{\alpha k}, \overset{0}{\pi}_{\alpha k}$,

(2) $Q_r, A_{kr}, B_{r\alpha}; \quad P_r, L_0^{rs}, T_0^{rs}$,

(3) $\overset{0}{q}_{\alpha\beta}=\overset{0}{q}_{\beta\alpha}, e_{\alpha k}; \quad \overset{0}{p}_{\alpha\beta}=\overset{0}{p}_{\beta\alpha}, L_0^{\alpha\beta}$.

While we were able to get an explicit expression for the kinetic energy in terms of the variables (2), this is not rigorously possible with the variables (3). From (48), (50) we get only

$$\sum_{\alpha,k}(\overset{0}{\pi}_{\alpha k})^2=\sum_{\alpha,\beta}\overset{0\dagger}{p}_{\alpha\beta}\overset{0}{p}_{\alpha\beta}+\frac{1}{4}\sum_{r,s}\frac{(L_0^{rs}-T_0^{rs})^2}{(Q_r+Q_s)^2}. \quad (61)$$

In the next section we shall see, however, that in the case of small deviations of the Q_r from a large common value $Q_r^0=D$, further simplifications are possible, and that the variables (3) are the most convenient ones in this case.

5. MINIMUM OF THE POTENTIAL ENERGY. STRONG COUPLING APPROXIMATION

We determine first the minimum of the total potential energy of the zero field which is, according to (18), (36), (37), equal to

$$E_{\text{pot}}^0=\frac{1}{2I}\sum_{r=1}^3 Q_r^2+\frac{g}{\kappa\sqrt{2}}\sum_r Q_r\epsilon_r \quad (\epsilon_1\epsilon_2\epsilon_3=-1). \quad (62)$$

The minimum corresponds to

$$\epsilon_1=\epsilon_2=\epsilon_3=-1, \quad Q_1=Q_2=Q_3=D=\frac{g}{\kappa\sqrt{2}}I,$$

$$E_{\min}^0=-\frac{3}{4}\frac{g^2}{\kappa^2}I. \quad (63)$$

According to (53) the corresponding field is given by

$$\overset{0}{\varphi}_{\alpha k}=De_{\alpha k} \quad (64)$$

or, in vector notation

$$\boldsymbol{\phi}_\alpha{}^0 = D\mathbf{e}_\alpha. \tag{64a}$$

This field corresponds to the smallest eigenvalue of the interaction energy, determined by (36), and to the absence of free mesons [we neglected φ'][15] but still contains the q numbers $\mathbf{e}_\alpha$. Moreover, it corresponds to the state of the τ and σ where

$$\sum_{\alpha,k} \tau_\alpha \sigma_k e_{\alpha k} = -3.$$

By a suitable S transformation of the Hamiltonian (see Appendix) we can bring this to the form

$$S\Big(\sum_{\alpha,k} \tau_\alpha \sigma_k e_{\alpha k}\Big) S^{-1} = \sum_{\alpha=1}^{3} \tau_\alpha \sigma_\alpha. \tag{65}$$

The S transformation is not uniquely determined, just as is true for the A and B matrices; it is, for instance, sufficient in this case to transform one system of the matrices τ_α or σ_k alone. In view of the application to the charged pseudoscalar theory, which is discussed in Section 6, we decided to leave the τ_α's unchanged and to transform the σ_k's,

$$S\tau_\alpha S^{-1} = \tau_\alpha; \quad S\Big(\sum_k e_{\alpha k}\sigma_k\Big) S^{-1} = \sigma_\alpha. \tag{65a}$$

This is equivalent to

$$\sigma_k' \equiv S\sigma_k S^{-1} = \sum_\alpha e_{\alpha k}\sigma_\alpha. \tag{65b}$$

The state in question can be described as the singlet state inasmuch as the composition of the τ_α and σ_α is analogous to the composition of two spins of equal magnitude. This state is not degenerate according to (36'), while the three other eigenvalues of the interaction energy are equal:

$$E_1 = -(g/\kappa\sqrt{2})3D, \quad E_2 = E_3 = E_4 = (g/\kappa\sqrt{2})D. \tag{66}$$

In the following we assume that it is legitimate to restrict our attention to the lowest, or singlet state. This implies a condition on the magnitude of such terms in the Hamiltonian as couple the lowest to the three upper states of the interaction energy.

For the eigenvalue E_1, the following expressions are diagonal:

$$\tau_1\sigma_1 = \tau_2\sigma_2 = \tau_3\sigma_3 = -1; \quad \tau_1\sigma_2 + \tau_2\sigma_1 = 0, \cdots \tag{67}$$

[15] It will be shown in Section 7 that the field φ' describes free mesons.

On the other hand, the matrices τ_r, σ_r, and $\tau_1\sigma_2 - \tau_2\sigma_1$, $\cdots$ are not diagonal. We shall simply neglect terms in the energy in which these matrices appear as a factor. In Section 6, we shall discuss the region of validity of this approximation.

As is shown in the Appendix, the S transformation changes the angular momentum $\mathbf{L}$ according to

$$\mathbf{L}' = S\mathbf{L}S^{-1} = \mathbf{L} - \tfrac{1}{2}\boldsymbol{\sigma}' = \mathbf{L} - \tfrac{1}{2}\sum_\alpha \sigma_\alpha \mathbf{e}_\alpha. \tag{68}$$

As a consequence of this and (54) we have the relation

$$SL_0{}^{\alpha\beta}S^{-1} = L_0{}^{\alpha\beta} - \tfrac{1}{2}\sigma_{\alpha\beta}. \tag{69}$$

One checks directly that $\mathbf{L}'$ commutes with $\boldsymbol{\sigma}'$ if $\mathbf{L}$ commutes with $\boldsymbol{\sigma}$ using (55). As the σ_α can be disregarded in our strong coupling approximation if they do not occur multiplied by the τ_α's, the $\mathbf{L}'$ have in this approximation the same eigenvalues as the $\mathbf{L}$, while the total sum L'^2 [see (42)] has eigenvalues $\frac{1}{4}$ larger than L^2. Moreover, the eigenfunction $\Psi' = S\Psi$ is double-valued in the angles which enter in S and in which Ψ is one-valued. Therefore $(L')^2$ has the eigenvalues $\frac{1}{4} + j(j+1)$ with half-integer j.

We now split the variables $\overset{0}{q}_{\alpha\beta}$ defined by (52) into two parts according to (64)

$$\overset{0}{q}_{\alpha\beta} = D\delta_{\alpha\beta} + \overset{(1)}{q}_{\alpha\beta}, \tag{70}$$

of which we consider the second part as small. With D given by (63)

$$E_{\text{pot}} = \frac{1}{2I}\sum_{\alpha,k} (\overset{0}{\varphi}_{\alpha k})^2 + \frac{g}{\kappa\sqrt{2}}\sum_{\alpha,k} \tau_\alpha\sigma_k \overset{0}{\varphi}_{\alpha k}.$$

This leads, by the S transformation (65) which does not change the $\overset{0}{\varphi}_{\alpha k}$ but does change the $\overset{0}{\pi}_{\alpha k}$, to

$$E'_{\text{pot}} = SE_{\text{pot}}S^{-1} = \frac{1}{2I}\sum_{\alpha,\beta} (\overset{0}{q}_{\alpha\beta})^2 + \frac{g}{\kappa\sqrt{2}}\sum_{\alpha,\beta} \overset{0}{q}_{\alpha\beta}\,\tfrac{1}{2}(\tau_\alpha\sigma_\beta + \sigma_\beta\tau_\alpha).$$

Using (67) we have

$$E'_{\text{pot}} = \frac{1}{2I}\sum_{\alpha,\beta} (\overset{0}{q}_{\alpha\beta})^2 - \frac{g}{\kappa\sqrt{2}}\sum_{\alpha,\beta} \overset{0}{q}_{\alpha\beta},$$

which simply reduces to

$$E'_{\text{pot}} = -\frac{3}{4}\frac{g^2}{\kappa^2}I + \frac{1}{2I}\sum_{\alpha,\beta} (\overset{(1)}{q}_{\alpha\beta})^2. \tag{71}$$

We now introduce (64) into (22_0), which means that we disregard $q^{(1)}_{\alpha\beta}$ and get

$$L^0_{ik}=D\sum_\alpha (e_{\alpha i}\pi^0_{\alpha k}-e_{\alpha k}\pi^0_{\alpha i}).$$

and from (54)

$$-L_0{}^{\alpha\beta}=D\sum_k (e^0_{\alpha k}\pi^0_{\beta k}-e^0_{\beta k}\pi^0_{\alpha k}).$$

It therefore follows from (59) that

$$\pi^0_{\alpha k}=\sum_\beta e_{\beta k}\left(p^0_{\alpha\beta}+\frac{1}{2D}L_0{}^{\alpha\beta}\right)$$

$$=\sum_\beta \left(p^{0\dagger}_{\alpha\beta}+\frac{1}{2D}L_0{}^{\alpha\beta}\right)e_{\beta k}. \quad (72)$$

Inserting $\varphi^0_{\alpha k}=De_{\alpha k}$ one can finally check directly

$$T_0{}^{\alpha\beta}=-L_0{}^{\alpha\beta}, \quad (73)$$

where the disregarded terms are of the relative order of magnitude D^{-2} in comparison with the main term. This is in agreement with the result of the last section. If we introduce $T_0{}^{rs}=-L_0{}^{rs}$ and $Q_r+Q_s=2D$ in the last term in (48) we get (72) directly. The relation (73) has the important consequence that the total square of the isotopic spin is equal to the total square of the angular momentum; after the S transformation, both correspond to half-integer quantum numbers. Therefore the quantum number n, which is equal to the charge number minus $\frac{1}{2}$ [see Eqs. (9), (10)], always has for the zero field (that means in absence of free mesons) an absolute value smaller than the total angular momentum quantum number j:

$$-j\leqq n\leqq j. \quad (74)$$

This is of course due to the fact that the τ_α and σ_α are in the "singlet state" defined by (67); this also enables us to disregard the terms linear in τ and σ as already mentioned.

If we introduce $\langle p^0_{\alpha\beta}\rangle_H=\frac{1}{2}(p^0_{\alpha\beta}+p^{0\dagger}_{\alpha\beta})$, the $\langle\ \rangle_H$ denoting Hermitization, we get

$$\pi^0_{\alpha\beta}=\sum_\beta e_{\beta k}\langle p^0_{\alpha\beta}\rangle_H+\frac{1}{2D}\langle L_0{}^{\alpha\beta}e_{\beta k}\rangle_H. \quad (72')$$

This leads to the following expression for the kinetic energy of the zero field (neglecting an additive constant in the term proportional to D^{-2}):

$$\frac{N}{2}\sum_{\alpha,k}(\pi^0_{\alpha k})^2=\frac{N}{2}\left\{\sum_{\alpha,\beta}(p^0_{\alpha\beta})_H{}^2+\frac{1}{2D^2}L_0{}^2\right\}, \quad (72a)$$

where the square of the total angular momentum is given by (42). A result identical with (72a) is obtained from (61) if we insert in the last term $Q_r+Q_s=2D$, $-T_0{}^{rs}=L_0{}^{rs}$. We note that the only result of the S transformation is that j gets half-integral values, the constant $\frac{1}{4}$ added to $L_0{}^2$ being negligible for our applications.

Inserting (71), (72), (72a) into the Hamiltonian (I), we get the "reduced" Hamiltonian of the strong coupling approximation

$$H=-\frac{3}{4}\frac{g^2}{\kappa^2}I+\frac{1}{2}N\left\{\sum_{\alpha,\beta}\langle p^0_{\alpha\beta}\rangle^2_H+\frac{1}{2D^2}L_0{}^2\right\}$$

$$+\frac{1}{2I}\sum_{\alpha,\beta}(q^{(1)}_{\alpha\beta})^2+(4\pi)^{\frac{1}{2}}\sum_{\alpha,\beta,k}e_{\beta k}\langle p^0_{\alpha\beta}\rangle_H$$

$$\times\int\frac{\partial K}{\partial x_k}\pi_\alpha'(x)dV+\frac{1}{2}\sum_\alpha\int\pi_\alpha'^2dV$$

$$+\frac{1}{2}\sum_\alpha\int\varphi_\alpha'(-\Delta+\kappa^2)\varphi_\alpha'dV$$

$$+(4\pi)^{\frac{1}{2}}\sum_{\alpha,\beta,k}\frac{1}{2D}\langle e_{\beta k}L_0{}^{\alpha\beta}\rangle_H\int\frac{\partial K}{\partial x_k}\pi_\alpha'(x)dV. \quad (II)$$

Inspection with respect to the approximation contained in (72) shows that the disregarded terms in H are of the following type: terms of the order D^{-2} independent of L^0_{ik}; terms of the order D^{-2} linear in the L^0_{ik} and in the $q^{(1)}_{ik}$; and terms of higher order than D^{-2}. We shall see in the next two sections that such terms are of no importance for the questions which are treated in this paper. The last term in (II), however, will be essential.

6. THE EXCITED STATES (ISOBARS) OF THE NUCLEON

We shall now treat two different kinds of problems. In the first kind we investigate the states of the nucleon in the absence of free mesons, while in the second kind we treat the scattering of free mesons by the nucleon and its proper field. It will turn out in the next section that the field which is described by $p^0_{\alpha\beta}$, $\pi_\alpha'(x)$; $q^{(1)}_{\alpha\beta}$, $\varphi_\alpha'(x)$ represents free mesons, which are partly undisturbed plane waves, partly scattered waves. On the other hand the problem described by e_{ak}, $L^0_{\alpha\beta}$ is the problem of the possible states of the free nucleon in the absence of free mesons.

For the latter we have to retain the terms up to the order D^{-2} but we can omit terms of the order D^{-2} which are independent of L_{ik}^{0} or terms of the order D^{-2} linear in L_{ik}^{0} which are at the same time linear in $q_{ik}^{(1)}$ or bilinear in $\pi_\alpha'(x_1)$ and $\varphi_\beta'(x_2)$. The latter terms do not have an expectation value of the order D^{-2} in the state where the corresponding waves are unexcited, and the terms independent of L_{ik}^{0} do not influence the energy difference between the excited states of the nucleon and the ground state (isobar separation). These more complicated terms, however, give rise to a correction of higher order to the scattering of free mesons, which question is not treated in this paper. In the following section we treat the meson scattering only as a problem of the order D^0 and disregard all terms of higher order, while in this section we treat the problem of the nucleon in the absence of free mesons up to the order D^{-2}.

In order to get rid of the last terms in (II) we have to shift the zero point of $\pi_\alpha'(x)$ but in such a way that the orthogonality relation (12′), namely $\int \pi_\alpha'(\partial\xi/\partial x_k)dV=0$ is not violated. The suitable assumption is

$$\pi_\alpha'(x)=\pi_\alpha''(x)-\frac{(4\pi)^{\frac{1}{2}}}{2D}\sum_{k,\beta}\langle e_{\beta k}L_0^{\alpha\beta}\rangle_H \times\left\{\frac{\partial K}{\partial x_k}-\frac{\partial\xi/\partial x_k}{\int(\partial\xi/\partial x)^2dV}\right\},^{16} \quad (75)$$

which agrees with the orthogonality condition (12′) because of (15). Indeed, we have, again using (12′),

$$\sum_\alpha \tfrac{1}{2}\int(\pi_\alpha'')^2dV=\sum_\alpha \tfrac{1}{2}\int(\pi_\alpha')^2dV +\frac{(4\pi)^{\frac{1}{2}}}{2D}\sum_{k,\alpha,\beta}\langle e_{\beta k}L_0^{\alpha\beta}\rangle_H\int\frac{\partial K}{\partial x_k}\pi_\alpha'(x)dV +\frac{4\pi}{2D^2}L_0^{2}\tfrac{1}{2}\int\left\{\frac{\partial K}{\partial x}-\frac{\partial\xi/\partial x}{\int(\partial\xi/\partial x)^2dV}\right\}^2dV.$$

Taking into account (15) and the definition (23) of N we find

$$4\pi\int\left\{\frac{\partial K}{\partial x}-\frac{\partial\xi/\partial x}{\int(\partial\xi/\partial x)^2dV}\right\}^2Vd=N-\frac{4\pi}{\int(\partial\xi/\partial x)^2dV}.$$

[16] We omit the index on the variable x if an integral has the same value for all three values of this index.

The term with N just gives the second term in (II); therefore we get finally, inserting $\xi(x)=\mathrm{X}(x)/I$ and the value (63) of D

$$H=\frac{\kappa^2}{2g^2}\frac{4\pi}{\int(\partial\mathrm{X}/\partial x)^2dV}L_0^2-\frac{3}{4}\frac{g^2}{\kappa^2}I+H_1, \quad (76)$$

$$H_1=\tfrac{1}{2}N\sum_{\alpha,\beta}\langle p_{\alpha\beta}^{0}\rangle_H^2+\frac{1}{2I}\sum_{\alpha,\beta}(q_{\alpha\beta}^{(1)})^2 +(4\pi)^{\frac{1}{2}}\sum_{\alpha,\beta,k}\langle p_{\alpha\beta}^{0}\rangle_H e_{\beta k}\int\frac{\partial K}{\partial x_k}\pi_\alpha''(x)dV +\tfrac{1}{2}\sum_\alpha\int(\pi_\alpha'')^2dV +\tfrac{1}{2}\sum_\alpha\int\varphi_\alpha'(-\Delta+\kappa^2)\varphi_\alpha'dV. \quad (77)$$

In the third term of the shift of $\pi_\alpha'(x)$ does not give any contribution, because

$$\sum_{\alpha,\beta}L_0^{\alpha\beta}p_{\alpha\beta}=0,$$

$L_0^{\alpha\beta}$ being antisymmetric, $p_{\alpha\beta}$ symmetric in α and β.

Before we proceed, it is necessary to complete the discussion of the shift (75) of $\pi_\alpha'(x)$. As this shift depends on $L_0^{\alpha\beta}$ and $e_{\beta k}$ it is a q number and necessitates corrections to $L_0^{\alpha\beta}$ and $e_{\beta k}$ themselves to insure that they commute with the new $\pi_\alpha''(x)$ and at the same time maintain their own commutation relations. This goal is reached by the canonical transformation

$$F=e^{iU}F'e^{-iU}=F'+i[U,F'] +\frac{i^2}{2!}[U,[U,F']]+\cdots. \quad (78)$$

We can substitute for F the old variables $\pi_\alpha'(x)$, $L_0^{\alpha\beta}$, $e_{\beta k}$, for F' the new variables $\pi_\alpha''(x)$, $L_0^{\alpha\beta\prime}$, $e_{\beta k}'$ if we choose for U

$$U=\frac{(4\pi)^{\frac{1}{2}}}{2D}\sum_{\alpha,\beta,k}\langle e_{\beta k}'L_0^{\alpha\beta\prime}\rangle_H\int\frac{\partial\xi}{\partial x_k}\varphi_\alpha'(x)dV \times\left[\int\left(\frac{\partial\xi}{\partial x}\right)^2dV\right]^{-1}, \quad (79)$$

which again gives the shift (75) for the first-order correction to $\pi_\alpha'(x)$ as a result of (21).

Fortunately it is not necessary to give here the explicit formulas for the corrections to $L_0^{\alpha\beta\prime}$,

e'_{ak} and the second-order corrections to $\pi_a'(x)$ because the additional terms in the Hamiltonian of the order D^{-2} are either independent of $L_0^{\alpha\beta}$ or linear in $L_0^{\alpha\beta}$ and at the same time linear in $\varphi_a'(x)$ or bilinear in $\pi_a'(x)$, $\varphi_\beta'(x)$. The expectation value of the terms linear in $L_0^{\alpha\beta}$ is zero in the stationary states of the Hamiltonian (76), (77). It may be noted that L^0_{ik} is only an approximate integral of the motion, but if we replace it in (76) by the exact integral (22′) of the total angular momentum, the additional terms in the Hamiltonian are again of the type which is disregarded here.

Because the eigenvalues of L_0^2 are $j(j+1)$ with half-integer j after the transformation (54), we get directly from (76) for the energy of excitation of the levels of the nucleon above the ground level

$$\Delta E=\frac{3}{2}\frac{\kappa^2}{g^2}\frac{4\pi}{\int(\nabla \mathrm{X})^2dV}\{j(j+1)-\tfrac{3}{4}\}. \quad (80)$$

The charge quantum number n does not enter but is restricted by (74) to values less than or equal to j. It is characteristic of the *symmetrical* pseudoscalar theory that the system is degenerate and the energy of all states with the same j and different charges has the same value. For the ground state, $j=\frac{1}{2}$, the number n has the two possible values $n=-\frac{1}{2}$ and $n=\frac{1}{2}$, which correspond to neutron and proton.

The integral

$$\frac{1}{4\pi}\int(\nabla \mathrm{X})^2dV=-\frac{1}{4\pi}\int \mathrm{X}\Delta \mathrm{X}dV$$
$$=\int \mathrm{X}KdV-\frac{\kappa^2}{4\pi}\int \mathrm{X}^2dV,$$

[see (13)] and can be evaluated in the two limiting cases of small sources $\kappa a\ll 1$ and large sources $\kappa a\gg 1$ as follows. Consider the expression

$$\int \mathrm{X}KdV=\int\int K(x')\frac{e^{-\kappa r}}{r}K(x)dVdV'.$$

In the first limit we may substitute 1 for $e^{-\kappa r}$, the error being of the relative order κa. This means, according to (4), that we put $\int \mathrm{X}KdV=a^{-1}$. In this limit the second integral $(\kappa^2/4\pi)\int \mathrm{X}^2dV$ can be disregarded because it becomes independent of a if κa is small. Therefore we get

$$\frac{1}{4\pi}\int(\nabla \mathrm{X})^2dV=\frac{1}{a},$$
$$\frac{\Delta E}{\mu c^2}=\frac{3}{2}\frac{\kappa a}{g^2}\{j(j+1)-\tfrac{3}{4}\}\ \text{for}\ \kappa a\ll 1. \quad (80a)$$

The expression $(\Delta E/\mu c^2)$, μ being the rest mass of the meson, refers to ordinary units of the energy and it is equal to $\Delta E/\kappa$ in our units.

For large sources $\kappa a\gg 1$ it is possible to integrate (13) by the following development

$$\mathrm{X}(x)=\frac{4\pi}{\kappa^2}\left(1-\frac{1}{\kappa^2}\Delta\right)^{-1}K(x)$$
$$=\frac{4\pi}{\kappa^2}\left(1+\frac{1}{\kappa^2}\Delta+\frac{1}{\kappa^4}\Delta\Delta+\cdots\right)K(x),$$

which corresponds to a development in increasing powers of $(\kappa a)^{-1}$ in the resulting integrals. The leading term gives [see (23)]

$$\frac{1}{4\pi}\int(\nabla \mathrm{X})^2dV=\frac{4\pi}{\kappa^4}\int(\nabla K)^2dV=\frac{3}{\kappa^4}N.$$

Hence we get, using $N=\alpha a^{-5}$ (with a numerical factor α depending on the shape of the source function)

$$\frac{1}{4\pi}\int(\nabla \mathrm{X})^2dV=3\alpha(\kappa a)^{-4}a^{-1},$$
$$\frac{\Delta E}{\mu c^2}=\frac{1}{\alpha}\frac{(\kappa a)^5}{g^2}\{j(j+1)-\tfrac{3}{4}\}\ \text{for}\ \kappa a\gg 1. \quad (80b)$$

We have now to consider the various terms neglected and the conditions which are implied by such procedures. In the first place, we neglected terms in the Hamiltonian which had as factors τ_r, σ_r, since these had no diagonal matrix elements for the system of states chosen, but introduced coupling between them. In order of magnitude, such terms are given by

$$h\sim\frac{\kappa^2}{g^2}\left[\int(\nabla \mathrm{X})^2dV\right]^{-1}.$$

For small sources ($\kappa a\ll 1$) we get from (80a)

$$h\sim\kappa^2 a/g^2.$$

The energy of separation between the states of (62) is of the order g^2I/κ^2. An evaluation of the

integral I, defined by (14), shows that in the limit $\kappa a \ll 1$, $I \sim 1/a^3$. Consequently, if we demand that h be small compared with the energy of separation we get

$$\kappa a/g \ll 1. \tag{81}$$

The second approximation was introduced in (70) and (72) when $q^{(1)}_{\alpha\beta}$ was treated as small compared to D; we restricted ourselves at this point to small oscillations of the field about its position of equilibrium. This restriction is not necessarily essential to the strong coupling hypothesis, but was introduced for mathematical simplicity. If it failed, the isobar energy (80) would have had a more complicated dependence on the angular momentum quantum number j. We estimate the validity of the approximation by computing $\langle (q^{(1)}_{\alpha\beta})^2 \rangle_H / D^2$; we do this for the case where no free mesons are present, so that the only contribution to $\langle (q^{(1)}_{\alpha\beta})^2 \rangle_H$ comes from the zero-point oscillations of the field. We find for small sources

$$\langle (q^{(1)}_{\alpha\beta})^2 \rangle_H \sim a^{-4} \text{ for } \kappa a \ll 1.$$

In the same limit $D = gI/\kappa \sim g/\kappa a^3$. Once again, the criterion proves to be

$$\kappa a/g \ll 1.$$

Finally, we consider the unitary transformation (78). To the first order, its effect was simply to shift $\pi_\alpha'(x)$ according to (75) in such a way as to separate the Hamiltonian completely into a bound part and a part (77) associated with unbound mesons. However, higher order terms in (78) spoil this separation; they give a dependence of the isobar energy on the distribution of free mesotrons, or conversely a dependence of the scattering of mesotrons on the isobaric state. They make possible such processes as the transition from one isobaric state to another with the inelastic scattering of mesons. If we demand that the ratio of these terms to the isobar separation be small (i.e., that the half-width of the isobaric states be small compared to their separation), we arrive at the condition

$$\int \frac{\partial \xi}{\partial x_k} \varphi_\alpha'(x) dV \Big/ \int \left(\frac{\partial \xi}{\partial x}\right)^2 dV \ll 1. \tag{82}$$

Again we substitute for φ_α' values corresponding to the zero-point oscillation of the unbound meson field. Evaluating the expressions in the small source limit, we find[17]

$$\frac{(\kappa a)^2 \ln \kappa a}{g^2} \ll 1. \tag{83}$$

For $\kappa a < 1$, this condition is certainly fulfilled for values of g large enough to satisfy (81). For comparison we give the preceding expressions in the large source limit ($\kappa a \gg 1$):

$$h \sim \kappa^6 a^5/g^2, \quad I \sim 1/\kappa^2 a^5, \quad D \sim g/\kappa^3 a^5,$$
$$\langle (q^{(1)}_{\alpha\beta})^2 \rangle_H \sim 1/\kappa a^5.$$

Condition (81) for the first and second neglects is replaced by

$$(\kappa a)^5/g^2 \ll 1. \tag{81a}$$

Inequality (81a) also expresses the validity of (82) for this limit.

7. THE SCATTERING OF FREE MESONS

As mentioned already, in this paper we treat the scattering with disregard of all terms of order D^{-2} which means that we do not distinguish between elastic and inelastic scattering. Our treatment of the problem therefore will give us the total scattering cross section. Omitting the irrelevant self-energy constant, we can use here the Hamiltonian (77) directly, where the difference between $\pi_\alpha'(x)$ and $\pi_\alpha''(x)$ can be disregarded. The quantities $\mathbf{e}_\alpha$ or $e_{\alpha k}$ can be treated here as c numbers for they commute with all other observables in the Hamiltonian.[18] It is convenient to go back from the variables in (77) with the help of (16), (16′), (70), (72), to the functions

$$p_\alpha(x) = (4\pi)^{\frac{1}{2}} \sum_{i,\beta} \overset{0}{p}_{\alpha\beta} e_{\beta i} \frac{\partial K}{\partial x_i} + \pi_\alpha'(x)$$
$$= \pi_\alpha(x) - \frac{1}{2D} \sum_{\beta,k} e_{\beta k} L_0{}^{\alpha\beta} \frac{\partial K}{\partial x_k}, \tag{84}$$

$$q_\alpha(x) = 1/(4\pi)^{\frac{1}{2}} \sum_{i,\beta} q^{(1)}_{\alpha\beta} e_{\beta i} (\partial \xi/\partial x_i) + \varphi_\alpha'(x)$$
$$= \varphi_\alpha(x) - 1/(4\pi)^{\frac{1}{2}} \textstyle\sum_k e_{\alpha k} (\partial \xi/\partial x_k). \tag{85}$$

[17] The condition from which (82) was derived also restricts the values of j for which the approximation holds. We find $j \ll g/\kappa a$.

[18] If, on the other hand, one uses a matrix representation where $\overset{0}{T}_{12}$, $\overset{0}{L}_{12}$, and $L_0{}^2$ are diagonal, the e_{ak} are matrices which are a generalization of the rotator matrices already used by Heitler and Ma (reference 8).

We see that $p_\alpha(x)$, $q_\alpha(x)$ represents a field of free mesons, the meson eigenfield of the nucleon being subtracted. It fulfills the commutation relations [see (21), (55)]

$$i[p_\alpha(\mathbf{x}_1), q_\beta(\mathbf{x}_2)]=\delta_{\alpha\beta}\delta(\mathbf{x}_1-\mathbf{x}_2)$$
$$-\tfrac{1}{2}\sum_k \frac{\partial K}{\partial x_{1k}}\frac{\partial \xi}{\partial x_{2k}}\delta_{\alpha\beta}+\tfrac{1}{2}\sum_{i,k} e_{\alpha k}e_{\beta i}\frac{\partial K}{\partial x_{1i}}\frac{\partial \xi}{\partial x_{2k}}. \quad (86)$$

These relations correspond to the fact that the symmetry of the $q^{(1)}_{\alpha\beta}$ and $p^{0}_{\alpha\beta}$ makes the field $p_\alpha(x)$, $q_\alpha(x)$ fulfill the subsidiary conditions [compare (12), (12′)]

$$\sum_k \left\{e_{\alpha k}\int \frac{\partial \xi}{\partial x_k}p_\beta dV-e_{\beta k}\int \frac{\partial \xi}{\partial x_k}p_\alpha dV\right\}=0, \quad (87a)$$

$$\sum_k \left\{e_{\alpha k}\int \frac{\partial K}{\partial x_k}q_\beta dV-e_{\beta k}\int \frac{\partial K}{\partial x_k}q_\alpha dV\right\}=0. \quad (87b)$$

On the other hand, the Hamiltonian (77) becomes formally a Hamiltonian for free plane waves

$$H=\tfrac{1}{2}\sum_\alpha \int p_\alpha^2 dV+\tfrac{1}{2}\sum_\alpha \int q_\alpha(-\Delta+k^2)q_\alpha dV. \quad (88)$$

The fact that the equations of motion differ from the wave equation of free particles is entirely due to the symmetry conditions or to the difference of the commutation relations (86) from the usual canonical ones.[19]

From (87a, b) and (88) we get, by the method of Lagrangian multipliers which have here the form of antisymmetric constants $\lambda_{\alpha\beta}=-\lambda_{\beta\alpha}$ and $\lambda'_{\alpha\beta}=-\lambda_{\beta\alpha}$, the equations of motion

$$\dot{q}_\alpha=p_\alpha-\sum_{\beta,k}\lambda_{\alpha\beta}e_{\beta k}(\partial\xi/\partial x_k),$$
$$-\dot{p}_\alpha=(-\Delta+k^2)q_\alpha-\sum_{\beta,k}\lambda'_{\alpha\beta}e_{\beta k}(\partial K/\partial x_k).$$

With the help of the time derivatives of (87a), (87b) in which one has to insert the expressions for $\dot{q}_\alpha$, $\dot{p}_\alpha$ one gets

$$\lambda_{\alpha\beta}=\tfrac{1}{2}\sum_k \int (p_\alpha e_{\beta k}-p_\beta e_{\alpha k})\frac{\partial K}{\partial x_k}dV, \quad \lambda'_{\alpha\beta}=0.$$

Therefore we get the equations of motion in the form

$$\dot{q}_\alpha=p_\alpha-\tfrac{1}{2}\sum_{i,k,\beta} e_{\beta k}\frac{\partial \xi}{\partial x_k}\times\int (p_\alpha e_{\beta i}-p_\beta e_{\alpha i})\frac{\partial K}{\partial x_i}dV, \quad (89a)$$

$$-\dot{p}_\alpha=(-\Delta+k^2)q_\alpha. \quad (89b)$$

The same equations follow from (86) with the help of the relation $\dot{f}=i[H,f]$ for $f=p_\alpha$ and $f=q_\alpha$.

If we first consider q_α, p_α as classical quantities, we can integrate (89a, b) by putting

$$p_\alpha=\dot{u}_\alpha, \quad q_\alpha=u_\alpha-\tfrac{1}{2}\sum_{i,k,\beta} e_{\beta k}\frac{\partial \xi}{\partial x_k}\times\int (u_\alpha e_{\beta i}-u_\beta e_{\alpha i})\frac{\partial K}{\partial x_i}dV, \quad (90)$$

where u_α has, according to (89b), to fulfill the wave equation

$$\left(-\Delta+k^2+\frac{\partial^2}{\partial t^2}\right)u_\alpha=\frac{4\pi}{2I}\sum_{i,k,\beta} e_{\beta k}\frac{\partial K}{\partial x_k}\times\int (u_\alpha e_{\beta i}-u_\beta e_{\alpha i})\frac{\partial K}{\partial x_i}dV \quad (91)$$

and the subsidiary condition

$$\sum_k \left\{e_{\beta k}\int \frac{\partial \xi}{\partial x_k}u_\alpha dV-e_{\alpha k}\int \frac{\partial \xi}{\partial x_k}u_\beta dV\right\}=0. \quad (91a)$$

This condition is, however, not independent of the wave Eq. (91), for the second time derivative of (91a) vanishes as a consequence of (91). The subsidiary condition essentially excludes only the static solution

$$u_\alpha{}^0=\sum_k e_{\alpha k}\frac{\partial \xi}{\partial x_k} \text{ of (91).}$$

The quantum-theoretical formalism leads to an analogous result. Let $u_\alpha{}^{(n)}$ be a normalized orthogonal set of functions (c numbers), which fulfill (with the usual boundary conditions in a hole)

$$(-\Delta+k^2-\omega_n{}^2)u_\alpha{}^{(n)}=\frac{4\pi}{2I}\sum_{i,k,\beta} e_{\beta k}\frac{\partial K}{\partial x_k}\times\int (u_\alpha{}^{(n)}e_{\beta i}-u_\beta{}^{(n)}e_{\alpha i})\frac{\partial K}{\partial x_i}dV, \quad (91b)$$

[19] The analogous result in the charged scalar theory was first obtained by J. Schwinger.

and the subsidiary condition (91a). We put

$$p_\alpha=\sum_n A_n u_\alpha^{(n)}\left(\frac{\omega_n}{2}\right)^{\frac{1}{2}}, \tag{92}$$

$$q_\alpha=\sum_n A_n(2\omega_n)^{-\frac{1}{2}}\Big\{u_\alpha^{(n)}-\frac{1}{2}\sum_{i,k,\beta}e_{\beta k}\frac{\partial\xi}{\partial x_k}\times\int(u_\alpha^{(n)}e_{\beta i}-u_\beta^{(n)}e_{\alpha i})\frac{\partial K}{\partial x_i}dV\Big\},$$

$$A_{-n}=A_n{}^+,\quad u_\alpha^{(-n)}=u_\alpha^{(n)*},\quad \omega_{-n}=\omega_n>0. \tag{92a}$$

If we assume

$$[A_n,\ A_m{}^+]=[A_n,\ A_{-m}]=\delta_{nm}, \tag{93}$$

we get just the commutation relation (86), the system $u_\alpha^{(n)}$ being incomplete because, as a result of (91a), the static solution $u_\alpha{}^0=\sum_k e_{\alpha k}(\partial\xi/\partial x_k)$ is missing. Moreover, the Hamiltonian (77) assumes the normal form

$$H=\textstyle\sum_n \omega_n(A_n{}^+A_n+\frac{1}{2}). \tag{94}$$

Our scattering problem is therefore reduced to the determination of the solution of (91) [or, aside from a factor $\exp(-i\omega t)$, of (91b)] which describes a plane wave incident in a given direction and an outgoing scattered wave. Corresponding to the three pseudoscalar fields u_α ($\alpha=1,\ 2,\ 3$) we shall get three linear independent solutions $u_\alpha^{(\rho)}$ or $u_\alpha^{(1)}$, $u_\alpha^{(2)}$, $u_\alpha^{(3)}$ of this problem, which correspond to an incident particle with $\rho=1$, $\rho=2$, or $\rho=3$.

Instead of this we can also use the solutions

$$u_\alpha{}^+=(1/\sqrt{2})(u_\alpha^{(1)}+iu_\alpha^{(2)}),$$

$$u_\alpha{}^-=(1/\sqrt{2})(u_\alpha^{(1)}-iu_\alpha^{(2)}),\ u_\alpha^{(3)},$$

which correspond to an incident positive or negative charged or neutral particle.

We now solve (91b) by the assumption

$$u_\alpha^{(\rho)}(x)=\delta_{\alpha\rho}\exp[ik(\mathbf{n}\cdot\mathbf{x})]+A\sum_{i,k}(\delta_{\alpha\rho}n_k-e_{\alpha i}e_{\rho k}n_i)\frac{\partial}{\partial x_k}\times\int K(x')\frac{e^{ikr}}{r}dV'. \tag{95}$$

Here $\rho=1,\ 2,\ 3$ enumerates the three different solutions, $\mathbf{n}$ is a unit vector in the direction of the incident wave, $k=(\omega^2-\kappa^2)^{\frac{1}{2}}$, and the constant A has to be determined. The first part, the plane wave, fulfills the wave equation for free particles without the right side of (91) while the scattered wave and therefore the whole expression (95) fulfills the equation

$$-(\Delta+k^2)u_\alpha^{(\rho)}=4\pi A\sum_{i,k}(\delta_{\alpha\rho}n_k-e_{\alpha i}e_{\rho k}n_i)(\partial K/\partial x_k). \tag{95'}$$

In order to check (91b) we introduce the abbreviations

$$\int K(x)\exp[ik(\mathbf{n}\cdot\mathbf{x})]dV=\int K(x)\frac{\sin kR}{kR}dV=F, \tag{96}$$

(where $R=|\mathbf{x}|$, $r=|\mathbf{x}-\mathbf{x}'|$)

$$\int\int\frac{\partial K(x)}{\partial x_i}\frac{\cos kr}{r}\frac{\partial K(x')}{\partial x_k'}dVdV'=\delta_{ik}J. \tag{97}$$

Further we have to evaluate the integral

$$\int\int\frac{\partial K(x)}{\partial x_i}\frac{\sin kr}{r}\frac{\partial K(x')}{\partial x_k'}dVdV'=\frac{1}{3}\int\int K(x)\left(-\Delta\frac{\sin kr}{r}\right)K(x')dVdV'=\frac{k^2}{3}\int\int K(x)\frac{\sin kr}{r}K(x')dVdV'.$$

But as a consequence of the fact that $\sin kr/kr$ has no singularity for $x=0$, $\int(\sin kr/r)K(x')dV'$ is a solution of the wave equation $(\Delta+k^2)u=0$, and therefore

$$\int(\sin kr/r)K(x')dV'=(\sin kR/R)C.$$

Moreover, $C=F$ because for $R=0$ the left side of the equation is equal to kF, the right side equal to kC. Therefore

$$\int\int\frac{\partial K(x)}{\partial x_i}\frac{\sin kr}{r}\frac{\partial K(x')}{\partial x_k'}dVdV'=\delta_{ik}\frac{k^3}{3}F^2, \tag{98}$$

and finally

$$\int\int\frac{\partial K(x)}{\partial x_i}\frac{e^{ikr}}{r}\frac{\partial K(x')}{\partial x_k}dVdV'=\delta_{ik}\left(J+i\frac{k^3}{3}F^2\right). \tag{99}$$

With the assumption (95) we get

$$\sum_k \int (e_{\beta k} u_\alpha^{(\rho)} - e_{\alpha k} u_\beta^{(\rho)}) \frac{\partial K}{\partial x_k} dV$$
$$= \sum_k (\delta_{\rho\alpha} e_{\beta k} n_k - \delta_{\rho\beta} e_{\alpha k} n_k) \times \left\{ -ikF + 2A\left(J + \frac{ik^3}{3}F^2\right)\right\}.$$

The differential Eq. (89b) therefore gives

$$-(\Delta + k^2) u_\alpha^{(\rho)} = \frac{4\pi}{2I}\left\{\sum_{i,k} (n_k \delta_{\alpha\rho} - e_{\rho k} e_{\alpha i} n_i) \frac{\partial K}{\partial x_k}\right\} \times \left\{ -ikF + 2A\left(J + \frac{ik^3}{3}F^2\right)\right\},$$

and the comparison with (95′) gives

$$IA = -\frac{ikF}{2} + A\left(J + \frac{ik^3}{3}F^2\right), \qquad A = \frac{ikF/2}{J - I + \frac{ik^3}{3}F^2}. \tag{100}$$

Introducing

$$\tan\delta = \frac{k^3}{3}F^2 \Big/ (J - I), \qquad \sin\delta = \frac{k^3}{3}F^2 \Big/ \left[(J-I)^2 + \left(\frac{k^3}{3}F^2\right)^2\right]^{\frac{1}{2}}, \tag{101}$$

we get

$$A = (3i/2k^2F)\sin\delta e^{i\delta}. \tag{100′}$$

We get the asymptotic behavior of the scattered wave for very large r in the direction $\mathbf{n}_s$ of the scattered wave by putting $r = R - ik(\mathbf{n}_s \cdot \mathbf{x})$, $\nabla = -ik\mathbf{n}_s$,

$$[u_\alpha^{(\rho)}(x)]_{\text{scatt}} \sim ikFA[\delta_{\rho\alpha}(\mathbf{n}\cdot\mathbf{n}_s) - (\mathbf{e}_\alpha\cdot\mathbf{n})(\mathbf{e}_\rho\cdot\mathbf{n}_s)](e^{ikR}/R). \tag{102}$$

We now compute the square of this amplitude for a given $\mathbf{n}_s$ and sum over α,

$$\sum_\alpha [u_\alpha^{(\rho)}(x)]^2_{\text{scatt}} = k^2F^2A^2[(\mathbf{n}\cdot\mathbf{n}_s)^2 - 2(\mathbf{n}\cdot\mathbf{n}_s)(\mathbf{e}_\rho\cdot\mathbf{n})(\mathbf{e}_\rho\cdot\mathbf{n}_s) + (\mathbf{e}_\rho\cdot\mathbf{n}_s)^2].$$

Further, we take the average over-all directions of the axis system $\mathbf{e}_\alpha$ and get for the right side,[20] with $\cos\theta = (\mathbf{n}\cdot\mathbf{n}_s)$, θ being the scattering angle

$$(kFA)^2\tfrac{1}{3}(1+\cos^2\theta).$$

[20] This is in the approximation where the energy loss of the meson in the scattering is disregarded, the same as averaging over-all directions of the angular momentum L_{ik}^0 in the initial and in the final states.

This is the cross section dq for the solid angle $d\Omega = 2\pi\sin\theta d\theta$; inserting (100′) we get

$$dq = \frac{\sin^2\delta}{k^2}\frac{3}{4}(1+\cos^2\theta)d\Omega, \tag{103}$$

and the total cross section

$$q = (\sin^2\delta/k^2)4\pi. \tag{104}$$

On the other hand, if we integrate the square of the amplitude over all angles θ, which means averaging over $\mathbf{n}_s$ without summation over α, we get

$$(kFA)^2\tfrac{1}{3}[\delta_{\alpha\rho} - 2\delta_{\alpha\rho}(\mathbf{e}_\rho\cdot\mathbf{n}) + (\mathbf{e}_\alpha\cdot\mathbf{n})^2].$$

Averaging over the orientations of the axis system gives

$$(kFA)^2\tfrac{1}{3}(\delta_{\alpha\rho}+1)$$

which means

$$q_\alpha = 4\pi(\sin^2\delta/k^2)\tfrac{1}{4}(1+\delta_{\alpha\rho}). \tag{105}$$

In other words, if the incident particle is a "1 particle" the number of scattered "1 particles," "2-particles," and "3-particles" is $\frac{1}{2}$, $\frac{1}{4}$, $\frac{1}{4}$. This also holds if one takes for "1," "2," "3" *in any order, neutral, positive, and negative* as can be shown by using the above-mentioned eigenfunctions

$$u_\alpha^+ = (1/\sqrt{2})(u_\alpha^{(1)} + iu_\alpha^{(2)}),$$
$$u_\alpha^- = (1/\sqrt{2})(u_\alpha^{(1)} - iu_\alpha^{(2)})$$

as well as $u_\alpha^{(3)}$.

Finally we evaluate the integrals J, I, and F for the physically important case $ka \ll 1$, $\kappa a \ll 1$. In this case we can first put $F = 1$. Further we have, according to (97),

$$3J = \int\int K(x)[(-\Delta)(\cos kr/r)]K(x')dVdV' = 4\pi\int K^2(x)dV + k^2\int\int K(x)(\cos kr/r)K(x')dVdV'.$$

In the same way

$$3I = \int\int K(x)\left[(-\Delta)\frac{e^{-\kappa r}}{r}\right]K(x')dVdV' = 4\pi\int K^2(x)dV - \kappa^2\int\int K(x)\frac{e^{-\kappa r}}{r}K(x')dVdV'.$$

Therefore

$$3(J-I)=\int\int K(x)(k^2\cos kr+\kappa^2 e^{-\kappa r})\times\frac{1}{r}K(x')dVdV'. \quad (106)$$

So far this result is exact, but for $ka\ll 1$, $\kappa a\ll 1$ we can substitute 1 for $\cos kr$ and $e^{-\kappa r}$ and get, with $\omega^2=k^2+\kappa^2$

$$3(J-I)=\omega^2/a \quad \text{for} \quad ka\ll 1, \quad \kappa a\ll 1, \quad (106')$$

hence

$$\sin\delta\sim\tan\delta\sim(k^3a/\omega^2)$$

and for (103), (104) we get finally on writing $v/c=p/E$ for k/ω

$$\left.\begin{aligned} dq&=\left(\frac{p}{E}\right)^4 a^2\tfrac{3}{4}(1+\cos^2\theta)d\Omega \\ q&=\left(\frac{p}{E}\right)^4 a^2 4\pi \end{aligned}\right\} ka\ll 1, \kappa a\ll 1, \quad (107)$$

which was quoted in the second section.

8. THE CHARGED PSEUDOSCALAR THEORY

Although the symmetrical theory is, from a mathematical standpoint, more elegant than the "charged pseudoscalar theory" which uses only positive and negative charged, but no neutral, mesons, it is also of interest to develop the corresponding results for the latter theory, because neutral mesons have never been observed and because in the case of strong coupling the charged theory also leads to forces between two like particles.

With a complex pseudoscalar field φ the Hamiltonian of this theory can be written

$$H=\int dV\left\{\pi^*\pi+(\nabla\varphi^*)\cdot(\nabla\varphi)+\kappa^2\varphi^*\varphi-\frac{g}{\kappa}(4\pi)^{\frac{1}{2}}K(x)(\nabla\varphi\cdot\tau_+\boldsymbol{\sigma}+\nabla\varphi^*\cdot\tau_-\boldsymbol{\sigma})\right\}, \quad (108)$$

where

$$\tau_+=\tfrac{1}{2}(\tau_1+i\tau_2), \quad \tau_-=\tfrac{1}{2}(\tau_1-i\tau_2). \quad (109)$$

In order to facilitate the comparison with the symmetrical theory we split π and φ into the real and imaginary parts which are normalized according to

$$\left.\begin{aligned} \pi&=\frac{1}{\sqrt{2}}(\pi_1+i\pi_2), \quad \varphi=\frac{1}{\sqrt{2}}(\varphi_1-i\varphi_2), \\ \pi^*&=\frac{1}{\sqrt{2}}(\pi_1-i\pi_2), \quad \varphi^*=\frac{1}{\sqrt{2}}(\varphi_1+i\varphi_2), \end{aligned}\right. \quad (110)$$

and get

$$H=\frac{1}{2}\sum_{\alpha=1}^{2}\left\{\int[\pi_\alpha^2+(\nabla\varphi_\alpha)^2+\kappa^2\varphi_\alpha^2]dV-\frac{g}{\kappa\sqrt{2}}(4\pi)^{\frac{1}{2}}\int K(x)\tau_\alpha\boldsymbol{\sigma}\cdot\nabla\varphi_\alpha dV\right\}. \quad (111)$$

We can therefore take over the whole development of Section 3 if we simply drop the field components π_3, φ_3 and let the summation index α take only the values $\alpha=1, 2$. Of course there exists as an integral of motion only the T_{12} component of the isotopic spin in this theory, which gives the electric charge minus $\frac{1}{2}$.

The determination of the eigenvalue of the interaction energy

$$H_{\text{int}}=\frac{g}{\kappa\sqrt{2}}\sum_{k=1}^{3}(\tau_1\sigma_k\overset{0}{\varphi}_{1k}+\tau_2\sigma_k\overset{0}{\varphi}_{2k})$$

here is somewhat simpler than in the case of the symmetrical theory. Computing the square of the interaction energy, we get,

$$[\tau_1(\boldsymbol{\sigma}\cdot\boldsymbol{\phi}_1^0)+\tau_2(\boldsymbol{\sigma}\cdot\boldsymbol{\phi}_2^0)]^2=(\boldsymbol{\phi}_1^0)^2+(\boldsymbol{\phi}_2^0)^2-2\tau_3(\boldsymbol{\sigma}\cdot[\boldsymbol{\phi}_1^0,\boldsymbol{\phi}_2^0]).$$

The four eigenvalues of the interaction energy are therefore

$$\begin{aligned} E_{\text{int}}&=\pm\frac{g}{\kappa\sqrt{2}}\{(\boldsymbol{\phi}_1^0)^2+(\boldsymbol{\phi}_2^0)^2\pm|[\boldsymbol{\phi}_1^0,\boldsymbol{\phi}_2^0]|\}^{\frac{1}{2}} \\ &=\pm\frac{g}{\kappa\sqrt{2}}\{(\boldsymbol{\phi}_1^0)^2+(\boldsymbol{\phi}_2^0)^2\pm 2[(\boldsymbol{\phi}_1^0)^2(\boldsymbol{\phi}_2^0)^2-(\boldsymbol{\phi}_1^0\cdot\boldsymbol{\phi}_2^0)^2]^{\frac{1}{2}}\}^{\frac{1}{2}}, \end{aligned} \quad (112)$$

with all possible combinations of the + and − signs.

The application of the formalism of Section 4 leads here to the case where one of the eigenvalues Q of (C) [Eq. (30)] or (C') [Eq. (30')] is zero because $\overset{0}{\varphi}_{3i}\equiv 0$. The matrix C' has therefore only two rows and two columns and is

given by

$$C'=\begin{pmatrix}(\boldsymbol{\phi}_1^0)^2 & (\boldsymbol{\phi}_1^0\cdot\boldsymbol{\phi}_2^0)\\ (\boldsymbol{\phi}_1^0\cdot\boldsymbol{\phi}_2^0) & (\boldsymbol{\phi}_2^0)^2\end{pmatrix}$$

and Q_1^2, Q_2^2 are the roots of the equation

$$\{(\boldsymbol{\phi}_1^0)^2-x\}\{(\boldsymbol{\phi}_2^0)^2-x\}-(\boldsymbol{\phi}_1^0\cdot\boldsymbol{\phi}_2^0)^2=0,$$

which gives

$$Q_{1,2}=\frac{1}{\sqrt{2}}\{(\boldsymbol{\phi}_1^0)^2+(\boldsymbol{\phi}_2^0)^2\pm[(\boldsymbol{\phi}_1^0)^2+(\boldsymbol{\phi}_2^0)^2-4((\boldsymbol{\phi}_1^0)^2(\boldsymbol{\phi}_2^0)^2-(\boldsymbol{\phi}_1^0\cdot\boldsymbol{\phi}_2^0)^2)]^{\frac{1}{2}}\}^{\frac{1}{2}}. \quad (113)$$

The expression (36) for the interaction energy

$$E_{\text{int}}=\frac{g}{\kappa\sqrt{2}}(\pm Q_1\pm Q_2) \quad (112')$$

is in agreement with (112). The orthogonal matrix $B_{r\alpha}$ has here only two rows and two columns and can be assumed as

$$B_{r\alpha}=\begin{pmatrix}\cos\theta & \sin\theta\\ -\sin\theta & \cos\theta\end{pmatrix}. \quad (114)$$

If we write $\mathbf{n}^{(r)}$ for A_{kr} the normal form (29) for $\overset{0}{\varphi}_{\alpha k}$ gives us

$$\begin{aligned}\boldsymbol{\phi}_1^0&=Q_1\cos\theta\mathbf{n}^{(1)}-Q_2\sin\theta\mathbf{n}^{(2)},\\ \boldsymbol{\phi}_2^0&=Q_1\sin\theta\mathbf{n}^{(1)}+Q_2\cos\theta\mathbf{n}^{(2)}.\end{aligned} \quad (115)$$

The significance of $\mathbf{n}^{(1)}$, $\mathbf{n}^{(2)}$ is therefore that $\mathbf{n}^{(3)}$ is orthogonal to the plane through $\boldsymbol{\phi}_1^0$ and $\boldsymbol{\phi}_2^0$ and the orientation of the $\mathbf{n}^{(1)}$, $\mathbf{n}^{(2)}$ axes which we may call for the moment the ξ and η axes is defined by the condition

$$\overset{0}{\varphi}_{1\xi}\overset{0}{\varphi}_{1\eta}+\overset{0}{\varphi}_{2\xi}\overset{0}{\varphi}_{2\eta}=0. \quad (116)$$

This can be immediately derived from (115) and means that the matrix C defined by (30) is diagonalized by going to the (ξ,η,ζ) axes, the diagonal matrix elements being Q_1, Q_2, 0.

In the Eqs. (45), (45′) we have to put

$$\overset{0}{\pi}_{3k}\equiv 0,\quad B_{3\alpha}\equiv 0,\quad B_{r3}\equiv 0 \text{ for } \alpha, r=1,2;\quad P_3\equiv 0;$$

hence

$$\sum_{\alpha=1,2}(\boldsymbol{\pi}_\alpha^0)^2=\sum_{r=1,2}P_r^+P_r+\frac{(L_0^{12}+T_0^{12})^2}{2(Q_1-Q_2)^2}+\frac{(L_0^{12}-T_0^{12})}{2(Q_1+Q_2)^2}+\sum_{r=1,2}\frac{(L_0^{r3})^2}{Q_r^2}. \quad (50c)^{21}$$

[21] We denote corresponding equations in the symmetric and charged theories with the same number and add in the latter a c.

The symmetrical quantities $\overset{0}{q}_{\alpha\beta}$, $\overset{0}{p}_{\alpha\beta}$ have to be defined only for $\alpha,\beta=1,2$ and according to (51) we get

$$\begin{aligned}\mathbf{e}^{(1)}&=\mathbf{n}^{(1)}\cos\theta-\mathbf{n}^{(2)}\sin\theta,\\ \mathbf{e}^{(2)}&=\mathbf{n}^{(1)}\sin\theta+\mathbf{n}^{(2)}\cos\theta,\\ \mathbf{e}^{(3)}&=\mathbf{n}^{(3)},\end{aligned} \quad (117)$$

and from (52)

$$\begin{aligned}\overset{0}{q}_{11}&=Q_1\cos^2\theta+Q_2\sin^2\theta,\\ \overset{0}{q}_{12}&=\overset{0}{q}_{21}=(Q_1-Q_2)\sin\theta\cos\theta,\\ \overset{0}{q}_{22}&=Q_1\sin^2\theta+Q_2\cos^2\theta.\end{aligned} \quad (118)$$

For the description of $\mathbf{n}^{(r)}$ and L_0^{rs} by Euler angles and their conjugate momenta, see Appendix.

For the minimum of the potential energy we get from (62) the old value (63) for $Q_1=Q_2=D$; but because $Q_3=0$ we now have

$$E_{\text{min}}^0=-\frac{D^2}{I}=-\frac{1}{2}\frac{g^2}{\kappa^2}I. \quad (63c)$$

In the approximation where $\overset{(1)}{q}_{\alpha\beta}$ is disregarded, we now get

$$\begin{aligned}L_0^{12}&=D\{(\mathbf{e}_\alpha\cdot\boldsymbol{\pi}_\beta^0)-(\mathbf{e}_\beta\cdot\boldsymbol{\pi}_\alpha^0)\},\\ L_0^{3\alpha}&=-L_0^{\alpha3}=D(\mathbf{e}_3\cdot\boldsymbol{\pi}_\alpha^0)\quad(\alpha=1,2).\end{aligned}$$

Therefore

$$\boldsymbol{\pi}_\alpha^0=\sum_{\beta=1,2}\left(\mathbf{e}_\beta\overset{0}{p}_{\alpha\beta}+\frac{1}{2D}\langle\mathbf{e}_\beta L_0^{\alpha\beta}\rangle_H\right)+\frac{1}{D}\mathbf{e}_3L_0^{\alpha3},$$

hence

$$\sum_\alpha(\boldsymbol{\pi}_\alpha^0)^2=\sum_{\alpha,\beta}(\overset{0}{p}_{\alpha\beta})^2+\frac{1}{2D^2}(L_0^{12})^2+\frac{1}{D^2}\sum_{\alpha=1,2}(L_0^{\alpha3})^2$$
$$=\sum_{\alpha,\beta}(\overset{0}{p}_{\alpha\beta})^2+\frac{1}{2D^2}[2L_0^2-(L_0^{12})^2].$$

This is in accordance with (50c) if we put in the last two terms $Q_1=Q_2=D$, $T_0^{12}=-L_0^{12}$. In (II) we have therefore to substitute $2L_0^2-(T_0^{12})^2$ for L_0^2.

In the same way we have to substitute in (75)

$$\frac{1}{2D}\{\sum_\beta e_{\beta i}L_0^{\alpha\beta}+2e_{3i}L_0^{\alpha3}\}\quad\text{for}\quad\frac{1}{2D}\sum_\beta e_{\beta i}L_0^{\alpha\beta}$$

and get instead of (76):

$$H=\frac{\kappa^2}{2g^2}\frac{4\pi}{\int(\partial X/\partial x)^2dV}[2L_0^2-(T_0^{12})^2]-\frac{1}{2}\frac{g^2}{\kappa^2}I+H_1 \quad (76c)$$

where H_1 is again given by (73), and instead of (80), (80a), (80b)

$$\Delta E=\frac{3}{2}\frac{\kappa^2}{g^2}\frac{4\pi}{\int(\nabla X)^2 dV}[2j(j+1)-n^2-5/4], \quad (80c)$$

$$\frac{\Delta E}{\mu c^2}=\frac{3}{2}\frac{\kappa a}{g^2}[2j(j+1)-n^2-5/4] \text{ for } \kappa a\ll 1, \quad (80ac)$$

$$\frac{\Delta E}{\mu c^2}=\frac{1}{\alpha}\frac{(\kappa a)^5}{g^2}[2j(j+1)-n^2-5/4] \text{ for } \kappa a\gg 1. \quad (80bc)$$

The restriction (74) $-j\leqq n\leqq j$ is of course unchanged.

In the computation of the scattering the following modifications of Section 7 take place. The functions $p_\alpha(x)$, $q_\beta(x)$ ($\alpha, \beta=1, 2$ only in the following) fulfill, besides (87a, b), the condition

$$\mathbf{e}_3\cdot\int\nabla K q_\alpha dV=0, \quad \mathbf{e}_3\cdot\int\nabla\xi p_\alpha dV=0, \quad (87c)$$

and the commutation relations (86) get a corresponding additional term:

$$i[p_\alpha(\mathbf{x}_1), q_\beta(\mathbf{x}_2)]=\delta_{\alpha\beta}\delta(\mathbf{x}_1-\mathbf{x}_2) -\frac{1}{2}\sum_k\frac{\partial K}{\partial x_{1k}}\frac{\partial\xi}{\partial x_{2k}}\delta_{\alpha\beta}+\frac{1}{2}\sum_{i,k}e_{\alpha k}e_{\beta i}\frac{\partial K}{\partial x_{1i}}\frac{\partial\xi}{\partial x_{2k}} -\delta_{\alpha\beta}\frac{1}{2}\sum_{i,k}e_{3i}e_{3k}\frac{\partial K}{\partial x_{1i}}\frac{\partial\xi}{\partial x_{2k}}. \quad (86c)$$

With

$$p_\alpha=\dot{u}_\alpha,$$

$$q_\alpha=u_\alpha-\frac{1}{2}\sum_{i,k}\frac{\partial\xi}{\partial x_k}\int(u_\alpha\delta_{ik}+u_\alpha e_{3i}e_{3k} -\textstyle\sum_\beta u_\beta e_{\beta k}e_{\alpha i})\dfrac{\partial K}{\partial x_i}dV, \quad (90c)$$

we now get

$$\mathbf{e}_\beta\cdot\int\nabla\xi u_\alpha dV-\mathbf{e}_\alpha\cdot\int\nabla\xi u_\beta dV=0,$$

$$\mathbf{e}_3\cdot\int\nabla\xi u_\alpha dV=0, \quad (91c)$$

$$(-\Delta+\kappa^2-\omega^2)u_\alpha=\frac{4\pi}{2I}\sum_{i,k,\beta}\frac{\partial K}{\partial x_k} \times\int\{u_\alpha(\delta_{ik}+e_{3i}e_{3k})-u_\beta e_{\beta k}e_{\alpha i}\}\frac{\partial K}{\partial x_i}dV. \quad (91c)$$

The solution is

$$u_\alpha^{(\rho)}(x)=\delta_{\rho\alpha}\exp[ik(\mathbf{n}\cdot\mathbf{x})] +A\{\delta_{\rho\alpha}[(\mathbf{n}\cdot\nabla)+(\mathbf{n}\cdot\mathbf{e}_3)(\mathbf{e}_3\cdot\nabla)] -(\mathbf{n}\cdot\mathbf{e}_\alpha)(\mathbf{e}_\rho\cdot\nabla)\}\int K(x')\frac{e^{ikr}}{r}dV', \quad (95c)$$

where A is again given by (88), (89). Asymptotically for large R we have

$$[u_\alpha^{(\rho)}(x)]_{\text{Scatt.}}\sim ikFA[\delta_{\rho\alpha}(\mathbf{n}\cdot\mathbf{n}_s)+\delta_{\rho\alpha}(\mathbf{n}\cdot\mathbf{e}_3)(\mathbf{n}_s\cdot\mathbf{e}_3) -(\mathbf{n}\cdot\mathbf{e}_\alpha)(\mathbf{n}_s\cdot\mathbf{e}_\rho)]\frac{e^{ikR}}{R}.$$

$$\sum_{\alpha=1,2}|u_\alpha^{(\rho)}(x)|^2_{\text{Scatt.}}=(kFA)^2\{[(\mathbf{n}\cdot\mathbf{n}_s) +(\mathbf{n}\cdot\mathbf{e}_3)(\mathbf{n}_s\cdot\mathbf{e}_3)]^2-2(\mathbf{n}\cdot\mathbf{n}_s)(\mathbf{n}\cdot\mathbf{e}_\rho)(\mathbf{n}_s\cdot\mathbf{e}_\rho) -2(\mathbf{n}\cdot\mathbf{e}_3)(\mathbf{n}\cdot\mathbf{e}_\rho)(\mathbf{n}_s\cdot\mathbf{e}_3)(\mathbf{n}_s\cdot\mathbf{e}_\rho) +(\mathbf{n}_s\cdot\mathbf{e}_\rho)^2-(\mathbf{n}\cdot\mathbf{e}_3)^2(\mathbf{n}_s\cdot\mathbf{e}_\rho)^2\}.$$

The process of averaging over the directions of the axis system $\mathbf{e}_1$, $\mathbf{e}_2$, $\mathbf{e}_3$ gives (for any value of ρ, and for the solutions which correspond to an incident charged particle)

$$dq=(\sin^2\delta/k^2)\tfrac{3}{4}(1+3\cos^2\theta)d\Omega, \quad (103c)$$

$$q=(\sin^2\delta/k^2)\tfrac{3}{2}4\pi, \quad (104c)$$

where for $\sin^2\delta/k^2$ we can again substitute

$$\left(\frac{v}{c}\right)^4 a^2=\left(\frac{p}{E}\right)^4 a^2$$

if $ka\ll 1$, $\kappa a\ll 1$.

If the incident particle has a + charge, we find for the total cross section (integrating over all scattering angles) for scattering with the same (+) and the opposite (−) charge, respectively,

$$q_+=(\sin^2\delta/k^2)4\pi(5/4), \quad q_-=(\sin^2\delta/k^2)4\pi(1/4), \quad (105c)$$

the sum of both agreeing with (104c).

9. THE MAGNETIC MOMENT OF THE NUCLEON

The meson field surrounding the heavy particle gives rise to a magnetic moment which will prove to be of equal magnitude, but of opposite sign for the proton and neutron, just as in the case

of the weak coupling theory.[22] The results of this section are equally valid for the symmetrical and charged pseudoscalar theories, since the neutral mesons give no contribution to the magnetic moment.

The magnetic moment is related to the current density S by

$$M=\tfrac{1}{2}e\int[\mathbf{x}\cdot\mathbf{S}]dV \tag{119}$$

or, in tensor notation,

$$M_{ik}=-M_{ki}=\tfrac{1}{2}e\int[x_iS_k-x_kS_i]dV, \tag{119a}$$

e being the absolute value of the elementary electric charge. The definition of the charge and current densities S_0 and $\mathbf{S}$ becomes essentially ambiguous in a theory which uses finite distance operators, such as the source function $K(x)$. Indeed, in such a theory it is not possible to fulfill the continuity equation

$$\partial S_0/\partial t+\operatorname{div}\mathbf{S}=0 \tag{120}$$

everywhere inside the source. It is fulfilled outside the source, as well as (on the average) over a volume V of dimensions of order a in which the source is included.

$$\int_V[\partial S_0/\partial t+\operatorname{div}\mathbf{S}]dV=0. \tag{120a}$$

Expressions for S_0 and $\mathbf{S}$ which fulfill this weaker condition and which agree with the definition (9) of the total charge are given by

$$S_0=\varphi_1\pi_2-\varphi_2\pi_1+\tfrac{1}{2}(1+\tau_3)K(x), \tag{121}$$

$$\mathbf{S}=(\varphi_2\,\mathbf{grad}\,\varphi_1-\varphi_1\,\mathbf{grad}\,\varphi_2)+\frac{g}{\kappa}(2\pi)^{\frac{1}{2}}(\phi_1\tau_2-\phi_2\tau_1)\boldsymbol{\sigma}K(x).$$

To prove that these satisfy the conservation conditions, we make use of the relations

$$\left(-\Delta+\kappa^2+\frac{\partial^2}{\partial t^2}\right)\varphi_a+\frac{g}{\kappa}(2\pi)^{\frac{1}{2}}\tau_a(\boldsymbol{\sigma}\cdot\mathbf{grad}\,K)=0,$$

$$\frac{1}{2}\frac{\partial\tau_3}{\partial t}=-\frac{g}{\kappa}(2\pi)^{\frac{1}{2}}\boldsymbol{\sigma}\cdot\int(\tau_2\,\mathbf{grad}\,\varphi_1-\tau_1\,\mathbf{grad}\,\varphi_2)K(x)dV.$$

These follow from the general rule $\partial f/\partial t=i[H,f]$ and the commutation relations (2), (6) applied to the Hamiltonian given by (1), (8) with $f=\pi_a(X)$, $\phi_a(X)$, τ_3. We obtain

$$\frac{\partial S_0}{\partial t}+\operatorname{div}\mathbf{S}=-\boldsymbol{\sigma}\cdot[\tau_2\,\mathbf{grad}\,\varphi_1-\tau_1\,\mathbf{grad}\,\varphi_2]K(x)+K(X)\boldsymbol{\sigma}\cdot\int dV(\tau_2\,\mathbf{grad}\,\varphi_1-\tau_1\,\mathbf{grad}\,\varphi_2)K(x).$$

Therefore the continuity condition is fulfilled both for points outside the source, where $K(x)=0$, and on the average over the source as indicated by (120a). As a result of the lack of validity of the continuity equation inside the source, we may apply the assumed expression for the current density to the computation of the magnetic moment only if this moment is generated in a volume large compared with the dimensions of the source; in other words, we are restricted to small source size, $\kappa a\ll 1$.

Introducing the strong coupling approximation, we apply the S transformation (65a, b) to the second part of the current (121b); then we insert the values (68) for $\tau_r\sigma_s$, namely $\tau_r\sigma_s=-\delta_{rs}$. This gives

$$\mathbf{S}=(\varphi_2\,\mathbf{grad}\,\varphi_1-\varphi_1\,\mathbf{grad}\,\varphi_2)-\frac{g}{\kappa}(2\pi)^{\frac{1}{2}}(\varphi_1\mathbf{e}^{(2)}-\varphi_2\mathbf{e}^{(1)})K(x). \tag{122}$$

We insert for the field its value corresponding to the absence of free mesons and the lowest eigenvalue of the interaction energy, (16), (64).

$$\varphi_\alpha(x)=\frac{1}{(4\pi)^{\frac{1}{2}}}D\mathbf{e}^{(\alpha)}\cdot\operatorname{grad}\xi\quad(\alpha=1,2).$$

If now we use

$$D=\frac{g}{\kappa\sqrt{2}}I\ [\text{Eq. (63)}],\quad \xi=\frac{1}{I}\mathrm{X}\ \text{Eq. (15)},$$

$$\varphi_\alpha(x)=\frac{1}{(4\pi)^{\frac{1}{2}}}\frac{g}{\kappa\sqrt{2}}\mathbf{e}^{(\alpha)}\cdot\operatorname{grad}\mathrm{X}.$$

The current becomes

$$S_k=\frac{g^2}{2\kappa^2}\sum_{l,m=1}^{3}\left\{\frac{1}{4\pi}(e_l^{(1)}e_m^{(2)}-e_l^{(2)}e_m^{(1)})\frac{\partial^2\mathrm{X}}{\partial x_k\partial x_l}\frac{\partial\mathrm{X}}{\partial x_m}-(e_l^{(1)}e_k^{(2)}-e_l^{(2)}e_k^{(1)})\frac{\partial\mathrm{X}}{\partial x_l}K(x)\right\}$$

[22] H. Fröhlich, W. Heitler, and N. Kemmer, Proc. Roy. Soc. **A166**, 154 (1938). Their result, given in Eq. (63) of their paper, agrees formally (apart from a numerical factor) with our result, Eq. (124) below.

and the magnetic moment (119a) becomes

$$M_{ik}=\frac{e}{2}\frac{g^2}{2\kappa^2}\sum_{l,m=1}^{3}\Big\{\int dV\frac{1}{4\pi}(e_l^{(1)}e_m^{(2)}-e_l^{(2)}e_m^{(1)})\times\Big(x_i\frac{\partial^2\mathrm{X}}{\partial x_k\partial x_l}-x_k\frac{\partial^2\mathrm{X}}{\partial x_i\partial x_l}\Big)\frac{\partial\mathrm{X}}{\partial x_m}$$
$$-\int dV[e_l^{(1)}e_k^{(2)}-e_l^{(2)}e_k^{(1)})x_i-(e_l^{(1)}e_i^{(2)}-e_l^{(2)}e_i^{(1)})x_k]\frac{\partial\mathrm{X}}{\partial x_l}K(x)\Big\}. \quad (123)$$

The first volume integral is transformed by partial integration with respect to $\partial/\partial x_l$, half the terms vanishing in the sum over l and m. In the second integral one substitutes for $K(x)$ its expression $(4\pi)^{-1}(-\Delta+\kappa^2)\mathrm{X}$ taken from (13) and gets

$$4\pi\int x_i\frac{\partial\mathrm{X}}{\partial x_l}K(x)dV=\int x_i\frac{\partial\mathrm{X}}{\partial x_l}(-\Delta+\kappa^2)\mathrm{X}dV$$
$$=\tfrac{1}{2}\int dVx_i\frac{\partial}{\partial x_l}\mathrm{X}(-\Delta+\kappa^2)\mathrm{X}$$
$$+\tfrac{1}{2}\sum_r\int dVx_i\frac{\partial}{\partial x_r}\Big(\mathrm{X}\frac{\partial^2\mathrm{X}}{\partial x_l\partial x_r}-\frac{\partial\mathrm{X}}{\partial x_l}\frac{\partial\mathrm{X}}{\partial x_r}\Big)$$
$$=\tfrac{1}{2}\delta_{il}\int\mathrm{X}\Delta\mathrm{X}dV-\frac{\kappa^2}{2}\delta_{il}\int\mathrm{X}^2dV$$
$$+\tfrac{1}{2}\int\Big(\frac{\partial\mathrm{X}}{\partial x_l}\frac{\partial\mathrm{X}}{\partial x_i}-\mathrm{X}\frac{\partial^2\mathrm{X}}{\partial x_l\partial x_i}\Big)dV$$
$$=-\tfrac{1}{2}\delta_{il}\int(\mathbf{grad}\ \mathrm{X})^2dV-\frac{\kappa^2}{2}\delta_{il}\int\mathrm{X}^2dV+\int\frac{\partial\mathrm{X}}{\partial x_l}\frac{\partial\mathrm{X}}{\partial x_i}dV.$$

Using the spherical symmetry of X we have

$$\int\frac{\partial\mathrm{X}}{\partial x_i}\frac{\partial\mathrm{X}}{\partial x_l}dV=\tfrac{1}{3}\delta_{il}\int(\mathbf{grad}\ \mathrm{X})^2dV.$$

We get

$$M_{ik}=+\frac{e}{8\pi}\frac{g^2}{2\kappa^2}(e_i^{(1)}e_k^{(2)}-e_i^{(2)}e_k^{(1)})\times\Big[-\tfrac{1}{3}\int(\mathbf{grad}\ \mathrm{X})^2dV+\kappa^2\int\mathrm{X}^2dV\Big].$$

As was shown in Section 4 the second integral can be neglected for $\kappa a\ll 1$ while

$$\frac{1}{4\pi}\int(\mathbf{grad}\ \mathrm{X})^2dV=1/a.$$

Changing to vector notation and using $[\mathbf{e}^{(1)}\times\mathbf{e}^{(2)}]=\mathbf{e}^{(3)}$ we get the final result

$$\mathbf{M}=-\frac{e}{\kappa}\frac{g^2}{\kappa a}\frac{1}{12}\mathbf{e}^{(3)}. \quad (124)$$

We now compute the component of $\mathbf{M}$ in a fixed direction, say along the x_3 axis. We introduce a matrix representation for the $e_k^{(\alpha)}$, where $L_{12}^0\equiv L_3^0$, $(L_0)^2$, and $T_0^{12}=-L_0^{(3)}$ [cf. Eq. (73)] are diagonal with eigenvalues m, $j(j+1)$, and n, respectively, with $-j\leq m\leq j$ and $-j\leq n\leq j$. From the commutation relations (39), (55), (56) it follows that $L^{(3)}\equiv L^{12}$ commutes with all L_k and is therefore diagonal with respect to j, m, and L_k.

Moreover, $e^{(3)}$ commutes with $L^{(3)}$ and is therefore diagonal with respect to n. However, $e_3^{(3)}$ is not diagonal with respect to j and we need the diagonal element $(j, n, m|e_3^{(3)}|j, n, m)$.

We have the following relations:

$$(m|L_1+iL_2|m-1)=[(j+m)(j-m+1)]^{\frac{1}{2}},$$
$$(m|L_1-iL_2|m+1)=[(j+m-1)(j-m)]^{\frac{1}{2}}.$$

To satisfy the commutation relations [analogous to (38)] of $e_l^{(3)}$ with L_{ik}^0 we set

$$(j, m, n|e_3^{(3)}|j, m, n)=(j, n|C|j, n)m,$$
$$(j, m, n|e_1^{(3)}+ie_2^{(3)}|j, m-1, n)=(j, n|C|j, n)[(j+m)(j-m+1)]^{\frac{1}{2}},$$
$$(j, m, n|e_1^{(3)}-ie_2^{(3)}|j, m+1, n)=(j, n|C|j, n)[(j+m+1)(j-m)]^{\frac{1}{2}}.$$

Inserting this in the equation

$$-(\mathbf{L}\cdot\mathbf{e}^{(3)})=-\mathbf{L}^{(3)}=\mathbf{T}^{(3)}$$

we get

$$-(j, n|C|j, n)j(j+1)=n$$

or

$$-(j, m, n|e_3^{(3)}|j, m, n)=\frac{nm}{j(j+1)}.$$

Therefore, for a given isobar, we find that to the leading order

$$M_3=-\frac{e}{\kappa}\frac{g^2}{\kappa a}\frac{1}{12}\frac{nm}{j(j+1)}. \quad (125)$$

For the proton $n=m=j=\frac{1}{2}$, hence

$$M_3=\frac{e}{\kappa}\frac{g^2}{\kappa a}\frac{1}{36}. \tag{126}$$

For the neutron $n=-\frac{1}{2}$, hence M_3 simply changes sign, as was mentioned above.

If, for a first orientation, we identify this magnetic moment with the total empirical magnetic moment of the neutron—1.93 proton magnetons—and assume a meson mass equal to 1/10 proton mass ($e/\kappa=10$ proton magnetons), we find $g^2/\kappa a\sim 6.95$. Inserting the value of $\kappa a\sim 0.1$ determined from consideration of the scattering, we find $g^2\sim 0.695$, or $g/\kappa a\sim 8.3$, well within the range of the strong coupling approximation.

However, the fact that the proton and neutron magnetic moments are not of equal magnitude cannot be explained in any simple way in this theory. Of course, (126) does not give the total magnetic moment, but only the part due to the meson cloud. To it must be added the moment due to the nucleon itself.[23] If we assume that a "bare" proton or neutron would have a magnetic moment or one or zero proton magnetons, respectively, then we can compute the nucleon moment in the two lowest states by calculating the expectation value of

$$\mathbf{M}'=\frac{e\hbar}{m_p c}\frac{1}{2}(1+\tau_3)\boldsymbol{\sigma}. \tag{127}$$

In the weak coupling theory τ_3 is diagonal with the value $+\frac{1}{2}$ for the proton and $-\frac{1}{2}$ for the neutron, giving rise to the same values for the moment which were assumed for the bare core. However, in the strong coupling theory we have, after performing the S transformation,

$$\mathbf{M}'=-\frac{e}{m_p c}\frac{1}{2}\mathbf{e}^{(3)},$$

the expectation value of $\boldsymbol{\sigma}$ being zero. We compute the component of M' along the x_3 axis as before and get

$$M_3'=\frac{1}{2}\frac{nm}{j(j+1)}\frac{e}{m_p c}. \tag{128}$$

This moment, while small compared to the empirical moments of proton and neutron, is again equal in magnitude and opposite in sign for the two. For the two states $n=\pm\frac{1}{2}$, $m=j=\frac{1}{2}$

$$M_3'=\pm\tfrac{1}{6}\text{ proton magneton.}$$

APPENDIX

1. Introduction of Polar Angles

It is possible to express by means of Euler angles the orthogonal matrices (or, in other words, the three orthogonal-unit-vectors) introduced in Section 2. For instance, we can put

$$\begin{aligned}
A_{1k}&=\cos\theta\cos\varphi\cos\psi-\sin\varphi\sin\psi,\\
&\quad\cos\theta\sin\varphi\cos\psi+\cos\varphi\sin\psi,\quad -\sin\theta\cos\psi,\\
A_{2k}&=-\cos\theta\cos\varphi\sin\psi-\sin\varphi\cos\psi,\\
&\quad -\cos\theta\sin\varphi\sin\psi+\cos\varphi\cos\psi,\quad \sin\theta\sin\psi,\\
A_{3k}&=\sin\theta\cos\varphi,\quad \sin\theta\sin\varphi,\quad \cos\theta,
\end{aligned} \tag{1}$$

which means that the right side is the transposed matrix **A**. In the same way we put for the matrix

$$\begin{aligned}
B_{1\alpha}&=\cos\Theta\cos\Phi\cos\Psi-\sin\Phi\sin\Psi,\\
&\quad\cos\Theta\sin\Phi\cos\Psi+\cos\Phi\sin\Psi,\quad -\sin\Theta\cos\Psi,\\
B_{2\alpha}&=-\cos\Theta\cos\Phi\sin\Psi-\sin\Phi\cos\Psi,\\
&\quad -\cos\Theta\sin\Phi\sin\Psi+\cos\Phi\cos\Psi,\quad \sin\Theta\sin\Psi,\\
B_{3\alpha}&=\sin\Theta\cos\Phi,\quad \sin\Theta\sin\Phi,\quad \cos\Theta
\end{aligned} \tag{2}$$

and for the e_{ak} defined by (51)

$$\begin{aligned}
e_{1k}&=\cos a\cos b\cos c-\sin b\sin c,\\
&\quad\cos a\sin b\cos c+\cos b\sin c,\quad -\sin a\cos c,\\
e_{2k}&=-\cos a\cos b\sin c-\sin b\cos c,\\
&\quad -\cos a\sin b\sin c+\cos b\cos c,\quad \sin a\sin c,\\
e_{3k}&=\sin a\cos b,\quad \sin a\sin b,\quad \cos a.
\end{aligned} \tag{3}$$

Defining the operators p_θ, p_φ, p_ψ simply by $p_\theta=-i\partial/\partial\theta$, $p_\varphi=-i\partial/\partial\varphi$, $p_\psi=-i\partial/\partial\psi$, we find from the volume element $\sin\theta d\theta d\varphi d\psi$ that p_φ, p_ψ are Hermitian, but

$$p_\theta^\dagger=(\sin\theta)^{-1}p_\theta\sin\theta;$$

similar expressions are found for $p_\Theta^\dagger$, $p_a^\dagger$.

A direct evaluation of the angular momentum operators gives

$$\begin{aligned}
L_1\equiv L_{23}&=-\sin\varphi p_\theta+(\cos\varphi/\sin\theta)(p_\psi-\cos\theta p_\varphi)\\
&=-p_\theta^\dagger\sin\varphi+(p_\psi-p_\varphi\cos\theta)(\cos\varphi/\sin\theta),\\
L_2\equiv L_{31}&=\cos\varphi p_\theta+(\sin\varphi/\sin\theta)(p_\psi-\cos\theta p_\varphi)\\
&=p_\theta^\dagger\cos\varphi+(p_\psi-p_\varphi\cos\theta)(\sin\varphi/\sin\theta),\\
L_3\equiv L_{12}&=p_\varphi,
\end{aligned} \tag{4}$$

and also

$$\begin{aligned}
L_1\equiv L_{23}&=-\sin b p_a+(\cos b/\sin a)(p_c-\cos a p_b)\\
&=-p_a^\dagger\sin b+(p_c-p_b\cos a)(\cos b/\sin a),\\
L_2=L_{31}&=\cos b p_a+(\sin b/\sin a)(p_c-\cos a p_b)\\
&=p_a^\dagger\cos b+(p_c-p_b\cos a)(\sin b/\sin a),\\
L_3=L_{12}&=p_b.
\end{aligned} \tag{5}$$

Analogously for the isotopic spin

$$\begin{aligned}
T_1\equiv T_{23}&=-\sin\Phi p_\Theta+(\cos\Phi/\sin\Theta)(p_\Psi-\cos\Theta p_\Phi)\\
&=-p_\Theta^\dagger\sin\Phi+(p_\Psi-p_\Phi\cos\Theta)(\cos\Phi/\sin\Theta),
\end{aligned}$$

[23] We are indebted to Dr. J. Schwinger for valuable discussion of this question.

$$T_2 \equiv T_{31} = \cos\Phi p_\Theta + (\sin\Phi/\sin\Theta)(p_\Psi - \cos\Theta p_\Phi) \quad (6)$$
$$= p_\Theta{}^\dagger \cos\Phi + (p_\Psi - p_\Phi \cos\Theta)(\sin\Phi/\sin\Theta),$$
$$T_3 \equiv T_{12} = p_\Phi.$$

For the components L^{rs} and T^{rs} we find

$$L^1 \equiv L^{23} = \sin\psi p_\theta + (\cos\psi/\sin\theta)(\cos\theta p_\psi - p_\varphi)$$
$$= p_\theta{}^\dagger \sin\psi + (p_\psi \cos\theta - p_\varphi)(\cos\psi/\sin\theta),$$
$$L^2 \equiv L^{31} = \cos\psi p_\theta - (\sin\psi/\sin\theta)(\cos\theta p_\psi - p_\varphi) \quad (7)$$
$$= p_\theta{}^\dagger \cos\psi - (p_\psi \cos\theta - p_\varphi)(\sin\psi/\sin\theta),$$
$$L^3 \equiv L^{12} = p_\psi,$$

$$T^1 \equiv T^{23} = \sin\Psi p_\Theta + (\cos\Psi/\sin\Theta)(\cos\Theta p_\Psi - p_\Phi)$$
$$= p_\Theta{}^\dagger \sin\Psi + (p_\Psi \cos\Theta - p_\Phi)(\cos\Psi/\sin\Theta),$$
$$T^2 \equiv T^{31} = \cos\Psi p_\Theta - (\sin\Psi/\sin\Theta)(\cos\Theta p_\Psi - p_\Phi) \quad (8)$$
$$= p_\Theta{}^\dagger \cos\Psi - (p_\Psi \cos\Theta - p_\Phi)(\sin\Psi/\sin\Theta),$$
$$T^3 \equiv T^{12} = p_\Psi.$$

And, analogously for the components $L^{\alpha\beta}$ which we write $L^{(1)}$, $L^{(2)}$, $L^{(3)}$ or $L^{(23)}$, $L^{(31)}$, $L^{(12)}$ to distinguish them from L^{rs}

$$L^{(1)} \equiv L^{(23)} = \sin c p_a + (\cos c/\sin a)(\cos a p_c - p_b)$$
$$= p_a{}^\dagger \sin c + (p_c \cos a - p_b)(\cos c/\sin a),$$
$$L^{(2)} \equiv L^{(31)} = \cos c p_a - (\sin c/\sin a)(\cos a p_c - p_b) \quad (9)$$
$$= p_a{}^\dagger \cos c - (p_c \cos a - p_b)(\sin c/\sin a),$$
$$L^{(3)} \equiv L^{(12)} = p_c.$$

We note that all components L^{rs}, T^{rs}, $L^{\alpha\beta}$ turn out to be Hermitian. For the total square of L and T we get

$$L^2 = p_\theta{}^\dagger p_\theta + \frac{(p_\psi - \cos\theta p_\varphi)^2}{\sin^2\theta} + p_\varphi{}^2$$
$$= p_\theta{}^\dagger p_\theta + \frac{(\cos\theta p_\psi - p_\varphi)^2}{\sin^2\theta} + p_\psi{}^2 \quad (10)$$

$$T^2 = p_\Theta{}^\dagger p_\Theta + \frac{(p_\Psi - \cos\Theta p_\Phi)^2}{\sin^2\Theta} + p_\Phi{}^2$$
$$= p_\Theta{}^\dagger p_\Theta + \frac{(\cos\Theta p_\Psi - p_\Phi)^2}{\sin^2\Theta} + p_\Psi{}^2 \quad (11)$$

and also

$$L^2 = p_a{}^\dagger p_a + \frac{(p_c - \cos a p_b)^2}{\sin^2 a} + p_b{}^2$$
$$= p_a{}^\dagger p_a + \frac{(\cos a p_c - p_b)^2}{\sin^2 a} + p_c{}^2. \quad (12)$$

The expressions (7), (8) can be substituted in the expression (50) for

$$\sum_{\alpha,k}{}^{0} (\pi_{\alpha k})^2$$

which, however, gets rather complicated even in the approximation where one puts $Q_r + Q_s = 2D$ because of the terms containing $Q_r - Q_s$. The analogous expression (50c) for the charged scalar theory is simpler, because here we have simply $T^{12} = T_{12} = p_\Phi$. In the approximation where we can put in the last two terms $Q_1 + Q_2 = 2D$, $Q_r = D$ we get

$$(\pi_1)^2 + (\pi_2)^2 = P_1{}^\dagger P_1 + P_2{}^\dagger P_2 + \frac{(p_c + p_\varphi)^2}{2(Q_1 - Q_2)^2} + \frac{(p_c - p_\varphi)^2}{8D^2}$$
$$+ \left\{ \frac{(\cos a p_c - p_b)^2}{\sin^2 a} + p_a{}^\dagger p_a \right\} D^{-2}. \quad (13c)$$

2. The S Transformation

By using the expression (3) for the $e_{\alpha k}$ the S transformation defined by Eq. (65a) is simply obtained by putting[24]

$$S = \exp\left(i\sigma_3 \frac{c}{2}\right) \exp\left(i\sigma_2 \frac{a}{2}\right) \exp\left(i\sigma_3 \frac{b}{2}\right);$$
$$S^{-1} = \exp\left(-i\sigma_3 \frac{b}{2}\right) \exp\left(-i\sigma_2 \frac{a}{2}\right) \exp\left(-i\sigma_3 \frac{c}{2}\right) \quad (14)$$

which can also be written out as

$$S = \cos\frac{a}{2}\left(\cos\frac{b}{2}\cos\frac{c}{2} - \sin\frac{b}{2}\sin\frac{c}{2}\right) I$$
$$+ i\sin\frac{a}{2}\left(-\sin\frac{b}{2}\cos\frac{c}{2} + \cos\frac{b}{2}\sin\frac{c}{2}\right)\sigma_1$$
$$+ i\sin\frac{a}{2}\left(\cos\frac{b}{2}\cos\frac{c}{2} + \sin\frac{b}{2}\sin\frac{c}{2}\right)\sigma_2$$
$$+ i\cos\frac{a}{2}\left(\sin\frac{b}{2}\cos\frac{c}{2} + \cos\frac{b}{2}\sin\frac{c}{2}\right)\sigma_3. \quad (15)$$

The expression for S^{-1} is obtained from it by changing i into $-i$. One easily finds

$$S p_a S^{-1} = p_a - \tfrac{1}{2}(\sigma_1 \sin c + \sigma_2 \cos c),$$
$$S p_b S^{-1} = p_b - \tfrac{1}{2}(-\sigma_1 \sin a \cos c + \sigma_2 \sin a \sin c + \sigma_3 \cos a), \quad (16)$$
$$S p_c S^{-1} = p_c - \tfrac{1}{2}\sigma_3.$$

Inserting this in the expressions (5) and (9) of the last section, one easily checks the Eqs. (69), (69[1]) of the text, namely

$$S\mathbf{L}S^{-1} = \mathbf{L} - \tfrac{1}{2}S\boldsymbol{\sigma}S^{-1} = \mathbf{L} - \tfrac{1}{2}\Sigma_\alpha \sigma_\alpha \mathbf{e}_\alpha,$$
$$S L^{\alpha\beta} S^{-1} = L^{\alpha\beta} - \tfrac{1}{2}\sigma_{\alpha\beta}.$$

[24] See W. Pauli, Helv. Phys. Acta **12**, 147 (1939), Section 3, where the special case $c = 0$ is treated.

The Fine Structure of Nuclear Energy Levels on the Alpha-Model*

CHARLES KITTEL**
Department of Physics, University of Wisconsin, Madison, Wisconsin
(Received February 24, 1942)

In studying the fine structure predictions of any proposed theory of nuclear forces it is important to know to what extent the results obtained are sensitive to the changes in the nuclear model employed in making the calculations. The present work is concerned with this. The splitting for He^5, which should be very similar to that for Li^5, is discussed on the alpha- and central field models. A deuteron group model for the alpha-particle is considered in addition to the simple alpha-group. Li^7 is treated from the standpoint of the theory of "holes" and also on a modified alpha-particle model. The contribution of the exchange terms to the splitting in He^5 is greater by a factor of the order of two or three on the alpha-model than on the central field model. The sign and magnitude of the total splitting are of about the same order on the two models. The deuteron group alpha-function gives essentially the same splitting as the ordinary alpha-function. So far as ordinary terms for Li^7 are concerned, the spin-orbit interaction of a "hole" in a concentrated closed shell with a closed shell is the same, apart from a numerical factor, as the spin-orbit interaction of a single particle with a closed shell. The exchange terms for Li^7 are approximately proportional to the degree of overlapping of the alpha- and triton groups. The exchange splitting has the same sign as the ordinary splitting. Energy splitting estimates on the alpha-model in which the exchange terms are neglected should give results reliable to an order of magnitude at least, as far as this model is concerned.

I. INTRODUCTION

VARIOUS experiments suggest that the lowest states of the nuclei He^5, Li^5, and Li^7 are doublets. Calculations of Feenberg and Wigner[1] indicate that the ground states of these nuclei should be ^2P. It is logical to interpret the doublets as consisting of the $^2P_{3/2}$ and $^2P_{1/2}$ parts of a ^2P state.

The evidence relating to He^5 comes from the experiments of Staub and Tatel[2] on the scattering of neutrons by helium. The variation with neutron energy of the backward scattering cross section indicates a doublet structure with a splitting of about 0.3 Mev. The sign of the splitting is not fixed.

Experiments by Heydenburg and Ramsey[3] on the scattering of protons by helium show a very broad maximum in the scattering of half-width over 1 Mev. There is no positive evidence of a doublet structure for Li^5.

In the case of Li^7 the ground state is stable, and its spin is[4–7] 3/2. Rumbaugh and Hafstad[8] found an excited state of this nucleus about 400 kev above the normal level.

Theoretical investigations of the fine structure of these nuclei can, as pointed out by Breit and Stehn,[9] throw light on the form of the interaction energy between pairs of nuclear particles. Also, since the fine structure matrix elements involve the derivative of the potential and hence may magnify the influence of the shape of some potentials at small interparticle separations, studies of fine structure offer a possible way of investigating the potential at small distances. It is difficult to obtain this knowledge from scattering experiments on elementary particles, since, according to Hoisington, Share, and Breit,[10] scattering results depend mostly on the shape of the outer region of the potential well.

In testing the fine structure predictions of any proposed theory of nuclear forces it is important to know to what extent the results obtained are sensitive to the changes in the nuclear model employed in making the calculations. The splitting for He^5, which on present ideas should be

* Submitted to the Graduate School of the University of Wisconsin in partial fulfillment of the requirements for the degree of Doctor of Philosophy.

** Now at Naval Ordnance Laboratory, Washington, D. C.

[1] E. Feenberg and E. Wigner, Phys. Rev. **51**, 95 (1937).

[2] H. Staub and H. Tatel, Phys. Rev. **58**, 820 (1940); see also H. Staub and W. E. Stephens, Phys. Rev. **55**, 131 (1939).

[3] N. P. Heydenburg and N. F. Ramsey, Phys. Rev. **57**, 1077 (1940).

[4] H. Schuler, Zeits. f. Physik **42**, 487 (1927).

[5] A. Harvey and F. A. Jenkins, Phys. Rev. **35**, 789 (1930).

[6] L. P. Granath, Phys. Rev. **42**, 44 (1932).

[7] M. Fox and I. I. Rabi, Phys. Rev. **48**, 746 (1935).

[8] L. H. Rumbaugh and L. R. Hafstad, Phys. Rev. **50**, 681 (1936).

[9] G. Breit and J. R. Stehn, Phys. Rev. **53**, 459 (1938).

[10] L. E. Hoisington, S. S. Share, and G. Breit, Phys. Rev. **56**, 884 (1939).

very similar to that for Li^5, will be discussed on the alpha-particle and central field models. Li^7 is treated on a modified alpha-model, the central field model having been discussed previously by Breit and Stehn.[9]

Dancoff[11] has given numerical estimates for the splitting in He^5 on a central field model, using the relativistic spin-orbit coupling and the tensor spin-orbit-spin coupling of meson theory. Inglis[12] has made estimates of the spin-orbit coupling on the alpha-model of light nuclei, including Li^7.

The theoretical basis for the alpha-particle model has been thoroughly discussed by Wheeler[13] in his papers on the resonating group model. For He^5 the relatively large binding energy of an alpha-particle suggests that the most important grouping of particles will be He^4+n^1, while for Li^7 it will be He^4+H^3. The internal motion of the particles in each group is described by a wave function depending on the interparticle distances; the relative motion of the groups is described by a function depending on the vector from the center of mass (c.m.) of one group to the c.m. of the other; the total wave function is the product of these functions.

To simplify the treatment of Li^7 the alpha-model is modified by introducing central field functions for the particles in the alpha-group and for the center of mass of the triton (H^3) group. On the basis of this model it will be shown that the contribution to the splitting from the exchange terms is approximately proportional to the degree of overlapping of the two groups, for small overlapping. This result should have application in approximate discussions of heavier nuclei.

Breit[14] has shown that the requirements of relativistic covariance of the wave equation for nuclear particles determines the spin-orbit interactions apart from certain adjustable parameters. From a consideration of the possible forms of wave equations for particles with spin he obtains the interaction energy

$$H=\sum \mathbf{B}_{kl}[a\boldsymbol{\sigma}_k+(a-1)\boldsymbol{\sigma}_l]-\sum{}' J_{kl}, \quad (1)$$

$$\mathbf{B}_{kl}=-(\hbar/4M^2c^2)[\mathbf{p}_k\times\nabla_k J_{kl}], \quad (2)$$

for Wigner forces. The particles in the nucleus are referred to by subscripts k, l; r_{kl} is the distance between particles k and l; the potential energy between two particles is $-J(r_{kl})$; the momentum operator is written $\mathbf{p}_k=(\hbar/i)\nabla$. $\sum'$ refers to sums over pairs of particles, and $\sum$ to sums over all values of k and l except $k=1$. The constant a is arbitrary. For particles interacting through the electromagnetic field the value of a is -1. The picture of each particle producing a scalar field defined in the reference system moving instantaneously with it corresponds to $a=1$. In the present work only $a=1$ is considered.

Note on Notation

Ψ^A is written for a complete antisymmetrized wave function, including spin; Ψ is the unsymmetrized product wave function, including spin; ψ is the space part of Ψ.

R, Q, $\mathfrak{R}$, ρ have different meanings on different models and must be watched carefully.

P_{ij} is the permutation operator, and interchanges i and j in the expression to its right.

$S_0(12)=(\alpha_1\beta_2-\alpha_2\beta_1)/\sqrt{2}$, where α and β are the usual spin functions. α is for spin up, β for spin down. Indices 1, 2, refer to the two particles.

$$\mathbf{1}=\mathbf{r}_1, \text{ etc.}; \quad x_{ij}=x_i-x_j.$$

II. FINE STRUCTURE OF He^5

The resonating group wave function assumed here for the $p_{3/2}$ state of He^5 is

$$\Psi^A=(1-P_{45}-P_{35})v[\mathbf{5}-(\mathbf{1}+\mathbf{2}+\mathbf{3}+\mathbf{4})/4]$$

$$\times u(r_{12}, r_{13}, r_{14}, r_{23}, r_{24}, r_{34})S_0(12)S_0(34)\alpha(5). \quad (3)$$

Particles 1 and 2 are protons; 3, 4, and 5 are neutrons. u describes the internal motion of the alpha-particle group and is an s function: unless specifically mentioned to the contrary u will be assumed symmetric in all particles in the alpha-group. The function v describes the motion of the outer neutron relative to the center of mass of the alpha-group. v is a p function as is explained by its dependence on x, y, z in Eq. (4).

Introducing

$$\boldsymbol{\rho}=\mathbf{5}-(\mathbf{1}+\mathbf{2}+\mathbf{3}+\mathbf{4})/4$$

$$=(x_\rho, y_\rho, z_\rho)$$

[11] S. M. Dancoff, Phys. Rev. **58**, 326 (1940).
[12] D. R. Inglis, Phys. Rev. **56**, 1175 (1939).
[13] J. A. Wheeler, Phys. Rev. **52**, 1083, 1106 (1939).
[14] G. Breit, Phys. Rev. **51**, 248 (1936).

in Cartesian coordinates, one writes

$$v(\varrho)=(x_\rho+iy_\rho)R(\rho), \tag{4}$$

where R is spherically symmetric.

The first-order perturbation energy for the $p_{3/2}$ state is

$$(\Delta E)_{3/2}=(\Psi^A, H'\Psi^A)/(\Psi^A, \Psi^A). \tag{5}$$

Neglecting the contribution from exchange terms, one finds

$$(\Psi^A, H'\Psi)_{\text{ordinary}}=(\lambda^2/4)\int u^2(1234)R^2(\rho) \times(2/3)(\varrho\cdot\nabla_5 J_{51})d\tau, \tag{6}$$

a form which shows clearly the dependence on the radial component of the force on the outside particle. A more convenient form is obtained by integrating the original equation by parts.

The total ΔE is three times the displacement of the $p_{3/2}$ state:

$$(\Delta E)_{\text{ordinary}}=-[3\lambda^2\int u^2(1234)J_{51}[2R^2(\rho) +(4/3)R(\rho)\rho R'(\rho)]d\tau]/ [(2/3)\int u^2(1234)\rho^2R^2(\rho)d\tau], \tag{7}$$

where only the ordinary term has been included in the numerator as well as in the denominator.

Evaluation of $(\Delta E)_{\text{ordinary}}$ for Gaussian Functions

Let

$$J=B\exp[-br^2], \tag{8a}$$

$$u(1234)=\exp[-\alpha(r_{12}^2+r_{13}^2+r_{14}^2+r_{23}^2+r_{24}^2+r_{34}^2)], \tag{8b}$$

$$R(\rho)=\exp[-\beta\rho^2], \tag{8c}$$

where B, b, α, and β are arbitrary constants.

The following general form of integral is needed:

$$\int \exp[-c_1r_1^2-c_2r_2^2-c_3r_3^2-c_4r_4^2-d_1r_{12}^2-d_2r_{13}^2 -d_3r_{14}^2-d_4r_{23}^2-d_5r_{24}^2-d_6r_{34}^2]d\tau_{1234} =\pi^6[c_1+c_2+c_3+c_4]^{-\frac{1}{2}}[(a+b+c)(a_3a_1+a_1a_2+a_2a_3) +b(a_3c+a_1a)+c(a_1a+a_2b)+a(a_3c+a_2b)+abc]^{-\frac{1}{2}}, \tag{9}$$

where

$$a_1=[(c_2c_3)/(c_1+c_2+c_3+c_4)]+d_4;$$
$$a_2=[(c_1c_3)/(c_1+c_2+c_3+c_4)]+d_2;$$
$$a_3=[(c_1c_2)/(c_1+\cdots)]+d_1;\quad a=[(c_1c_4)/(c_1+\cdots)]+d_3;$$
$$b=[(c_2c_4)/(c_1+\cdots)]+d_5;\quad c=[(c_3c_4)/(c_1+\cdots)]+d_6.$$

This integral was evaluated with the help of the standard form

$$\int \exp[-px^2\pm qx]dx=(\pi/p)^{\frac{1}{2}}\exp[q^2/4p].$$

The integrand in (9) is separable into the form $f(x)f(y)f(z)$, so that it is sufficient to evaluate $\int f(x)dx_1dx_2dx_3dx_4$ and then take the cube of the result.

The integral can also be expressed as (see Fig. 1)

$$\pi^6[\text{all quadruplets of lines except those forming triangles and quadrilaterals}]^{-\frac{1}{2}}. \tag{10}$$

There are 125 terms in the square brackets. Other integrals used in this work are obtained by differentiation with respect to the constants in the integrand.

One obtains

$$(\Delta E)_{\text{ordinary}}=-6\lambda^2Bb[(32\alpha\beta)/(16\alpha b+(32\alpha+3b)\beta)]^{3/2}. \tag{11}$$

Exchange Terms on the Alpha-Particle Model

The exchange integral in (5) simplifies to

$$\int v^*(\varrho)u(1234)[2B_{34}^2-6B_{41}^2-2B_{45}^2]v(\xi)u(1235)d\tau, \tag{12}$$

under the special assumption that u is of the form

$$\exp[-\alpha(r_{12}^2+r_{13}^2+r_{14}^2+r_{23}^2+r_{24}^2+r_{34}^2)]. \tag{13}$$

The evaluation of these integrals with Gaussian wave functions and potentials is exceedingly lengthy, and the results difficult to interpret. It is more instructive to consider the values of the integrals in the case of a long neutron range. This has some bearing on the physical situation, because the forces between the alpha-particle and the incoming neutron in a scattering experiment are thought to be relatively weak.

In the "long neutron range approximation" [15] it is assumed that $\alpha\gg\beta$. Particles 1, 2, 3 (in the unsymmetrized wave function) are assumed to be concentrated in a tight group. In what follows the "spread" of 1, 2, 3, will be neglected. The angular factors in the integral are considerably simplified under these conditions, and the integral over **1, 2, 3** may be replaced by an integral over **1** alone. One obtains a long formula for $(\Delta E)_{\text{exchange}}$ which the author will be glad to furnish to those interested.

Numerical results are given in Tables I–IV. The values of the constants used are, in nuclear units:

Formula	Constant	Value	Range in 10^{-13} cm
$J=B\exp(-br^2)$	b	20	$2.01=10^{+13}/\sqrt{b}$
$u=\exp[-\alpha\Sigma' r_{ij}^2]$	α	6.1	$3.64=10^{13}/\sqrt{\alpha}$
$R(\rho)=\exp(-\beta\rho^2)$	β	0.81	$10.0=10^{13}/\sqrt{\beta}$
		1.65	7.0
		5.06	4.0

The value of b chosen is in fair accord with the interpretation of experiments on the scattering of protons by protons. A variational calculation to be described later is the basis for the value of α. In an expression of the form $\exp[-cr^2]$, the range is defined as $1/\sqrt{c}$.

From Table I it is seen that the "long neutron range" [l.n.r.] approximation is reliable for the range of values for β considered. Table II gives the contribution to ΔE due to the exchange terms. Table III gives the contribution to ΔE from the ordinary terms, but differs from Table I in that exchange terms are included in the normalization integral now. Table IV gives the ratio of exchange terms to ordinary terms, with

[15] Referred to as l.n.r. approximation.

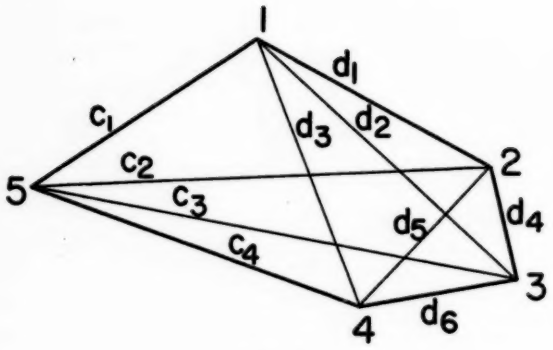

FIG. 1.

the normalization integral including exchange terms in both cases. It is seen from this table that the exchange terms give a very appreciable addition to the splitting on the alpha-particle model.

Central Field Model

Certain results obtained by Breit and Stehn in their treatment of the fine structure of the nuclear ground level of Li^7 can be used in the discussion of He^5 on the central field model. The wave function is

$$\Psi^A=(1/\sqrt{3})[1-P_{45}-P_{35}]\times[\xi_5 Q_5 R_3 R_4 S_0(34)\alpha(5)]R_1 R_2 S_0(12). \quad (15)$$

Here $\xi=x+iy$, Q describes the particle outside the alpha-shell, and R a particle in the alpha-shell. Suppose

$$J=A\exp[-ar^2],\quad Q=N_Q\exp[-\nu r^2/2],\quad R=N_R\exp[-\mu r^2/2].$$

Introduce the abbreviations:

$$d^2=(\mu+\nu)^2/4+a(\mu+\nu),\quad g^2=\mu\nu+a(\mu+\nu).$$

One has

$$\Delta E=[(\Delta E)_{s\pi}^{w1}-(\Delta E)_{s\nu}^{w1}+2(\Delta E)_{s\nu}^{w1}, \quad (16)$$

where the expressions on the right side are defined and evaluated in the work of Breit and Stehn. From this

$$\Delta E=-(3/2)\lambda^2 A a\nu^{5/2}\mu^{5/2}[4g^{-5}+d^{-5}]. \quad (17)$$

For $\mu=\nu$, it follows that $d=g$, and

$$\Delta E=-(15/2)\lambda^2 A a\nu^{5/2}\mu^{5/2}g^{-5}. \quad (18)$$

In this case the exchange term is 0.20 of the total ΔE.

As a preliminary to the comparison of the fine structure as calculated on different models, it is useful to have relations between the Gaussian function $u(1234)=\exp[-\alpha(r_{12}^2+\cdots+r_{34}^2)]$ in the interparticle distances, and the product function

$$u(1234)=\exp[-\mu r_{a1}^2/2]\exp[-\mu r_{a2}^2/2]\times\exp[-\mu r_{a3}^2/2]\exp[-\mu r_{a4}^2/2], \quad (19)$$

where $\mu/2$ is written for comparison with the central field function $R_1=N_R\exp[-\mu r_1^2/2]$, although in the present case r_{a1} differs from r_1, the former being taken relative to the center of mass of the alpha-particle group:

$$\mathbf{r}_{a1}=\mathbf{1}-(\mathbf{1}+\mathbf{2}+\mathbf{3}+\mathbf{4})/4,$$
$$\mathbf{r}_{a2}=\mathbf{2}-(\mathbf{1}+\mathbf{2}+\mathbf{3}+\mathbf{4})/4, \quad (20)$$
$$\cdots\cdots\cdots$$

If we let $\alpha=\mu/8$, $\beta=(8\nu+2\mu)/25$, or

$$\mu=8\alpha,\quad \nu=25\beta/8-2\alpha, \quad (21)$$

the product function in the five particles is found equal to the expression in $r_{12},\cdots,r_{34},\rho$.

Central field functions are referred to a fixed point—therefore the above relations are not strictly applicable. They will be used, however, in estimating the μ and ν to be used for comparison with a given α,β. This amounts to neglecting the center of mass motion on the central field model.

For $\mu=\nu$, $\alpha=\mu/8$; $\beta=2\mu/5$, or $\beta=16\alpha/5$. With $\alpha=6.1$, $\beta=19.52$ (range $\sim 2\times10^{-13}$ cm). This value of β is unlikely physically, but it is apparent from Table IV that on the alpha-particle model the exchange terms are relatively more important than on the central field model.

Using (21) one has for $(\Delta E)_{\text{ordinary}}$ on the central field model,

$$(\Delta E)_{\text{ordinary}}=-6\lambda^2 Bb[(25\alpha\beta-16\alpha^2)/(25\alpha\beta-16\alpha^2+b(25\beta/8+6\alpha))]^{5/2}. \quad (22)$$

TABLE I. Table of values of $(\Delta E)_{\text{ordinary}}/B$. Only ordinary terms included in normalization integral.

β	Exact	l.n.r. approx.
0.81	-9.48×10^{-5}	-9.50×10^{-5}
1.65	-4.46×10^{-4}	-4.50×10^{-4}
5.06	-3.33×10^{-3}	-3.41×10^{-3}

Geometrical Conditions for Vanishing of Exchange Terms on Alpha-Particle Model

It can be shown that on the alpha-group model of He^5 non-vanishing exchange integrals exist even when the alpha-group does not overlap the outside neutron. It is in fact necessary that r_b, the radius of the sphere about the center of mass of the alpha-particle from which the outside neutron is excluded, be greater than $5r_a/3$, where r_a is the radius of the alpha-particle, in order that a non-vanishing exchange integral exist. The reason for this behavior is that the center of mass of the original particles in the alpha-group is displaced when the outside neutron is exchanged with a neutron in the alpha-group.

III. DEUTERON GROUP MODEL OF THE ALPHA-PARTICLE

Up to now the alpha-particle wave function has been used in the form

$$u(1234)=\exp[-\alpha(r_{12}^2+\cdots+r_{34}^2)].$$

It is of interest to consider the effect on the level splitting of a change on the form of u. The alpha-group can be thought of as composed of two deuteron groups; u will be represented as the product of factors representing the internal motion of each deuteron with a factor describing the relative motion of the center of masses of the deuterons. The complete alpha-particle wave function is assumed to be

$$\begin{aligned}\Psi^A=\{&\exp[-\alpha_{\rm I}(r_{12}^2+r_{34}^2+r_{14}^2+r_{23}^2)\\&-\alpha_{\rm II}(r_{13}^2+r_{24}^2)]\\&+\exp[-\alpha_{\rm I}(r_{12}^2+r_{34}^2+r_{13}^2+r_{24}^2)\\&-\alpha_{\rm II}(r_{14}^2+r_{23}^2)]\}S_0(12)S_0(34).\end{aligned}\quad(23)$$

The relationship of this wave function to a deuteron grouping is seen from the relation

$$\begin{aligned}&\exp[-\alpha_{\rm I}(r_{12}^2+r_{34}^2+r_{14}^2+r_{23}^2)\\&-\alpha_{\rm II}(r_{13}^2+r_{24}^2)]=\exp[-\alpha_{\rm I}r_D^2\\&-(\alpha_{\rm I}+\alpha_{\rm II})(r_{13}^2+r_{24}^2)],\end{aligned}\quad(24)$$

TABLE II. Table of values of $(\Delta E)_{\rm exchange}/B$.

β	l.n.r. approx.
0.81	-4.50×10^{-5}
1.65	-2.47×10^{-4}
5.06	-2.48×10^{-3}

where $\mathbf{r}_D=\mathbf{1}+\mathbf{3}-\mathbf{2}-\mathbf{4}$, or twice the vector between the centers of mass of the two deuteron groups. This follows from

$$r_D^2=r_{12}^2+r_{14}^2+r_{23}^2+r_{34}^2-r_{13}^2-r_{24}^2.\quad(25)$$

Two terms in the spatial part of Ψ^A are necessary to make the space part symmetric in 1, 2 and 3, 4.

The ranges $\alpha_{\rm I}$ and $\alpha_{\rm II}$ will be determined by minimizing the energy integral

$$E=(\Psi^A, H\Psi^A)/(\Psi^A, \Psi^A),\quad(26)$$

$$H=T+V,\quad(27)$$

$$\begin{aligned}T=-\frac{\hbar^2}{M}\Big[&\sum{}'\Big(\frac{\partial^2}{\partial r_{kl}^2}+\frac{2}{r_{kl}}\frac{\partial}{\partial r_{kl}}\Big)\\&+\sum_{\substack{l,\,n\neq k\\ l<n}}^{4}\sum_{k=1}^{4}\Big(\cos(lkn)\frac{\partial^2}{\partial r_{kl}\partial r_{kn}}\Big)\Big],\end{aligned}\quad(28)$$

$$V=-\sum{}'[(1-g)P^M+gP^H]J_{ij};$$

$$J=A\exp[-br^2],\quad(29)$$

where P^M is the Majorana exchange operator, and P^H the Heisenberg exchange operator. The effect of g is to decrease the attraction between like particles relative to that between unlike particles.

The minimization of E is done by first minimizing the symmetric function with $\alpha_{\rm I}=\alpha_{\rm II}$. With the value of $\alpha_{\rm I}$ found in this manner, $\alpha_{\rm II}$ is varied in the general expression for E, and the minimum determined graphically. It is too laborious to minimize E simultaneously with respect to both $\alpha_{\rm I}$ and $\alpha_{\rm II}$. The results are given in

TABLE III. Table of values of $(\Delta E)_{\rm ordinary}/B$. Exchange terms included in normalization integral.

β	l.n.r. approx.
0.81	-9.48×10^{-5}
1.65	-4.43×10^{-4}
5.06	-2.94×10^{-3}

TABLE IV. Exchange terms included in normalization integral.

β	$[(\Delta E)_{\rm exchange}/(\Delta E)_{\rm ordinary}]$ l.n.r. approx.
0.81	0.475
1.65	0.557
5.06	0.843

Table V, in which we use as constants $A=85.0$, $b=20.0$, $g=0.22$. Nuclear units are used. For $\alpha_I=\alpha_{II}$, the minimum occurs at $\alpha_I=6.10$, where $E=-52.54\ mc^2$. With this value of α_I, a graph of E against α_{II} indicates a minimum at $\alpha_{II}=6.5\pm0.05$. The effect of g is to increase the internal binding of the deuteron subgroups.

An alternate form of deuteron grouping was tried in which the spin terms are built up of deuteron spin functions:

$$\Psi_1{}^A=\exp[-\alpha_I(r_{12}{}^2+r_{34}{}^2+r_{14}{}^2+r_{23}{}^2)-\alpha_{II}(r_{13}{}^2+r_{24}{}^2)]\mathcal{S}_1 -\exp[-\alpha_I(r_{12}{}^2+r_{13}{}^2+r_{34}{}^2+r_{23}{}^2) -\alpha_{II}(r_{14}{}^2+r_{23}{}^2)]\mathcal{S}_2; \quad (30)$$

$$\mathcal{S}_1=(1/\sqrt{3})(S_1(13)S_{-1}(24)-S_0(13)S_0(24) +S_{-1}(13)S_1(24)), \quad (31)$$

$$\mathcal{S}_2=(1/\sqrt{3})(S_1(14)S_{-1}(23)-S_0(14)S_0(23) +S_{-1}(14)S_1(23). \quad (32)$$

For $\alpha_I=\alpha_{II}$, this function becomes identical with the one previously considered. The binding energy is slightly less with the present function. It can be shown that $\Psi_1{}^A$ differs from Ψ^A only by the addition of a small term with like particle spins coupled parallel. Since Heisenberg forces favor antiparallel coupling, $\Psi_1{}^A$ is not as good a function as Ψ^A. The fine structure was not calculated for $\Psi_1{}^A$.

Estimates of $(\Delta E)_{\text{ordinary}}$ on the Different Models

Constants used: $b=20$, $\alpha=\alpha_I=6.10$, $\alpha_{II}=6.60$, $B=75$. Equation (22) used for central model.

$\beta=10$

$$(\Delta E)_{\text{alpha}}=-6\lambda^2Bb[0.1237]=-0.605\ mc^2,$$
$$(\Delta E)_{\text{alpha-deuteron}}=-6\lambda^2Bb[0.1248]=-0.612\ mc^2,$$
$$(\Delta E)_{\text{central}}=-6\lambda^2Bb[0.1054]=-0.516\ mc^2.$$

$\beta=19.52$ (when $\mu=\nu$)

$$(\Delta E)_{\text{alpha}}=(\Delta E)_{\text{central}} =-6\lambda^2Bb[0.224]=-1.1\ mc^2.$$

Concentrated Alpha-Particle $(\alpha\to\infty)$

$$(\Delta E)_{\text{alpha}}=-6\lambda^2Bb[2\beta/(b+2\beta)]^{5/2} =-6\lambda^2Bb[0.176] \quad \text{for} \quad \beta=10 =-6\lambda^2Bb[0.36] \quad \text{for} \quad \beta=20.$$

In this limit the exchange terms vanish, and the above values give the total splitting.

Central Model, letting $\mu\to\infty$

$$(\Delta E)_{\text{central}}=-6\lambda^2Bb[\nu/(\nu+b)]^{5/2}.$$

It is seen from these results that so far as the ordinary terms are concerned the "deuteron-grouping" alpha-function gives essentially the same ΔE as the simple alpha-function

$$u=\exp[-\alpha(r_{12}{}^2+\cdots+r_{34}{}^2)].$$

TABLE V. $\alpha_I=6.10$. Energy in mc^2.

$\alpha_{II}=$	5.0	6.1	6.2	6.6	7.0
Kinetic energy	103.1	109.80	110.32	112.631	114.961
Potential energy	−155.07	−162.34	−162.86	−165.244	−167.296
Total energy	−52.0	−52.54	−52.54	−52.61	−52.34

The results are not very different from those calculated on the central model with corresponding ranges. In comparing with the central model no correction has been made for the center of mass motion.

IV. SPLITTING DUE TO INTERACTION OF A CONCENTRATED s GROUP WITH AN ALPHA-GROUP

It will be shown that the spin-orbit interaction of an s group, in an $s_{1/2}$ state of internal motion, with an alpha-group is the same apart from a numerical factor as the interaction of a single particle with an alpha-group, in the limit of a very concentrated space function for the outside group. This calculation is of interest in connection with the theory of holes. The result will be given for the case of a $p_{3/2}$ state of the complete system.

Let N be the total number of particles, of which $N-4$ are in a group in an $s_{1/2}$ state of internal motion, and 4 are in an alpha-group. The exchange terms vanish in the limit of a concentrated function for the outside group; thus ordinary terms only will be considered. The result will be given for any odd integer N in order to exhibit the numerical constant mentioned above; in practice only $N=5$ and 7 are possible because of the exclusion principle.

The wave function is

$$\Psi=u(r_{12},\cdots,r_{34})w(r_{56},\cdots,r_{N-1,\,N})v(\boldsymbol{\varrho})S_0(12) \times S_0(34)S_0(56)\cdots S_0(N-2,\,N-1)\alpha(N);$$
$$v(\boldsymbol{\varrho})=(x_\rho+iy_\rho)R(|\rho|),$$

where

$$\boldsymbol{\varrho}=(\mathbf{5}+\mathbf{6}+\cdots+\mathbf{N})/(N-4)-(\mathbf{1}+\mathbf{2}+\mathbf{3}+\mathbf{4})/4. \quad (33)$$

One finds

$$(\Psi, H'\Psi)=-\lambda^2[N-4]^{-2}\int J_{N1}u(1234)w^2(5\cdots N) \times[2R^2(\rho)+4/3\rho R'(\rho)R(\rho)]d\tau_1\ldots_N. \quad (34)$$

To see the resemblance to the corresponding result for He^5, one introduces a delta-function for w:

$$w(5\cdots N)=[\delta(\mathbf{N}-\mathbf{5})\delta(\mathbf{N}-\mathbf{6})\delta(\mathbf{N}-\mathbf{7})\cdots \delta(\mathbf{N}-[\mathbf{N}-\mathbf{1}])]^{\frac{1}{2}}, \quad (35)$$

where $\delta(\mathbf{N}-\mathbf{5})$ denotes $\delta(x_N-x_5)\delta(y_N-y_5)\delta(z_N-z_5)$. Then the integral becomes

$$\int J_{N1}u^2(1234)[2R^2(\bar{\rho})+4/3\bar{\rho}R'(\bar{\rho})R(\bar{\rho})]d\tau_{1234N},$$

where $\bar{\boldsymbol{\varrho}}=\mathbf{N}-(\mathbf{1}+\mathbf{2}+\mathbf{3}+\mathbf{4})/4$. Finally

$$(\Delta E)=-3\lambda^2[\int u^2(1234)J_{N1}[2R^2(\bar{\rho}) +4/3\rho R'(\bar{\rho})R(\bar{\rho})]d\tau_{1234N}]/ [[N-4]^2 2/3\int u^2(1234)\bar{\rho}^2R^2(\bar{\rho})d\tau_{1234N}]$$
$$=[N-4]^{-2}(\Delta E)_{\text{ordinary, alpha-model, He}^5}. \quad (36)$$

The factor $[N-4]^{-2}$ can be understood from a classical model, according to which

$$\Delta E/\hbar=\omega=-\mathbf{v}\times\mathbf{a}/2c^2=-\dot{r}_\perp\ddot{r}_{\text{radial}}/2c^2. \quad (37)$$

For a given angular momentum $\dot{r}_\perp$ is $[N-4]^{-1}$ that for He^5, and $\ddot{r}_{\text{radial}}$ is $[N-4]^{-1}$ that for He^5, so that $[N-4]^{-2}$ enters the result.

The preceding results are also applicable to a model in which central field product functions are used for the alpha-particle, and also for the center of mass of the outside group. In this case one finds

$$(\Delta E)=[N-4]^{-2}(\Delta E)_{\text{ordinary, central model, He}^5}. \quad (38)$$

V. FINE STRUCTURE OF Li^7

The nucleus Li^7 is pictured on the alpha-particle model as built up from an alpha-particle group and a triton (H^3) group. The unsymmetrized wave function for the $p_{3/2}$ state is taken to be of the form

$$\Psi=u(1234)w(r_{56}, r_{57}, r_{67})v(\varrho)S_0(12)\times S_0(34)S_0(56)\alpha(7), \quad (39)$$

so that the antisymmetric wave function is

$$\Psi^A=(1-P_{17}-P_{27})(1-P_{35}-P_{36}-P_{45}-P_{46}+P_{35}P_{46})\Psi. \quad (40)$$

ψ will be used to denote the space part of Ψ. Particles 1, 2, 7 are protons; 3, 4, 5, 6 are neutrons; u is a central field product type function,

$$u(1234)=\Re(1)\Re(2)\Re(3)\Re(4), \quad (41)$$

$$v(\varrho)=(x_\rho+iy_\rho)Q(\rho), \quad (42)$$

where

$$\varrho=\tfrac{1}{3}(5+6+7).$$

This is a central field representation of $v(\varrho)$. w is an s function, and will be assumed symmetric in 5, 6, 7.

$$(\Psi^A, H'\Psi^A)=18(\Psi, H'\Psi^A). \quad (43)$$

$$(\Psi, H'\Psi^A)=I_0+I_1+I_2+I_3, \quad (44)$$

where I_0 contains the terms classified as ordinary, I_1 the terms with a single permutation operator, I_2 the terms with two permutation operators, and I_3 those with three permutation operators.

The ordinary terms can be evaluated from the equation for central field functions analogous to (34), with $N=7$. Setting

$$\begin{aligned} J&=B\exp[-br^2],\\ \Re&=\exp[-\alpha r^2],\\ Q&=\exp[-\beta\rho^2],\\ w&=\exp[-\gamma(r_{56}^2+r_{57}^2+r_{67}^2)], \end{aligned} \quad (45)$$

one has

$$(\Delta E)_{\text{ordinary}}=-(2\lambda^2/3)Bb[(2\alpha\beta\gamma)/(2\alpha\beta\gamma+b(\beta\gamma+\alpha\gamma+2\alpha\beta/9))]^{5/2}. \quad (46)$$

Consider various limiting cases of this result: For $\alpha\to\infty$; $\gamma\to\infty$ (concentrated alpha-group, concentrated triton)

$$(\Delta E)_{\text{ordinary}}=-(2\lambda^2/3)Bb[(2\beta)/(2\beta+b)]^{5/2}. \quad (47)$$

For $\alpha\to\infty$ (concentrated alpha-group)

$$(\Delta E)_{\text{ordinary}}=-(2\lambda^2/3)Bb\times[(2\beta)/(2\beta+b(1+(2/9)\beta/\gamma)]^{5/2}. \quad (48)$$

For $\gamma\to\infty$ (concentrated triton)

$$(\Delta E)_{\text{ordinary}}=-(2\lambda^2/3)Bb\times[(2\alpha\beta)/(2\alpha\beta+b(\beta+\alpha))]^{5/2}=1/9(\Delta E)_{\text{central model He}^5\text{, ordinary terms.}} \quad (49)$$

Discussion of Exchange Terms for Li^7, Alpha-Triton Model

It will be shown below that the exchange integrals in the limit of small overlapping of the group wave functions have a value proportional to the degree of overlapping. It is of great assistance to be able to eliminate double and triple exchange integrals from the calculations. This may be done by the following reasoning in the case of a small overlap. On a central field model of Li^7 one has the following sequence, where v is a central field function for a particle in the triton:

Ordinary:

$$\int R_1^2R_2^2R_3^2R_4^2v_5^2v_6^2v_7^2d\tau_1\cdots=1, \text{ say.}$$

Single exchange:

$$\int R_1^2R_3^2R_4^2v_5^2v_6^2d\tau_{13456}\int R_2v_2R_7v_7d\tau_{27}=x.$$

Double exchange:

$$\int R_1^2R_4^2v_6^2d\tau_{146}\int R_2v_2R_7v_7d\tau_{27}\times\int R_3v_3R_5v_5d\tau_{35}=x^2.$$

Triple exchange:

$$\int R_1^2 d\tau_1 \int R_4 v_4 R_6 v_6 d\tau_{46} \int R_3 v_3 R_5 v_5 d\tau_{35} \times \int R_2 v_2 R_7 v_7 d\tau_{27} = x^3.$$

If x is small, then x^2 and x^3 may be neglected. On going over now to the case of a group model for the triton, it will be seen that the corresponding double and triple exchange terms are smaller than x^2 and x^3, respectively. Suppose that the contribution x to the single exchange integral comes from a small region of space. It may not be possible for more than one particle in the triton to occupy this region simultaneously, because the center of mass of the triton is restricted in its motion to remain, say, outside of a certain spherical region. In this example the double and triple exchange terms would vanish. These terms may become as large as x^2 and x^3 only if the triton is completely included in the sphere of the alpha-particle.

The general plan of this section is to work out the single exchange terms in a form depending on the overlapping, and certain vector and scalar products. These products will first be estimated roughly in the limit of a very small overlap, and the values obtained in this manner will be the basis for a classification of the terms as large or small. The small terms will then be neglected. The terms which are not neglected will be estimated on a more refined model. Henceforth one assumes

$$(\Psi, H'\Psi^A) \leqq I_0 + I_1. \tag{50}$$

Division of Terms into Large and Small Parts

The division proceeds by calculating the averages of various vector and scalar products appearing in I_1, such as $[\mathbf{r}_5 \times \mathbf{r}_2]^2$ and $(\mathbf{r}_7 \cdot \boldsymbol{\rho})$, in the limiting case of small overlap for very simple group wave functions.

The result of the calculation of the averages is that

$$I_1 = -(\lambda^2/108) C \int \Re_1^2 \Re_2^2 \Re_4^2 \Re_3 \Re_5 w(567) \times w(367) Q_\rho Q_\eta [\boldsymbol{\rho} \cdot (10\mathbf{r}_7 - 4\mathbf{r}_3)] d\tau_1 \cdots 7, \tag{51}$$

where several small terms contributing about 1 percent of the result have been neglected. *This is free from any direct assumption about the wave functions.* It need be supposed only that the "small" terms are always negligible and that $J'/r = C$.

Measure of Overlap

The term $(\psi, P_{35}\psi)$ in the normalization integral will be used as a measure of the overlapping. It is supposed that $(\psi, \psi) = 1$.

$$(\psi, P_{35}\psi) = \int (\Re_1 \Re_2 \Re_4)^2 \Re_3 \Re_5 w(567) w(367) \times Q_\rho Q_\eta (x_\rho - iy_\rho)(x_\eta + iy_\eta) d\tau = (2/3) \int (\Re_1 \Re_2 \Re_4)^2 \Re_3 \Re_5 w(567) \times w(367) Q_\rho Q_\eta \rho^2 d\tau, \tag{52}$$

for small overlapping, in which case the whole contribution to the integral comes from $\boldsymbol{\rho} \leqq \mathbf{n}$.

Define

$$\Omega = (8d^2/3) \int (\Re_1 \Re_2 \Re_4)^2 \Re_3 R_5 w(567) \times w(367) Q_\rho Q_\eta d\tau, \tag{53}$$

which is the value of the above integral for triton radius = alpha-radius = d in the limit of small overlap. It is, however, approximately valid as a measure of overlap for finite overlap—the error is that of replacing $(\boldsymbol{\rho} \cdot \mathbf{n})$ in the integral by the constant $2d^2$.

On this model,

$$I_1 = -7\lambda^2 C\Omega/16, \tag{54}$$

and to the same approximation

$$(\Psi, \Psi^A) = (\psi, \psi) - 3(\psi, P_{35}\psi) = 1 - 3\Omega, \tag{55}$$

when we take $(\psi, \psi) = 1$. Thus the complete splitting is

$$(\Delta E) = -(\lambda^2/2)[(\Re_1 \Re_2 \Re_3 \Re_4)^2 \times J_{71}[2Q_\rho^2 + 4\rho Q'_\rho Q_\rho/3] w^2(567) d\tau + 7C\Omega/16]/[\int (\Re_1 \Re_2 \Re_3 \Re_4 \times Q_\rho w(567))^2 d\tau - 3\Omega]. \tag{56}$$

It is instructive to evaluate (ΔE) wholly on the model used for the exchange term:

$$(\Delta E) = -\lambda^2[-C(\psi, \psi) + 7C\Omega/16]/[(\psi, \psi) - 3\Omega] \leqq C\lambda^2(1 + 2.6\Omega). \tag{57}$$

The exchange term has the same sign as the

ordinary term, in agreement with the central model result. The doublet is inverted, since C is negative.

The overlapping can be calculated directly, with Gaussian functions and a product type central field representation of the alpha-group as in (46):

$$\Omega=[12\alpha\beta/(3\alpha^2+6\beta\gamma+6\alpha\gamma+14\alpha\beta/3)]^{\frac{1}{2}}, \quad (58)$$

where several very small terms have been omitted.

The range of the wave function $\mathfrak{R}$ should be corrected for the center of mass motion. This can be estimated from the result for the mean square displacement of the center of mass of the alpha-particle:

$$\langle\zeta^2\rangle_{Av}=[\int(\mathfrak{R}_1\mathfrak{R}_2\mathfrak{R}_3\mathfrak{R}_4)^2 \times(r_1^2+r_2^2+r_3^2+r_4^2)d\tau_{1\ldots4}]/ [16\int(\mathfrak{R}_1\mathfrak{R}_2\mathfrak{R}_3\mathfrak{R}_4)^2d\tau_{1\ldots4}] =3\alpha/16, \quad (59)$$

where ζ is the coordinate of the c.m. of the alpha-particle group. Suppose now α on an independent particle model is given, and one wishes to find the corrected range. The apparent range is $1/\sqrt{\alpha}=r_\alpha$; then the corrected range is

$$r_\alpha-(\langle\zeta^2\rangle_{Av})^{\frac{1}{2}}=(1/\alpha)^{\frac{1}{2}}-(3/16)^{\frac{1}{2}}(1/\alpha)^{\frac{1}{2}} =(1-\sqrt{3}/4)r_\alpha.$$

The overlap integral $(\psi, P_{35}\psi)=\Omega$ can be approximately related to the periods of motion of the particles in the alpha-group and the center of mass of the triton, considering the triton group to be very concentrated. By utilizing the uncertainty principle, we have

$$\begin{aligned}\Omega &\leqq \text{range particles in alpha-group/ range c.m. of triton}\\ &\leqq \text{momentum c.m. of triton/ momentum particles in alpha-group}\\ &\leqq \sqrt{\text{ period particles in alpha-group/ period c.m. of triton.}}\end{aligned} \quad (60)$$

If the alpha-group is considered to be very concentrated,

$$\Omega=\sqrt{\text{ period c.m. of alpha-group/ period particles in triton.}} \quad (61)$$

Similar estimates can be made by using the W. K. B. approximation as a solution of the radial wave equations for the various particles and groups, but no exact connection can be made between the overlap and the periods of motion, because the spatial characteristics of wave functions such as the presence of "tails" affect the overlap integrals.

The splitting for Li^7 on a true alpha-particle model in which only relative coordinates appear has not been discussed because of the great amount of labor involved in treating such a model. An investigation of the geometrical conditions for the vanishing of the exchange terms has been carried out, however, in a manner similar to that employed on the same question for He^5. It turns out that for non-overlapping groups the single and double exchange integrals I_1 and I_2 vanish, but the triple exchange integral I_3 does not vanish until the distance between the c.m.'s of the two groups is at least 7/3 the radius of the alpha-group.

VI. CONCLUSIONS

1. The contribution of the exchange terms relative to ordinary to the splitting in He^5 is greater by a factor of the order of two or three on the alpha-model than on the central field model. The sign and magnitude of the total splitting are of about the same order on the two models.

2. The "deuteron-grouping" alpha-function gives for He^5 a splitting within a few percent of that for the ordinary alpha-function.

3. The exchange terms for Li^7 are approximately proportional to the degree of overlapping of the alpha- and triton groups. The exchange splitting has the same sign as the ordinary splitting.

4. Energy splitting estimates on the alpha-model in which the exchange terms are neglected should give results reliable to an order of magnitude at least so far as this model is concerned. On reasonable assumptions the value of the exchange terms is of the order of one-half of that of the ordinary terms.

I wish to acknowledge my great indebtedness to Professor G. Breit for many discussions and suggestions on this work.

Electromagnetic Properties of Nuclei in the Meson Theory

S. T. MA AND F. C. YU
Department of Physics, National University of Peking, Kunming, China
(Received May 22, 1942)

The mathematical treatment of the interaction of a meson field with an electromagnetic field is simplified by using Pauli's method. A discussion of calculation of exchange multipole moments of nuclei by the method of canonical transformation and the results for dipole moments in the pseudoscalar theory are given.

1. INTRODUCTION

THE theory of the interaction of a meson field and an electromagnetic field has been developed by several authors.[1] More details have been worked out by Bhabha. The latter has given complete expressions for the electromagnetic interaction of a meson field in the presence of nuclear particles and also equations of continuity for the meson current and the current of nuclear particles separately. Both the mathematical treatment and the final result can be simplified if we adopt a method used by Pauli.[2] Pauli's treatment is based on the general properties of the Lagrangian function instead of the explicit form of Proca's equations which are derivable from the Lagrangian function as variational equations. The method is therefore quite general and is applicable not only to the vector meson theory, but also to the scalar, pseudovector, and pseudoscalar theories as well. Pauli treated only the electromagnetic interaction of a free meson. We give below a generalization of his method to include nuclear particles.

Owing to the exchange nature of the meson theory, it becomes now necessary, in treating the interaction of a nucleus with an external electromagnetic field, to take into account not only the direct influence of the electromagnetic field on the nuclear particles, but also the interaction of the external field with the exchange meson field. Investigations in this direction have recently been made by several authors.[3] It has been shown that the electromagnetic interaction of a nuclear system can be expressed in terms of interactions between the external field and the electric and magnetic multipole moments of the nuclear system. The electric and magnetic dipole moments and the electric quadripole moment have been calculated on the vector theory by means of the ordinary perturbation method in quantum theory. It might appear objectionable to use a perturbation method for this purpose, because perturbations of as high as the third order are involved in such calculations. It can be shown, however, that all the previous results can be obtained, in a simpler manner, as the first approximation in the canonical transformation carried out by Møller and Rosenfeld.[4] We give below a discussion of the calculation of the exchange multipole moments by the method of canonical transformation and also give results in the pseudoscalar theory.

2. GENERAL THEORY OF THE INTERACTION OF MESON FIELD WITH ELECTROMAGNETIC FIELD

We give below a mathematical treatment of the interaction of a meson field with an electromagnetic field in the vector meson theory on the basis of Pauli's method. Pauli's method may be easily extended to other forms of meson theory. We give at the end of this section the results for the pseudoscalar theory, which can be similarly derived.

The vector meson field is described by a four vector U_ρ, with $U_4=\epsilon U_0$, ϵ being the square root of -1 introduced by Proca.[5] Let the complex conjugates of the field variables U_ρ be denoted

[1] Yukawa, Sakata, Kobayasi, and Taketani, Proc. Phys. Math. Soc. Japan **20**, 319, 720 (1938); Fröhlich, Heitler, and Kemmer, Proc. Roy. Soc. **A166**, 154 (1938); Kemmer, Proc. Roy. Soc. **A166**, 127 (1938); Bhabha, Proc. Roy. Soc. **A166**, 501 (1938).
[2] W. Pauli, Report of the Solvay Conference (1939).
[3] A. J. F. Siegert, Phys. Rev. **52**, 787 (1937); W. E. Lamb, Jr. and L. I. Schiff, Phys. Rev. **53**, 651 (1938); Fröhlich, Heitler, and Hahn, Proc. Roy. Soc. **A174**, 85 (1940); S. T. Ma, Proc. Camb. Phil. Soc. **36**, 351, 438 (1940).
[4] Møller and Rosenfeld, K. Danske Vidensk. Selskab. **17**, 8 (1940).
[5] Proca, J. de phys. et rad. **7**, 347 (1936).

by U_ρ^*. We introduce the operators

$$\pi_\nu=\nabla_\nu-i\Phi_\nu,\quad \pi_\nu^*=\nabla_\nu+i\Phi_\nu, \tag{1}$$

where $\nabla_\nu=\partial/\partial x_\nu$, $(\Phi_1, \Phi_2, \Phi_3)=(e/\hbar c)(A_1, A_2, A_3)$ and $\Phi_0=\Phi_4/\epsilon=(e/\hbar c)A_0$, $\mathbf{A}$ and A_0 being the electromagnetic potentials from which the antisymmetric tensor $f_{\rho\nu}$ representing the field strengths can be derived. We also adopt the notations

$$\begin{aligned} &U_{\rho\nu}=\pi_\nu U_\rho, \qquad U_{\rho\nu}^*=\pi_\nu^* U_\rho^*,\\ &U_{\rho\nu\lambda}=\pi_\lambda\pi_\nu U_\rho, \quad U_{\rho\nu\lambda}^*=\pi_\lambda^*\pi_\nu^* U_\rho^*. \end{aligned} \tag{2}$$

From these we define the new field variables

$$G_{\rho\nu}=U_{\nu\rho}-U_{\rho\nu},\quad G_{\rho\nu}^*=U_{\nu\rho}^*-U_{\rho\nu}^*. \tag{3}$$

It follows from the relations

$$\pi_\nu\pi_\lambda-\pi_\lambda\pi_\nu=-\frac{ie}{\hbar c}f_{\nu\lambda},\quad \pi_\nu^*\pi_\lambda^*-\pi_\lambda^*\pi_\nu^*=\frac{ie}{\hbar c}f_{\nu\lambda} \tag{4}$$

that

$$\begin{aligned} &U_{\rho\nu\lambda}-U_{\rho\lambda\nu}=+\frac{ie}{\hbar c}f_{\nu\lambda}U_\rho,\\ &U_{\rho\nu\lambda}^*-U_{\rho\lambda\nu}^*=-\frac{ie}{\hbar c}f_{\nu\lambda}U_\rho^*. \end{aligned} \tag{5}$$

Furthermore, for two complex scalar quantities A and B, we have

$$(\pi_\rho^* A^*)B+A^*(\pi_\rho B)=\nabla_\rho(A^*B). \tag{6}$$

Let the wave functions of the nuclear particles be denoted by Ψ which consists of the relativistic wave functions of the proton and the neutron. On introducing the notations

$$\Psi^\dagger=\epsilon\Psi^*\gamma^4,\quad \gamma^\rho=-i\beta\alpha^\rho,\quad \alpha^4=\epsilon, \tag{7}$$

where α^1, α^2, α^3, β are Dirac's matrices, we obtain the following four vectors and six vectors:

$$\begin{aligned} &\Psi_P^\dagger\Pi\gamma^\rho\Psi_N=\Gamma^\rho, \qquad \Psi_N^\dagger\Pi^*\gamma^\rho\Psi_P=\Gamma^{\rho*},\\ &\Psi_P^\dagger\Pi\gamma^\rho\gamma^\nu\Psi_N=\Gamma^{\rho\nu}, \quad \Psi_N^\dagger\Pi^*\gamma^\rho\gamma^\nu\Psi_P=\Gamma^{\rho\nu*}. \end{aligned} \tag{8}$$

The complete Lagrangian function for the system of nuclear particles, the meson field, their mutual interaction, and their interaction with the external electromagnetic field may be written as follows:

$$L=L^P+L^N+L^M+L^{PN}+L^{NP}, \tag{9}$$

$$\begin{aligned} &L^P=-i\Psi_P^\dagger(c\hbar\gamma^\rho\pi_\rho+M_Pc^2)\Psi_P,\\ &L_N=-i\Psi_N^\dagger(c\hbar\gamma^\rho\nabla_\rho+M_Nc^2)\Psi_N, \end{aligned} \tag{10}$$

$$L^M=\kappa^2U_\rho^*U_\rho+\tfrac{1}{2}G_{\rho\nu}^*G_{\rho\nu}, \tag{11}$$

$$\begin{aligned} &L^{PN}=-g_1\Gamma^\rho U_\rho-\frac{g_2}{2\kappa}\Gamma^{\rho\nu}G_{\rho\nu},\\ &L^{NP}=-g_1\Gamma^{\rho*}U_\rho^*-\frac{g_2}{2\kappa}\Gamma^{\rho\nu*}G_{\rho\nu}^*. \end{aligned} \tag{12}$$

It follows from the variational principle

$$\delta\int\int\int\int L dx_1dx_2dx_3dx_4=0 \tag{13}$$

that

$$\pi_\nu^*\frac{\partial L}{\partial U_{\rho\nu}}=\frac{\partial L}{\partial U_\rho},\quad \pi_\nu\frac{\partial L}{\partial U_{\rho\nu}^*}=\frac{\partial L}{\partial U_\rho^*}, \tag{14}$$

$$\pi_\nu^*\frac{\partial L}{\partial \Psi_{P\nu}}=\frac{\partial L}{\partial \Psi_P},\quad \pi_\nu\frac{\partial L}{\partial \Psi_{P\nu}^*}=\frac{\partial L}{\partial \Psi_P^*}, \tag{15}$$

$$\nabla_\nu\frac{\partial L}{\partial \Psi_{N\nu}}=\frac{\partial L}{\partial \Psi_N},\quad \nabla_\nu\frac{\partial L}{\partial \Psi_{N\nu}^*}=\frac{\partial L}{\partial \Psi_N}. \tag{16}$$

From these equations we obtain

$$\begin{aligned} &\nabla_\nu\left(\frac{\partial L}{\partial U_{\lambda\nu}}U_\lambda\right)=\frac{\partial L}{\partial U_\lambda}U_\lambda+\frac{\partial L}{\partial U_{\lambda\nu}}U_{\lambda\nu},\\ &\nabla_\nu\left(U_\lambda^*\frac{\partial L}{\partial U_{\lambda\nu}^*}\right)=U_\lambda^*\frac{\partial L}{\partial U_\lambda^*}+U_{\lambda\nu}^*\frac{\partial L}{\partial U_{\lambda\nu}^*},\\ &\nabla_\nu\left(\frac{\partial L}{\partial U_{\lambda\nu}}U_{\lambda\rho}\right)=\frac{\partial L}{\partial U_\lambda}U_{\lambda\rho}+\frac{\partial L}{\partial U_{\lambda\nu}}U_{\lambda\rho\nu},\\ &\nabla_\nu\left(U_{\lambda\rho}^*\frac{\partial L}{\partial U_{\lambda\nu}^*}\right)=U_{\lambda\rho}^*\frac{\partial L}{\partial U_\lambda^*}+U_{\lambda\rho\nu}^*\frac{\partial L}{\partial U_{\lambda\nu}^*}. \end{aligned} \tag{17}$$

The Lagrangian function defined above, besides being relativistically invariant, is invariant under a gauge transformation. A gauge transformation for the wave functions of the protons, neutrons, and mesons is

$$\begin{aligned} &\Psi_P\rightarrow\Psi_Pe^{i\alpha},\quad \Psi_P^*\rightarrow\Psi_P^*e^{-i\alpha},\\ &\Psi_N\rightarrow\Psi_N,\qquad \Psi_N^*\rightarrow\Psi_N^*,\\ &U_\rho\rightarrow U_\rho e^{i\alpha},\quad U_\rho^*\rightarrow U_\rho^*e^{-i\alpha}, \end{aligned} \tag{18}$$

where α is an arbitrary function of x_1, x_2, x_3, and x_4. The corresponding gauge transformation for the electromagnetic fields is

$$\Phi_\nu\rightarrow\Phi_\nu+\nabla_\nu\alpha. \tag{19}$$

From (18) and (19) it follows that

$$\pi_\nu\rightarrow\pi_\nu-i\nabla_\nu\alpha,\quad \pi_\nu^*\rightarrow\pi_\nu^*+i\nabla_\nu\alpha, \tag{20}$$

and therefore

$$\begin{aligned} &U_{\rho\nu}\to U_{\rho\nu}e^{i\alpha}, \quad && U^*_{\rho\nu}\to U^*_{\rho\nu}e^{-i\alpha},\\ &U_{\rho\nu\lambda}\to U_{\rho\nu\lambda}e^{i\alpha}, \quad && U^*_{\rho\nu\lambda}\to U^*_{\rho\nu\lambda}e^{-i\alpha},\\ &\Psi_{P\nu}\to\Psi_{P\nu}e^{i\alpha}, \quad && \Psi^*_{P\nu}\to\Psi^*_{P\nu}e^{-i\alpha},\\ &\Psi_{N\nu}\to\Psi_{N\nu}, \quad && \Psi^*_{N\nu}\to\Psi^*_{N\nu}, \end{aligned} \tag{21}$$

and also that

$$\begin{aligned} &\Gamma^{\nu}\to\Gamma^{\nu}e^{-i\alpha}, \quad && \Gamma^{\nu *}\to\Gamma^{\nu *}e^{i\alpha},\\ &\Gamma^{\rho\nu}\to\Gamma^{\rho\nu}e^{-i\alpha}, \quad && \Gamma^{\rho\nu *}\to\Gamma^{\rho\nu *}e^{i\alpha}. \end{aligned} \tag{22}$$

Since L is invariant under a gauge transformation, we have

$$\partial L/\partial\alpha=0.$$

Putting $\alpha=0$ in this equation we obtain

$$\frac{\partial L}{\partial U_\nu}U_\nu+\frac{\partial L}{\partial U_{\nu\rho}}U_{\nu\rho}+\frac{\partial L}{\partial\Psi_P}\Psi_P+\frac{\partial L}{\partial\Psi_{P\nu}}\Psi_{P\nu}=U_\nu{}^*\frac{\partial L}{\partial U_\nu{}^*}+U^*_{\nu\rho}\frac{\partial L}{\partial U^*_{\nu\rho}}+\Psi_P{}^*\frac{\partial L}{\partial\Psi_P{}^*}+\Psi^*_{P\nu}\frac{\partial L}{\partial\Psi^*_{P\nu}}. \tag{23}$$

With the help of this equation we obtain

$$\nabla_\rho L=U^*_{\lambda\rho}\frac{\partial L}{\partial U_\lambda{}^*}+\frac{\partial L}{\partial U_\lambda}U_{\lambda\rho}+U^*_{\lambda\nu\rho}\frac{\partial L}{\partial U^*_{\lambda\nu}}+\frac{\partial L}{\partial U_{\lambda\nu}}U_{\lambda\nu\rho}+\left(\Psi_\rho{}^*\frac{\partial L}{\partial\Psi^*}+\frac{\partial L}{\partial\Psi}\Psi_\rho+\Psi^*_{\nu\rho}\frac{\partial L}{\partial\Psi_\nu{}^*}+\frac{\partial L}{\partial\Psi_\nu}\Psi_{\nu\rho}\right)_{P,N}. \tag{24}$$

The energy and momentum tensor may be defined as

$$T_{\rho\nu}=U^*_{\lambda\rho}\frac{\partial L}{\partial U^*_{\lambda\nu}}+\frac{\partial L}{\partial U_{\lambda\nu}}U_{\lambda\rho}+\left(\Psi_\rho{}^*\frac{\partial L}{\partial\Psi_\nu{}^*}+\frac{\partial L}{\partial\Psi_\nu}\Psi_\rho\right)_{P,N}-L\delta_{\rho\nu}. \tag{25}$$

By (17),

$$\nabla_\nu T_{\rho\nu}=U^*_{\lambda\rho\nu}\frac{\partial L}{\partial U^*_{\lambda\nu}}+\frac{\partial L}{\partial U_{\lambda\nu}}U_{\lambda\rho\nu}+U^*_{\lambda\rho}\frac{\partial L}{\partial U_\lambda{}^*}+\frac{\partial L}{\partial U_\lambda}U_{\lambda\rho}+\left(\Psi^*_{\rho\nu}\frac{\partial L}{\partial\Psi_\nu{}^*}+\frac{\partial L}{\partial\Psi_\nu}\Psi_{\rho\nu}+\Psi_\rho{}^*\frac{\partial L}{\partial\Psi^*}+\frac{\partial L}{\partial\Psi}\Psi_\rho\right)_{P,N}-\nabla_\rho L. \tag{26}$$

Substituting (24) into this expression we obtain the result

$$\nabla_\nu T_{\rho\nu}=f_{\rho\nu}s_\nu, \tag{27}$$

where

$$s_\nu=-\frac{ie}{\hbar c}\left(U_\lambda{}^*\frac{\partial L}{\partial U^*_{\lambda\nu}}-\frac{\partial L}{\partial U_{\lambda\nu}}U_\lambda+\Psi_P{}^*\frac{\partial L}{\partial\Psi^*_{P\nu}}-\frac{\partial L}{\partial\Psi_{P\nu}}\Psi_P\right) \tag{28}$$

may be interpreted as the four vector expressing the current and charge densities of the nuclear system including the nuclear particles and the meson field. From (28) we have

$$\nabla_\nu s_\nu=-\frac{ie}{\hbar c}\left(U_\lambda{}^*\frac{\partial L}{\partial U_\lambda{}^*}-\frac{\partial L}{\partial U_\lambda}U_\lambda+U^*_{\lambda\nu}\frac{\partial L}{\partial U^*_{\lambda\nu}}-\frac{\partial L}{\partial U_{\lambda\nu}}U_{\lambda\nu}+\Psi_P{}^*\frac{\partial L}{\partial\Psi_P{}^*}-\frac{\partial L}{\partial\Psi_P}\Psi_P+\Psi^*_{P\nu}\frac{\partial L}{\partial\Psi^*_{P\nu}}-\frac{\partial L}{\partial\Psi_{P\nu}}\Psi_{P\nu}\right). \tag{29}$$

The equation of continuity for the total current

$$\nabla_\nu s_\nu=0 \tag{30}$$

follows from (29) and (23).

The current s_ν can be separated into two parts: the proton and the meson current defined, respectively, by

$$s_\nu{}^P=-\frac{ie}{\hbar c}\left(\Psi_P{}^*\frac{\partial L}{\partial\Psi^*_{P\nu}}-\frac{\partial L}{\partial\Psi_{P\nu}}\Psi_P\right), \tag{31}$$

$$s_\nu{}^M=-\frac{ie}{\hbar c}\left(U_\lambda{}^*\frac{\partial L}{\partial U^*_{\lambda\nu}}-\frac{\partial L}{\partial U_{\lambda\nu}}U_\lambda\right). \tag{32}$$

The two parts do not satisfy (30) separately because of the exchange of charge. We have

$$\nabla_\nu s_\nu{}^P = -\frac{ie}{\hbar c}\left(\Psi_P{}^*\frac{\partial L}{\partial \Psi_P{}^*}+\Psi^*_{P\lambda}\frac{\partial L}{\partial \Psi^*_{P\lambda}}-\frac{\partial L}{\partial \Psi_P}\Psi_P-\frac{\partial L}{\partial \Psi_{P\lambda}}\Psi_{P\lambda}\right).$$

On account of the relations

$$\Psi_P{}^*\frac{\partial L}{\partial \Psi_P{}^*}=L^P+L^{PN},\quad \frac{\partial L}{\partial \Psi^*_{P\lambda}}=0,\quad \frac{\partial L}{\partial \Psi_{P\lambda}}\Psi_{P\lambda}+\frac{\partial L}{\partial \Psi_P}\Psi_P=L^P+L^{NP},$$

we obtain the result

$$\nabla_\nu s_\nu{}^P=-\nabla_\nu s_\nu{}^M=-\frac{ie}{\hbar c}(L^{PN}-L^{NP}). \tag{33}$$

This equation expresses the rate of flow of the exchange current into or out of the nuclear particles. It has been given by Bhabha[1] but it is here given in a much simpler form.

The explicit expressions for the variational equations and the current densities are

$$\pi_\rho{}^* G'^*_{\rho\nu}=\kappa^2 U_\nu{}^*-g_1\Gamma^\nu,\quad \pi_\rho G'_{\rho\nu}=\kappa^2 U_\nu-g_1\Gamma^{\nu*}, \tag{34}$$

$$s_\nu{}^P=e\Psi_P{}^\dagger\gamma^\nu\Psi_P,\quad s_\nu{}^M=-\frac{ie}{\hbar c}(U_\lambda{}^* G'_{\nu\lambda}-G'^*_{\nu\lambda}U_\lambda), \tag{35}$$

where

$$G'_{\rho\nu}=G_{\rho\nu}-\frac{g_2}{\kappa}\Gamma^{\rho\nu*},\quad G'^*_{\rho\nu}=G^*_{\rho\nu}-\frac{g_2}{\kappa}\Gamma^{\rho\nu}. \tag{36}$$

Let us now write the four and six vectors in terms of ordinary vectors and scalars as follows:

$$\begin{gathered}U_\rho=(\mathbf{U},\ V),\quad G'_{\rho\nu}=(\mathbf{G},\ \mathbf{F}),\quad (G'_{12}=G_3,\quad G'_{01}=F_1,\ \text{etc.}),\\ g_1\Gamma^\rho=(\mathbf{M},\ N)=(g_1\Psi_P{}^*\Pi\boldsymbol{\alpha}\Psi_N,\ g_1\Psi_P{}^*\Pi\Psi_N),\\ -\frac{g_2}{\kappa}\Gamma^{\rho\nu}=(\mathbf{S},\ \mathbf{T})=\left(\frac{g_2}{\kappa}\Psi_P{}^*\Pi\boldsymbol{\beta\sigma}\Psi_N,\ \frac{ig_2}{\kappa}\Psi_P{}^*\Pi\boldsymbol{\beta\alpha}\Psi_N\right).\end{gathered} \tag{37}$$

Equations (34) and (36) become then

$$\begin{gathered}\left(\frac{1}{c}\frac{\partial}{\partial t}+i\Phi_0\right)\mathbf{F}=(\boldsymbol{\nabla}-i\boldsymbol{\Phi})\times\mathbf{G}+\kappa^2\mathbf{U}-\mathbf{M}^*,\\ \kappa^2 V=-(\boldsymbol{\nabla}-i\boldsymbol{\Phi})\cdot\mathbf{F}+\mathbf{N}^*,\\ \mathbf{G}=(\boldsymbol{\nabla}-i\boldsymbol{\Phi})\times\mathbf{U}+\mathbf{S}^*,\\ \left(\frac{1}{c}\frac{\partial}{\partial t}+i\Phi_0\right)\mathbf{U}=-\mathbf{F}-(\boldsymbol{\nabla}-i\boldsymbol{\Phi})V+\mathbf{T}^*,\end{gathered} \tag{38}$$

together with the complex conjugates of these equations. The meson current and charge densities are, in the present notations,

$$\mathbf{j}=c(s_1,\ s_2,\ s_3)=-\frac{ie}{\hbar}(\mathbf{U}^*\times\mathbf{G}-\mathbf{U}\times\mathbf{G}^*+V^*\mathbf{F}-V\mathbf{F}^*), \tag{39}$$

$$\rho=s_4/\epsilon=-\frac{ie}{c\hbar}(\mathbf{U}^*\cdot\mathbf{F}-\mathbf{F}^*\cdot\mathbf{U}). \tag{40}$$

In order to link up the present notations with that of reference 3, we divide $\mathbf{U}$ and $\mathbf{F}$ into longi-

tudinal and transverse parts and put

$$\mathbf{U}_l=\frac{1}{(4\pi)^{\frac{1}{2}}}\boldsymbol{\phi},\quad \mathbf{F}_c=-\frac{\kappa}{(4\pi)^{\frac{1}{2}}}\boldsymbol{\psi}.$$

The longitudinal part of $\mathbf{U}$ and the transverse part of $\mathbf{F}$ may then be expressed in terms of $\boldsymbol{\phi}$ and $\boldsymbol{\psi}$ with the help of (38) with Φ_0, $\boldsymbol{\Phi}$, $\mathbf{M}$, N, $\mathbf{S}$, and $\mathbf{T}$ omitted. We have

$$\mathbf{U}=\frac{1}{(4\pi)^{\frac{1}{2}}}\left(\boldsymbol{\phi}-\frac{1}{c\kappa}\dot{\boldsymbol{\psi}}\right),\quad \mathbf{F}=-\frac{\kappa}{(4\pi)^{\frac{1}{2}}}\left(\boldsymbol{\psi}+\frac{1}{c\kappa}\dot{\boldsymbol{\phi}}\right). \tag{41}$$

The Hamiltonian is equal to the 44 component of the energy-momentum tensor

$$T_{\rho\nu}=-L\delta_{\rho\nu}+U^*_{\lambda\rho}G'_{\nu\lambda}+G'^*_{\nu\lambda}U_{\lambda\rho}-ic\hbar\Psi^\dagger\gamma^\nu(\nabla_\rho-i\Phi_\rho\tau_P)\Psi \tag{42}$$

multiplied by -1. Since

$$U^*_{\lambda\rho}G'_{\nu\lambda}=G^*_{\rho\lambda}G_{\nu\lambda}-\frac{g_2}{\kappa}G^*_{\rho\lambda}\Gamma^{\nu\lambda *}+U^*_{\rho\lambda}G'_{\nu\lambda},$$

and

$$\begin{aligned}\nabla_\nu(U^*_{\rho\lambda}G'_{\nu\lambda})&=\nabla_\nu\nabla_\lambda(U_\rho{}^*G'_{\nu\lambda})+\nabla_\nu[U_\rho{}^*(\kappa^2U_\nu-g_1\Gamma^{\nu *})]\\&=\nabla_\nu[U_\rho{}^*(\kappa^2U_\nu-g_1\Gamma^{\nu *})],\end{aligned}$$

we may write

$$T_{\rho\nu}=-L\delta_{\rho\nu}-ic\hbar\Psi^\dagger\gamma^\nu(\nabla_\rho-i\Phi_\rho\tau_P)\Psi+G^*_{\rho\lambda}G_{\nu\lambda}+\kappa^2U_\rho{}^*U_\nu-g_1\Gamma^\nu U_\rho-\frac{g_2}{\kappa}\Gamma^{\nu\lambda}G_{\rho\lambda}+\text{the complex conjugate}. \tag{43}$$

Hence

$$\begin{aligned}H=-T_{44}=L+ic\hbar\Psi^\dagger\gamma^4(\nabla_4-i\Phi_4\tau_P)\Psi-2(G^*_{4\lambda}G_{4\lambda}+\kappa^2U_4{}^*U_4)\\+g_1\Gamma^4U_4+\frac{g_2}{\kappa}\Gamma^{4\lambda}G_{4\lambda}+\text{the complex conjugate}\\=-i\Psi^\dagger[c\hbar\boldsymbol{\gamma}\cdot(\boldsymbol{\nabla}-i\boldsymbol{\Phi}\tau_P)+(M_P\tau_P+M_N\tau_N)c^2]\Psi+\kappa^2\mathbf{U}^*\cdot\mathbf{U}+\tfrac{1}{2}\sum_{i,j=1}^{3}G^*_{ij}G_{ij}\\+\frac{1}{\kappa^2}|\boldsymbol{\pi}\cdot\mathbf{F}-N^*|^2+|\mathbf{F}-\mathbf{T}^*|^2-\mathbf{M}\cdot\mathbf{U}+\tfrac{1}{2}\sum_{i,j=1}^{3}S^{ij}G_{ij}+\text{the complex conjugate}.\end{aligned} \tag{44}$$

This result can be separated into a term independent of the electromagnetic field and a term describing the electromagnetic interaction, namely,

$$\begin{aligned}H_0=-i\Psi^\dagger[c\hbar(\boldsymbol{\gamma}\cdot\boldsymbol{\nabla})+(M_P\tau_P+M_N\tau_N)c^2]\Psi+\kappa^2\mathbf{U}^*\cdot\mathbf{U}+\mathbf{F}^*\cdot\mathbf{F}\\+\frac{1}{\kappa^2}|\boldsymbol{\nabla}\cdot\mathbf{F}|^2+|\boldsymbol{\nabla}\times\mathbf{U}|^2-M\cdot U-\frac{1}{\kappa^2}N(\boldsymbol{\nabla}\cdot\mathbf{F})+\mathbf{S}\cdot(\boldsymbol{\nabla}\times\mathbf{U})-\mathbf{F}\cdot\mathbf{T}\\+\text{the complex conjugate}+\text{terms containing } g_1^2,\ g_2^2,\end{aligned} \tag{45}$$

and

$$H_I=-\frac{1}{c}\mathbf{j}\cdot\mathbf{A}. \tag{46}$$

In the second equation terms proportional to the square of the A's have been omitted. In order to obtain the interaction with an external electrostatic field A_0 we have further to introduce into the Hamiltonian the zero term

$$A_0\left(\rho-\frac{1}{4\pi}\boldsymbol{\nabla}\cdot\mathbf{E}\right), \tag{47}$$

where ρ is the charge density given by (40) and $\mathbf{E}$ is the electric field strength.[6]

[6] Heisenberg and W. Pauli, Zeits. f. Physik **59**, 168 (1930).

Equation (44) can also be reduced to the form

$$H=-i\Psi^\dagger[c\hbar\boldsymbol{\gamma}\cdot(\boldsymbol{\nabla}-i\boldsymbol{\Phi}\tau_P)+(M_P\tau_P+M_N\tau_N)c^2]\Psi+\kappa^2\mathbf{U}^*\cdot\mathbf{U}+\mathbf{G}^*\cdot\mathbf{G}+\kappa^2V^*V$$
$$+\mathbf{F}^*\cdot\mathbf{F}-\mathbf{F}\cdot\mathbf{T}-\mathbf{F}^*\cdot\mathbf{T}^*-\mathbf{M}\cdot\mathbf{U}-\mathbf{M}^*\cdot\mathbf{U}^*, \quad (48)$$

if we add the relativistically invariant term

$$\frac{1}{2}\frac{g_2^2}{\kappa^2}\Gamma^{\rho\nu*}\Gamma^{\rho\nu}=\mathbf{S}^*\cdot\mathbf{S}-\mathbf{T}^*\cdot\mathbf{T}$$

to the Lagrangian function (9).

The treatment of other forms of meson theory is similar to the above. We state briefly the results in the pseudoscalar theory. Let ψ be a pseudoscalar describing the meson field and $\psi_\rho=\pi_\rho\psi$ be the pseudovector derived from ψ. For the nuclear particles we have the following pseudovector and pseudoscalar:

$$\begin{gathered}\Gamma^{\rho\nu\lambda}=i\epsilon\Psi_P^\dagger\Pi\gamma^\rho\gamma^\nu\gamma^\lambda\Psi_N, \quad \Gamma^{\rho\nu\lambda*}=i\epsilon\Psi_N^\dagger\Pi^*\gamma^\rho\gamma^\nu\gamma^\lambda\Psi_P,\\ (\Gamma^{234},\ \Gamma^{314},\ \Gamma^{124},\ \Gamma^{321})=(\Gamma^{1'},\ \Gamma^{2'},\ \Gamma^{3'},\ \Gamma^{4'}),\\ (\Gamma^{234*},\ \Gamma^{314*},\ \Gamma^{124*},\ \Gamma^{321*})=(\Gamma^{1'*},\ \Gamma^{2'*},\ \Gamma^{3'*},\ \Gamma^{4'*}),\\ \Gamma^{1234}=-i\epsilon\Psi_P^\dagger\Pi\gamma^1\gamma^2\gamma^3\gamma^4\Psi_N=\Gamma', \quad \Gamma^{1234*}=-i\epsilon\Psi_N^\dagger\Pi^*\gamma^1\gamma^2\gamma^3\gamma^4\Psi_P=\Gamma'^*.\end{gathered} \quad (49)$$

While the Lagrangian function for the nuclear particles is still given by (10), for the meson field and its interactions we have

$$L^M=\kappa^2\psi^*\psi+\psi_\rho^*\psi_\rho, \quad L^{PN}=-f_1\Gamma'\psi-\frac{f_2}{\kappa}\Gamma'^\rho\psi_\rho, \quad L^{NP}=-f_1\Gamma'^*\psi^*-\frac{f_2}{\kappa}\Gamma'^\rho{}^*\psi_\rho{}^*. \quad (50)$$

The variational equations for the pseudoscalar meson field are

$$\pi_\nu{}^*\partial L/\partial\psi_\nu=\partial L/\partial\psi, \quad \pi_\nu\partial L/\partial\psi_\nu{}^*=\partial L/\partial\psi^*, \quad (51)$$

or

$$\pi_\rho\varphi_\rho=-\kappa^2\psi+f_1\Gamma'^*, \quad \pi_\rho{}^*\varphi_\rho{}^*=-\kappa^2\psi^*+f_1\Gamma', \quad (52)$$

where

$$\varphi_\rho=-\psi_\rho+\frac{f_2}{\kappa}\Gamma^{\rho'*}, \quad \varphi_\rho{}^*=-\psi_\rho{}^*+\frac{f_2}{\kappa}\Gamma^{\rho'}. \quad (53)$$

The present scheme is also gauge invariant and therefore (23) still holds. From the energy-momentum tensor

$$T_{\rho\nu}=\psi_\rho{}^*\frac{\partial L}{\partial\psi_\nu{}^*}+\frac{\partial L}{\partial\psi_\nu}\psi_\rho+\left(\Psi_\rho{}^*\frac{\partial L}{\partial\Psi_\nu{}^*}+\frac{\partial L}{\partial\Psi_\nu}\Psi_\rho\right)_{P,N}-L\delta_{\rho\nu} \quad (54)$$

it follows that the four vector of the current and charge density is given by

where

$$s_\nu=s_\nu{}^P+s_\nu{}^M,$$
$$s_\nu{}^M=\frac{ie}{\hbar c}(\psi^*\varphi_\nu-\varphi_\nu{}^*\psi). \quad (55)$$

The proof of the equations of continuity (30) and (33) is the same as in the vector theory.

Let us rewrite the above four-dimensional pseudovectors and pseudoscalars in terms of three-dimensional pseudovectors and pseudoscalars as follows:

$$\varphi_\rho=(\boldsymbol{\Gamma},\ \varphi), \quad (56)$$

$$f_1\Gamma'=R, \quad \frac{f_2}{\kappa}(\Gamma^{1'},\ \Gamma^{2'},\ \Gamma^{3'})=\mathbf{P}, \quad \frac{f_2}{\kappa}\Gamma^{0'}=Q. \quad (57)$$

Then (52) and (53) become

$$\left(\frac{1}{c}\frac{\partial}{\partial t}+i\Phi_0\right)\psi=\varphi-Q^*,\quad -\left(\frac{1}{c}\frac{\partial}{\partial t}+i\Phi_0\right)\varphi=\kappa^2\psi+(\nabla-i\mathbf{\Phi})\cdot\mathbf{\Gamma}-R^*,\quad \mathbf{\Gamma}=-(\nabla-i\mathbf{\Phi})\psi+P^*, \tag{58}$$

together with the complex conjugates of these equations, and (55) takes the form

$$\mathbf{j}^M=(ie/\hbar)(\psi^*\mathbf{\Gamma}=\mathbf{\Gamma}^*\psi), \tag{59}$$

$$\rho^M=(ie/\hbar c)(\psi^*\varphi-\varphi^*\psi). \tag{60}$$

The Hamiltonian is given by

$$H=-i\Psi^\dagger\{c\hbar\boldsymbol{\gamma}\cdot(\nabla-i\mathbf{\Phi}\tau_P)+(M_P\tau_P+M_N\tau_N)c^2\}\Psi+\kappa^2\psi^*\psi+|\boldsymbol{\pi}\psi|^2+\varphi^*\varphi-f_1\Gamma'\psi$$
$$-\frac{f_2}{\kappa}(\Gamma^{0'}\varphi+\sum_{k=1}^{3}\Gamma^{k'}\pi_k\psi)+\text{the complex conjugate}+\frac{f_2^2}{\kappa^2}\Gamma^{0'*}\Gamma^{0'}, \tag{61}$$

in which the term describing the electromagnetic interaction is of the form (46), $\mathbf{j}^M$ being now given by (59). Equation (61) may be rewritten in the form

$$H=-i\Psi^\dagger\{c\hbar\boldsymbol{\gamma}\cdot(\nabla-i\mathbf{\Phi}\tau_P)+(M_P\tau_P+M_N\tau_N)c^2\}\Psi+\kappa^2\psi^*\psi+\varphi^*\varphi+\mathbf{\Gamma}^*\cdot\mathbf{\Gamma}-R\psi$$
$$-Q\varphi-R^*\psi^*-Q^*\varphi^*+|Q|^2-|\mathbf{P}|^2, \tag{62}$$

which is the expression given in reference 4.

3. CALCULATION OF EXCHANGE MULTIPOLE MOMENTS

As in the case of the nuclear forces the multipole moments of a nuclear system due to exchange processes may be calculated either by using the ordinary method of quantum theory or by adopting the method of canonical transformation in reference 4. Calculations of the multipole moments by the former method have been given in reference 3. We discuss below the method of canonical transformation and also calculate the multipole moments in the pseudoscalar theory.

Let us take as an example the exchange magnetic moment of the deuteron in the vector theory. The static parts of the field variables are given by

$$\begin{aligned}
V^0(\mathbf{r}')&=\int N^*(\mathbf{r})\varphi(\mathbf{r}-\mathbf{r}')d\mathbf{r},\\
\mathbf{U}^0(\mathbf{r}')&=-\int\nabla\times\mathbf{S}^*(\mathbf{r})\varphi(\mathbf{r}-\mathbf{r}')d\mathbf{r},\\
\mathbf{F}^0(\mathbf{r}')&=-\int\nabla N^*(\mathbf{r})\varphi(\mathbf{r}-\mathbf{r}')d\mathbf{r},\\
\mathbf{G}^0(\mathbf{r}')&=\kappa^2\int\mathbf{S}^*(\mathbf{r})\varphi(\mathbf{r}-\mathbf{r}')d\mathbf{r}-\int\nabla(\nabla\cdot\mathbf{S}^*(\mathbf{r}))\varphi(\mathbf{r}-\mathbf{r}')d\mathbf{r},
\end{aligned} \tag{63}$$

together with the complex conjugates of these equations, in which

$$\varphi(\mathbf{r}-\mathbf{r}')=\frac{1}{4\pi}\frac{\exp(-\kappa|\mathbf{r}-\mathbf{r}'|)}{|\mathbf{r}-\mathbf{r}'|}. \tag{64}$$

The exchange magnetic moment is given by

$$\mathfrak{y}=\frac{1}{2c}\int \mathbf{r}\times\mathbf{j}^0 d\mathbf{r}=\frac{ie}{2c\hbar}\int\{\mathbf{r}\times\mathbf{F}^{0*}V^0-\mathbf{r}\times\mathbf{F}^0V^{0*}-\mathbf{r}\times(\mathbf{G}^{0*}\times\mathbf{U}^0)+\mathbf{r}\times(\mathbf{G}^0\times\mathbf{U}^{0*})\}d\mathbf{r}. \tag{65}$$

Take any point O as the origin. Let the vectors OP and ON from O to the proton and the neutron, respectively, be denoted by $\mathbf{R}_1$ and $\mathbf{R}_2$. We write $\mathbf{R}_1-\mathbf{R}_2=\mathbf{R}$, $\mathbf{R}_1+\mathbf{R}_2=\boldsymbol{\varrho}$, $\mathbf{r}-\mathbf{R}_1=\mathbf{r}_1$, $\mathbf{r}-\mathbf{R}_2=\mathbf{r}_2$. Then the first term in the integrand of (65) gives a contribution

$$-\int\int\int \mathbf{r}\times(\boldsymbol{\nabla}_2 N_2)N_1^*\varphi(r_1)\varphi(r_2)d\mathbf{r}d\mathbf{R}_1d\mathbf{R}_2.$$

With the help of the relation

$$\int\varphi(r_1)\varphi(r_2)d\mathbf{r}=\frac{1}{8\pi\kappa}e^{-\kappa R}, \tag{66}$$

we obtain

$$-\frac{1}{16\pi\kappa}\int\int\boldsymbol{\varrho}\times(\boldsymbol{\nabla}_2N_2)N_1^*e^{-\kappa R}d\mathbf{R}_1d\mathbf{R}_2=\frac{1}{16\pi}\int\int N_1^*N_2(\boldsymbol{\varrho}\times\mathbf{R})\frac{e^{-\kappa R}}{R}d\mathbf{R}_1d\mathbf{R}_2.$$

The first two terms in the integrand of (65) give therefore a contribution

$$\frac{ie}{16\pi c\hbar}\int\int N_1^*N_2(\boldsymbol{\varrho}\times\mathbf{R})\frac{e^{-\kappa R}}{R}d\mathbf{R}_1d\mathbf{R}_2=\frac{1}{2c}\frac{ie}{\hbar}\int\int\left(\frac{\boldsymbol{\varrho}}{2}\times\mathbf{R}\right)N_1^*N_2\varphi(R)d\mathbf{R}_1d\mathbf{R}_2. \tag{67}$$

It is known that (see reference 3) the total exchange current between the proton and the neutron is equal to $(ie/\hbar)J$, J being the nuclear potential between the proton and the neutron due to exchange processes. Equation (67) is therefore just one part of the magnetic moment due to the exchange current with respect to the point O. If we choose the origin at the midpoint of the two particles then $\boldsymbol{\varrho}=0$ and (67) vanishes. Henceforth we shall omit all terms containing $\boldsymbol{\varrho}$ in the final result.

The contribution of the third and fourth terms in the integrand of (65) can be similarly calculated with the help of the general formula for partial integration

$$\int\mathbf{uv}\cdot(\boldsymbol{\nabla}\times\mathbf{w})d\mathbf{r}=\int(\mathbf{v}\times\mathbf{w})\cdot\boldsymbol{\nabla}\mathbf{u}d\mathbf{r}+\int\mathbf{uw}\cdot(\boldsymbol{\nabla}\times\mathbf{v})d\mathbf{r}. \tag{68}$$

The final result for the exchange magnetic moment with respect to the midpoint of P and N is

$$\mathfrak{y}=\frac{ie}{16\pi\mu}(\mathbf{S}_1^*\times\mathbf{S}_2)(\nabla^2+\kappa^2)e^{-\kappa R}=\frac{ieg_2^2}{8\pi\mu\kappa^2}\Pi_1^*\Pi_2(\boldsymbol{\sigma}_1\times\boldsymbol{\sigma}_2)\left(\kappa^2-\frac{\kappa}{R}\right)e^{-\kappa R}, \tag{69}$$

in agreement with the result obtained in reference 3.

In the pseudoscalar theory the exchange magnetic dipole moment is given by

$$\mathfrak{y}=\frac{ie}{2\hbar c}\int\mathbf{r}\times(\psi^{0*}\boldsymbol{\Gamma}^0-\boldsymbol{\Gamma}^{0*}\psi^0)d\mathbf{r}$$

$$=\frac{ie}{2\hbar c}\int\int\int\mathbf{r}\times[(\kappa^2\mathbf{P}_2+\boldsymbol{\nabla}_2\times\boldsymbol{\nabla}_2\times\mathbf{P}_2)(\boldsymbol{\nabla}_1\cdot\mathbf{P}_1^*)-(\kappa^2\mathbf{P}_1^*+\boldsymbol{\nabla}_1\times\boldsymbol{\nabla}_1\times\mathbf{P}_1^*)(\boldsymbol{\nabla}_2\cdot\mathbf{P}_2)]\varphi(r_1)\varphi(r_2)d\mathbf{r}d\mathbf{R}_1d\mathbf{R}_2.$$

On evaluating the integral as above, we find

$$\mathfrak{y}=\frac{ief_2^2}{8\pi\mu}\Pi_1^*\Pi_2\left[\frac{(\boldsymbol{\sigma}_1\times\boldsymbol{\sigma}_2)\cdot\mathbf{R}}{R}\frac{\mathbf{R}}{R}\left(1+\frac{1}{\kappa R}\right)-(\boldsymbol{\sigma}_1\times\boldsymbol{\sigma}_2)\right]e^{-\kappa R}. \tag{70}$$

The result is antisymmetric in the spins of the two nuclear particles. A deuteron in any stationary state has therefore no extra non-additive magnetic moment due to meson exchange in the pseudoscalar theory as well as the vector theory.

In contrast to the result in the vector theory, in the pseudoscalar theory a proton-neutron pair has no exchange electric dipole moment that reacts with an electrostatic field. There is also no electric quadripole moment that reacts with an electrostatic field.

In conclusion the writers would like to thank Professor W. Heitler for a comment at the early stage of this work.

AUGUST 1 AND 15, 1942 PHYSICAL REVIEW VOLUME 62

Tensor Forces and Heavy Nuclei

G. M. VOLKOFF*
Department of Physics, University of British Columbia, Vancouver, British Columbia, Canada
(Received May 18, 1942)

It has been suggested that the interaction between a pair of nuclear particles contains, in addition to a central force term, a tensor term, and quantitative estimates of the relative magnitudes of these two terms have been given. In this paper a rough quantitative estimate of the relative contributions of these two terms to the binding energy of a nucleus is made on the basis of a highly simplified nuclear model. It is found that a tensor interaction between two nuclear particles of the form suggested by the neutral meson field theory of nuclear forces with constants determined to fit the experimental data on the two-particle neutron-proton system would lead to the existence of moderately light nuclei having binding energies, spins, and deviations from spherical shape much greater than those observed.

1. INTRODUCTION

THE discovery of the electric quadrupole moment of the deuteron[1] suggests the existence of a term lacking spherical symmetry in the interaction between a proton and a neutron. The current assumption of equality of forces between all pairs of nuclear particles then implies the existence of a similar term in the interaction between two like particles. General considerations of invariance[2] indicate that such a term should contain the operator

$$S_{12}=3(\boldsymbol{\sigma}_1\cdot\mathbf{r}\boldsymbol{\sigma}_2\cdot\mathbf{r}/r^2)-\boldsymbol{\sigma}_1\cdot\boldsymbol{\sigma}_2. \qquad (1)$$

Field theories of nuclear forces have been proposed[3] which lend support to this view. They predict the existence of terms containing S_{12} as a factor, but little reliance can be placed on the detailed form of the interaction given by these theories because of divergence difficulties from which they suffer.

The influence of the S_{12} tensor term on the two-particle proton-neutron system has been investigated by Rarita and Schwinger[4] and by Bethe.[5] The former develop a purely phenomenological theory adopting simplified rectangular well potentials with constants chosen to fit the binding energy and quadrupole moment of the deuteron, and the scattering of slow neutrons in hydrogen. The range of the forces is taken equal to that deduced from proton-proton scattering. Bethe employs the form of the interaction predicted by the single-meson theory of nuclear forces cutting off at small distances to avoid divergence. The value of the "cut-off" distance and the strength of the interaction is determined to fit the deuteron binding energy

---

* The greater part of this work was completed during the spring term of 1940 while the author was in the Department of Physics at Princeton University, Princeton, New Jersey, on a Research Fellowship granted by the Royal Society of Canada.

[1] J. M. B. Kellogg, I. I. Rabi, N. F. Ramsey, Jr., and J. R. Zacharias, Phys. Rev. **55**, 318 (1939) and **57**, 677 (1940).

[2] E. Wigner, Phys. Rev. **51**, 106 (1937).

[3] H. A. Bethe, Phys. Rev. **57**, 260 (1940) (gives a list of references); R. E. Marshak, Phys. Rev. **57**, 1101 (1940).

[4] W. Rarita and J. Schwinger, Phys. Rev. **59**, 436 (1941) and Phys. Rev. **59**, 556 (1941).

[5] H. A. Bethe, Phys. Rev. **57**, 390 (1940).

and the scattering cross section of slow neutrons in hydrogen. A discussion of H^3 and He^4 based on the use of tensor forces is given by Gerjuoy and Schwinger.[6]

It seems of interest to investigate the effect of the tensor interaction on the binding energy, spin, and shape of heavy nuclei. Wigner and Eisenbud[7] pointed out that forces of the general type of those used by Rarita and Schwinger and by Bethe will not have the property of saturation. Bethe[3] also mentioned the possibility of the tensor part of the interaction becoming predominant in heavy nuclei with the consequences not only of non-saturation, but also of large nuclear spin and markedly non-spherical shape of the nucleus. The object of the present paper is twofold: (a) On the basis of a highly simplified nuclear model, we obtain a rough estimate of the relative contributions of the spherically symmetrical and of the tensor interaction to the nuclear binding energy. (b) The application of these results to the "neutral" theory type interactions using the numerical constants as determined by Bethe[5] shows that the difficulties mentioned above will become pronounced well within the range of existing nuclei. The same holds for the values of the constants as determined by Schwinger and Rarita[4] if the spherically symmetrical part of the interaction is due to an ordinary potential. The case that it is an exchange interaction is not considered in the present paper and may well lead to a different conclusion. This makes it very probable that in the Schwinger and Rarita theory, the $J_0(r)$ of (2) has to be replaced by an exchange interaction.

2. THE FORM OF THE NUCLEAR INTERACTION

The general form of the interaction between two nuclear particles predicted by the neutral meson theory is given by

$$V=J_0(r)+J_1(r)\boldsymbol{\sigma}_1\cdot\boldsymbol{\sigma}_2+J_2(r)S_{12}. \qquad (2)$$

The symmetrical theory introduces an additional factor $\boldsymbol{\tau}_1\cdot\boldsymbol{\tau}_2$, while the charged meson theory gives no interaction between like particles, and

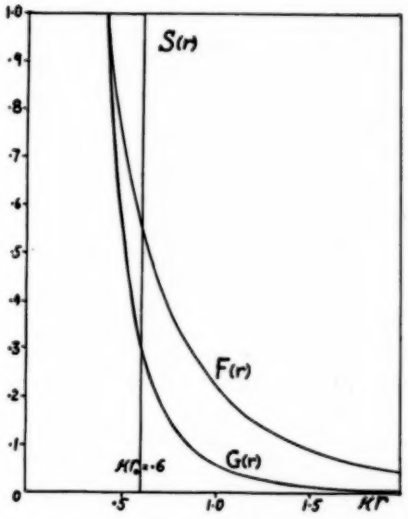

FIG. 1. The factor giving the dependence of the nuclear interaction on the distance (in units of $1/\kappa=2.18\times10^{-13}$ cm) between the particles. $F(r)$ and $G(r)$ are Bethe's results on the neutral straight cut-off theory for the spherically symmetric and the tensor parts of the interaction. $S(r)$ is the step function used to replace both in the present calculations.

introduces a factor $(1+\boldsymbol{\tau}_1\cdot\boldsymbol{\tau}_2)$ in the interaction between a proton and a neutron.

Bethe[5] arbitrarily assumed the spin independent term J_0 to be entirely absent, and took the other two terms to be of the form predicted by the meson theory of nuclear forces:

$$J_0(r)=0, \quad J_1(r)=\frac{2}{3}f^2\frac{e^{-\kappa r}}{r},$$
$$J_2(r)=-f^2e^{-\kappa r}\left\{\frac{1}{\kappa^2r^2}+\frac{1}{\kappa r}+\frac{1}{3}\right\}, \qquad (3)$$

where $1/\kappa=\hbar/\mu c=2.18\times10^{-13}$ cm on the assumption that $\mu=177$ m, and f^2 is a constant. To avoid divergence these interactions must be cut off at some value of $r=a$. Using straight cut-off ($J(r)\equiv J(a)$ for $r<a$) and the interaction (2) of the neutral theory Bethe obtained

$$f^2=0.0770\hbar c, \quad \kappa a=0.405. \qquad (4)$$

J_1 and J_2 may then be rewritten as

$$J_1(r)=AF(r), \quad J_2(r)=BG(r), \qquad (5)$$

where $F(r)$ and $G(r)$ are unity for $r\leqq a$, and for $r>a$

$$F(r)=J_1(r)/J_1(a), \quad G(r)=J_2(r)/J_2(a). \qquad (6)$$

[6] E. Gerjuoy and J. Schwinger, Phys. Rev. **61**, 138 (1942).
[7] E. Wigner and L. Eisenbud, Phys. Rev. **56**, 214 (1939).

TABLE I. Values of the function $W_1(k, \delta)$.

k	$\delta=0$	0.5	0.6	0.7	0.8	0.9	1.0	1.5	2.0	3.0
0.1	1.000		0.968		0.801		0.624	0.342	0.207	
0.2	1.000	1.000	1.000		0.946		0.805	0.483	0.300	
0.4	1.000	1.000	1.000	1.000	0.999		0.946	0.641	0.404	0.172
0.6	1.000	1.000	1.000	1.000	1.000		0.988	0.723	0.448	0.183
0.8	1.000	1.000	1.000	1.000	1.000	1.000	0.999	0.759	0.465	0.187
1.0	1.000	1.000	1.000	1.000	1.000	1.000	1.000	0.768	0.469	0.188
1.5	1.000	1.000	1.000	1.000		0.997	0.985	0.741	0.457	0.185
2.0	1.000	1.000	1.000	1.000		0.975	0.943	0.692	0.436	0.180
3.0	1.000	0.998		0.975		0.893	0.843	0.598	0.394	0.170
4.0	1.000	0.994		0.923		0.810	0.755	0.524	0.357	0.161
8.0	1.000	0.879		0.717		0.588	0.537	0.361	0.259	0.134
20.0	1.000	0.606		0.437		0.346	0.311	0.208	0.152	0.091

TABLE II. Values of the function $W_2(k, \delta)$.

k	$\delta=0$	0.5	0.6	0.7	0.8	0.9	1.0	1.5	2.0	3.0
0.1	−0.939		−0.908		−0.742		−0.566	−0.290	−0.162	
0.2	−0.833	−0.833	−0.833		−0.779		−0.641	−0.336	−0.177	
0.4	−0.595	−0.595	−0.595	−0.595	−0.594		−0.543	−0.283	−0.121	−0.029
0.6	−0.370	−0.370	−0.370	−0.370	−0.370		−0.359	−0.175	−0.069	−0.016
0.8	−0.172	−0.172	−0.172	−0.172	−0.172	−0.172	−0.171	−0.076	−0.029	−0.006
1.0	0.000	0.000	0.000	0.000	0.000	0.000	0.000	0.000	0.000	0.000
1.5	0.338	0.338	0.338	0.338		0.333	0.310	0.124	0.046	0.010
2.0	0.582	0.582	0.582	0.582		0.535	0.483	0.194	0.073	0.016
3.0	0.906	0.906		0.858		0.708	0.621	0.263	0.103	0.023
4.0	1.111	1.101		0.962		0.754	0.654	0.290	0.119	0.028
8.0	1.496	1.252		0.937		0.693	0.595	0.290	0.140	0.036
20.0	1.778	0.953		0.662		0.484	0.419	0.223	0.128	0.043

A and B are constants given by

$$A=J_1(a)=7.7 \text{ Mev}, \quad B=J_2(a)=-102 \text{ Mev}. \quad (7)$$

$F(r)$ and $G(r)$ are plotted in Fig. 1 together with the step function $S(r)$ of range r_0 defined by

$$\begin{aligned} S(r)&=1 \quad 0\leqq r\leqq r_0 \\ &=0 \quad r>r_0. \end{aligned} \quad (8)$$

Bethe also found that the factor $\tau_1\cdot\tau_2$ introduced by the symetmric theory alters the values of a and f^2 and leads to several serious difficulties.

Rarita and Schwinger[4] assumed rectangular well potentials of equal range, but different depths:

$$\begin{aligned} J_0(r)&=-(1-\tfrac{1}{2}g)\,V_0S(r)=-13.39S(r), \\ J_1(r)&=-\tfrac{1}{2}gV_0S(r) \quad =-\ 0.50S(r), \\ J_2(r)&=-\gamma V_0S(r) \quad =-10.75S(r). \end{aligned} \quad (9)$$

$S(r)$ is the step function defined by (8), and the constants g, γ, V_0, and r_0 were evaluated to be:

$$g=0.0715, \quad \gamma=0.775, \quad V_0=13.89 \text{ Mev}, \quad r_0=2.80\times10^{-13} \text{ cm}. \quad (10)$$

The known properties of the ground state of the deuteron and low energy collision phenomena are insufficient to discriminate on the basis of a purely phenomenological theory between the interaction (2) and those obtained from it by the inclusion of the factors $-\frac{1}{3}\tau_1\cdot\tau_2$ or $-\frac{1}{2}(1+\tau_1\cdot\tau_2)$, which both have the value unity for states antisymmetrical in the charge.

3. THE SIMPLIFIED NUCLEAR MODEL

The following model is used in the present calculations:

(a) The interaction V between two particles is assumed to be of the form (2) corresponding to the neutral meson theory. The particles are taken to have all their spins parallel. V then becomes an ordinary potential depending on the distance r between the two particles, and the angle θ which r makes with the direction of their spins:

$$V=[J_0(r)+J_1(r)]+(3\cos^2\theta-1)J_2(r). \quad (11)$$

(b) The functions $J(r)$ are replaced by rectangular potential wells of appropriate range r_0. The ranges need not all be the same, but will

be taken the same for convenience. Then:

$$V=AS(r)+BS(r)(3\cos^2\theta-1). \quad (12)$$

(c) The nucleus is taken to have the shape of an ellipsoid of revolution with its axis of symmetry parallel to the spins of the particles. The shape of the ellipsoid is specified by the ratio k of its length along the axis of symmetry to the diameter of its greatest circular cross section ($k>1$ corresponds to prolate, and $k<1$ to oblate ellipsoids). The volume Ω of the ellipsoid is specified by δ which is defined by $\Omega=(\pi/6)(\delta r_0)^3$; i.e., δ is the ratio of the diameter of the sphere having the same volume as the ellipsoid to the range r_0 of the step functions used.

(d) The density ρ of the particles is assumed to be uniform over the volume of the nucleus.

(e) The Coulomb energy, and the exchange integrals of the purely nuclear interaction are neglected, the total energy being calculated as the sum of the direct nuclear interaction and the kinetic energy of all the particles.

If the Coulomb and the exchange integrals are not neglected, and if the surface effect[8] is properly taken into account then calculations based on the above crude model must *necessarily* give an overestimate of the total energy and hence an underestimate of the binding energy, so that any conclusions as to lack of saturation for such a model would *a fortiori* hold for a better one. The additional approximation made in neglecting the Coulomb, the exchange, and the surface energy makes this argument somewhat less conclusive, but the results obtained below are still suggestive enough to make such a model of interest.

4. EVALUATION OF THE POTENTIAL ENERGY

On the above model the potential energy is given by

$$\text{P.E.}=\tfrac{1}{2}\int\int\rho(\mathbf{x})\,V(\mathbf{x}-\mathbf{x}')\,\rho(\mathbf{x}')d\mathbf{x}d\mathbf{x}' \quad (13)$$

$$=\tfrac{1}{2}N^2[A\,W_1(k,\delta)+BW_2(k,\delta)]\equiv W(k,\delta)N^2.$$

Here N is the number of particles in the nucleus and

$$W_1(k,\delta)\equiv\frac{1}{\Omega^2}\int\int S(|\mathbf{x}-\mathbf{x}'|)d\mathbf{x}d\mathbf{x}',$$

$$W_2(k,\delta)\equiv\frac{1}{\Omega^2}\int\int S(|\mathbf{x}-\mathbf{x}'|)(3\cos^2\theta-1)d\mathbf{x}d\mathbf{x}', \quad (14)$$

both integrations being extended twice over the volume of the nucleus. The integrals in (14) may be carried out analytically, and the results are stated in the appendix. From these results, Tables I and II, giving numerical values of $W_1(k,\delta)$ and $W_2(k,\delta)$ as functions of k and δ for several selected values of these parameters, were constructed.

5. KINETIC ENERGY

In the statistical model the wave function of each individual particle is taken to be that of a free particle in a box of a size and shape corresponding to the particular nuclear model under investigation. The number of particles in each level is restricted by the Pauli exclusion principle. Usually two particles are allowed in each level corresponding to the two possible spin orientations. In our case, where the spins are all taken

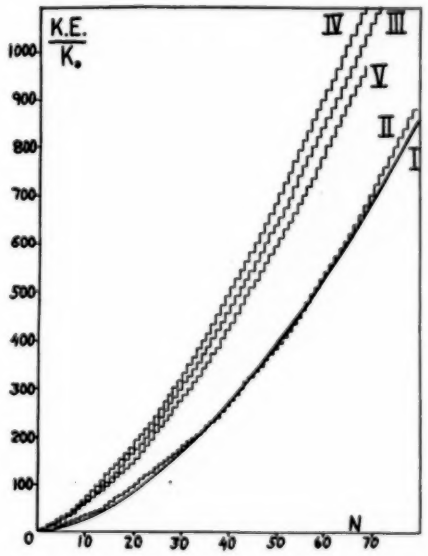

FIG. 2. The total kinetic energy (in units of $K_0=\pi^2\hbar^2/2M\Omega^{\frac{2}{3}}$) of N particles obeying the exclusion principle confined to a box of volume Ω. I—Approximate calculation. II—Cubical box, periodic boundary conditions. III—Cubical box, zero boundary conditions. IV—Rectangular box, ratio of sides 1 : 1 : 3, zero boundary conditions. V—Spherical box, zero boundary conditions.

[8] H. A. Bethe and R. F. Bacher, Rev. Mod. Phys. **8**, 82 (1936); E. Feenberg, Phys. Rev. **60**, 204 (1941).

TABLE III. Values of the function

$$W_B(k,\delta)=\tfrac{1}{2}[7.7W_1(k,\delta)-102W_2(k,\delta)]$$

in Mev.

k	$\delta=0.50$	0.70	0.90	1.0	1.5	2.0	3.0
1.0	3.8	3.8	3.8	3.8	3.0	1.8	0.7
1.5	−13.4	−13.4	−13.1	−12.0	− 3.5	−0.6	0.2
2.0	−25.8	−25.8	−23.5	−21.0	− 7.2	−2.1	−0.1
3.0	−42.4	−40.0	−32.7	−28.4	−11.1	−3.8	−0.5
4.0	−52.3	−45.5	−35.3	−30.4	−12.8	−4.7	−0.8
8.0	−60.5	−45.0	−33.1	−28.2	−13.4	−6.2	−1.3
20.0	−46.3	−32.1	−23.3	−20.2	−10.6	−5.9	−1.8

parallel, there are still two particles in each level—a proton and a neutron.

The familiar formula for the kinetic energy of a large number N of particles obeying the exclusion principle and restricted to a volume Ω, obtained by assigning two particles to each cell of size h^3 in phase space, is

$$\text{K.E.}=\frac{3}{5}\left(\frac{3}{\pi}\right)^{2/3}\frac{\pi^2\hbar^2}{2M\Omega^{2/3}}N^{5/3}=0.582K_0N^{5/3}, \quad (15)$$

where

$$K_0\equiv\pi^2\hbar^2/2M\Omega^{2/3}. \quad (16)$$

This is seen to depend on the mass M of each particle, and on the volume Ω of the box, but not on its shape. However, a more detailed calculation for a small number of particles shows that the result does depend on the shape of the volume Ω, and also on the type of boundary conditions used. Results are given below for a few simple cases.

The simplest case is that of a rectangular box of sides a, k_2a, k_3a and volume $\Omega=k_2k_3a^3$. Two types of boundary conditions are possible: periodic or zero boundary conditions. The wave functions are complex exponentials in the former case, and sines in the latter. The corresponding expressions for the kinetic energy are:

$$(\text{K.E.})_{\exp}=4(k_2k_3)^{\frac{1}{2}}K_0\times\sum[n_1^2+n_2^2/k_2^2+n_3^2/k_3^2]; \quad (17)$$

$$(\text{K.E.})_{\sin}=(k_2k_3)^{\frac{1}{2}}K_0\times\sum[n_1^2+n_2^2/k_2^2+n_3^2/k_3^2]. \quad (18)$$

K_0 is defined by (16). The summation in (17) extends over zero, positive, and negative integral values of n_1, n_2, n_3, while in (18) it extends only over the positive integral values.

TABLE IV. Values of $N_0^{\frac{1}{2}}=-107/\delta^2W_B(k,\delta)$.

k	$\delta=0.50$	0.70	0.90	1.0	1.5	2.0	3.0
1.0							
1.5	32.0	16.3	10.1	8.9	13.7	44.7	
2.0	16.6	8.4	5.6	5.1	6.6	13.0	91.7
3.0	10.1	5.5	4.0	3.8	4.3	7.1	22.4
4.0	8.2	4.8	3.7	3.5	3.7	5.7	15.2
8.0	7.1	4.8	4.0	3.8	3.5	4.3	9.1
20.0	9.3	6.8	5.7	5.3	4.5	4.5	6.5

TABLE V. Average energy per particle in Mev (from Bethe's interaction) for a nucleus containing 45 particles.

k	$\delta=0.9$	1.0	1.5	2.0
3.0	202	76	101	169
4.0	82	−16	25	126
8.0	183	82	−2	61
20.0	621	445	125	72

TABLE VI. Average energy per particle in Mev (from Bethe's interaction) for a nucleus containing 216 particles.

k	$\delta=0.7$	0.9	1.0
3.0	− 778	−2298	−2283
4.0	−1965	−2871	−2723
8.0	−1864	−2388	−1349

Another simple case is that of a spherical box with zero boundary conditions for which

$$\text{K.E.}=(4/3\pi^2)^{\frac{1}{2}}K_0\sum_{n,i}Z^2_{n,i}, \quad (19)$$

where K_0 is given by (16), and $Z_{n,i}$ ($i=1, 2, 3, \cdots$) are zeros of Bessel's functions of order $n=1/2, 3/2, 5/2, \cdots$, the sum being taken over a sufficient number of the lower lying zeros.

Figure 2 gives the ratio K.E./K_0 as a function of the total number of particles for five different cases:

I. Calculated from (15).
II. Calculated from (17) with $k_2=k_3=1$.
III. Calculated from (18) with $k_2=k_3=1$.
IV. Calculated from (18) with $k_2=1$, $k_3=3$.
V. Calculated from (19).

It is of interest to note that although for a given volume of the box the K.E. does not depend strongly on its shape (cubical, oblong, and spherical, respectively, in III, IV, V), it does depend markedly on the type of boundary conditions used (periodic in II, zero in III). For a very large number of particles the ratio of

the K.E. obtained from any of the formulae above to that given by (15) must necessarily approach unity. But for small N it is seen that zero boundary conditions, which lead to a greater concentration of particles towards the center of the box, give a considerably higher energy than the periodic boundary conditions, which for all values of N give results very close to those obtained from (15).

Since in our simple model of the nucleus the density of particles is assumed to be constant over the nucleus, it is consistent to use the periodic rather than the zero boundary conditions on the wave functions in calculating the kinetic energy, the former giving a more uniform particle density. Since the dependence of the kinetic energy on the shape of the nucleus is slight, for simplicity expression (15) is used for all values of k and δ. Rewritten in terms of δ, (15) becomes:

$$\text{K.E.} = KN^{5/3}\delta^{-2}, \tag{20}$$

TABLE VII. Values of the function

$$W_{RS}(k, \delta) = \tfrac{1}{2}[-13.89W_1(k, \delta) - 10.75W_2(k, \delta)]$$

in Mev.

k	$\delta=0.5$	0.7	0.9	1.0	1.5	2.0	3.0
1	−6.94	−6.94	−6.94	−6.94	−5.33	−3.26	−1.30
1.5	−8.76	−8.76	−8.72	−8.51	−5.81	−3.42	−1.34
2.0	−10.07	−10.07	−9.65	−9.15	−5.85	−3.42	−1.34
3.0	−11.81	−11.39	−10.01	−9.19	−5.57	−3.29	−1.31
4.0	−12.83	−11.58	−9.71	−8.76	−5.20	−3.12	−1.27
8.0	−12.84	−10.02	−7.81	−6.93	−3.94	−2.55	−1.12
20.0	−9.33	−6.60	−5.01	−4.42	−2.64	−1.74	−0.86

TABLE VIII. Values of $N_0^{\frac{1}{3}} = -23.3/\delta^2 W_{RS}(k, \delta)$.

k	$\delta=0.5$	0.7	0.9	1.0	1.5	2.0	3.0
1	13.41	6.84	4.14	3.35	1.92	1.79	1.98
1.5	10.63	5.42	3.30	2.74	1.77	1.70	1.93
2.0	9.24	4.72	2.98	2.54	1.75	1.70	1.93
3.0	7.88	4.17	2.87	2.53	1.84	1.77	1.98
4.0	7.26	4.10	2.96	2.66	1.97	1.87	2.04
8.0	7.25	4.74	3.68	3.36	2.60	2.28	2.31
20.0	9.98	7.20	5.74	5.27	3.88	3.34	2.99

TABLE IX. Average energy per particle in Mev (from Rarita and Schwinger's interaction) for a nucleus containing 9 particles.

k	$\delta=1.0$	1.5	2.0
1	38.2	−3.6	−4.1
1.5	24.1	−7.9	−5.6
2.0	18.4	−8.3	−5.6
3.0	18.0	−5.7	−4.4

where

$$K = \frac{9\pi}{5}\left(\frac{3}{2\pi}\right)^{\frac{1}{3}} \frac{\hbar^2}{Mr_0^2} = \frac{38.4}{(\kappa r_0)^2} \text{ Mev}, \tag{21}$$

with $1/\kappa = 2.18\times10^{-13}$ cm.

6. CALCULATION OF TOTAL ENERGY FROM BETHE'S CONSTANTS

Our approximation to the total energy of a heavy nucleus is obtained by adding (13) and (20):

$$E = W(k, \delta)N^2 + KN^{5/3}\delta^{-2}. \tag{22}$$

In order to apply this to Bethe's[5] neutral theory interaction with straight cut-off the functions $F(r)$ and $G(r)$ of Fig. 1 are replaced by the step function $S(r)$ whose range r_0 is so chosen that the area under $G(r)$ is the same as that under $S(r)$. $F(r)$ could be replaced by a step function of a different range, but A is numerically so much smaller than B in (7) as to make the contribution of $W_1(k, \delta)$ to the total energy relatively unimportant, so that for convenience $F(r)$ and $G(r)$ are replaced by the same step function $S(r)$ of range determined by

$$\kappa r_0 = 0.6. \tag{23}$$

The value of K_B is then obtained from (21):

$$K_B = 107 \text{ Mev}, \tag{24}$$

and $W_B(k, \delta)$ calculated from

$$W_B(k, \delta) = \tfrac{1}{2}[7.7W_1(k, \delta) - 102W_2(k, \delta)] \text{ Mev} \tag{25}$$

is given for selected values of k and δ in Table III. The value of N for which $E=0$ is given by

$$N_0^{\frac{1}{3}} = -\frac{K_B}{\delta^2 W_B(k, \delta)} = -\frac{107}{\delta^2 W_B(k, \delta)}. \tag{26}$$

For values of N greater than N_0, E rapidly becomes more and more negative, very soon numerically exceeding the observed value of

TABLE X. Average energy per particle in Mev (from Rarita and Schwinger's interaction) for a nucleus containing 216 particles.

k	$\delta=0.9$	1.0	1.5
2.0	−1048	−1137	−891
3.0	−1126	−1146	−830
4.0	−1062	−1053	−750

roughly $-8N$ Mev. Table IV gives the values of $N_0^{\frac{1}{3}}$ from (26) for selected values of k and δ. In this table the lowest value of $N_0=(3.5)^3=43$ is seen to occur for $k=4$, $\delta=1$. Table V gives the values of the average energy per particle E/N in Mev when $N=45$, and Table VI gives the average energy per particle when $N=216$. If the range r_0 of the step function $S(r)$ replacing $F(r)$ and $G(r)$ in the above calculations is increased so as to satisfy $\kappa r_0=0.7$ instead of $\kappa r_0=0.6$, the lowest value of N_0 is further reduced to $N_0=17$.

The dimensions of the ellipsoid specified by $k=4$, $\delta=1$, $\kappa r_0=0.6$ are: major axis $=3.3\times10^{-13}$ cm, minor axis $=0.83\times10^{-13}$ cm. The ellipsoid is of the order of magnitude of nuclear dimensions, but is excessively elongated.

7. CALCULATION OF TOTAL ENERGY FROM RARITA AND SCHWINGER'S CONSTANTS

Rarita and Schwinger[4] use the step function $S(r)$ of range $r_0=2.80\times10^{-13}$ cm, i.e.,

$$\kappa r_0=1.285. \tag{27}$$

The corresponding value of K_{RS} from (21) is

$$K_{RS}=23.3 \text{ Mev}, \tag{28}$$

and $W_{RS}(k, \delta)$ calculated from

$$W_{RS}(k, \delta)=\tfrac{1}{2}[-13.89W_1(k, \delta) -10.75W_2(k, \delta)] \text{ Mev} \tag{29}$$

is given for selected values of k and δ in Table VII. The value of N for which $E=0$ is given by

$$N_0^{\frac{1}{3}}=-\frac{K_{RS}}{\delta^2W_{RS}(k, \delta)}=-\frac{23.3}{\delta^2W_{RS}(k, \delta)}. \tag{30}$$

Table VIII gives the values of $N_0^{\frac{1}{3}}$ from (30) for selected values of k and δ. In this table the lowest value of $N_0=(1.7)^3=5$ is seen to occur for $k=2$, $\delta=2$. Table IX gives the values of the average energy per particle E/N in Mev when $N=9$, and Table X gives the average energy per particle when $N=216$.

The dimensions of the ellipsoid specified by $k=2$, $\delta=1.5$, $\kappa r_0=1.285$ are: major axis $=6.7\times10^{-13}$ cm, minor axis $=3.4\times10^{-13}$ cm.

8. DISCUSSION

Although the model used in the above calculations has little meaning when applied to nuclei containing as few particles as the values of N_0 obtained above, nevertheless the inference may be drawn from these calculations that interactions of the type suggested by the neutral meson field theory of nuclear forces, although useful for describing the lighter nuclei, will allow stable nuclei having large spins, excessive binding energies, and deviating appreciably from spherical shape to exist well within the range of the atomic weights of the periodic table, contrary to experimental evidence.

The small values of N_0 given by (26) are due to the large negative values of $W_B(k, \delta)$ obtained by using Bethe's interaction. The feature of the interaction responsible for this is the excessive depth of the attractive tensor term as compared with the magnitude of the repulsive spherically symmetric term. This disparity in the relative strengths of the two parts of the interaction between a proton and a neutron is, however, required to give the observed binding energy of the deuteron, if the wave function for the ground state of the deuteron is not to deviate appreciably from spherical symmetry.

The values of $W_{RS}(k, \delta)$ obtained by using Rarita and Schwinger's interaction are numerically much smaller than those of $W_B(k, \delta)$ because in their interaction the tensor and the spherically symmetric terms are both attractive, and consequently the observed binding energy of the deuteron can be obtained with relatively shallow potential wells. In spite of this the values of N_0 given by (30) are even smaller than those given by (26) because K_{RS} in (30) is much smaller than K_B in (26). This is because the width of the potential well used by Rarita and Schwinger is twice the width of the square well introduced above to replace Bethe's potential. The greater is the width of the square well used, the more important is the potential energy relative to the kinetic energy, since the particles can occupy a larger volume, and hence have less kinetic energy, for the same value of the potential energy.

The author takes great pleasure in expressing his gratitude to Professor E. Wigner, under whose direction the work was carried out, for suggesting the problem, and for continued interest and aid during the course of the work. The grant by the Royal Society of Canada of

a Research Fellowship under which this work was carried out is gratefully acknowledged. The author also takes pleasure in acknowledging his debt to the Dean of the Graduate School, and the members of the Physics Department of Princeton University for the many privileges and courtesies extended to him during his three months' stay there.

APPENDIX

The analytical expressions for the functions $W_1(k, \delta)$ and $W_2(k, \delta)$ defined by (14) are given below.

$k \geqq 1$ (Prolate Ellipsoids)

$$\begin{aligned} W_1(k,\delta) &= 1 && \text{for } \delta \leqq k^{-2/3}, \\ &= 8\delta^{-3} - B(k)\delta^{-4} + C(k)\delta^{-6} \\ &\quad - (k^2-1)^{-1/2} D(\delta k^{-1/3}) && \text{for } k^{-2/3} \leqq \delta \leqq k^{1/3}, \\ &= 8\delta^{-3} - B(k)\delta^{-4} + C(k)\delta^{-6} && \text{for } k^{1/3} \leqq \delta, \end{aligned}$$

where

$$\begin{aligned} B(k) &\equiv \tfrac{9}{2} k^{-4/3}[(k^2-1)^{-1/2} \cos^{-1}(k^{-1}) + k^{-2}], \\ C(k) &\equiv \tfrac{1}{4}[3 + 2k^{-2} + 3k^2(k^2-1)^{-1/2} \cos^{-1}(k^{-1})], \\ D(x) &\equiv \tfrac{3}{4}(x^{-2}-1)^{5/2} + 1\tfrac{1}{2}(x^{-2}-1)^{3/2} \\ &\quad + 1\tfrac{5}{4}(x^{-2}-1)^{1/2} - \tfrac{9}{2}(x^{-4} - \tfrac{1}{6}x^{-6}) \cos^{-1} x, \end{aligned}$$

and

$$\begin{aligned} W_2(k,\delta) &= E(k), && \text{for } \delta \leqq k^{-2/3}, \\ &= F(k)\delta^{-4} - G(k)\delta^{-6} + H(k,\delta) && \text{for } k^{-2/3} \leqq \delta \leqq k^{1/3}, \\ &= F(k)\delta^{-4} - G(k)\delta^{-6} && \text{for } k^{1/3} \leqq \delta, \end{aligned}$$

where

$$\begin{aligned} E(k) &\equiv (k^2-1)^{-1}(2k^2+1) - 3k^2(k^2-1)^{-3/2} \cos^{-1}(k^{-1}), \\ F(k) &\equiv \tfrac{9}{8} k^{4/3}[(k^2-4)(k^2-1)^{-3/2} \cos^{-1}(k^{-1}) \\ &\quad + (1+2k^{-2})(k^2-1)^{-1}], \\ G(k) &\equiv \tfrac{1}{8}[3k^2(k^2-2)(k^2-1)^{-3/2} \cos^{-1}(k^{-1}) \\ &\quad + (3k^2 - 4 + 4k^{-2})(k^2-1)^{-1}], \\ H(k,\delta) &\equiv \tfrac{3}{8} k^2(k^2-1)^{-3/2}[(k^2-2)\delta^{-6} - 3(k^2-4)k^{-2/3}\delta^{-4} - 8] \\ &\quad \times \cos^{-1}(\delta k^{-1/3}) + 1\tfrac{5}{4}(k^2-1)^{-1/2}(k^{2/3}\delta^{-2} - 1)^{1/2} \\ &\quad - \tfrac{1}{8}(k^2+44)(k^2-1)^{-3/2}(k^{2/3}\delta^{-2} - 1)^{3/2} \\ &\quad + \tfrac{3}{8}(k^2-2)(k^2-1)^{-3/2}(k^{2/3}\delta^{-2} - 1)^{5/2}. \end{aligned}$$

$k \leqq 1$ (Oblate Ellipsoids)[9]

$$\begin{aligned} W_1(k,\delta) &= 1 && \text{for } \delta \leqq k^{1/3}, \\ &= 1 + (1-k^2)^{-1/2} D'(\delta k^{-1/3}) && \text{for } k^{1/3} \leqq \delta \leqq k^{-2/3}, \\ &= 8\delta^{-3} - B'(k)\delta^{-4} + C'(k)\delta^{-6} && \text{for } k^{-2/3} \leqq \delta, \end{aligned}$$

where

$$\begin{aligned} B'(k) &\equiv \tfrac{9}{2} k^{4/3}[(1-k^2)^{-1/2} \cosh^{-1}(k^{-1}) + k^{-2}], \\ C'(k) &\equiv \tfrac{1}{4}[3 + 2k^{-2} + 3k^2(1-k^2)^{-1/2} \cosh^{-1}(k^{-1})], \\ D'(x) &\equiv \tfrac{3}{4}(1-x^{-2})^{5/2} - 1\tfrac{1}{2}(1-x^{-2})^{3/2} \\ &\quad + 1\tfrac{5}{4}(1-x^{-2})^{1/2} - \tfrac{9}{2}(x^{-4} - \tfrac{1}{6}x^{-6}) \cosh^{-1} x, \end{aligned}$$

and

$$\begin{aligned} W_2(k,\delta) &= -E'(k) && \text{for } \delta \leqq k^{1/3}, \\ &= -E'(k) + H'(k,\delta) && \text{for } k^{1/3} \leqq \delta \leqq k^{-2/3}, \\ &= -F'(k)\delta^{-4} + G'(k)\delta^{-6} && \text{for } k^{-2/3} \leqq \delta, \end{aligned}$$

where

$$\begin{aligned} E'(k) &\equiv (1-k^2)^{-1}(2k^2+1) - 3k^2(1-k^2)^{-3/2} \cosh^{-1}(k^{-1}), \\ F'(k) &\equiv \tfrac{9}{8} k^{4/3}[(k^2-4)(1-k^2)^{-3/2} \cosh^{-1}(k^{-1}) \\ &\quad + (1+2k^{-2})(1-k^2)^{-1}], \\ G'(k) &\equiv \tfrac{1}{8}[3k^2(k^2-2)(1-k^2)^{-3/2} \cosh^{-1}(k^{-1}) \\ &\quad + (3k^2 - 4 + 4k^{-2})(1-k^2)^{-1}], \\ H'(k,\delta) &\equiv \tfrac{3}{8} k^2(1-k^2)^{-3/2}[(k^2-2)\delta^{-6} \\ &\quad - 3(k^2-4)k^{-2/3}\delta^{-4} - 8] \cosh^{-1}(\delta k^{-1/3}) \\ &\quad - 1\tfrac{5}{4}(1-k^2)^{-1/2}(1 - k^{2/3}\delta^{-2})^{1/2} \\ &\quad + \tfrac{1}{8}(k^2+44)(1-k^2)^{-3/2}(1 - k^{2/3}\delta^{-2})^{3/2} \\ &\quad + \tfrac{3}{8}(k^2-2)(1-k^2)^{-3/2}(1 - k^{2/3}\delta^{-2})^{5/2}. \end{aligned}$$

The three separate ranges of validity of all the above results correspond, respectively, to the range r_0 of the step function $S(r)$ being greater than the maximum dimension of the ellipsoid, intermediate between the maximum and minimum dimensions, and less than the minimum dimension.

As $\delta \to \infty$ the values of $W_1(k, \delta)$, $W_2(k, \delta)$, and $W_2(k, \delta)/W_1(k, \delta)$ all approach zero for all values of k.

As $k \to \infty$ for any finite value of δ the values of $W_1(k, \delta)$ and $W_2(k, \delta)$ both approach zero, while their ratio $W_2(k, \delta)/W_1(k, \delta)$ approaches 2.

As $k \to 0$ for any finite value of δ the values of $W_1(k, \delta)$ and $W_2(k, \delta)$ both approach zero, while their ratio $W_2(k, \delta)/W_1(k, \delta)$ approaches -1.

$W_1(k, \delta)$ is always positive, while $W_2(k, \delta)$ is positive for prolate ellipsoids ($k > 1$), negative for oblate ellipsoids ($k < 1$), and zero for a sphere ($k = 1$).

The values of $W_1(k, \delta)$ and $W_2(k, \delta)$ calculated from the above formulae for selected values of k and δ are given in Tables I and II.

[9] The formulae for the oblate case were also obtained independently by W. Rarita and J. Schwinger. I am indebted to them for communicating to me their results and the following numerical values of $W_1(k, \delta)$ and $W_2(k, \delta)$ some of which supplement those already listed in Tables I and II:

δ	k	1	0.9	0.8	0.7	0.6	0.5	0.4	0.3	0.2	0.1
1	$W_1(k,\delta)$	1.000	1.000	0.999	0.996	0.988	0.973	0.945	0.896	0.805	0.624
	$W_2(k,\delta)$	0.000	−0.082	−0.172	−0.266	−0.360	−0.454	−0.542	−0.612	−0.642	−0.566
0	$W_1(k,\delta)$	1.000	1.000	1.000	1.000	1.000	1.000	1.000	1.000	1.000	1.000
	$W_2(k,\delta)$	0.000	−0.082	−0.172	−0.268	−0.370	−0.480	−0.594	−0.714	−0.832	−0.940

A Note on Exchange Tensor Forces in Heavy Nuclei

G. M. VOLKOFF*
Department of Physics, University of British Columbia, Vancouver, British Columbia, Canada
(Received June 9, 1942)

Short range *spherically symmetrical exchange* forces between elementary nuclear particles were first introduced into nuclear theory to account for the observed saturation of nuclear forces. More recently additional *tensor* forces between elementary particles have been proposed. The object of this note is to point out that if tensor forces, whether of the ordinary or the exchange type, are assumed to be the *dominant* forces between nuclear particles, they will not lead to saturation, but will permit the existence of nuclei with excessive values of binding energy, spin, and isotopic number. The presence of a sufficiently strong spherically symmetrical exchange term in the nuclear interaction thus seems to be required to counteract this effect of the tensor forces.

THE Hartree method is used to obtain an estimate of the nuclear energy.[1] The nucleus is described by the completely antisymmetrical wave function

$$\Psi=\begin{vmatrix} \psi_1(\xi_1) & \psi_2(\xi_1) & \cdots & \psi_N(\xi_1) \\ \psi_1(\xi_2) & \psi_2(\xi_2) & \cdots & \psi_N(\xi_2) \\ \cdot & \cdot & & \cdot \\ \cdot & \cdot & & \cdot \\ \cdot & \cdot & & \cdot \\ \psi_1(\xi_N) & \psi_2(\xi_N) & \cdots & \psi_N(\xi_N) \end{vmatrix}. \quad (1)$$

The wave functions $\psi_i(\xi_j)$ describing the individual particles are taken to be products of three factors, one depending only on the space coordinates $\mathbf{r}_j$ of the particle, the second only on its spin, and the third only on its isotopic spin, i.e., specifying whether a given particle is a proton or a neutron. Let the spin wave function be α or β depending on whether the spin component in a given direction Z is $+\frac{1}{2}$ or $-\frac{1}{2}$, and the isotopic spin wave function be p or n according to whether a given particle is a proton or a neutron. Then a given $\psi_i(\xi_j)$ will consist of some spatial wave function $\phi_i(\mathbf{r}_j)$ multiplied by one of the four possible combinations: $\alpha(s_j)p(\tau_j)$, $\beta(s_j)p(\tau_j)$, $\alpha(s_j)n(\tau_j)$, $\beta(s_j)n(\tau_j)$. Let the interaction between a pair of particles be denoted by $V(\xi_i, \xi_j)$, and the kinetic energy of each particle by T_i. The total energy of the nucleus on this model is then given by:[1]

$$E=\sum_{i=1}^{N} T_i+\tfrac{1}{2}\sum_{i=1}^{N}\sum_{k=1}^{N} \times\Big[\int\int \psi_i^*(1)\psi_k^*(2)\,V(1,2)\psi_i(1)\psi_k(2)d\xi_1 d\xi_2 - \int\int \psi_i^*(1)\psi_k^*(2)\,V(1,2)\psi_k(1)\psi_i(2)d\xi_1 d\xi_2\Big]. \quad (2)$$

The integrations in (2) imply summations over the spin and isotopic spin as well as integrations over the space coordinates. After the explicit expression for $V(1, 2)$ has been substituted in (2) and the summations over the spin and isotopic spin coordinates have been carried out two types of space integrals may appear in the result: the "direct" integrals

$$J_{ik}\equiv\int\int \phi_i^*(1)\phi_k^*(2)\,V(\mathbf{r}_{12})\phi_i(1)\phi_k(2)d\mathbf{r}_1 d\mathbf{r}_2, \quad (3)$$

and the "exchange" integrals

$$K_{ik}\equiv\int\int \phi_i^*(1)\phi_k^*(2)\,V(\mathbf{r}_{12})\phi_k(1)\phi_i(2)d\mathbf{r}_1 d\mathbf{r}_2. \quad (4)$$

Using plane waves for $\phi_i(\mathbf{r}_j)$ the following properties of these integrals may be demonstrated.[1] The sum

$$\sum_{i=1}^{N}\sum_{k=1}^{N} J_{ik}=\int\int \rho(1)\,V(\mathbf{r}_{12})\rho(2)d\mathbf{r}_1 d\mathbf{r}_2 \quad (5)$$

is, for small R, proportional to N^2, while the sum

$$\sum_{i=1}^{N}\sum_{k=1}^{N} K_{ik}=\int\int |\rho(1,2)|^2 V(\mathbf{r}_{12})d\mathbf{r}_1 d\mathbf{r}_2 \quad (6)$$

* This note was written while the author was visiting at the Department of Physics, University of California, Berkeley, California. It is a pleasure for him to record his gratitude for the hospitality extended to him.

[1] Cf. H. A. Bethe and R. F. Bacher, Rev. Mod. Phys. **8**, 82 (1936).

is proportional to N. Here

$$\rho(\mathbf{r}) \equiv \sum_{i=1}^{N} |\phi_i(\mathbf{r})|^2$$

and

$$\rho(\mathbf{r}_1, \mathbf{r}_2) \equiv \sum_{i=1}^{N} \phi_i^*(\mathbf{r}_1)\phi_i(\mathbf{r}_2) \tag{7}$$

are the total particle density, and Dirac's "mixed density," respectively. The former may be taken constant over the nucleus and of the order NR^{-3} where R is the nuclear radius. The latter is of order NR^{-3} when $\mathbf{r}_1$ and $\mathbf{r}_2$ coincide, and falls off rapidly as soon as $|\mathbf{r}_1-\mathbf{r}_2|$ becomes greater than $RN^{-\frac{1}{3}}$.

In order to bring out the characteristic features of spherically symmetrical and tensor forces responsible for the difference in their behavior with respect to saturation we substitute for $V(\xi_1, \xi_2)$ in (2) the following four expressions in turn:

	Ordinary	Exchange	
Spherically symmetrical	$J(r)$	$-\frac{1}{3}\boldsymbol{\tau}_1\cdot\boldsymbol{\tau}_2 J(r)$	(8)
Tensor	$J(r)S_{12}$	$-\frac{1}{3}\boldsymbol{\tau}_1\cdot\boldsymbol{\tau}_2 J(r)S_{12}$.	

Here $J(r)$ is a spherically symmetrical potential. S_{12} is defined by

$$S_{12} \equiv 3\frac{\boldsymbol{\sigma}_1\cdot\mathbf{r}\boldsymbol{\sigma}_2\cdot\mathbf{r}}{r^2} - \boldsymbol{\sigma}_1\cdot\boldsymbol{\sigma}_2, \tag{9}$$

which reduces in the case of the two spins pointing in the same direction to

$$S_{12} = 3\cos^2\theta - 1. \tag{10}$$

The exchange operator $-\frac{1}{3}\boldsymbol{\tau}_1\cdot\boldsymbol{\tau}_2$ has the value $+1$ for a state antisymmetrical in the charge (e.g., the ground state of the deuteron), and $-\frac{1}{3}$ for a state symmetrical in the charge (e.g., two protons, or two neutrons). Also by analogy with similar results[1] for the case of the ordinary spin operator $\boldsymbol{\sigma}_1\cdot\boldsymbol{\sigma}_2$:

$$\begin{aligned} &\boldsymbol{\tau}_1\cdot\boldsymbol{\tau}_2 p(1)p(2) = p(1)p(2), \\ &\boldsymbol{\tau}_1\cdot\boldsymbol{\tau}_2 p(1)n(2) = -p(1)n(2) + 2n(1)p(2). \end{aligned} \tag{11}$$

With $V(\xi_1, \xi_2) = J(r)$ the direct integrals J_{ik} all have the same sign as $J(r)$ irrespective of the values of the spin and the isotopic spin of the individual particles, so that (5) is directly applicable resulting in lack of saturation for an attractive $J(r)$. The introduction of the additional exchange operator $-\frac{1}{3}\boldsymbol{\tau}_1\cdot\boldsymbol{\tau}_2$ helps to avoid this difficulty by making the direct integrals between *like* particles contribute *positive* amounts to the total energy counteracting the *negative* contributions of the direct integrals between *unlike* particles. In virtue of (11) the contribution of all the direct integrals from (2) will now be given not by (5) but by

$$-\tfrac{1}{3}\int\int [\rho_p(1)-\rho_n(1)] \times J(r_{12})[\rho_p(2)-\rho_n(2)]d\mathbf{r}_1 d\mathbf{r}_2, \tag{12}$$

where ρ_p and ρ_n are now separately the proton and the neutron densities. If the individual wave functions in (1) are chosen in such a way that there is always both a proton and a neutron in each space-spin state, then $\rho_p-\rho_n$, and hence (12), will be identically zero. For any other distribution of protons and neutrons among the space-spin states (e.g., the extreme case of a nucleus consisting of only protons or only neutrons) such that $\rho_p-\rho_n$ is always of one sign, the total contribution of the direct integrals given by (12) is always *repulsive* for an attractive $J(r)$. When (12) vanishes the binding energy is due entirely to the contributions of the exchange integrals K_{ik}, so that according to (6) saturation will result. Saturation in this case therefore depends on the fact that the direct integral of the interaction $-\frac{1}{3}\boldsymbol{\tau}_1\cdot\boldsymbol{\tau}_2 J(r)$ between two like particles is *necessarily* repulsive for an attractive $J(r)$.

The feature of the tensor forces which produces lack of saturation is the fact that by a proper choice of individual particle wave functions in (1) it is always possible to make *all* the direct integrals J_{ik} give an attractive contribution. Take all the nuclear particles with their spins parallel, so that S_{12} can be replaced by (10). The ordinary tensor interaction is then given by

$$V(\mathbf{r}_{12}) = J(r)(3\cos^2\theta - 1). \tag{13}$$

The contribution of all the direct integrals will be given by (5), and can *always* be made attractive by choosing a particle distribution concentrated along the polar axis (prolate) if $J(r)$ is

negative, or in the equatorial plane (oblate) if $J(r)$ is positive. To show that the exchange tensor force $-\frac{1}{3}\tau_1\cdot\tau_2 V(\mathbf{r}_{12})$ also leads to lack of saturation choose the individual particles not only with all their spins parallel, but also all of the same kind, so that $-\frac{1}{3}\tau_1\cdot\tau_2=-\frac{1}{3}$ for all pairs, which is equivalent to reversing the sign of $J(r)$ in (13). With spherically symmetrical forces such a reversal of sign necessarily leads to a repulsive total contribution proportional to N^2. With tensor forces the reversal of sign of $J(r)$ can be compensated for by a suitable change (prolate to oblate) in the distribution of particles. Therefore if tensor forces alone are assumed to act between elementary nuclear particles they would allow the existence of heavy nuclei composed of only protons or only neutrons, deviating appreciably from spherical shape and having excessive values of the spin and the binding energy.

The presence of a sufficiently strong spherically symmetrical exchange term of the right sign will counteract this tendency of the tensor forces to produce non-saturation. If the spherically-symmetrical exchange term is assumed to be the dominant one, while the tensor force is considered as a perturbation, then it will favor nuclei composed of proton-neutron pairs in identical space-spin states, as was seen above. The exclusion principle will further favor the presence of two protons of opposite spin, and two neutrons of opposite spin in each space state. For such a combination of individual particle wave functions the direct integrals J_{ik} of the tensor part of the interaction will all cancel out pair by pair, as in the spherically symmetrical case, because of the relations

$$\begin{aligned}&\sum_{\tau_1,\tau_2}\sum_{s_1,s_2}\alpha(1)p(1)\alpha(2)p(2)\\&\quad\times S_{12}\tau_1\cdot\tau_2\alpha(1)p(1)\alpha(2)p(2)=3\cos^2\theta-1,\\&\sum_{\tau_1,\tau_2}\sum_{s_1,s_2}\alpha(1)p(1)\beta(2)p(2)\\&\quad\times S_{12}\tau_1\cdot\tau_2\alpha(1)p(1)\beta(2)p(2)=-3\cos^2\theta+1,\end{aligned}\tag{14}$$

and similar relations for neutrons, and likewise for the ordinary tensor force with the $\tau_1\cdot\tau_2$ operator left out. Since the contribution of the direct integrals in this case vanishes saturation again becomes possible.

In a recent paper[2] the influence on heavy nuclei of *non-exchange* interactions combining spherically symmetrical and tensor terms proposed by Bethe and by Rarita and Schwinger was investigated. It was concluded that such interactions would lead to difficulties even for relatively light nuclei. On the basis of the above discussion it would seem that the inclusion of the exchange operator $-\frac{1}{3}\tau_1\cdot\tau_2$ in Rarita and Schwinger's potential will overcome non-saturation and related difficulties, since the spherically symmetric term in their interaction has a depth of 13.39 Mev, while the depth of the tensor term is only 10.75 Mev. On the other hand in Bethe's interaction the tensor term having a depth of 102 Mev far exceeds the 7.7 Mev spherically symmetrical term, so that the inclusion of an exchange operator will not prevent non-saturation.

It is a pleasure to thank Professor J. R. Oppenheimer for his interest in this work, and for valuable discussions.

[2] G. M. Volkoff, Phys. Rev. **62**, 126 (1942).

The Absence of the $M\beta$ X-Ray Satellite Intensity Anomaly*

F. R. HIRSH, JR.
Pasadena, California

(Received January 19, 1942)

The absence of the $M\beta$ x-ray satellite intensity maximum is shown, and explained in terms of the relative probability of Auger transitions, the relative probabilities being determined by means of diagram line widths.

INTRODUCTION

IN a former study of the $M\alpha_1$ and $M\beta$ satellites,[1] the writer especially noted the similarity of the "semi-Moseley" graphs for the maxima of these two groups: they are practically identical. Moreover, in a subsequent paper[2] the writer pointed out how similarly shaped the $M\alpha_1$ and $M\beta$ lines of Bi(83) were (Fig. 7, reference 2). In that same paper,[2] the present writer proposed that the $M\alpha_1$ satellites were due to the transition $M_{\text{V}}N_{\text{IV,V}} \rightarrow N_{\text{VII}}N_{\text{IV,V}}$ effected by the radiationless transition $M_{\text{III}} \rightarrow M_{\text{V}}$ with ejection of an $N_{\text{IV,V}}$ electron; that the $M\beta$ satellites were due to the transition $M_{\text{IV}}N_{\text{IV,V}} \rightarrow N_{\text{VI,}}N_{\text{IV,V}}$ effected by the radiationless transition $M_{\text{III}} \rightarrow M_{\text{IV}}$ with ejection of an $N_{\text{IV,V}}$ electron. Thus the satellites of both the $M\alpha_1$ and $M\beta$ groups could be accounted for by the Auger effect. Moreover, the very similar nature of the two, single-electron transitions between doubly-ionized states, just mentioned, practically ensures the similarity of the semi-Moseley graph groups for $M\alpha_1$ and $M\beta$ as well as that of the over-all line shapes. In Munier, Bearden, and Shaw's article,[3] the $M\alpha$ and $M\beta$ groups for W(74), (p. 541), are very similar, except for fine detail.

With this situation in mind, the present writer investigated the plates from which the measurements of reference 1 were made. It was simple to show photographically that the $M\alpha_1$ lines revealed a maximum of intensity[4] for their satellites near the proper atomic number. In the case of the $M\beta$ satellites, the energy curve for the radiationless transition $M_{\text{III}} \rightarrow M_{\text{IV}}$ intersects and passes above the ionization-energy curve for the $N_{\text{IV,V}}$ shell (necessarily for $Z+1$ as an inner M electron is missing), at $Z=84$ (see Fig. 1). Thus we might expect the Auger effect to occur and doubly ionize atoms below $Z=84$, producing an Auger intensity maximum (anomaly), as in the case of the $M\alpha_1$ satellites.

EXPERIMENTAL

The plates for the $M\beta$ lines[1] (all lines except those for Pt and Ir were taken with a calcite crystal; the two named were taken with a quartz crystal) were photometered by using a Koch microphotometer; the constants were secured and density plotted as a function of wave-length for each x-ray line. The range of the present wave-lengths, from 3.7 to 6.0A, has been studied by the writer[5] who has shown density to be proportional to exposure (intensity constant), over a considerable range of densities. The present writer is not alone in this result.[5] Having

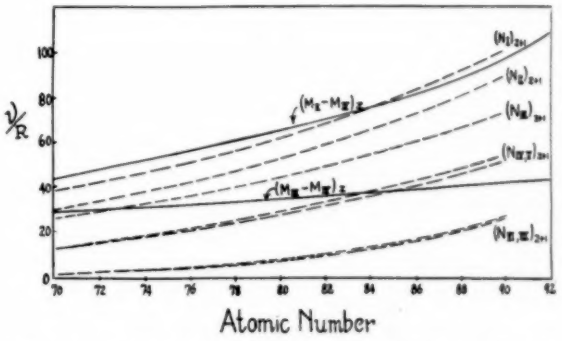

FIG. 1. Coster-Kronig diagram for the satellites of the $M\beta$ line: energy released by the radiationless transitions $M_{\text{II}} \rightarrow M_{\text{IV}}$ and $M_{\text{III}} \rightarrow M_{\text{IV}}$ plotted as a function of atomic number (full line); ionization energies for the various N shells, plotted for $Z+1$ as an M electron is missing (dashed lines).

* The absence of the $M\beta$ satellite intensity anomaly was briefly commented on in a Letter to the Editor of *The Physical Review* [Phys. Rev. **59**, 766 (1941)].

[1] F. R. Hirsh, Jr., Phys. Rev. **38**, 914 (1931).

[2] F. R. Hirsh, Jr., Phys. Rev. **50**, 191 (1936).

[3] J. H. Munier, J. A. Bearden, and C. H. Shaw, Phys. Rev. **58**, 537 (1940).

[4] F. R. Hirsh, Jr., Phys. Rev. **57**, 662 (1940).

[5] F. R. Hirsh, Jr., J. Opt. Soc. Am. **25**, 229 (1935); **28**, 463 (1938).

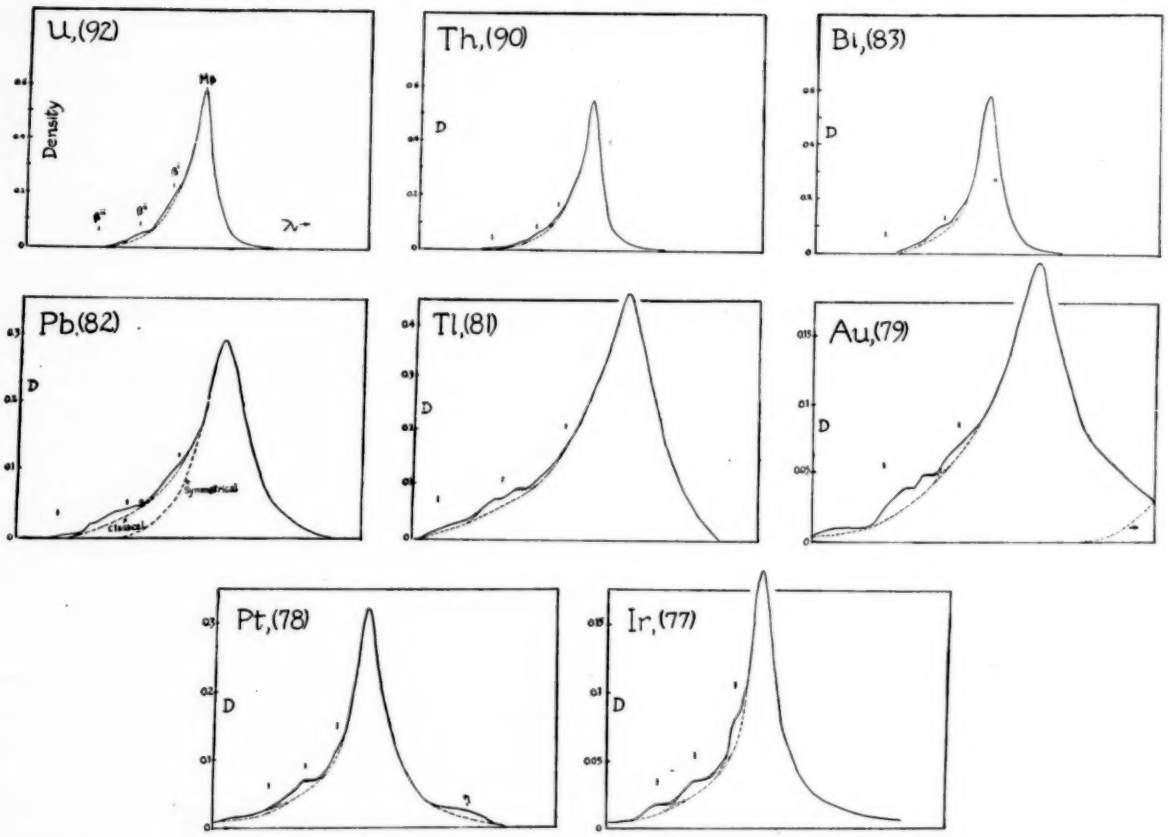

FIG. 2. Density (intensity) plots for $M\beta$ x-ray lines of the elements from U(92) to Ir(77). Vertical lines indicate visual measurements of maxima on the original plates (reference 1).

secured the true over-all intensity shapes for each line (see Fig. 2), a suitable and "reasonable" background for each satellite group was drawn in with a spline and the satellites were delineated. Next, the microphotometer magnification was secured, the Δ's (satellite separations) were computed easily from the Δλ values of reference 1, and the spectrograph radius was known to be 36.728 cm. These Δ values are seen to be quite accurately related to the satellites of Fig. 2, with one exception: the *satellite* $M\beta^{ii}$ is seen from the density (intensity) plots *to be double* (two components) *for* Pb(82), Tl(81), *and* Au(79), *showing without a doubt that the semi-Moseley graph group for the* $M\beta$ *satellites is the exact counterpart of the semi-Moseley graph group for the* $M\alpha_1$ *satellites.*

In each case the $M\beta^{ii}$ satellite is seen to be the most intense component, and easily the best defined. For this reason the intensity of the $M\beta^{ii}$ group, with respect to the parent line, was taken as a measure of x-ray line energy produced by double ionization as compared with the x-ray line energy produced by single ionization. These data are presented in Table I. While there should be an increase in the relative energy (ratio S/P) starting just below $Z=84$, coming to a maximum and falling off with decreasing atomic number, it is quite evident that *the intensity maximum is not present for the* $M\beta$ *satellites.*

The absence of the intensity maximum for the $M\beta$ satellites is made very obvious in an illustration (made from these same plates taken by the

TABLE I. Relative energy (by areas) for the $M\beta^{ii}$ satellite.

Element	$M\beta^{ii}$ satellite area (S)	Parent line area (P)	Ratio S/P
U(92)	0.01×10 sq. in.	0.50×10 sq. in.	0.020
Th(90)	0.01	0.44	0.023
Bi(83)	0.01	0.49	0.020
Pb(82)	0.03	1.22	0.025
Tl(81)	0.045	1.97	0.023
Au(79)	0.07	2.76	0.025
Pt(78)	0.02	0.78	0.026
Ir(77)	0.028	0.86	0.032

present author[1]) on page 305 of H. E. White's book, *Introduction to Atomic Spectra*. Here the satellites of $M\alpha_1$ show an unmistakable maximum of intensity at Pb(82), while it is absent for the $M\beta$ satellites.

DISCUSSION OF EXPERIMENTAL RESULTS

One fact that is evident in Fig. 1, is that the radiationless transition $M_{II} \rightarrow M_{IV}$ can eject an N_I electron at $Z=84$, and below that atomic number. Thus *there are two Auger transitions possible at and below $Z=84$: one which will produce the $M\beta$ satellite group, ($M_{III} \rightarrow M_{IV}$) and one which will not*, ($M_{II} \rightarrow M_{IV}$). If it could be shown that the radiationless transition $M_{II} \rightarrow M_{IV}$ was more probable than the radiationless transition $M_{III} \rightarrow M_{IV}$, the first transition would rob the second to its effective exclusion. This seems to be actually the fact, and will now be discussed.

A very interesting fact, which is not necessarily essential to this argument, but which tells us what intra-level transfers are effective as radiationless transitions, is that *all the known radiationless transitions, which cause the known x-ray satellite intensity anomalies, are permitted by the x-ray quantum number selection rules:* $\Delta j = \pm 1, 0$; $\Delta k = \pm 1$; Δn is arbitrary. For $L_I \rightarrow L_{III}$ ($L\alpha_1$ and $L\beta_2$ satellites), $\Delta j = -1$, and $\Delta k = -1$; for $L_I \rightarrow L_{II}$ ($L\beta_1$ satellites), $\Delta j = 0$ and $\Delta k = -1$; for $M_{III} \rightarrow M_V$ ($M\alpha_1$ satellites), $\Delta j = -1$ and $\Delta k = -1$. Similarly for the two radiationless transitions under discussion: for $M_{III} \rightarrow M_{IV}$, $\Delta j = 0$ and $\Delta k = -1$; for $M_{II} \rightarrow M_{IV}$, $\Delta j = -1$ and $\Delta k = -1$.

Theoreticians might immediately raise a protest as to the significance of these last observations. However, it will be remembered that in 1922 D. Coster[6] was searching for radiations corresponding to the transition $L_I \rightarrow L_{III}$ (permitted by selection rules). He failed in this first search; he later reported[7] that radiation had been observed very faintly for a few atomic numbers. We now know why this search failed at first: $L_I \rightarrow L_{III}$ is much more probable as a radiationless transition (see reference 7). Such electron jumps are *intra-level transfers* as compared with the usual *inter-level transfers* which give rise to the ordinary x-ray diagram lines. Thus it would seem evident that *these intra-level transfers, while probable to some extent as ordinary permitted transitions yielding radiation, are much more probable as radiationless transitions.* The significance of the radiationless transitions being permitted by selection rules is that the *selection rules point out where the radiationless transitions are sure to occur.*

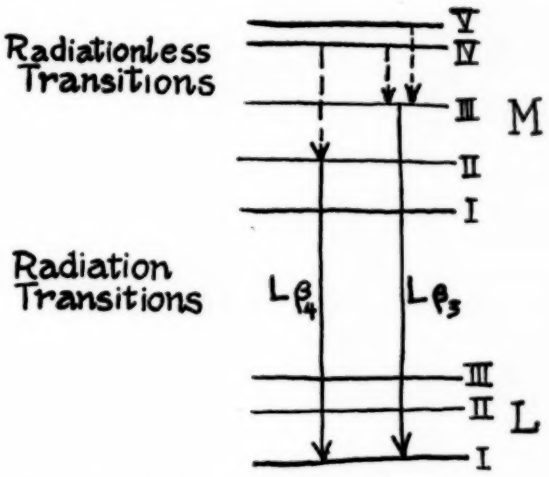

FIG. 3. Energy level diagram showing relation of radiationless transitions to radiation transitions in interpreting Auger probabilities in terms of line widths.

With this last fact well in mind, let us proceed to the solution of the problem caused by the absence of the $M\beta$ x-ray satellite intensity anomaly. Figure 3 shows the situation as regards the radiationless transitions: all are permitted by selection rules; two result in ionization of the M_{IV} shell ($M_{III} \rightarrow M_V$ ionizes the M_V shell), but the $M_{III} \rightarrow M_{IV}$ transition alone could cause enhancement of the $M\beta$ satellite group, as has been previously discussed in this paper. The facts are as follows: $M_{III} \rightarrow M_{IV}$ and $M_{III} \rightarrow M_V$ both broaden the M_{III} level by decreasing its mean ionized life; $M_{II} \rightarrow M_{IV}$ broadens the M_{II} level similarly by decreasing its mean ionized life. If the M_{II} level is broader than the M_{III} level, we would immediately see that $M_{II} \rightarrow M_{IV}$ has an extremely high probability of occurrence. Ramberg and Richtmyer[8] *ascribe practically the entire breadth of such levels to Auger transitions.* How may we measure the breadth of the M_{II} and M_{III} levels? Fortunately, there are two radiation transitions starting from these levels and ending in a common level: $L\beta_4$ and $L\beta_3$ (see Fig. 3). Any difference in the width of the $L\beta_4$ line as

[6] D. Coster, Phil. Mag. **43**, 1089 (1922).
[7] D. Coster and R. DeL. Kronig, Physica **2**, 13 (1935).
[8] E. Ramberg and F. K. Richtmyer, Phys. Rev. **51**, 913 (1937).

TABLE II. Corrected line breadths (ev).

	Yb(70)	Lu(71)	Ta(73)	W(74)	Re(75)	Os(76)	Ir(77)	Pt(78)	Au(79)	Tl(81)
$L\beta_4$	13.9	—	14.1	15.1	16.4	17.1	17.7	18.4	19.6	20.4
$L\beta_3$	12.9	12.8	11.7	12.3	13.6	14.7	14.9	16.1	17.2	18.4
Diff.	1.0	—	2.4	2.8	2.8	2.4	2.8	2.3	2.4	2.0

compared with the $L\beta_3$ line, must be due to the greater width of the M_{II} level compared with the M_{III} level. The breadth of a diagram line has been shown to be equal to the sum of the breadths of the two energy levels between which the electron transition takes place.[9]

One way of expressing the Bohr-Heisenberg indeterminacy principle is:

$$\Delta E_l \cdot \Delta T_l \approx \hbar, \tag{1}$$

where ΔE_l is the uncertainty in measuring the energy of a certain atomic phenomenon, and ΔT_l is the uncertainty in measuring the time of its occurrence. Equation (1) is dimensionally equivalent to the more commonly quoted form. Let ΔE_l be considered to be the energy breadth of a given electron energy level, and ΔT_l the mean ionized life: we then see that the indeterminacy principle applies to our problem. Let $\Gamma_l = 1/\Delta T_l$, where Γ_l is the reciprocal of the mean ionized life. Then

$$\Delta E_l \approx \hbar \cdot \Gamma_l. \tag{2}$$

But

$$\Gamma_l = \sum_{(A)} \gamma_l^{(A)} + \sum_{(R)} \gamma_l^{(R)}, \tag{3}$$

which says that for a particular level Γ_l is the sum of all the γ's contributed by the Auger transitions, plus the sum of all the γ's contributed by ordinary radiation transitions.[8]

Now Ramberg and Richtmyer[8] have shown that in the M and N levels where the Auger transitions are the chief contributors to the breadth of levels:

$$\Gamma_l = \sum_{(A)} \gamma_l^{(A)}, \tag{4}$$

i.e.,

$$\sum_{(A)} \gamma_l^{(A)} \gg \sum_{(R)} \gamma_l^{(R)}.$$

Then from (2) and (4) we have

$$\Delta E_l \approx \hbar \sum_{(A)} \gamma_l^{(A)}. \tag{5}$$

From (5), for the M_{II} level:

$$\Delta E_{M_{II}} \approx \hbar \gamma_{(M_{II} \to M_{IV})}. \tag{6}$$

For the M_{III} level:

$$\Delta E_{M_{III}} \approx \hbar \{\gamma_{(M_{III} \to M_{IV})} + \gamma_{(M_{III} \to M_V)}\}. \tag{7}$$

For the $L\beta_4$ line Weiskopf and Wigner have shown:[9]

$$\Delta E_{L\beta_4} = \Delta E_{M_{II}} + \Delta E_{L_I}. \tag{8}$$

For the $L\beta_3$ line:

$$\Delta E_{L\beta_3} = \Delta E_{M_{III}} + \Delta E_{L_I}. \tag{9}$$

Subtracting (9) from (8) we have:

$$\Delta E_{L\beta_4} - \Delta E_{L\beta_3} = \Delta E_{M_{II}} - \Delta E_{M_{III}}. \tag{10}$$

Substituting in (10) from (6) and (7) we then have:

$$\Delta E_{L\beta_4} - \Delta E_{L\beta_3} \approx \hbar \{\gamma_{(M_{II} \to M_{IV})} - [\gamma_{(M_{III} \to M_{IV})} + \gamma_{(M_{III} \to M_V)}]\}. \tag{11}$$

But $\Delta E_{L\beta_4} - \Delta E_{L\beta_3}$ is always + (positive) between $Z=70$ and $Z=81$ as is shown in Table II, data from the thesis of Dr. John N. Cooper,[10] written at Cornell University in 1940. I am indebted to Dr. Cooper for an admirable presentation of the subject of line breadths.

This, then, affirms the idea that $M_{II} \to M_{IV}$ is more probable, according to line widths, than $M_{III} \to M_{IV}$ and $M_{III} \to M_V$ combined; this fact prevents the occurrence of the $M\beta$ satellite intensity anomaly.

ACKNOWLEDGMENTS

The writer wishes to acknowledge that the original $M\beta$ line plates were taken at the Cornell X-Ray Laboratory.

The author especially wishes to thank Dr. Millikan for extending research privileges at the California Institute.

[9] V. Weiskopf and E. Wigner, Zeits. f. Physik **63**, 54 (1930); **65**, 18 (1930).

[10] J. N. Cooper, Phys. Rev. **61**, 224 (1942).

The Absorption Spectra of CdF and SnCl

CHARLES A. FOWLER, JR.
Department of Physics, University of California, Berkeley, California
(Received May 21, 1942)

Cadmium fluoride, vaporized in an electric furnace, shows no absorption in the region λλ1950–7000 at temperatures below 1350°C, but above this temperature a band system of CdF appears at λλ2716–2924. Strong continuous absorption is observed at higher temperatures. The spectrum of SnCl is photographed in absorption for the first time. The spectrum consists of the two band systems observed in emission, a new system in the farther ultraviolet, and two continua. Its similarity to the absorption spectrum of the homologous molecule SnF is discussed.

I. CdF

PEARSE and Gaydon have shown[1] that the only spectrum previously attributed to CdF was actually due to the presence of CaF as an impurity. They have listed six other bands between λ2819 and λ3005 as possibly due to CdF inasmuch as they could not be traced to any known impurity, but have hesitated to attribute them definitely to this molecule because of their weakness and general behavior. Since those investigations were carried out in arc emission, it was thought that an attempt to observe the spectrum in absorption might give less ambiguous results.

The absorbing vapor was produced by heating a small amount (~10 g) of CdF_2 in a carbon-tube furnace previously described.[2] The spectral region λλ1950–7000 was surveyed under low dispersion and regions showing band structure were photographed in the first order of the 30,000 lines-per-inch, 21-foot concave grating with average dispersion of 1.3A/mm. The experimental technique has been fully described in a previous article.[3]

At the lower furnace temperatures no bands were observed but at about 1350°C some narrow regions of absorption around λ2800 appeared. With the vapor at 1600° the bands were quite strong (Fig. 1), but at higher temperatures continuous absorption, coming in from shorter wave-lengths, began to cover up the region. High dispersion spectrograms revealed six bands shaded to the red and spaced almost equally, their intensities decreasing from band to band in the direction of shorter wave-lengths. Although the first two bands of longest wave-length are the strongest of the system, they have very diffuse heads. The third has a fairly definite head while those of the fourth, fifth, and sixth are of increasing sharpness. Each of the third, fourth, and fifth bands has a weak satellite associated with the strong head. A narrow continuum with its maximum at λ2824 and a group of three closely spaced heads apparently not belonging to the principal system constitute the remaining features of the spectrum. Measured wave-lengths of the heads and the corresponding wave numbers in vacuum are given in Table I together with an assignment of probable values for $v'-v''$. The individual quantum numbers cannot be assigned with certainty because only a single progression is observed, the higher members of each sequence being covered by the first member. The values of $v'-v''$ in Table I are the most probable when one considers the great likelihood of a v' progression in absorption, despite the fact that the trend of

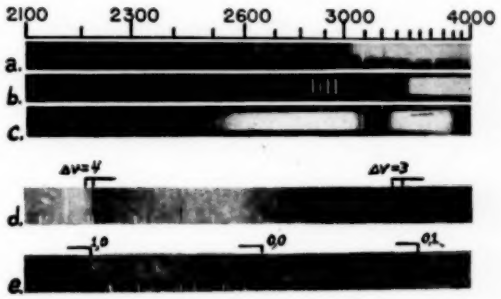

FIG. 1. Low dispersion absorption spectra of (*a*) CdF, (*b*) SnCl with the vapor density high, (*c*) SnCl with the vapor density low. High dispersion spectrograms of (*d*) part of the CdF band system and (*e*) the lower energy component of the $C^2\Pi$, $X^2\Pi$ system of SnCl.

[1] R. W. B. Pearse and A. G. Gaydon, Proc. Roy. Soc. **50**, 711 (1938).
[2] F. A. Jenkins and G. D. Rochester, Phys. Rev. **52**, 1135 (1937).
[3] C. A. Fowler, Jr., Phys. Rev. **59**, 645 (1941).

TABLE I. Band heads of CdF.

$v'-v''$	λ	ν	ΔG
0	2923.5 A	34196 cm^{-1}	
			509 cm^{-1}
1	2880.6	34705	
			514
2	2838.5	35219	
			522
3	2797.1	35741	
			529
4	2756.3	36270	
			535
5	2716.2	36805	
Satellite heads			
2	2837.2	35236	
			519
3	2796.0	35755	
			526
4	2755.5	36281	
Unclassified heads			
—	2788.2	35855	
			22
—	2786.5	35877	
			20
—	2784.9	35897	

the first differences indicates otherwise. Such a trend of the differences is possible, however, if the rotational and vibrational constants have certain, nearly equal values in the two electronic states involved in the transition.

A visual inspection shows that the over-all extent of each band is not large and that the rotational structure is unresolved except near the tail of the band, indicating a very small value for $B'-B''$, so that the band heads are formed at high J values and at considerable distances from the band origins. Furthermore, the distance between each band head and its origin will decrease rapidly with increasing v'. Therefore, although the first differences of the origin wave numbers will decrease with v', the first differences of the band heads may increase. Two features of the CdF bands support this assumption. The low (long wave-length) members of the progression whose heads should be formed at very high values of J show an almost headless nature, while the heads of the higher members are increasingly sharp. Furthermore, the third, fourth, and fifth bands possess satellite heads of increasing sharpness, which would not be expected in the lower members owing to the high J values at such heads. The diffuseness and lack of resolution is increased by the approximate superposition of the many bands of each sequence, superimposed because of the near equality of ω_e' and ω_e''. It is evident from the foregoing that all of the $v'-v''$ might well have values less by one than those given in Table I.

The vibrational constants cannot be accurately determined because only one progression of heads is measurable. Moreover, the first differences are poor representations of the $\Delta G(v+\frac{1}{2})$ when B' and B'' are nearly equal. The data indicate that ω_e' and ω_e'' are almost equal and somewhat greater than 535 cm^{-1}. A comparison of the normal state vibration frequencies of CdCl (330.5 cm^{-1}), CdBr (230.0 cm^{-1}), and CdI (178.5 cm^{-1}) with those of the various alkaline earth halides[4] reveals strikingly similar trends, and predicts for CdF a vibration frequency of about 540 cm^{-1}. Such a comparison also predicts for ZnF a normal state vibration frequency of about 630 cm^{-1}, in close agreement with the 620 cm^{-1} reported by Rochester and Olsson.[5]

No other bands were observed between λ1950 and λ7000. It is to be noted that although they lie in the same general region, there is no correlation in wave-lengths or first differences between these bands and those of Pearse and Gaydon.

II. SnCl

The spectrum of SnCl has been observed only in emission where it shows two band systems, a $^2\Delta$, $^2\Pi$ system[6] at $\lambda\lambda$3486–3910 and a $^2\Sigma$, $^2\Pi$ system[7] in the region $\lambda\lambda$2830–3405. The $^2\Pi$ level, with doublet separation of 2360 cm^{-1}, is common to both systems and is assumed to be the normal state. The occurrence of a $^2\Pi$ lower state in the absorption spectrum of the SnF molecule[2] implies the same type of normal state for all of the halides of Si, Ge, Sn, and Pb.

This investigation was undertaken to test the possibility of observing any shorter wave-length band systems analogous to those of SnF by observing the spectrum in absorption.

[4] G. Herzberg, *Molecular Spectra and Molecular Structure*, I (Prentice-Hall, 1939), pp. 483–494.
[5] G. D. Rochester and E. Olsson, Zeits. f. Physik **114**, 495 (1939).
[6] W. F. C. Ferguson, Phys. Rev. **32**, 607 (1929).
[7] W. Jevons, Proc. Roy. Soc. **A110**, 365 (1926).

With furnace temperatures ranging from below the boiling point of $SnCl_2$ (605°C) to 1000°C a weak, general absorption due to $SnCl_2$ was observed, but only by superheating the vapor to higher temperatures did the bands and continua characteristic of SnCl become evident. At 1200°C the higher energy component of the $B^2\Sigma \leftarrow X^2\Pi$ system is of considerable intensity, but the lower energy component is hidden by a strong, sharply defined continuum covering the region λλ3000–3500. A second continuum extends from λ2500 to the ultraviolet limit of observation at λ1950. At these temperatures the salt was quickly vaporized, and the vapor density slowly decreased by diffusion from the carbon tube. The rate of this diffusion can be governed by regulating the temperature, and a series of low dispersion spectrograms showed that the continua decrease in extent as time goes on. At one stage the more refrangible component of the $A^2\Delta \leftarrow X^2\Pi$ system (λ3488) could be observed under the edge of the weakening continuum. In the same manner the short wave-length continuum in retreating to the ultraviolet revealed a new band system at λλ2250–2450 consisting of a number of heads shaded to the ultraviolet (Fig. 1).

High dispersion plates of this system were taken with a furnace temperature of 1300°C and were exposed only during a predetermined 15-minute interval for which the vapor density was suitable for the bands to appear. The heads of the system fall readily into two groups, three faint bands at λλ2436, 2416, 2393 and six stronger ones between λ2249 and λ2326. These constitute the two components of a doublet system, the heads of the higher energy component being represented by the equation

$$\nu = 43656.1 + 392.8u' - 1.40u'^2 - 352.8u'' + 1.00u''^2.$$

TABLE II. Wave-lengths and intensities of the band heads of the $C \leftarrow X$ system of SnCl.

v', v''	λ	I	v', v''	λ	I
2,0	2248.86	8	0,1	2307.42	5
1,0	2268.62	10		2436.38	0
	2393.08	1	0,2	2326.16	2
0,0	2288.88	9	1,3	2323.80	3
	2415.67	1			

The observed wave-lengths and the estimated intensities are given in Table II.

A difference of 2292.2 cm^{-1} exists between the two 0,0 heads. Inasmuch as the $^2\Pi$ normal state has a separation of 2360.1 cm^{-1}, the new upper state must also be double, i.e., $^2\Pi$ or $^2\Delta$, since a $^2\Sigma$ upper level would produce two sub-bands whose separation equals the lower state interval. In both $^2\Pi, {}^2\Pi$ and $^2\Delta, {}^2\Pi$ transitions only two sub-bands are expected because of the selection rules, and the wave number difference must be the difference (or the sum) of the doublet separations of the two levels involved. Hence the new upper state is a doublet with a separation of 67.9 cm^{-1}. That the heads are apparently single implies that the upper state is $^2\Pi$, but this is not conclusive because of the low intensity of the bands.

The intensity ratio of the two sub-bands depends upon the temperature of the vapor and the splitting of the normal state if a Boltzmann distribution is assumed, and is given by $e^{-E/kT} = \frac{1}{9}$ for the temperature of 1300°C. This agrees well with a visual estimate of the 0,0 bands. Comparison of the intensities of the two sub-bands is very difficult, however, because of a rapid fall of background intensity toward shorter wave-lengths. This is an inherent characteristic of the H_2 continuum used as the source, and is here accentuated by a partially overlying absorption continuum.

The analogy between the electronic states of SnCl and SnF is quite obvious. Both possess $^2\Pi$ normal states. The $A^2\Delta$ and $B^2\Sigma$ states of SnCl correspond to the $B^2\Delta$ and $A^2\Sigma$ states, respectively, of SnF as pointed out by Jenkins and Rochester,[2] while the new state of SnCl is probably $^2\Pi$ corresponding to the $C^2\Pi$ state of the fluoride. Failure to observe the D state can be attributed to the strong overlying continuum. The two continua, because of their close association with the band systems, must be attributed to SnCl. They indicate the existence of the repulsive states E and F, and these, like the stable excited states, have somewhat smaller energies than their SnF analogues.

In conclusion the writer wishes to thank Professor F. A. Jenkins for his assistance and criticism in these investigations.

The β-ray Spectra of Rubidium^{86}, Strontium^{89}, Ekatantalum, and Protactinium*

EDITH HAGGSTROM
Department of Physics, Columbia University, New York, New York

(Received June 4, 1942)

The theory of the action of a recently developed β-ray spectrograph is discussed briefly and an account is given of several improvements. In particular a baffle system of greater resolving power and a G-M counting system of greater stability are described in detail. The β-ray spectra of rubidium^{86}, strontium^{89}, ekatantalum, and protactinium were measured. The use of thin collodion for the backing of sources and windows of counter permitted accurate measurements down to 50 kev. The upper energy end points were found to be: rubidium^{86}—1.60±.03 Mev; strontium^{89}—1.32±0.03 Mev; ekatantalum—230 kev. The Fermi and K-U plots of Rb^{86} and Sr^{89} are given.

A NEW solenoidal type β-ray spectrograph has been described recently by Witcher and co-workers[1] which has as its greatest advantage a good combination of resolving power and efficiency. The relatively high value of the efficiency (1 percent of the total number of particles emitted can be detected) has been found extremely useful for the study of many artificially radioactive substances of small intensities. One of the major advantages of this instrument is that radioactive sources covering fairly large circular areas may be utilized without decreasing the resolution seriously. This permits the use of extremely thin sources and minimizes dispersion due to scattering within the source material.

As originally constructed the resolution of the instrument (half-width of line divided by $H\rho=5$ percent) was satisfactory for continuous spectra, but the complete resolution of many line spectra such as ekatantalum required a baffle system of greater resolving power. Further work has therefore been done on this instrument to increase its usefulness by designing an alternate baffle system which could be substituted when stronger sources were available and when it was desirable to study a line spectrum in more detail. The new baffle system, besides reducing the spread of the beam, introduces some improvements in the geometry of the spectrograph, i.e., it enables the source, slits, and counter to be more accurately lined up and centered.

This type of spectrograph requires a special form of Geiger-Mueller counter which, in general, does not have the characteristics which make the ordinary counter a satisfactory detector for β-rays. Further work has therefore been done to improve the counter characteristics and to make it useful for work at low energies.

THE BAFFLE SYSTEM AND THE RESOLUTION OF THE SPECTROGRAPH

In this spectrograph a homogeneous magnetic field is used to focus the electrons. The field is produced by a solenoid and that portion of the solenoidal field is utilized which is homogeneous to within 1 percent. The path of an electron with an initial momentum making an angle α with the magnetic field is a helix of radius $(mcv/eH)\sin\alpha$ and pitch $(2\pi mcv/eH)\cos\alpha$, whose axis is parallel to the magnetic field. An electron emerging from a point source on the solenoidal axis will return to the axis after completing one revolution, the distance between the source and the point where it returns being equal to the pitch of the helix. If z denotes the displacement of the electron in the direction of the axis (the source taken as origin) and R the displacement of the electron from the axis in a direction perpendicular to it, then $R=(2mcv/eH)\cdot\sin\alpha\cdot\sin(eHz/2mcv\cos\alpha$. If we write $D=2mcv/eH$, then

$$R=D\cdot\sin\alpha\cdot\sin(z/D\cos\alpha).$$

For fixed z_1 and D_1 (at a plane distant z_1 from the source and for a fixed ratio of electron velocity to field strength), R will vary with the angle of emission α, and the mathematical condition that will give a point of focus at $R=R_1$, is that $dR/d\alpha=0$. The symmetry of the field about the

* Publication assisted by the Ernest Kempton Adams Fund for Physical Research of Columbia University.

[1] Witcher, O'Conor, Haggstrom, and Dunning, Phys. Rev. **55**, 1135A (1939); Witcher, Phys. Rev. **60**, 32 (1941).

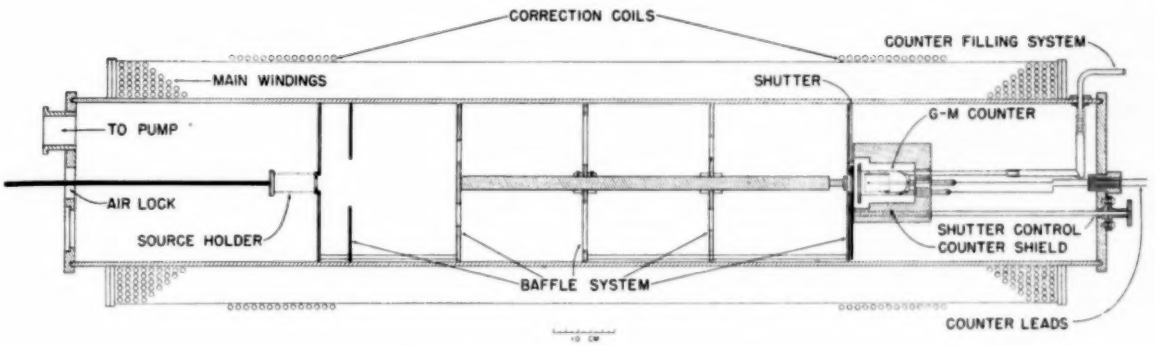

FIG. 1. Solenoidal β-ray spectrograph.

axis then leads to the focusing of all electrons with the same velocity and an angle of emergence α in a ring of radius R_1, in the plane $z=z_1$. A point focus is obtained if R_1 vanishes concurrently with $dR/d\alpha$. This requires that α be equal to 0, and since in this case there is no separation of the different velocities the focal ring must be of finite radius.

A diaphragm situated at a distance z_1 from the source and having an annular slit of radius R_1, will permit the focused electrons to pass through the instrument. A system consisting of a source and one such diaphragm would allow other electrons besides those which are focused at the slit to pass through, and an additional diaphragm is necessary to determine completely the helix within the limits set by the finite widths of the slits, if it can be assumed that no electron makes more than one revolution. By having a rod of material situated along the axis for most of the length of the spectrograph, the possibility of an electron making more than one revolution is ruled out.

FIRST BAFFLE SYSTEM

While only two slits are necessary, the baffle system originally designed contained a large number of slits which outlined the paths taken by the electrons of maximum and minimum velocity and angle of emergence that were allowed to pass through the spectrograph. An inner series of disks which are supported on a rod coincident with the axis outlines the curve $7.16 \sin (z\pi/90)$. The brass wall of the solenoid at its central point together with the inner diameters of two rings on either side of the center lies on the sine curve $12.5 \sin (z\pi/90)$. This baffle system, though more complicated than necessary and especially difficult to study exactly when computations of the average efficiency of extended sources are being made, has been designed to reduce scattering. There has been no evidence of any error due to scattering when this baffle system has been used. It was constructed so that the electrons were focused 86 cm distant from the source; the inner radius of the annular slit at that plane was 1 cm, and the outer radius was 1.5 cm. The value of D for which the efficiency of the spectrograph is a maximum is $94.7/\pi$. The emergent angles of the electrons which constitute the beam vary between 12° 36′ and 23° 30′. The solid angle at maximum efficiency is 1 percent and the half-width of the resolution curve (the plot of efficiency against D) is 5 percent. The choice of this geometry which leads to a good combination of resolution and efficiency under the practical restrictions of the size and power of the available solenoid has been discussed previously by Witcher.[1] He has also discussed the theoretical and experimental resolution curves for an extended circular source 2 cm in diameter.

SECOND BAFFLE SYSTEM

In the new baffle system the number of defining slits has been reduced to three. Two additional diaphragms whose slits are so large that they do not intercept the beam have been introduced to eliminate scattering. The annular ring slits are carefully centered with respect to the axis by means of bars connecting the outside ring to the inner disk. The β-ray source is in the form of a circular area 0.5 cm in diameter centered on the

axis of the instrument. The Geiger-Mueller counter has an open area greater than that of the last slit and is situated 1 cm behind the diaphragm where the electrons come to a focus. The maximum solid angle is obtained for $D=30$ and for this value of D the angles α range from 8.9° to 18.7°. The half-value of the resolution curve divided by the $H\rho$ value at the peak is 2.5 percent. Figure 1 shows the spectrograph with the new baffle system in place.

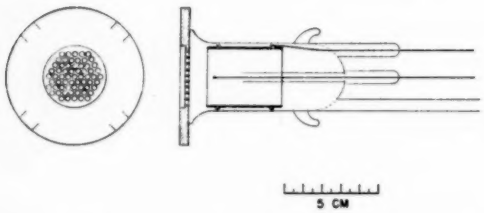

FIG. 2. G-M counter for use with spectrograph.

SOURCE

While the geometry of the instrument determines the efficiency for any point on an extended source, the intensity for any given source is a function of the diameter of the source. The resolution becomes greater as the diameter of the source is decreased. Sources up to 2 cm in diameter may be used.

The source, which is made by dropping the radioactive material in the center of a film of collodion of the order of 0.7-μ thickness, supported by an aluminum ring, is placed in position by fitting the ring into a diaphragm which has a central hole. Scattering from the collodion film support should be negligible for electrons above 30 kev.[2]

To minimize the small residual scattering that might take place by multiple scattering from the brass wall of the instrument, a sheet of fiber board 1/64″ thick is rolled to cover the wall of the solenoid between the source and the final slit.

GEIGER-MUELLER COUNTER

Inasmuch as the solenoidal spectrograph focuses the electrons in an annular ring, the electrons must enter the counter at one end and the cylindrical electrode must therefore be at least 3 cm in diameter. To keep the background of the counter low, the length of the cylinder was made relatively small (4 cm) and the central wire was covered by glass tubing leaving an active region of only 2-cm length exposed. The effect of this restricted geometry is that the pulses generated are small. Previously, the counter window was mounted on a metal grill and it was found necessary to apply a potential intermediate between that on the central wire and the cylindrical electrode to prevent spontaneous discharges through the counter to the grill. The counter characteristics have been improved by substituting a plastic grill with 60 percent open area ($\frac{1}{8}$″ holes) which results in increased stability and a wider plateau.

0.5-mil thick Cellophane windows are satisfactory for use down to 1900 $H\rho$ and approximate corrections can be made down to 800 $H\rho$. For accurate spectra below this energy, thinner collodion windows were used to close the counter. The film is made by dropping a half-and-half solution of collodion and amyl acetate on distilled water. The size of the holes in the grill determines the strength, i.e., the thickness necessary to withstand the pressure in the counter. In order to obtain a film that was tight over the comparatively large area of 10 cm², a film made of 12 superimposed layers of original film was necessary. Since each film is approximately 0.08μ thick the total thickness is about 1μ.

The collodion film when laid over the open area of the grill extends only about 2 mm beyond the open area and the pressure in the counter is sufficient to seal the thin film to the grill. A thin film of stopcock grease provides a satisfactory seal between the ground edge of the counter and the ground plastic grill, the two being held together by means of rubber bands that pass over hooks on counter and grill. A counter gas mixture of 9 cm of argon and 1 cm of alcohol has been found satisfactory, a five-gallon ballast flask being connected to the system to stabilize the pressure over a long period against possible porosity in the thin films. The operating characteristics of the counter are now very satisfactory with the threshold at 800 volts and a plateau of more than 150 volts. The counter is shown in Fig. 2.

Such a counter closed with a thin window of approximately 1-μ thickness of collodion will give

[2] A. Flammersfeld, Zeits. f. Physik **112**, 727 (1939).

accurate spectra for electrons ranging down to 50 kev without appreciable corrections.[2] Since the collodion films will vary somewhat in thickness, it is not possible to extrapolate accurately to zero thickness by placing one, two, and three additional thicknesses in the path of the beam by means of a shutter. It is therefore necessary to determine the region in which the spectra are not distorted by absorption in another way. This is done by placing one additional film in the path of the beam, varying the energy of the beam, and determining the point at which the intensity of the beam is not reduced by the film. For all energies above this point, the spectra are accurate.

COUNTER STANDARDIZATION

As a check on the sensitivity of the counter, a source of uranium oxide electroplated on copper is placed in one of the shutter windows. The use of this β-ray source has been found preferable to a radium γ-ray standard outside the instrument, especially when it is necessary to compare the operation of the counter over long periods of time. It is thus possible to measure the decay of a spectrum with accuracy. The counter is completely shielded from the uranium when the shutter is turned through 180°, and the background of the counter, which is about 20 per minute, is not affected by the presence of the uranium in the spectrograph.

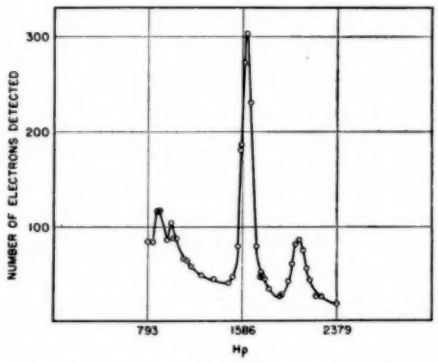

FIG. 3. Uncorrected spectrum of $_{91}$ekatantalum^{233}.

THE SPECTRA OF EKATANTALUM AND PROTACTINIUM

A. V. Grosse, E. T. Booth, and J. R. Dunning[3] have reported on the preparation of a β-emitting isotope of the naturally radioactive protactinium. Thorium in the form of a solution freed from the naturally radioactive protactinium is irradiated by slow neutrons from the Columbia cyclotron. The irradiated thorium shows a strong β-activity having a half-life of 25 minutes which could be explained by the formation of Th^{233} by resonance capture in an (n, γ) reaction which disintegrates by β-emission into an isotope of protactinium—$_{91}$ekatantalum^{233}.

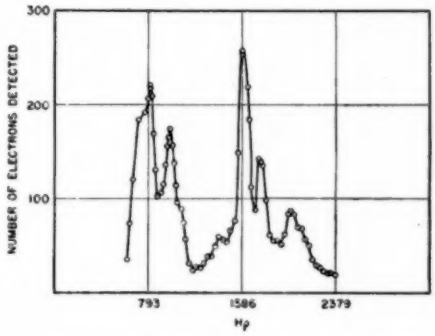

FIG. 4. Uncorrected spectrum of $_{91}$protactinium^{231}.

The chemical separation of ekatantalum from the irradiated thorium gives a product which is again β-active, tests on an ionization chamber giving the half-life as 27.4 ± 0.3 days. The decay of this substance by the emission of an electron would give rise to a new nucleus, presumably an unstable isotope of uranium, $_{92}U^{233}$. To establish definitely that the ekatantalum emitted nuclear electrons, the β-ray spectrum was examined.

The source after preparation by Dr. Grosse was placed over a 2-cm diameter area on a thin collodion film about 0.7μ thick. The layer of material was very thin so as to produce no effect from back scattering above the energy at which the accuracy of the instrument is limited by absorption in the Cellophane counter window. The comparison of the spectra obtained from two sources whose thickness and backing were different, established that errors due to back scattering were not apparent in the region of the spectrum reported on. The counter window was of 0.5-mil Cellophane.

The spectrum of ekatantalum shown in Fig. 5 has been obtained from the experimental results plotted in Fig. 3 by correcting for decay, division of ordinates by H to allow for the varying resolu-

[3] A. V. Grosse, E. T. Booth, and J. R. Dunning, Phys. Rev. **59**, 322 (1941); G. T. Seaborg, J. W. Gofman, and J. W. Kennedy, Phys. Rev. **59**, 321 (1941).

tion of the instrument, and by correcting for absorption in the Cellophane window. This last is done by placing one, two, and three additional layers of Cellophane in front of the counter window and extrapolating to zero thickness. The correction curve as a function of the energy is shown in Fig. 6 and gives the factor by which the actual intensity must be multiplied to yield a corrected spectrum. These corrections have been applied down to $H\rho = 800$ although it is difficult

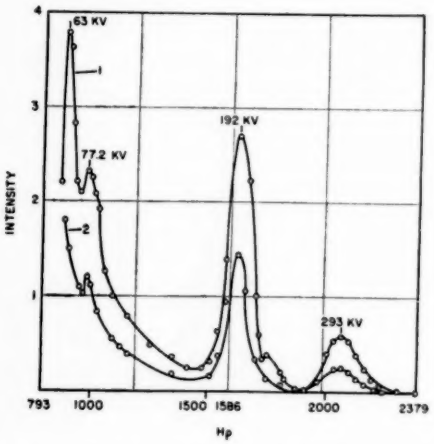

FIG. 5. Corrected β-ray spectrum of $_{91}$ekatantalum^{233}.

to establish just where the approximation becomes to poor to apply.

The spectrum of ekatantalum contains at least four γ-ray conversion lines at 63 kev, 77.2 kev, 192 kev, and 293 kev. Two of these lines, those at 192 kev and 293 kev, appear to be complexes of unresolved lines. The spectrum above 230 kev seems to consist of conversion lines alone; the lines below 230 kev appear to be superimposed on a continuous background. The spectrum has been followed with an accuracy of 2 percent on the peaks and the points have been taken too close together to admit of any undiscovered line of any intensity in the portion of the continuous background between 1000 and 1500 $H\rho$. If we rule out the possibility of this portion of the curve having been formed by a large number of lines all of small intensity, it can be concluded that the ekatantalum emits nuclear electrons, and that a uranium isotope $_{92}U^{233}$ is formed. The maximum energy end point is masked by the line at 192 kev. By subtracting this line from the continuous spectrum, the end point of the continuous spectrum appears to lie in the neighborhood of 230 kev.

A source of naturally radioactive protactinium $_{91}Pa^{231}$ prepared by Dr. Grosse was examined in order to compare it with its isotope and thereby establish independently the purity of the ekatantalum. Although Figs. 3 and 4 (plot of number of electrons detected against current or corresponding $H\rho$) show a similarity in the positions of some of the most intense conversion lines, the relative intensities and positions of the lines differ markedly. The spectrum of protactinium obtained checks as far as the resolved lines are concerned with the spectrum obtained by L. Meitner.[4]

To check further the purity of the sources and the modes of decay, both the ekatantalum and protactinium were remeasured after 27 days. The curve 2 of Fig. 5 shows that all parts of the ekatantalum curve decay at the same rate. The half-life of the ekatantalum measured on the spectrograph by taking an average of the decay at various points along the curve was 26.0 ± 0.5 days which checks well with the observed decay period for the bulk material. Since there was no

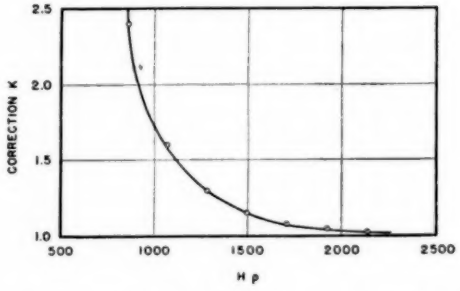

FIG. 6. Correction factor for absorption in 0.5-mil Cellophane window.

observable change in the shape of the ekatantalum curve, it was not possible to make any discovery as to the mode of decay of the product uranium nucleus. The natural protactinium showed no decay at the second measurement as is to be expected if the sample is pure. The spectra shown in Figs. 3 and 4 are the experimental plots of the electron intensity against the current or corresponding $H\rho$.

[4] L. Meitner, Zeits. f. Physik **50**, 15 (1928).

THE SPECTRUM OF RUBIDIUM[86]

Helmholz, Pecher, and Stout[5] have succeeded in producing a radioactive product with a period of 19.5 days by the bombardment of Sr with 16-Mev deuterons by the (d, α) reaction. They definitely established this product to be rubidium. By comparing their results with those of Snell[6] (who found an 18-min. and 18-day period after the bombardment of Rb^{85} and Rb^{87} with slow neutrons giving rise to the isotopes Rb^{86} and Rb^{88}), they concluded that the radioactive Rb was Rb^{86}, since this is the only Rb of the two that could be formed by the Sr (d, α) reaction, Sr^{88} being the heaviest Sr.

Three microcuries of Rb^{86} were prepared in the form of Rb Cl for examination in the spectrograph. The solution was dropped onto a collodion film about 0.7μ thick resulting in an invisible layer of Rb Cl when dry. The spectrum was first studied with a counter window of 0.4-mil thick Pliofilm, and a careful study made of the upper energy region. For the low energy region a counter window of approximately 1-μ thick collodion was employed. The curves from these two measurements were reduced to the same intensity

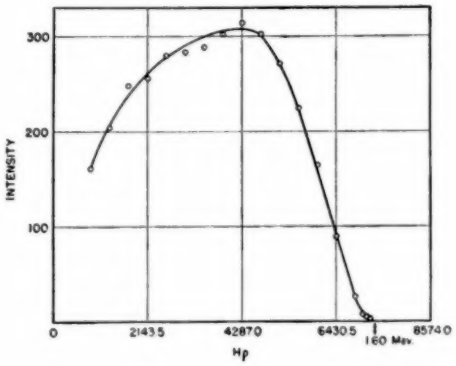

FIG. 7. β-ray spectrum of rubidium[86].

at a point above the energy at which absorption occurs in the Pliofilm window.

Figure 7 shows the corrected spectrum of Rb^{86}. It is seen that the upper end point of the experimental spectrum lies at $H\rho = 7288$. After correcting this upper energy end point for the finite spread of the resolution curve the value 1.60 Mev ±.03 is obtained as the true end point. The value obtained by Helmholz, Pecher, and Stout from absorption measurements is 1.56 Mev calculated from Feather's rule.

THE SPECTRUM OF STRONTIUM[89]

Sr^{89} is produced by bombarding Sr^{88} with deuterons in the (d, p) reaction. A source of 2.78 microcuries of this Sr^{89} was prepared for study.

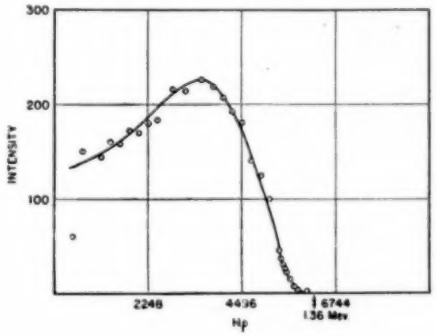

FIG. 8. β-ray spectrum of strontium[89].

The solution was prepared in the lactate form and after placing a drop of the concentrated solution on the center of the 0.7-μ thick collodion film the source after drying was invisible. There is little probability that an error in the spectrum has occurred due to back scattering from the source.

As in the case of rubidium the spectrum was first examined with a 0.4-mil Pliofilm window closing the counter and a second run was taken at the low energy end with a collodion film of approximately 1-μ thickness on the counter. The source strength was such as to give a counting rate of only 144 counts per minute at the peak. The counting period was such as to give an accuracy of ±2 percent on most of the points of the curve except at the upper and lower energy end of the spectrum. Figure 8 shows the spectrum thus obtained. The upper energy end point when corrected for the finite spread of the resolution curve is 1.32 Mev ±0.03. The half-life of this substance is 55 days.

[5] A. C. Helmholz, C. Pecher, P. Stout, Phys. Rev. **59**, 902 (1941).
[6] A. H. Snell, Phys. Rev. **52**, 1007 (1937).

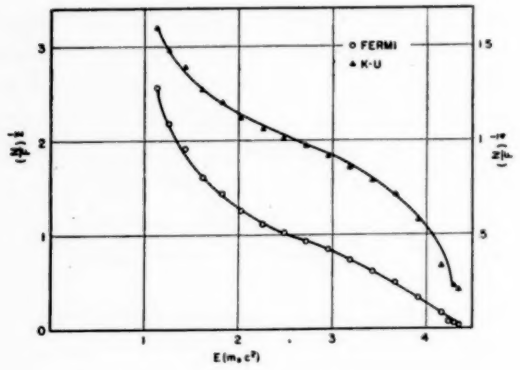

FIG. 9. Fermi and K-U plots for rubidium[86].

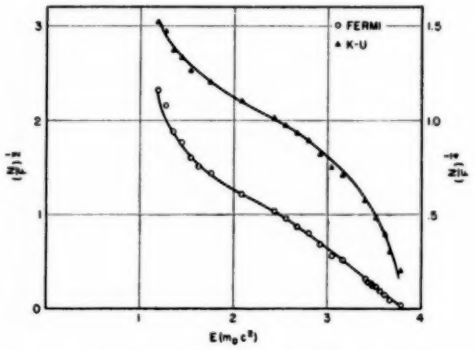

FIG. 10. Fermi and K-U plots for strontium[89].

THE SHAPE OF THE SPECTRA

Since both rubidium[86] and strontium[89] lie on the second forbidden Sargent curve, it is not to be expected that the Fermi plot for these elements be straight lines. To facilitate comparison between these and other doubly forbidden spectra such as P^{32}, the Fermi and K-U plots of Rb^{86} and Sr^{89} are shown, in Figs. 9 and 10. N represents the intensity and $F(\eta, Z)$ is the Fermi function for low Z

$$F(\eta, Z)=\eta^2(2\pi y/1-e^{-2\pi y});\ y=Z[(1+\eta^2)^{\frac{1}{2}}/137\eta].$$

It is seen that toward the upper energy end points of both of these spectra the Fermi plot is very nearly a straight line but at low energies it is convex toward the axis and lies above the extended straight line.

I wish to express my sincere thanks to Professor J. R. Dunning and Dr. E. T. Booth for their constant suggestions and advice during the course of this work, and to my co-workers, Dr. C. M. Witcher and J. O'Conor, S. J., for their cooperation and assistance in the research. I am indebted to Dr. A. V. Grosse and Dr. J. M. Kenny for their aid in procuring radioactive sources.

The Vibration-Rotation Spectrum of SiH_4

CHARLES H. TINDAL,* JOSEPH W. STRALEY,** AND HARALD H. NIELSEN
Mendenhall Laboratory of Physics, The Ohio State University, Columbus, Ohio

(Received May 15, 1942)

The infra-red bands of SiH_4, measured originally by Steward and Nielsen, have been remeasured at considerably higher resolving power. From a rotational analysis of the bands the equilibrium value of B and values of B for the vibration states ν_2, ν_3, ν_4, $\nu_2+\nu_3$, and $\nu_3+\nu_4$ have been determined, B being $h/8\pi^2Ic$. These have, respectively, the values $B_0=3.00$ cm^{-1}, $B''=2.96$ cm^{-1}, $B'(\nu_3)=2.95$ cm^{-1}, $B_+'(\nu_2)=3.06$ cm^{-1}, $B_-'(\nu_2)=3.02$ cm^{-1}, $B'(\nu_4)=2.89$ cm^{-1}, $B_+'(\nu_3+\nu_4)=3.05$ cm^{-1}, $B_0'(\nu_3+\nu_4)=2.97$ cm^{-1}, $B_-'(\nu_3+\nu_4)=2.94$ cm^{-1}, $B_+'(\nu_2+\nu_3)=3.05$ cm^{-1}, and $B_-'(\nu_2+\nu_3)=2.98$ cm^{-1}. The centers of the bands have been determined to be the following: $\nu_2=974.6$, $\nu_3=2190.6$ cm^{-1}, $\nu_4=914.2$ cm^{-1}, $(\nu_2+\nu_3)=3148.8$, $(\nu_3+\nu_4)=3100.2$. The value of $\zeta_4=\frac{1}{2}-\zeta_3=0.454$ is in good agreement with the value predicted by Jahn for valence force fields. From the band centers the valence force constants are calculated.

I. INTRODUCTION

THE infra-red spectrum of SiH_4 was investigated originally by Steward and Nielsen[1] who observed three principal absorption regions near 900 cm^{-1}, 2200 cm^{-1}, and 3100 cm^{-1}, all of which were partially resolved into rotational structure. The first two of these were bands exhibiting P, Q, and R branches and were identified with the fundamental vibration frequencies ν_4 and ν_3, respectively. The third region was found to consist of two overlapping bands with centers at 3095 cm^{-1} and 3153 cm^{-1} which may be identified as $\nu_3+\nu_4$ and $\nu_2+\nu_3$, respectively.

These measurements revealed, moreover, that the rotational structure, especially in the 11-μ region, was much more complex than was consistent with the simple theory of tetrahedrally symmetric molecules prevalent at that time. This structure has since been studied by Murphy[2] who has given a qualitative description of it on the basis of a theory proposed first by Childs and Jahn[3] and by Jahn[4] and subsequently verified by Shaffer, Nielsen, and Thomas,[5] that because the frequency ν_4 has nearly the same value as the twofold degenerate frequency ν_2 a resonance interaction of the Coriolis type is set up. This interaction removes the degeneracy in the rotational quantum number K so that a rotation level is split into $(J+1)$ component levels. The result is that a multiplet line should occur where on the basis of the simple theory a single line was predicted.

The data of Steward and Nielsen were not sufficiently good, however, to yield very accurate information concerning the structure of the molecule. Since then the experimental techniques have been so much improved that almost complete resolution of the bands might now be hoped for. In an effort to obtain data which might yield reliable information concerning the intermolecular distances and, perhaps, the force constants we have undertaken to remeasure these bands.

II. EXPERIMENTAL

The spectrometer used to remeasure this spectrum was the same used in similar investigations carried out in this laboratory. For these measurements two echellette gratings were used, one ruled with 900 lines per inch for the region 9.0μ to 12μ and another ruled with 4800 lines per inch for the regions 3.2μ and 4.6μ.

Two absorption cells were required; one 6 cm long was most useful for the regions near 11.0μ and 4.6μ and another 20 cm long was best suited for the work at 3.2μ. These were of glass tubing closed at the ends by polished plates of rocksalt.

In all cases it was possible to operate the spectrometer with slits adjusted to subtend an angle equivalent to 0.25 cm^{-1}. Deflections of the

* Now at Mt. Holyoke College, South Hadley, Massachusetts.
** Now at University of Toledo, Toledo, Ohio.
[1] W. B. Steward and H. H. Nielsen, Phys. Rev. **47**, 878 (1935).
[2] G. M. Murphy, J. Chem. Phys. **8**, 71 (1940).
[3] W. H. T. Childs and H. A. Jahn, Proc. Roy. Soc. **A169**, 451 (1939).
[4] H. A. Jahn, Proc. Roy. Soc. **A168**, 469 (1938).
[5] W. H. Shaffer, H. H. Nielsen, and L. H. Thomas, Phys. Rev. **56**, 1052 (1939).

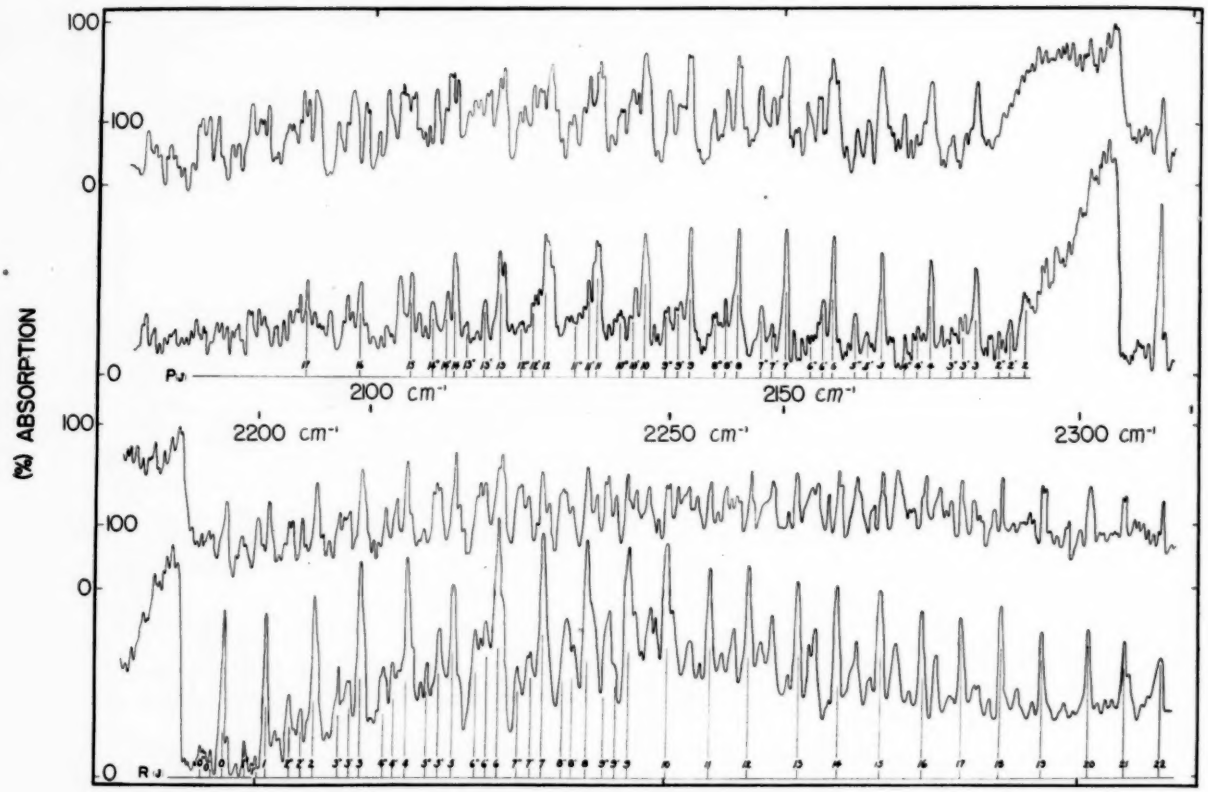

FIG. 1. 4.6-μ region of SiH_4.

galvanometer were recorded with the absorption cell in the light beam and with the cell out of the light beam so that the data could be recorded in terms of percent absorption. Records of the data were made at intervals on the spectrometer circle equivalent to about 0.2 cm^{-1}.

The SiH_4 gas used was taken from the same container from which the samples used by Steward and Nielsen were obtained. The gas had been prepared for them by Professor Warren C. Johnson of the University of Chicago.

The Absorption Band at 4.6μ

The measurements made on the absorption region near 4.6μ, plotted in percent absorption against a scale of frequencies, are shown in Fig. 1. The upper curve (A) represents the pattern obtained by using the 6-cm absorption cell filled with SiH_4 gas to a pressure of 12 cm Hg and the lower curve (B) was obtained with the same cell filled with SiH_4 to a pressure of only 6 cm Hg. Each curve represents the characteristics which were repeated in three independent runs over this region. Curve A may be said to reproduce the data of Steward and Nielsen with high fidelity when one considers that the slit widths and the corresponding intervals on the circle at which data were recorded were in this case roughly one-sixth of those of the earlier attempt. The second curve is much better resolved, shows much more detail and much sharper lines than the upper curve. The actual heights of the principal lines are not altered appreciably, but the relative intensities of the satellite lines to the principal lines are quite different. This suggests that in curve A the spectrum may be regarded as much "over-exposed" and that curve B presents a far more accurate picture of the 4.6μ band than does A. In the first column of Table I are set down the frequency positions of the principal lines and the more important satellite lines.

The Region 9.0μ to 12.0μ

Figure 2 represents the details which were repeated in three independent sets of data taken on the absorption by SiH_4 gas between 9.0μ and

12.0μ. The region from 800 cm^{-1} to 950 cm^{-1} is by far the more intense and for the measurements on this region a cell 6 cm long filled with SiH_4 gas to a pressure of 5 cm Hg was found suitable. In order to make measurements on the absorption by SiH_4 in the region from 950 cm^{-1} on, it was necessary to increase the pressure of the gas to 12 cm Hg. The absorption pattern shown in Fig. 2 reproduces quite faithfully the earlier measurements by Steward and Nielsen except that much more detail is revealed. In the first column of Table II are set down the frequency positions of the more prominent peaks measured throughout this region.

The Absorption Bands at 3.2μ

In Fig. 3 are shown the reproducible details of three independent sets of measurements made over the absorption region near 3.2μ in the spectrum of SiH_4. This region consists of two overlapping bands with centers near 3.17μ and 3.23μ. The bands are considerably better resolved and much more detail is discernible in the present set of data, but in general details the pattern obtained by S and N for this region is well reproduced. To obtain these measurements it was necessary to use a cell 20 cm long containing gas at a pressure of 40 cm Hg. In Table III are recorded the frequency positions of the more important lines measured in this region of absorption.

III. DISCUSSION OF THE RESULTS

The vibration and rotation of the tetrahedrally symmetric XY_4 type molecule have been studied in considerable detail by several authors. Such molecules may oscillate in four different normal modes with the frequencies ω_1, ω_2, ω_3, and ω_4. The first is frequently referred to as the breathing frequency and corresponds to a symmetrical periodic motion of the Y particles to and from the X particle. It is non-degenerate and induces zero electric moment. The vibration ω_2 is perhaps best visualized as one where the four Y particles move approximately in small ellipses about their positions of equilibrium. This frequency is twofold degenerate and like ω_1 induces zero electric moment. The frequency ω_3 is essentially a vibration of the four Y particles along the XY bonds in such a manner that two Y particles are approaching the X particle while the other two are receding. This can take place in three independent ways so that the frequency ω_3 is threefold degenerate. The frequency ω_4 is essentially a deformation frequency where one XYX angle decreases in magnitude while the opposite XYX band angle increases in size. Also this type of

TABLE I. Frequency positions and identifications of absorption lines near 4.4μ.

Frequency positions	Identifications	Frequency positions	Identifications
2091.2	$P(17)$	2210.1	$R''(3)$
2092.0		2211.3	$R'(3)$
2097.2	$P(16)$	2212.9	$R(3)$
2098.8		2215.6	$R''(4)$
2103.2	$P(15)$	2216.9	$R'(4)$
2104.8		2218.4	$R(4)$
2107.4	$P''(14)$	2221.0	$R''(5)$
2109.0	$P'(14)$	2222.5	$R'(5)$
2109.9	$P(14)$	2224.1	$R(5)$
2111.3	$P''(13)$	2226.8	$R''(6)$
2113.9	$P'(13)$	2228.0	$R'(6)$
2115.2	$P(13)$	2229.5	$R(6)$
2115.8		2232.2	$R''(7)$
2118.4	$P''(12)$	2233.4	$R'(7)$
2120.0	$P'(12)$	2234.8	$R(7)$
2121.1	$P(12)$	2237.1	$R''(8)$
2124.1	$P''(11)$	2238.5	$R'(8)$
2126.1	$P'(11)$	2240.3	$R(8)$
2127.2	$P(11)$	2242.9	$R''(9)$
2130.1	$P''(10)$	2243.9	$R'(9)$
2131.3	$P'(10)$	2245.2	$R(9)$
2132.8	$P(10)$	2246.2	
2135.5	$P''(9)$	2248.0	
2137.0	$P'(9)$	2250.2	$R(10)$
2138.6	$P(9)$	2251.2	
2141.4	$P''(8)$	2252.6	
2142.9	$P'(8)$	2253.9	
2144.5	$P(8)$	2255.1	$R(11)$
2147.2	$P''(7)$	2256.8	
2148.5	$P'(7)$	2258.2	
2150.2	$P(7)$	2260.0	$R(12)$
2153.1	$P''(6)$	2262.8	
2154.9	$P'(6)$	2264.5	
2156.1	$P(6)$	2265.8	$R(13)$
2158.8	$P''(5)$	2268.1	
2160.1	$P'(5)$	2269.6	
2161.9	$P(5)$	2270.8	$R(14)$
2165.3	$P''(4)$	2272.9	
2166.5	$P'(4)$	2274.8	
2168.0	$P(4)$	2276.0	$R(15)$
2170.6	$P''(3)$	2277.9	
2172.2	$P'(3)$	2279.2	
2173.5	$P(3)$	2281.2	$R(16)$
2179.2	$P(2)$	2282.5	
2185.1	$P(1)$	2284.5	
2193.2	$R''(0)$	2285.7	$R(17)$
2194.6	$R'(0)$	2287.2	
2196.2	$R(0)$	2289.5	
2199.6	$R''(1)$	2290.6	$R(18)$
2200.8	$R'(1)$	2292.0	
2201.3	$R(1)$	2294.0	
2204.9	$R''(2)$	2295.8	$R(19)$
2206.0	$R'(2)$	2300.3	$R(20)$
2207.2	$R(2)$	2305.5	$R(21)$
		2310.2	$R(22)$

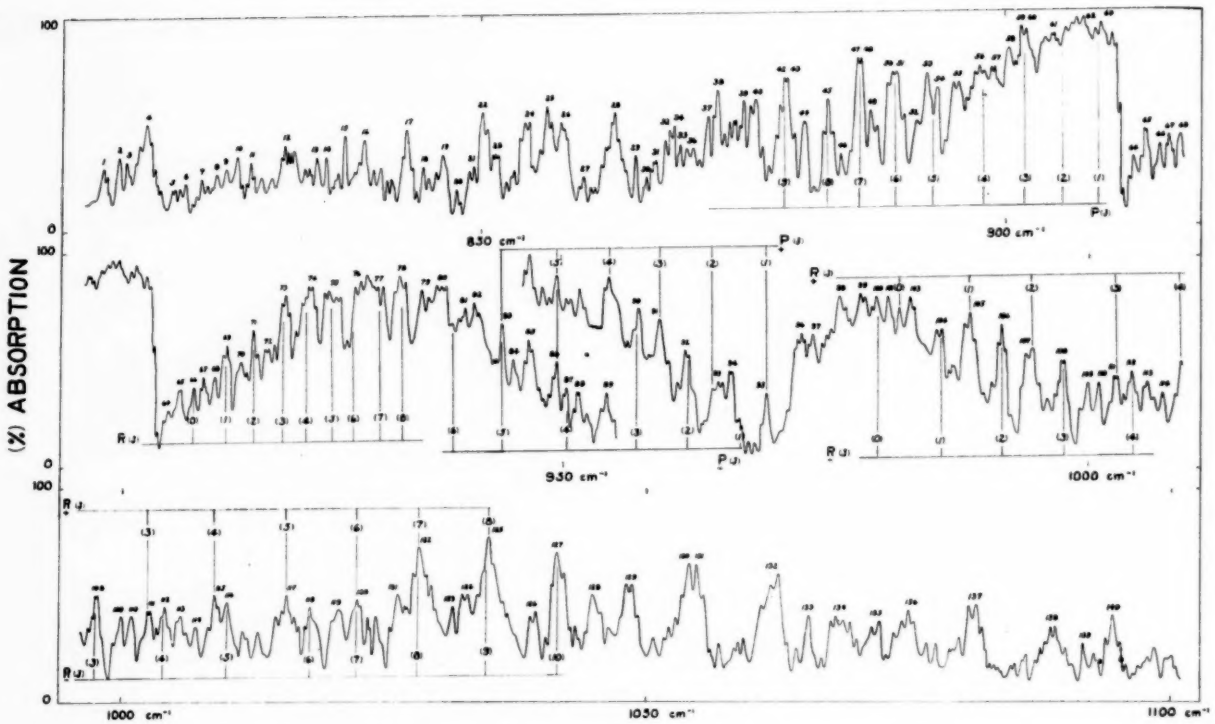

FIG. 2. The region 9μ to 12μ of SiH_4.

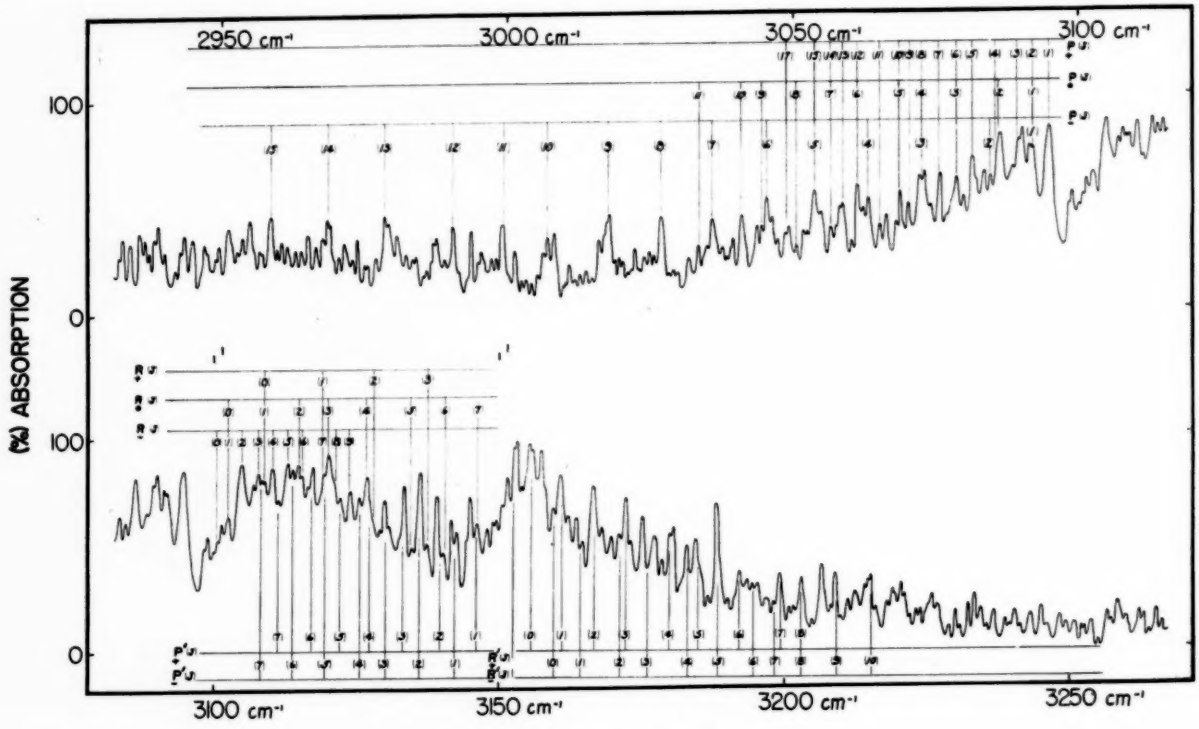

FIG. 3. 3.2-μ region of SiH_4.

TABLE II. Frequency positions (cm^{-1}) and identifications of absorption lines from 9.0μ to 12.0μ.

Line No.	Frequency position	Line No.	Frequency position	Ident.	Line No.	Frequency position	Ident.	Line No.	Frequency position	Ident.
1	813.8	38	872.5			927.1		103	983.3	
2	815.4	39	875.0	$P_4(10)$	75	927.5	$R_4(5)$	104	985.9	$R_-(1)$
3	816.2	40	875.7			928.1		105	988.5	$R_+(1)$
4	817.9	41	876.1			928.6		106	991.7	$R_-(2)$
5	820.6	42	878.9	$P_4(9)$		930.0		107	995.0	$R_+(2)$
6	821.7	43	879.2		76	930.5	$R_4(6)$	108	997.7	$R_-(3)$
7	823.2	44	880.7			931.1		109	1000.0	
8	824.6	45	882.6	$P_4(8)$		931.4		110	1001.0	
9	825.5	46	884.2		77	932.2	$R_4(7)$	111	1002.6	$R_+(3)$
10	826.7	47	886.0	$P_4(7)$		932.7		112	1004.1	$R_-(4)$
11	827.9	48	886.4			933.8		113	1005.2	
12	831.5	49	887.1		78	934.2	$R_4(8)$	114	1007.1	
13	834.2	50	888.8			934.8		115	1008.9	$R_+(4)$
14	835.1	51	889.2	$P_4(6)$	79	936.5		116	1010.1	$R_-(5)$
15	836.9	52	891.8		80	938.2		117	1015.7	$R_+(5)$
16	838.7	53	892.5		81	939.1	$P_-(6)$	118	1017.5	$R_-(6)$
17	842.8	54	893.5	$P_4(5)$	82	941.3		119	1021.0	
18	844.4	55	895.3		83	944.0	$P_+(6)$ $P_-(5)$	120	1022.5	$R_-(7)$ $R_+(6)$
19	846.4	56	897.5	$P_4(4)$	84	945.1		121	1026.5	
20	847.6	57	898.7		85	946.6		122	1028.4	$R_+(7)$ $R_-(8)$
21	849.2	58	900.4		86	949.2	$P_+(5)$	123	1031.6	
22	850.0	59	901.4	$P_4(3)$	87	950.3	$P_-(4)$	124	1032.8	
23	851.3	60	902.0		88	951.4		125	1035.0	$R_+(8)$ $R_-(9)$
24	854.6	61	905.1	$P_4(2)$	89	954.1	$P_+(4)$	126	1039.3	
25	856.2	62	907.1	$P_4(1)$	90	956.5	$P_-(3)$	127	1041.5	
26	857.6	63	909.0		91	959.1	$P_+(3)$	128	1045.0	
27	859.6	64	912.2		92	961.8	$P_-(2)$	129	1048.4	
28	862.7	65	913.4		93	964.1	$P_+(2)$	130	1054.1	
29	864.7	66	914.7	$R_4(0)$	94	966.8	$P_-(1)$	131	1054.7	
30	865.7	67	915.5		95	969.5	$P_+(1)$	132	1061.9	
31	866.5	68	916.8		96	972.7		133	1065.5	
32	867.6	69	917.7	$R_4(1)$	97	973.8		134	1068.5	
33	868.0	70	919.3		98	976.2		135	1071.7	
34	868.4	71	920.3	$R_4(2)$	99	978.2		136	1074.9	
35	869.0	72	926.6		100	979.7	$R_-(0)$	137	1081.1	
36	869.9	73	923.1	$R_4(3)$	101	980.8		138	1088.6	
37	871.6	74	925.4	$R_4(4)$	102	982.0	$R_+(0)$	139	1091.6	
								140	1094.5	

motion may take place in three independent ways so that ω_4 is threefold degenerate. The frequencies ω_3 and ω_4 will evidently give rise to a variation in the electric moment. In zero order of approximation the vibration energy of the XY_4 type of molecule will be

$$E_0/hc=\sum_{i=1}^{4}(V_i+g_i/2)\omega_i, \qquad (1)$$

where g_i takes the value of the order of the degeneracy of ω_i.

When all the nuclei are in their positions of equilibrium the tetrahedrally symmetric XY_4 type molecule will have three identical moments of inertia. For such a molecule, regarding it as a rigid rotator, one obtains as the rotational energy

$$E_R/hc=B_0J(J+1), \qquad (2)$$

where $B_0=h/[8\pi^2I_0c]$, I_0 being the equilibrium value of the moment of inertia of the molecule. In higher orders of approximation the vibration-rotation energy is found to be

$$T=E/hc=T_V+B(V,J,K)J(J+1)+C(V,J,K)K^2-\epsilon B_0-D_JJ^2(J+1)^2-D_{JK}J(J+1)K^2-D_KK^4. \qquad (3)$$

In (3) T_V is the oscillational term value, $B(V,J,K)=h/8\pi^2I(V,J,K)c$, $I(V,J,K)$ being the effective moment of inertia for a given vibration-rotation state, $C(V,J,K)$ is a constant for any one vibration-rotation state and D_J, $D_{J,K}$, and D_K are the centrifugal distortion coefficients. The term $\epsilon B(0)$ is the energy contribution of the Coriolis interaction originating with the degenerate states $V_i\omega_i+V_3\omega_3+V_4\omega_4$. When $V_3=V_4=0$ the coefficient is always zero, but when either V_3 or V_4 is equal to one, ϵ takes the three values $\epsilon_+=2J\zeta_{3,4}$, $\epsilon_0=-2\zeta_{3,4}$, $\epsilon_-=-2(J+1)\zeta_{3,4}$

where ζ_3 and ζ_4 are constants depending upon the nature of the normal frequencies ω_3 and ω_4. It is readily shown that $\zeta_3+\zeta_4=\frac{1}{2}$.

The constants $B(V, K, L)$ and $C(V, J, K)$ depend in a complicated manner upon J and K, but the dependence is always of the order $(J\times K)$ to the zero power. It is, therefore, probably legitimate to neglect entirely their dependence on J and K and consider them as constants for any one vibration state. Moreover, these constants contain terms which have as denominators $(\omega_2-\omega_3)$ and $(\omega_2-\omega_4)$. These originate with the Coriolis forces between ω_2 and the frequencies ω_3 and ω_4. In the case of such molecules as CH_4, SiH_4, and GeH_4 the potential function is such that ω_2 and ω_4 are nearly the same. This paves the way for a resonance interaction which manifests itself in that as the molecule makes a transition from the normal state to the states ω_2 and ω_4 the $B(V, J, K)$ and $C(V, J, K)$ values increase and decrease, respectively, above and below their values when the molecule is in the normal vibration state. Except for those states involving $V_2\omega_2$ and $V_4\omega_4$ the constant $C(V, J, K)$ is so small that it may completely be neglected.

The selection rules for the rotation quantum numbers for molecules of this type are $\Delta J=\pm 1, 0$. In the case of the vibration levels $V_1\omega_1+V_2\omega_2+\omega_3$ and $V_1\omega_1+V_2\omega_2+\omega_4$ the threefold degeneracies are removed by the Coriolis perturbation and the levels split up into three components. In these cases the selection rule for J becomes $\Delta J=1$, 0, or -1 depending upon whether the transition is from the normal state to the $+$, 0, or $-$ component levels in ω_3 or ω_4. For combination states between ω_3 and ω_4 the situation is considerably more complicated and we shall consider only one case, namely, $\omega_3+\omega_4$, in this paper. We defer this discussion to a somewhat later point.

With the aid of the above selection rules and the energy relations (3) one may derive the following combination relations if the term containing $C(V)$ and the centrifugal stretching terms are neglected:

$$R(J-1)-P(J+1)=2(2J+1)(B''-\zeta_iB_0), \quad (4a)$$

$$R(J)-P(J)=2(2J+1)(B'-\zeta_iB_0). \quad (4b)$$

These relations may be taken to hold quite generally for all bands except for combination bands between ω_3 and ω_4. In the above ζ_i is the amplitude of the internal angular momentum associated with the frequency ω_i; B'' and B' are $h/8\pi^2c$ times the reciprocals of the moments of inertia of the molecule in the normal state and in the excited state, respectively. For the frequency ω_1 which is non-degenerate and for ω_2 which is twofold degenerate it is readily verified that the ζ's are identically zero. Neither of the quantities ζ_3 nor ζ_4 can in general be equal to zero, but must satisfy the relation $\zeta_3+\zeta_4=\frac{1}{2}$. The relations (4a) and (4b) differ from the usual combination relations only by the presence of the term ζ_iB_0. They do not, except in cases where $\zeta_i=0$, enable one to evaluate the B'' or B' themselves unless the value of ζ_i can be determined by some other method. If, however, a band occurs in the spectrum for which ζ is zero the value B' can be determined.

TABLE III. Frequency positions and identifications of absorption lines near 3.3μ.

Frequency position	Identifications	Frequency position	Identifications
2958.5	$P_-(15)$	3114.0	$P_-'(6)$
2968.5	$P_-(14)$	3115.3	$R_0(2)$
2978.4	$P_-(13)$	3115.5	$R_-(6)$
2990.5	$P_-(12)$	3116.8	$P_+'(6)$
2999.3	$P_-(11)$	3118.6	$R_+(1)$
3006.1	$P_-(10)$	3119.4	$R_-(7)$
3015.9	$P_-(9)$	3119.6	$P'(5)$
3026.7	$P_-(8)$	3120.4	$R_-(8)$ $R_0(3)$
3033.4	$P_0(11)$	3121.0	$P_+'(5)$
3035.7	$P_-(7)$	3124.2	$R_-(9)$
3041.0	$P_0(10)$	3124.5	$P_-'(4)$
3045.5	$P_-(6)$ $P_0(9)$	3127.0	$P_+'(4)$
3049.0	$P_+(17)$	3127.5	$R_0(4)$
3050.6	$P_0(8)$	3128.0	$R_+(2)$
3053.8	$P_+(15)$ $P_-(5)$	3130.7	$P_-'(3)$
3056.7	$P_0(7)$ $P_+(14)$	3133.0	$P_+'(3)$
3058.6	$P_+(13)$	3135.0	$R_0(5)$
3061.4	$P_0(6)$ $P_+(12)$	3136.0	$P_-'(2)$
3063.3	$P_-(4)$	3137.0	$R_+(3)$
3065.4	$P_+(11)$	3138.7	$P_+'(2)$
3068.2	$P_0(5)$ $P_+(10)$	3140.9	$R_0(6)$
3070.2	$P_+(9)$	3142.0	$P_-'(1)$
3073.1	$P_-(3)$ $P_0(4)$ $P_+(8)$	3144.4	$P_+'(1)$
3076.0	$P_+(7)$	3145.5	$R_0(7)$
3079.8	$P_+(6)$ $P_0(3)$	3153.0	$R_-'(0)$
3081.6 (?)	$P_-(2)$	3155.7	$R_+'(0)$
3083.7	$P_+(5)$	3159.0	$R_-'(1)$
3086.6	$P_0(2)$ $P_+(4)$	3161.8	$R_+'(1)$
3088.6	$P_+(3)$ (?)	3164.4	$R_-'(2)$
3091.6	$P_-(1)$ $P_+(2)$ $P_0(1)$	3167.8	$R_+'(2)$
3094.3	$P_+(1)$	3170.5	$R_-'(3)$
3100.9	$R_-(0)$	3173.7	$R_+'(3)$
3102.7	$R_0(0)$ $R_-(1)$	3175.6	$R_-'(4)$
3105.2	$R_-(2)$	3179.0	$R_+'(4)$
3108.0	$P_-'(7)$	3182.0	$R_-'(5)$
3108.4	$R_-(3)$	3185.0	$R_+'(5)$
3109.4	$R_+(0)$ $R_0(1)$	3187.5	$R_-'(6)$
3110.6	$R_-(4)$	3192.5	$R_+'(6)$
3111.4	$P_+'(7)$	3193.0	$R_-'(7)$
3112.7	$R_-(5)$	3198.7	$R_+'(7)$

Since B'' is characteristic of the normal state its value must be the same when determined from other bands where $\zeta_i \neq 0$. This principle may be employed to determine the value of ζ_i for other bands when the quantities $(B''-\zeta_i B_0)$ have been obtained from experiment.

The regions which have been measured in the spectrum of SiH_4 have been interpreted in the following manner. The region near 4.6μ (2190 cm^{-1}) which is a region of intense absorption is identified as the band ν_3 and the very intense band at 11.0μ (914 cm^{-1}) is taken to be ν_4. The absorption band near 10μ (976 cm^{-1}) is much less intense than the band ν_4 which it partly overlaps. This band is identified with the vibration ν_2. This frequency should, according to what has already been said, be optically inactive in the infra-red. There exists, however, a resonance Coriolis interaction between these two nearly degenerate oscillations and the rotation of the molecule which is large enough so that the wave functions of the two vibration states become sufficiently "mixed" that the frequency ν_2 may borrow enough optical activity from ν_4 to become observable in the spectrum. There remains to consider the identity of the two overlapping bands which make up the region of absorption near 3.2μ. Of these the band of higher frequency (3150 cm^{-1}) is probably $\nu_2+\nu_3$ while the other (3097 cm^{-1}) is undoubtedly $\nu_3+\nu_4$. The reasons for this choice we shall have occasion to consider subsequently with more care. Each of the bands referred to above shall be considered in turn and an interpretation of them follows hereafter.

The Frequency ν_3

This band consists of a set of quite sharp and well-defined lines lying on each side of the central line or Q branch. Each intense line is accompanied by two less intense peaks also observed by Steward and Nielsen. These satellite peaks we believe to be the lines of the P and R branches of the bands ν_3 from the spectra of the molecules $Si^{(29)}H_4$ and $Si^{(30)}H_4$. From Fig. 1, curve B, it is evident that they are much less intense than the principal lines, a fact which is consistent with the relative abundance of the isotopes of silicon. The identification of the lines in this band is given in Table I. With the aid of Eqs. (4a) and (4b) we obtain from these sets of lines the values for $(B''-\zeta_3 B_0)$ and $(B'-\zeta_3 B_0)$ tabulated in Table IV.

The Frequency ν_4

Because of the close proximity of this band to the frequency ν_2 it is not justifiable to neglect $C(V)$ in the expression (3) for the vibration-rotation energy. The effect of this term is to remove the degeneracy in the quantum number K and thus split each level up into $J+1$ components. This means, of course, that the combination relations (4a) and (4b) are not correct as they stand for this case, but should contain other terms also. The splitting of the rotation levels due to the term $K^2C(V)$ in the energy is not extremely large, however, particularly for small values of J so that the effect upon the spectrum will be to break up what otherwise would have been a single line into a group of components frequently too close together to be resolved experimentally. We have attempted to identify the lines in the P and R branches in ν_4, taking a line to mean the center of what in some cases becomes a fairly broad band of unresolved component lines. This has been fairly satisfactory, although it will subsequently be highly desirable to make a detailed study of the structure of this band from the standpoint of the K splitting. This we hope to do at a later date. In this manner we have accounted for about nine lines on either side of the center. For lines corresponding to higher J values the structure becomes too complex to proceed in this manner.[6] On the high frequency side the structure of ν_4 is further obscured by the overlapping with ν_2. Our identification of the lines is given in the third column of Table II and from the combination relations we have arrived at values for $(B''-\zeta_4 B_0)$ and $(B''(\nu_4)-\zeta_4 B_0)$. These are found in Table V.

The Frequency ν_2

As we have already seen, a Coriolis resonance interaction exists between the two frequencies ω_4

[6] It is suggested that the rather complex region near 875 cm^{-1} is due to the Q branch of the first upper stage band. It will be seen to resemble the Q branch of the fundamental to a considerable degree. No attempt has been made to identify any of the lines in the P and R branches of this band since they must be weak and can scarcely be distinguished from the complex fine structure lines.

TABLE IV. Rotational constants for SiH_4 molecules derived from the band ν_3.

	$Si^{(28)}H_4$	$Si^{(29)}H_4$	$Si^{(30)}H_4$
$(B''-\zeta_3 B_0)$	2.82 cm^{-1}	2.83 cm^{-1}	2.84 cm^{-1}
$(B'-\zeta_3 B_0)$	2.81 cm^{-1}	2.82 cm^{-1}	2.82 cm^{-1}

TABLE V. Rotational constants of SiH_4 for the states ν_2, $\nu_2+\nu_3$, and ν_4.

	ν_2^+	ν_2^-	$(\nu_2+\nu_3)^+$	$(\nu_2+\nu_3)^-$	ν_4
$(B''-\zeta_4 B_0)$	2.96 cm^{-1}	2.96 cm^{-1}	2.86 cm^{-1}	2.82 cm^{-1}	1.60 cm^{-1}
$(B'-\zeta_4 B_0)$	3.06 cm^{-1}	3.02 cm^{-1}	2.91 cm^{-1}	2.84 cm^{-1}	1.53 cm^{-1}

and ω_2. Here as in the preceding case we may expect the rotation lines to be split or broadened because here also the quantity $C(\nu_2)$ is large enough to be of some importance. It is readily shown, moreover, that for the frequency ω_2 the internal angular momentum is equal to zero; i.e., $\zeta_2=0$. We should, therefore, expect the interval between two rotation lines to be about $\Delta\nu=2B$. We take, as before, a rotation line to mean the center of a group of unresolved component lines. From the data on the bands ν_3 and ν_4 we can estimate this interval to be about 6 cm^{-1}. Two sets of lines, apparently independent of each other and of about the same intensities, can be found in the band ν_2. When the combination relations are applied to the lines in the two sets the same value of B'' is obtained, indicating that both sets of lines originate in the same lower state. The values of the B' are slightly different. The explanation for this, we believe, is found in the papers by Shaffer, Nielsen, and Thomas. Because of the tetrahedral symmetry of the molecule a term is permitted in the anharmonic part of the potential energy which removes the degeneracy in the frequency ω_2 so that it will split into ω_2^+ and ω_2^-, say. From their discussion it is also clear that the effective moments of inertia associated with these component states will be slightly different. The principal lines in ν_2 have been accounted for on this basis up to about the ninth line on either side of the center. Beyond this the K splitting obscures the identification. Our identification is given in the third column of Table II and the values obtained for $(B''-\zeta_2 B_0)$ and $(B'-\zeta_2 B_0)$ (where, however, $\zeta_2\equiv 0$) are given in Table V.

The Frequency $\nu_2+\nu_3$

The band whose center lies near 3160 cm^{-1} must almost certainly be $\nu_1+\nu_4$ or $\nu_2+\nu_3$. The frequency ν_2 is known from Raman data to be 2187.0 cm^{-1}.[7] The frequency ν_4, we have seen, is about 914 cm^{-1}. The combination frequency $\nu_1+\nu_4$ should then be about 3100 cm^{-1} which is nearly 60 cm^{-1} less than the measured value. On the other hand ν_2 and ν_3 have, respectively, been found to be about 975 cm^{-1} and 2191 cm^{-1}. Their combined frequency would then be about 3166 cm^{-1} which is in satisfactory agreement with experiment. If this band is to be explained in this manner we should be able to find, as in the case of ν_2, two sets of independent rotation lines, one set associated with what has been termed $(\nu_2+\nu_3)^+$ and another with $(\nu_2+\nu_3)^-$. This does, indeed, appear to be the case and on this basis we have been able to identify about seven lines on either side of the center of each component band. Beyond this, overlapping with the other band made the identification impossible. The identifications are indicated in the third column of Table III and in Table V may be found the values of $(B''-\zeta B_0)$ and $(B'-\zeta B_0)$ obtained when the combination relations are applied to the band. It is obvious that the ζ appropriate for $(\nu_2+\nu_3)$ is equal to ζ_3.

The Frequency $\nu_3+\nu_4$

The first-order Coriolis interaction causes the level $\nu_3+\nu_4$ to split up into nine component levels. The amount of the splitting depends in a complicated manner upon the values of ζ_3 and ζ_4. In our analysis of the data on $\nu_3+\nu_4$ we shall anticipate the values of ζ_3 and ζ_4 which may be obtained from the information which goes before. It will be shown in the next section that $\zeta_3=0.046$ and that $\zeta_4=0.454$. With these values we may calculate the nine values of ϵ required in (3) to give the energy values of the molecule for a given value of J. Because ζ_3 is so nearly equal to zero the pattern becomes that of three closely spaced triplet components.

For the sake of simplicity we have taken ζ_3 exactly equal to zero and ζ_4 exactly equal to $\frac{1}{2}$. This is equivalent to letting each of the three triplet components for a given J value degenerate

[7] F. B. Stitt and D. M. Yost, J. Chem. Phys. **4**, 82 (1936).

into a single level. There will then be three different values of ϵ_i, ϵ_+, ϵ_0, and ϵ_-, each of which is repeated three times. These are $\epsilon_+ = 2J\zeta$, $\epsilon_0 = -2\zeta$, $\epsilon_- = -2(J+1)\zeta$. While the ϵ's are identical with those for the state ν_4 the selection rules for J will be more complicated. When the discussion of Shaffer, Nielsen, and Thomas is applied to this case one finds, in fact, that transitions of the type $\Delta J = \pm 1, 0$ may take place to each of the above three component levels ϵ_+, ϵ_0, and ϵ_- of any value J. These selection rules yield, in effect, three different bands, $(\nu_3+\nu_4)_+$, $(\nu_3+\nu_4)_0$, and $(\nu_3+\nu_4)_-$, which will overlap with each other. With the aid of the above selection rules we obtain the following relations for the positions of the lines in the P, Q, and R branches of each band:

$$P(J)(^+0_-) = (T_V - 2\zeta B_0) + J(J-1)B' - J(J+1)B'' + 2a(J)B_0, \quad (5)$$

where $a(J)$ takes, respectively, the values $J\zeta$, 0, and $-(J-1)\zeta$;

$$Q(J)(^+0_-) = (T_V - 2\zeta B_0) + J(J+1)(B' - B'') + 2a(J+1)B_0, \quad (6)$$

and

$$R(J)(^+0_-) = T_V - 2\zeta B_0) + (J+1)(J+2)B' - J(J+1)B'' + 2a(J+2)B_0. \quad (7)$$

These relations will in turn yield the following combination relations:

$$R(J-1)(^+0_-) - P(J+1)(^+0_-) = 2(2J+1)B'', \quad (8a)$$

$$R(J)(^+0_-) - P(J)(^+0_-) = 2(2J+1)B' + 4(^+1 0_{-1})\zeta B_0. \quad (8b)$$

The band $\nu_3+\nu_4$ overlaps rather badly with the band $\nu_2+\nu_3$, but the low frequency side is quite unobstructed. From the relation (5) it is clear that the lines of the component band $(\nu_3+\nu_4)_-$ will spread to lower frequencies than the lines of the other two component bands. In fact it will be seen that two lines in the P branch of this component band will be separated by an interval of about $2(B''+\zeta B_0)$ which is roughly 3/2 the normal rotation spacing. This appears consistent with the frequency intervals of the most prominent lines in the low frequency side of this band. It has been possible to account for most of the prominent peaks in $\nu_3+\nu_4$ on this basis and their identification is given in Table III in the third column. The values of the rotational constants from this band from the combination relations are set down in Table VI. No great accuracy for these values can be claimed, however, because of the approximation which was made that $\zeta_4 = \zeta = 0.5$ exactly.

IV

In the tables of Section III are summarized the data arrived at from a remeasurement of the bands in the spectrum of SiH_4. From our analysis of these data it has been possible to arrive at values for the rotational constants $(B''-\zeta_i B_0)$ and $(B'-\zeta_i B_0)$ characteristic of the normal state and the excited vibration states, respectively. From these values and from the knowledge that $\zeta_3+\zeta_4 = 0.50$ and that $\zeta_2 \equiv 0$ it is possible to arrive at values for the quantities B_0, B'', and $B'(\nu_i)$, as well as the values of ζ_3 and ζ_4. The values obtained are set down in Table VI.

From the value of B_0 given in the table above it is possible to compute the equilibrium value of the moment of inertia I_0 of the SiH_4 molecule. Taking h to be 6.624×10^{-27} one obtains for I_0 the value 9.33×10^{-40} g cm^2. From this value it is in turn possible to determine the equilibrium values of the distances between the silicon atom and the hydrogen atoms and the distances between two hydrogen atoms. It is readily verified that $I_0 = (8/3)m_H(r_{Si-H})^2 = m_H(r_{H-H})^2$. This leads to the values $(r_{Si-H}) = 1.55\times10^{-8}$ cm and $(r_{H-H}) = 2.58\times10^{-8}$ cm.

It is of interest to note in connection with the values of the rotational constants that the value of $[B''-\langle B'(\nu_2)\rangle_{Av}] = -0.08$ cm^{-1}, where we mean by $\langle B'(\nu_2)\rangle_{Av}$ the average value of $B_+'(\nu_2)$ and $B_-'(\nu_2)$, is very nearly equal to the negative of $[B''-B'(\nu_4)] = 0.07$ cm^{-1}. This suggests that the variation of $B'(\nu_2)$ and $B'(\nu_4)$ from B'' is essentially due to the Coriolis interaction between the two frequencies and that the other contributions are small. It is further of interest to note that the values of the ζ's obtained from the data are in good agreement with those predicted by Jahn on the basis of valence force fields.

With a knowledge of the rotational constants at hand it is possible at once to infer what are the centers of the bands. This information is gathered together in Table VII.

TABLE VI. Rotational constants of the SiH_4 molecule.

$B_0=3.00\ cm^{-1}$	$B'(\nu_3)=2.95\ cm^{-1}$	$B_+'(\nu_3+\nu_4)=3.05\ cm^{-1}$
$B''=2.96\ cm^{-1}$	$B'(\nu_4)=2.89\ cm^{-1}$	$B_0'(\nu_3+\nu_4)=2.97\ cm^{-1}$
$B_+'(\nu_2)=3.06\ cm^{-1}$	$B_+'(\nu_2+\nu_3)=3.05\ cm^{-1}$	$B_-'(\nu_3+\nu_4)=2.94\ cm^{-1}$
$B_-'(\nu_2)=3.02\ cm^{-1}$	$B_-'(\nu_2+\nu_3)=2.98\ cm^{-1}$	$\zeta_4=\frac{1}{2}-\zeta_3=0.454$

TABLE VII. Positions of the centers of the vibration-rotation bands in SiH_4.

ν_1	ν_2	ν_3	ν_4	$\nu_2+\nu_3$	$\nu_3+\nu_4$
$2187.0\ cm^{-1}(R)$	$974.6\ cm^{-1}$	$2190.6\ cm^{-1}$	$914.2\ cm^{-1}$	$3148.8\ cm^{-1}$	$3100.2\ cm^{-1}$

The potential energy functions of the tetrahedrally symmetric XY_4 have been discussed by several authors.[8] The most general form may be written

$$V=\tfrac{1}{2}\{k_1\sum_{i=1}^{3}\xi_i^2+2k_2\sum_{i=1}^{3}\eta_i\xi_i+k_3\sum_{i=1}^{3}\eta_i^2+k_4\sum_{i=1}^{3}\zeta_i^2+k_5\sum_{i=1}^{3}{}'\zeta_i\zeta_j\},\quad(9)$$

where the k's are complicated relations involving nine arbitrary and independent potential energy constants $K_1\cdots K_9$. We do not have available enough data to evaluate all of these. It is possible, however, to evaluate the five constants $k_1\cdots k_5$ since five independent pieces of information are available. Four of these are supplied by the values of the normal frequencies and the fifth is available when we make use of the fact that ζ_3 and ζ_4 are functions also of the potential energy constants. The values of the centers of the fundamental bands are, of course, different from the actual values of the fundamental normal frequencies because of the anharmonicity. For this effect we have no means at our disposal to make corrections. We may, however, to a fair degree of approximation simply use for the normal frequencies the centers of the fundamental bands. The values of the constants $k_1\cdots k_5$ arrived at on this basis are the following: $k_1=1.177\times10^5$, $k_2=1.4891\times10^5$, $k_3=3.963\times10^5$, $k_4=1.315\times10^5$, $k_5=0.754\times10^5$ dyne cm. It is of interest also to evaluate the five constants which will occur in a generalized valence force potential energy function. Such a generalized valence potential energy function will take the form:

$$V=\tfrac{1}{2}\{K_1\sum_{i=1}^{4}\delta r_i^2+K_2r_0^2\sum\delta\alpha_{ij}^2+K_3r_0\sum\delta\alpha_{ij}(\delta r_i+\delta r_j)+2K_4\sum_{\substack{i=1\\j=1\\i>j}}^{4}{}'\delta r_i\delta r_j+2K_5r_0^2\sum{}'\delta\alpha_{ij}\delta\alpha_{jk}\},\quad(10)$$

where δr_i is the change in the distance between the central atom and the ith hydrogen atom and $\delta\alpha_{ij}$ is the variation in the H_i-Si-H_i valence band angle. In an unpublished work Shaffer[9] has shown that the following relationships hold between the k's and the K's.

$$\begin{aligned}K_1&=\tfrac{1}{4}[k_1+2k_2+k_3+(k_4+2k_5)],\\K_2&=\tfrac{1}{12}[4k_1-4k_2+k_3],\\K_3&=(\sqrt{2}/6)[-2k_1-k_2+k_3],\\K_4&=\tfrac{1}{6}[-k_1-2k_2-k_3+3(k_4+2k_5)],\\K_5&=\tfrac{1}{3}[k_1-k_2+\tfrac{1}{4}k_3-k_4+k_5].\end{aligned}\quad(11)$$

From these we may evaluate the K's and their values are given below:

$$\begin{aligned}K_1&=2.735\times10^5\ \text{dyne cm},\\K_2&=0.2262\times10^5\ \text{dyne cm},\\K_3&=0.0283\times10^5\ \text{dyne cm},\\K_4&=0.0295\times10^5\ \text{dyne cm},\\K_5&=0.0196\times10^5\ \text{dyne cm}.\end{aligned}$$

We observe that the constants K_3, K_4, and K_5 are all of the order of $\frac{1}{10}$ of K_2; i.e., they are of a smaller order of magnitude than either K_1 or K_2. This fact is consistent with the point of view that the valence force field concept represents a legitimate approximation to the actual force fields in the SiH_4 molecule.

[8] D. M. Dennison, Astrophys. J. **62**, 84 (1925); J. E. Rosenthal, Phys. Rev. **45**, 538 (1934); W. H. Shaffer, H. H. Nielsen, and L. H. Thomas, reference 5.

[9] W. H. Shaffer, unpublished work. We are grateful to Dr. Shaffer for making this work available to us.

The Vibration-Rotation Spectrum of GeH_4

JOSEPH W. STRALEY,* CHARLES H. TINDAL,** AND HARALD H. NIELSEN
Mendenhall Laboratory of Physics, The Ohio State University, Columbus, Ohio

(Received May 15, 1942)

Two of the infra-red bands of SiH_4, originally measured by Steward and Nielsen, have been remeasured at much increased resolving power. In addition a new band near 13.0μ has been located and measured. The bands have been identified as follows: their centers having been determined to be $\nu_2=930.9$ cm^{-1}, $\nu_3=2113.6$ cm^{-1}, and $\nu_4=819.3$ cm^{-1}. From a rotational analysis of these bands the equilibrium value of B and the values of B for the vibration states ν_2, ν_3, and ν_4 have been determined, B being $h/8\pi^2Ic$. These have, respectively, the values $B_0=2.90$ cm^{-1}, $B''=2.87$ cm^{-1}, $B'(\nu_2)=2.96$ cm^{-1}, $B'(\nu_4)=2.79$ cm^{-1}. The values of ζ are found to be the following: $\zeta_4=\frac{1}{2}-\zeta_3=0.476$. From the above data four independent relations existing between the generalized valence force constant are computed.

I. INTRODUCTION

IN a recent paper[1] we have reported on our remeasurement of the infra-red absorption bands due to SiH_4. The results were so gratifying that it was decided to remeasure also the absorption bands in the spectrum of the GeH_4 molecule. Such an investigation would moreover present an opportunity to hunt for the forbidden vibration transition ν_2 which by analogy to the SiH_4 case might be expected to be intense enough to be observed.

Such an investigation could easily be carried out. No major adjustments of the spectrometer were required inasmuch as the absorption bands in the spectrum of GeH_4 lie in the same general regions as do the bands in the SiH_4 spectrum. The same diffraction gratings were used, respectively, as in the preceding case; the slits were maintained at the same sizes; in fact experimentally all conditions remained the same. The absorption cells containing the GeH_4 gas were simply made to replace the cells which contained the SiH_4 gas. Nothing further need therefore be said concerning the experimental procedure.

II. THE ABSORPTION BANDS OF GeH_4

The 4.5μ Band

For measurements on this region a cell 6 cm long filled with GeH_4 gas to a pressure of 10 cm Hg was used. The data are represented by the upper curve in Fig. 1. In it one can readily detect the peaks referred to by Lee and Sutherland[2] and which also were observed by Steward and Nielsen,[3] but with much less relative intensities. When, however, enough of the gas in the cell is removed so that the pressure is reduced to 6 cm Hg the data are represented by the lower curve which is quite consistent with the earlier data of S and N when one takes account of the fact that for the present curve, galvanometer deflections were taken at intervals of about $\frac{1}{6}$ of those of S and N. We believe the lower curve to be a far more accurate picture of the absorption region than the upper curve. The principal lines have approximately the same heights as before, but are much sharper. The subsidiary peaks of L and S we believe are in reality quite weak, but can be brought out quite strongly when enough gas is used so that the principal lines are strongly "overexposed."

In the first column of Table I are given the frequency positions of the more important lines in the band and their identifications are set down in the second column of the same table. The identifications have been made particularly with reference to the lower curve in Fig. 1. We have identified this absorption region as due principally to the fundamental vibration ν_3. For these we have

$$(B''-\zeta_3 B_0)=2.80 \text{ cm}^{-1}$$

* Now at the University of Toledo, Toledo, Ohio.
** Now at Mt. Holyoke College, South Hadley, Massachusetts.
[1] C. H. Tindal, J. W. Straley, and H. H. Nielsen, Phys. Rev. (this issue).
[2] E. Lee and G. B. B. M. Sutherland, Proc. Camb. Phil. Soc. **35**, 341 (1939).
[3] W. B. Steward and H. H. Nielsen, Phys. Rev. **48**, 861 (1935).

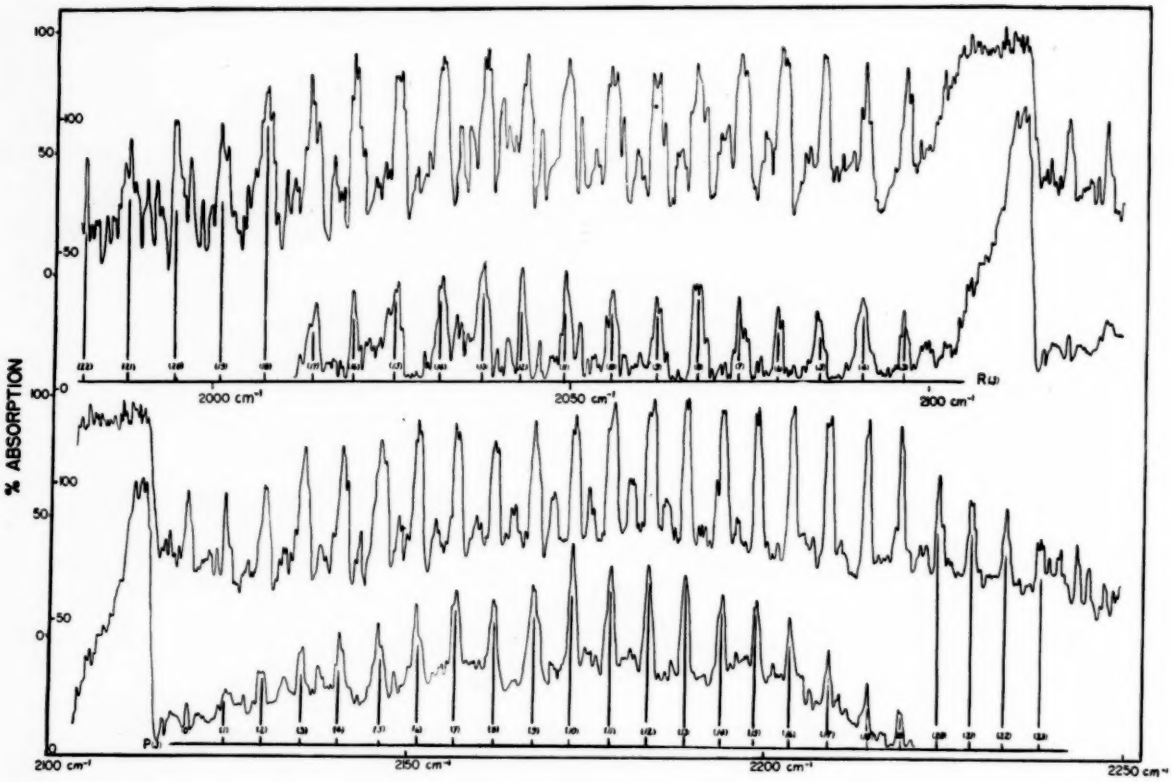

FIG. 1. 4.7-μ region of GeH_4.

TABLE I. Frequency positions and identifications of lines in the GeH_4 spectrum at 4.7μ.

Freq. (cm^{-1})	Ident.	Freq. (cm^{-1})	Ident.	Freq. (cm^{-1})	Ident.	Freq. (cm^{-1})	Ident.	Freq. (cm^{-1})	Ident.	Freq. (cm^{-1})	Ident.
2000.8	$P(19)$	2031.5	$P(14)$	2061.2	$P(9)$	2102.5	$P(2)$	2149.0		2188.5	$R(13)$
2004.6		2034.0		2062.8		2107.9	$P(1)$	2151.4	$R(6)$	2191.0	
2005.8		2035.8		2065.0		2116.2		2154.0		2193.6	$R(14)$
2007.5	$P(18)$	2037.5	$P(13)$	2067.3	$P(8)$	2119.3	$R(0)$	2156.6	$R(7)$	2198.7	$R(15)$
2011.4		2039.5		2071.3		2121.0		2159.5		2203.2	$R(16)$
2012.2		2041.5		2073.5	$P(7)$	2122.1		2162.1	$R(8)$	2208.0	$R(17)$
2014.3	$P(17)$	2044.0	$P(12)$	2076.5		2124.5	$R(1)$	2165.1		2212.5	$R(18)$
2016.2		2045.4		2079.1	$P(6)$	2130.3	$R(2)$	2167.8	$R(9)$	2217.8	$R(19)$
2017.5		2046.8		2082.8		2132.5		2170.5		2222.6	$R(20)$
2019.6	$P(16)$	2049.4	$P(11)$	2085.3	$P(5)$	2135.6	$R(3)$	2173.0	$R(10)$	2227.0	$R(21)$
2024.0		2051.2		2090.9	$P(4)$	2138.0		2175.8		2232.0	$R(22)$
2025.7	$P(15)$	2053.2		2093.0		2141.0	$R(4)$	2178.2	$R(11)$	2236.6	$R(23)$
2027.8		2055.3	$P(10)$	2096.6	$P(3)$	2143.4		2180.5		2241.2	$R(24)$
2029.5		2057.0				2146.3	$R(5)$	2183.6	$R(12)$		
		2059.2						2186.0			

and

$$(B'(\nu_3) - \zeta_3 B_0) = 2.78 \text{ cm}^{-1}.$$

There are five isotopes of germanium and one might expect, therefore, as in the case of SiH_4 to find a band ν_3 for each isotopic molecule. Unfortunately, however, the centers of these isotopic lines may be expected to lie so nearly superimposed that they cannot be resolved Experimentally no real evidence of these separations is to be found. The above rotational constants must therefore be regarded as average values for the several isotopic molecules.

No explanation for the weaker structure in between the principal lines is very obvious. Lee

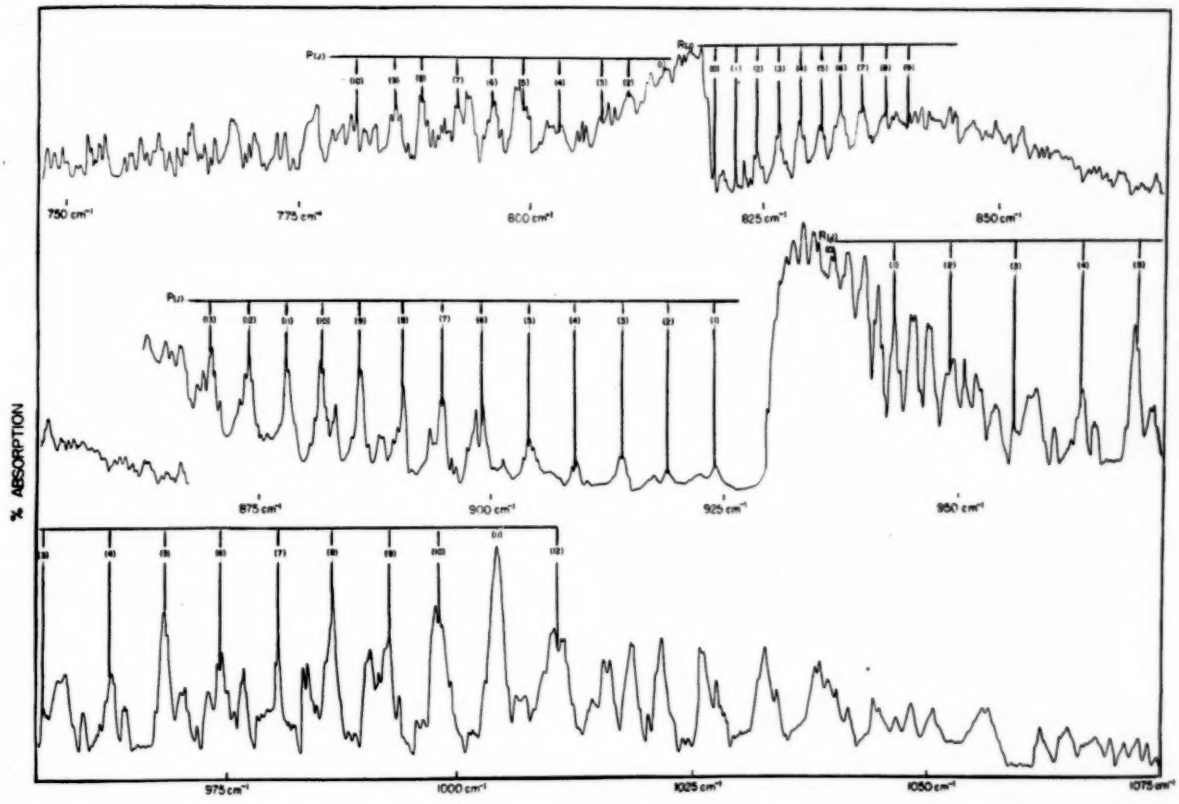

FIG. 2. The region 10μ to 14μ of GeH_4.

TABLE II. Frequency positions and identifications of lines in absorption bands near 12.0μ.

Freq. (cm^{-1})	Ident.	Freq. (cm^{-1})	Ident.	Freq. (cm^{-1})	Ident.	Freq. (cm^{-1})	Ident.	Freq. (cm^{-1})	Ident.	Freq. (cm^{-1})	Ident.
749.5		795.7	$P(6)$	837.9	$R(8)$	890.7	$P'(8)$	940.0		975.0	$R'(6)$
752.3		799.4	$P(5)$	839.0		893.6		941.5		977.6	
754.2		803.3	$P(4)$	840.4	$R(9)$	894.9	$P'(7)$	943.0	$R'(1)$	981.3	$R'(7)$
758.0		805.5		845.0	$R(11)$	898.4		945.2		984.3	
759.8	$P(15)$	807.5	$P(3)$	847.3	$R(12)$	899.0	$P'(6)$	947.0		987.2	$R'(8)$
763.5	$P(14)$	810.5	$P(2)$	849.6	$R(13)$	904.3	$P'(5)$	949.3	$R'(2)$	991.0	
766.0		814.1	$P(1)$	851.4	$R(14)$	909.2	$P'(4)$	950.6		993.3	$R'(9)$
768.0	$P(13)$	819.7	$R(0)$	863.0		914.2	$P'(3)$	952.0		998.6	$R'(10)$
770.5		820.5		865.0		917.5		954.0		1004.7	$R'(11)$
772.7 }	$P(12)$	822.0	$R(1)$	866.6		919.0	$P'(2)$	956.0	$R'(3)$	1011.3	$R'(12)$
773.6 }		822.8		869.7	$P'(13)$	922.0		958.0		1015.6	
776.8	$P(11)$	824.3	$R(2)$	874.0	$P'(12)$	924.1	$P'(1)$	960.3		1019.3	$R'(13)$
781.1	$P(10)$	826.4	$R(3)$	878.0	$P'(11)$	932.5		962.6	$R'(4)$	1022.5	
785.2	$P(9)$	828.9	$R(4)$	881.7	$P'(10)$	933.5		964.5		1026.8	$R'(14)$
788.2	$P(8)$	831.2	$R(5)$	883.2		934.5		969.5	$R'(5)$	1028.4	
792.5	$P(7)$	833.0	$R(6)$	886.1	$P'(9)$	936.3	$R'(0)$	971.0		1033.5	$R'(15)$
793.1		835.5	$R(7)$	888.3		938.3		973.7		1039.5	$R'(16)$

and Sutherland have suggested that these lines arise in some manner from interactions between vibration and rotation. This view receives little support from the theory in its present state although until the selection rules have been investigated to higher orders of approximation this question can probably not definitely be settled. It is suggested here that these lines might just conceivably be due to the overtone band $3\nu_4$.

The Region 10μ to 14μ

The region reported by Steward and Nielsen near 10.5μ was first remeasured. The data were here obtained by using an absorption cell 6 cm long containing GeH_4 gas at a pressure of 10 cm Hg. These measurements repeated the earlier data quite satisfactorily, especially on the high frequency side, when one takes into account that the galvanometer deflections were taken at intervals one-sixth as large as in the earlier work. It was soon discovered, however, that on the long wave-length side, about where the data of S and N stopped, a new and much more intense band set in. This region extended out to beyond 14.0μ and for measurements on this band enough gas was removed from the cell to reduce the pressure to 6 cm Hg. The data taken are shown graphically in Fig. 2 and the frequency positions of the more intense lines throughout the region are set down in Table II.

Steward and Nielsen identified the band at 10.5μ as the fundamental frequency ν_4 and never looked farther for another band. In the light of this investigation it becomes clear that their identification was wrong and that this band was in reality the forbidden band ν_2 and that the much more intense band at 820 cm^{-1} must be the fundamental frequency ν_4.

The rotation lines will here as in the spectra of SiH_4 and CH_4 be split into fine structure because of the resonance Coriolis interaction between ν_2 and ν_4. The splitting is, however, not very great, especially for the smaller quantum numbers. In the same manner as we preceded with the SiH_4 bands, so here also we have taken a line to mean a group of component lines too closely spaced to be resolved spectroscopically. On this basis we have identified a considerable number of the rotation lines in the P and R branches in both of the bands ν_2 and ν_4. Our identification of the lines in these two bands is set down in the second column of Table II.

In the case of the SiH_4 spectrum it appeared that the twofold degeneracy of the frequency ν_2 was removed. This does not appear to be the case here. It does not seem possible to find more than one set of lines in the band ν_2. There are certain lines in ν_2 which remain unaccounted for, but they are probably to be ascribed to K splitting of the principal lines. The $B'(\nu)$ values seem to decrease with increasing quantum numbers, particularly beyond $J=6$, but this effect may be due to centrifugal stretching. With the aid of the combination relations we obtain the following rotational constants from the band ν_4:

$$(B''-\zeta_4 B_0)=1.49\ cm^{-1},$$
$$(B'(\nu_4)-\zeta_4 B_0)=1.41\ cm^{-1}$$

and from the band ν_2 we get, remembering that $\zeta_2\equiv 0$, $B''=2.87$ cm^{-1} and $B'(\nu_2)=2.96$ cm^{-1}.

The Combination Frequencies near 3.3μ

It was found that there was not enough GeH_4 gas available to fill a cell long enough to remeasure these bands. We refer, therefore, to the earlier measurements reported by S and N. We alter their identification of the band at 3031.0 cm^{-1}, however, from $\nu_1+\nu_4$ to $\nu_2+\nu_3$, but retain their identification of the band at 2922.7 cm^{-1} as $\nu_3+\nu_4$. In support of this identification we shall point out that for $\nu_2+\nu_3$ the appropriate ζ value will be ζ_3. This should therefore lead to a spacing between rotation lines, particularly near the center, of about 5.6 cm^{-1}. This value agrees very well with the data of Steward and Nielsen. The band at 2936 cm^{-1} overlaps badly with that at 3031 cm^{-1}, but the low frequency side remains quite unobscured. Our discussion of the frequency $\nu_3+\nu_4$ for the SiH_4 molecule is equally applicable for the frequency $\nu_3+\nu_4$ for the GeH_4 molecule. We should therefore expect to find a separation between lines in the low frequency end of the P branch of about 8.7 cm^{-1}. This seems in excellent agreement with the spacings between the first six lines shown in the diagram of S and N.

III. DISCUSSION OF THE RESULTS

From the rotational constants derived from an analysis of the bands ν_2, ν_3, and ν_4 one may, with the aid of the condition $\zeta_3+\zeta_4=\frac{1}{2}$, obtain the values for B'', $B'(\nu)$, ζ_3, and ζ_4 themselves. The values obtained are given in Table III. It is worthy of note that, here also as in the case of SiH_4 spectrum, one finds $[B''-B'(\nu_4)]$ is very nearly equal to the negative of $[B''-B'(\nu_2)]$ which indicates that the principal contribution to the change in B for these frequencies comes from the resonance Coriolis interaction.

From the value of B_0 we can compute the equilibrium value of the moment of inertia I_0. We find this to be 9.65×10^{-40} g-cm^2. From I_0 we may then deduce the equilibrium values of the H−H distance and the Si−H distance. We find these, respectively, to be $r_{H-H}=2.41\times10^{-8}$ cm and $r_{Si-H}=1.48\times10^{-8}$ cm.

With a knowledge of the values of the rotational constants we may infer at once where the centers of the aforementioned bands lie. The

TABLE III. Numerical values for the rotational constants of the GeH_4 molecule.

B_0	B''	$B'(\nu_2)$	$B'(\nu_3)$	$B'(\nu_4)$	ζ_3	ζ_4
2.90 cm^{-1}	2.87 cm^{-1}	2.96 cm^{-1}	2.85 cm^{-1}	2.79 cm^{-1}	0.024	0.476

values we find are the following: $\nu_2=930.9$ cm^{-1}, $\nu_3=2113.6$ cm^{-1}, and $\nu_4=819.3$ cm^{-1}. No data on the Raman spectrum of GeH_4 seem to be available. The value of ν_1 is therefore not known. There are consequently only four independent bits of knowledge from which to deduce the values of the potential energy constants. These are the values of the band centers ν_2, ν_3, ν_4, and the ζ's. As a consequence we cannot here compute more than four of the independent relations among the constant k_i [4] which would occur in the general potential energy function for such a molecule. If we take the values of the fundamental frequencies ω_s to be equal, respectively, to the values of the band centers ν_s, these we find are: $k_1=1.117\times10^5$ dyne cm, $k_2=\pm1.471\times10^5$ dyne cm, $k_3=3.709\times10^5$ dyne cm, $k_4-k_5=5.116\times10^5$ dyne cm. From these we may in turn calculate four independent relations between the constants K_s which will be present in the generalized valence potential energy function. The relations are $K_1-\frac{1}{2}K_4=2.589\times10^5$ dyne cm; $K_2=0.191\times10^5$ dyne cm; $K_3=0.0011\times10^5$ dyne cm; $K_5=0.0104\times10^5$ dyne cm. It should be noted that similar to the case of the SiH_4 molecule the constants K_3 and K_5 are small compared to K_2 and $K_1-\frac{1}{2}K_4$. It seems therefore quite likely also that K_4 (which is the coefficient of the cross product terms

$$\sum_{\substack{i=1\\ i=1}}^{4}{}' \delta r_i \delta r_j)$$

will be small compared to these, say of the order of 1 percent of K_1. The value of K_1 is probably not very much different from $K_1-\frac{1}{2}K_4$. We shall here assume that K_4 is of the order of 1 percent of K_1 and then calculate the value of ν_1. For ν_1 calculated on this basis we obtain 2090 cm^{-1} which seems a quite reasonable value.

[4] See either Shaffer, Nielsen, and Thomas, Phys. Rev. **56**, 895 (1939) or our paper dealing with SiH_4.

Theory of the Magnetron

II. Oscillations in a Split-Anode Magnetron

LÉON BRILLOUIN*
University of Wisconsin, Madison, Wisconsin
(Received May 7, 1942)

A theoretical study is made of the possible oscillations in split-anode magnetrons. It is found that large oscillations can occur in certain frequency ranges, these ranges depending upon the number of segments. In Fig. 6 these frequency ranges are indicated with $y=21310/\lambda H$ as a function of the number of segments ($2n$). The large oscillations occur in the first and fourth region as tabulated at the top of the figure.

1. SPLIT-ANODE MAGNETRON—GENERAL REMARKS

THE behavior of a magnetron operated under steady conditions was studied in a previous paper[1] where the conditions of oscillation were also discussed for the case of a magnetron with one anode of cylindrical shape. This first paper will be referred to under the title "Magnetron I," and a numeral I will be added to its equation numbers to avoid confusion with the present paper.

The aim of the present work is a study of oscillation conditions in a split-anode magnetron. Such magnetrons are built with an anodic structure consisting of an even number of shells equally spaced so as to form an almost complete cylinder about the filament. The most popular type has two half-cylindrical anodes, but other models with as many as twelve or more anodes have also been successfully used. The oscillating circuit is connected by one of its terminals to the odd-numbered shells, the second terminal being connected to the even-numbered shells, as shown schematically in Fig. 1.

The exact field distribution in such magnetrons would be very difficult to compute, but a reasonable theoretical attempt is possible under the assumption of very small sinusoidal oscillations. This is illustrated in Fig. 2. Let us call b the radius of the anodic structure and $2n$ the number of anodes. The position of the anodes as a function of θ is indicated along the θ axis. Let V_c be the average constant potential of the anodes and $\pm U_a e^{i\omega t}$ the additional alternating potential, the + sign corresponding to the odd anodes and the − sign to the even ones. The potential distribution on the anode circle is represented by the curve in Fig. 2. Such a broken curve can easily be expanded in a Fourier series. Let α be the angle subtended by one anode while β is the angle between two successive anodes. Then $\alpha+\beta=\pi/n$. The potential on the radius $r=b$ is given by the series

$$V(b)=V_c(b)+U_a e^{i\omega t}\frac{8}{\pi n\beta}\times\sum_p \frac{1}{p^2}\sin(\tfrac{1}{2}pn\beta)\sin(pn\theta). \quad p \text{ odd} \quad (1)$$

The first term $p=1$ is the most important and the next term $p=3$ can be made zero by taking

$$\sin(3/2)n\beta=0, \quad \beta=2\pi/3n, \quad \alpha=\pi/3n,$$

which means that the distance between the anodes is twice the width of the anodes.

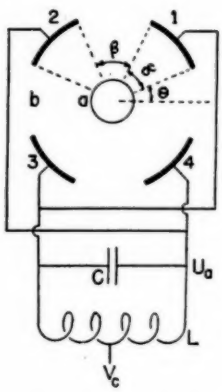

FIG. 1. Connections of terminals to oscillator.

* Now at Brown University, Providence, Rhode Island.
[1] L. Brillouin, Phys. Rev. **60**, 385 (1941); also Elec. Communication **20**, 112 (1941).

The calculations will be made under the assumption that the alternating term U_a is very small with an ϵ coefficient the highest power of which will be neglected. Furthermore, we shall keep only the first term of the Fourier expansion.

$$V(b) = V_c(b) + \epsilon V_a(b) e^{i\omega t} \sin(n\theta),$$
$$\epsilon V_a(b) = U_a(8/\pi n\beta) \sin(\tfrac{1}{2}n\beta). \tag{2}$$

This is the assumed distribution of potential on the circle $r=b$, but one should keep in mind the fact that a magnetron built with $2n$ anodes may eventually work on one of the higher modes corresponding to $2n'$ anodes with $n'=3n, 5n, \cdots$. It is easily seen that these higher modes of oscillation will increase in probability if the interval β between the anodes is very small. At the limit $\beta=0$, $\alpha=\pi/n$, the amplitude of the pth term becomes

$$\lim_{\beta=0} \frac{8}{\pi n\beta} \frac{1}{p^2} \sin(\tfrac{1}{2}pn\beta) = \frac{4}{\pi p}. \tag{3}$$

2. FUNDAMENTAL EQUATIONS

The fundamental equations are Maxwell's relations which will be written in cylindrical coordinates r, θ, z, where z is the axis taken along the filament. It will be assumed that all quantities are independent of z. The current density components J_r, J_θ, including Maxwell's displacement current, are

$$J_r = \rho v_r + \frac{\epsilon_0}{4\pi} \frac{\partial E_r}{\partial t},$$
$$J_\theta = \rho v_\theta + \frac{\epsilon_0}{4\pi} \frac{\partial E_\theta}{\partial t}. \tag{4}$$

v_r and v_θ are the components of the velocities of the electrons, ρ the space charge density, E_r and E_θ the components of the electric field, and $E_z=0$. The coefficients ϵ_0, μ_0 represent the dielectric power and the magnetic permeability in vacuum. Electrostatic c.g.s. units will be consistently used, making

$$\epsilon_0 = 1, \quad \mu_0 = c^{-2}. \tag{5}$$

$J_r r d\theta$ is the radial current flowing through $r d\theta$, per unit of length z, while $J_\theta dr$ is the angular component of the current through dr, per unit z. The total radial current per unit of length of z is

$$I_r = \int_0^{2\pi} J_r r d\theta. \tag{6}$$

It is well known that the introduction of Maxwell's displacement terms secures the following relation:

$$\operatorname{div} J = \frac{1}{r}\frac{\partial}{\partial r}(rJ_r) + \frac{1}{r}\frac{\partial}{\partial \theta}(J_\theta) = 0. \tag{7}$$

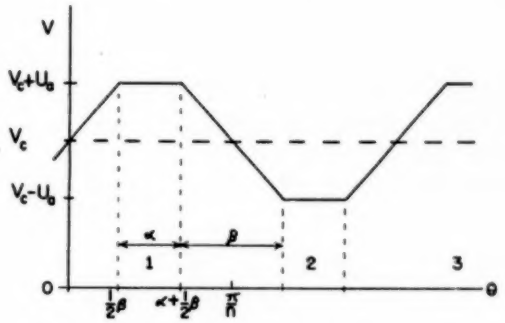

FIG. 2. Potential distribution on the anode circle.

This may easily be verified, with the conservation equation for electric charge

$$\partial\rho/\partial t = -\operatorname{div}(\rho v) = -\frac{1}{r}\frac{\partial}{\partial r}(r\rho v_r) - \frac{1}{r}\frac{\partial}{\partial \theta}(\rho v_\theta), \tag{8}$$

together with one of Maxwell's equations:

$$\operatorname{div} E = \frac{1}{r}\frac{\partial}{\partial r}(rE_r) + \frac{1}{r}\frac{\partial}{\partial \theta}E_\theta = 4\pi\rho/\epsilon_0. \tag{9}$$

Let us call H_r, H_θ, H_z the components of the oscillating magnetic field. The symmetry of the problem shows that H_r and H_θ are zero. Consequently

$$\operatorname{div} H = \partial H_z/\partial z = 0, \tag{10}$$

which proves that H_z is independent of z. Maxwell's equations yield

$$\operatorname{rot} H = 4\pi J \begin{cases} \partial H_z/r\partial\theta = 4\pi J_r, \\ -\partial H_z/\partial r = 4\pi J_\theta; \end{cases} \tag{11}$$

$$\operatorname{rot} E = -\mu_0 \partial H/\partial t,$$
$$\partial(rE_\theta)/r\partial r - \partial E_r/r\partial\theta = -\mu_0 \partial H_z/\partial t. \tag{12}$$

This system reduces to three relations: (11.1), (11.2), and (12). Equation (7) shows that the

relations (11.1) and (11.2) are compatible as it gives

$$\partial^2 H_z/\partial r\partial\theta = \partial^2 H_z/\partial\theta\partial r.$$

Hence we can write

$$H_z = 4\pi \int r J_r d\theta = -4\pi \int J_\theta dr, \tag{13}$$

and we are left with one relation

$$\frac{\partial(rE_\theta)}{r\partial r} - \frac{\partial E_r}{r\partial\theta} = -4\pi\mu_0 \frac{\partial}{\partial t} \int r J_r d\theta, \tag{14}$$

which is to be used together with (9) to define the electric field. It is well known that any field E can be represented as the sum of an irrotational field (grad V) and a field E' with no divergence.

$$E_r = -\frac{\partial V}{\partial r} + E'_r,$$
$$E_\theta = -\frac{1}{r}\frac{\partial V}{\partial\theta} + E'_\theta, \tag{15}$$

$$\text{div } E' = \frac{\partial(rE'_r)}{r\partial r} + \frac{\partial E'_\theta}{r\partial\theta} = 0. \tag{16}$$

Substituting in Eqs. (9) and (14) we obtain

$$\Delta V = -\frac{1}{r}\frac{\partial}{\partial r}\left(r\frac{\partial V}{\partial r}\right) + \frac{1}{r^2}\frac{\partial^2 V}{\partial\theta^2} = -\frac{4\pi\rho}{\epsilon_0}; \tag{17}$$

$$\frac{\partial(rE'_\theta)}{r\partial r} - \frac{\partial E'_r}{r\partial\theta} = -4\pi\mu_0 \frac{\partial}{\partial t} \int r J_r d\theta. \tag{18}$$

The assumption will now be made that the second field E' is very small compared to grad V and can be consistently neglected. This will be proved later on to be a reasonable hypothesis in most cases, provided the dimensions of the magnetron are small compared with the wavelength λ in vacuum.

$$b \ll \lambda. \tag{19}$$

Some special cases where this assumption would lead to error will be discussed. Most of them lie outside the actual operation conditions of the magnetron. Equation (18) may be reduced by the use of (16). One differentiates (18) with respect to θ and replaces $\partial E'_\theta/\partial\theta$ by its value $-\partial rE'_r/\partial r$, which yields

$$\Delta(rE'_r) = -\frac{1}{r}\frac{\partial}{\partial r}\left(r\frac{\partial}{\partial r}\right)rE'_r + \frac{1}{r}\frac{\partial^2 E'_r}{\partial\theta^2} = 4\pi\mu_0 \partial(rJ_r)/\partial t. \tag{20}$$

This equation will be used later in the discussion of the order of magnitude of E'_r and the conditions for its negligibility.

The preceding equations must be combined with the equations of motion for the electrons [Eqs. I.1) to (I.8)].

$$d^2 r/dt^2 = \frac{e}{m}E_r + r\dot\theta^2 - 2r\omega_H\dot\theta,$$
$$d(r^2\dot\theta)/dt = \frac{e}{m}rE_\theta + 2\omega_H r\dot r, \tag{21}$$

in which

$$\omega_H = -\tfrac{1}{2}\mu_0(e/m)H$$

Larmor's angular velocity. (22)

The second equation in (21) may also be written

$$\frac{d}{dt}[r^2(\dot\theta - \omega_H)] = \frac{e}{m}rE_\theta. \tag{23}$$

According to the assumption about the field, only grad V will be used in these equations.

The derivative of a function $f(r, \theta, t)$ is often to be taken following the motion of one electron. The symbol d/dt will be used on such occasions:

$$d/dt = \partial/\partial t + v_r\partial/\partial r + v_\theta\partial/r\partial\theta. \tag{24}$$

Applying this definition, using Eqs. (4) and (17) and neglecting E', one obtains, since $\epsilon_0 = 1$ (e.s.u.),

$$\frac{d}{dt}(r\partial V/\partial r) = r\partial^2 V/\partial r\partial t + v_r\frac{\partial}{\partial r}(r\partial V/\partial r) + v_\theta\partial^2 V/\partial r\partial\theta$$
$$= -4\pi r J_r - v_r\partial^2 V/r\partial\theta^2 + v_\theta\partial^2 V/\partial r\partial\theta. \tag{25}$$

In a similar way

$$\frac{d}{dt}\left(\frac{\partial V}{\partial\theta}\right) = \partial^2 V/\partial\theta\partial t + v_r\partial^2 V/\partial\theta\partial r + v_\theta\partial^2 V/r\partial\theta^2$$
$$= -4\pi r J_\theta + v_r\partial^2 V/\partial\theta\partial r - v_\theta\frac{\partial}{\partial r}(r\partial V/\partial r). \tag{26}$$

These two important formulae are the generalization of Eq. (I.41). They are very useful because they no longer contain the space charge density ρ. Our fundamental equations thus reduce to Eqs. (7), (21), (23), (25), and (26).

3. SMALL OSCILLATIONS IN A SPLIT-ANODE MAGNETRON

As in "Magnetron I" (Section 6) it is assumed that very small oscillations are superimposed on the static potential and current distributions. The smallness of these oscillations is secured by a parameter ϵ, the higher powers of which will be consistently neglected. We thus assume

$$\left.\begin{aligned} V(r,\theta,t) &= V_c(r)+\epsilon V_a(r,\theta,t),\\ J_r(r,\theta,t) &= I_c/2\pi r+\epsilon J_{ar}(r,\theta,t),\\ J_\theta(r,\theta,t) &= \rho_c r\dot\theta_c+\epsilon J_{a\theta}(r,\theta,t). \end{aligned}\right\} \tag{27}$$

The potential V_c and the current I_c are those defined in "Magnetron I" for the magnetron operated under steady conditions.

$$\dot\theta_c(r)=\omega_H(1-a^2/r^2). \tag{28}$$

In the new field of force electron trajectories are slightly modified. Let us follow one particular electron leaving the filament at a time t_0; its position at time t is

$$\begin{aligned} &r_c,\ \theta_c \quad \text{in the unperturbed motion.}\\ &r=r_c+\epsilon r_a(r_c,\theta_c,t),\quad \theta=\theta_c+\epsilon\theta_a(r_c,\theta_c,t) \quad \text{in the perturbed motion.} \end{aligned} \tag{29}$$

In the unperturbed motion the electron describes the static trajectory calculated in "Magnetron I," while in the perturbed motion its position at time t is at a distance ϵr_a, $\epsilon\theta_a$ from the unperturbed location. It is necessary to calculate the value of quantities such as V at the point where the electron is actually located. Let f be such a quantity. Then Eq. (27) would read

$$f(r,\theta,t)=f_c(r,\theta)+\epsilon f_a(r,\theta,t). \tag{30}$$

If this quantity be measured at the point $r_c+\epsilon r_a$, $\theta_c+\epsilon\theta_a$ where the electron is located, we must write

$$\begin{aligned} f(r_c+\epsilon r_a,\theta_c+\epsilon\theta_a,t)=f_c(r_c,\theta_c)\\ +\epsilon[r_a\partial f_c/\partial r+\theta_a\partial f_c/\partial\theta+f_a], \end{aligned} \tag{31}$$

terms in ϵ^2, ϵ^3, $\cdots$ being consistently neglected.

The fundamental equations can now be written with the expansions (27) to (31). Equation (7) first yields a very simple relation

$$\partial(rJ_{ar})/\partial r=-\partial J_{a\theta}/\partial\theta. \tag{32}$$

Equation (21) gives

$$\begin{aligned} &d^2r_c/dt^2+\epsilon d^2r_a/dt^2\\ &\quad=-\frac{e}{m}[\partial V_c/\partial r+\epsilon r_a\partial^2V_c/\partial r^2+\epsilon\partial V_a/\partial r]\\ &\qquad-2\omega_H[r_c\dot\theta_c+\epsilon(r_c\dot\theta_a+r_a\dot\theta_c)]\\ &\qquad\cdot\qquad+r_c\dot\theta_c{}^2+\epsilon[r_a\dot\theta_c{}^2+2r_c\dot\theta_c\dot\theta_a]. \end{aligned} \tag{33}$$

Terms independent of ϵ correspond to the static formula (I.19). In ϵ terms we use (28) for $\dot\theta_c$ and get finally

$$\begin{aligned} &d^2r_a/dt^2+r_a\left(\frac{e}{m}\partial^2V_c/\partial r^2+\omega_H{}^2-\omega_H{}^2a^4/r^4\right)\\ &\qquad=-\frac{e}{m}\partial V_a/\partial r-2\omega_Ha^2\dot\theta_a/r_c. \end{aligned} \tag{34}$$

Equation (23) is treated in the same way. Writing only ϵ terms one finds

$$\begin{aligned} &\frac{d}{dt}(r_c{}^2\dot\theta_a+2r_cr_a(\dot\theta_c-\omega_H))\\ &\qquad=\frac{d}{dt}\left(r_c{}^2\dot\theta_a-2\omega_Hr_a\frac{a^2}{r_c}\right)=-\frac{e}{m}\partial V_a/\partial\theta. \end{aligned} \tag{35}$$

Turning to Eq. (25) and applying (31), we get from the ϵ terms

$$\begin{aligned} &\frac{d}{dt}[r_a\partial V_c/\partial r+r_cr_a\partial^2V_c/\partial r^2+r_c\partial V_a/\partial r]\\ &\quad=-4\pi r_cJ_{ar}-\frac{\dot r_c}{r_c}\partial^2V_a/\partial\theta^2+r_c\dot\theta_c\partial^2V_a/\partial r\partial\theta. \end{aligned} \tag{36}$$

Equation (26) yields

$$\begin{aligned} &\epsilon\frac{d}{dt}(\partial V_a/\partial\theta)=-4\pi\Big[\rho_cr_c{}^2\dot\theta_c+\epsilon r_a\frac{\partial}{\partial r_c}(\rho_cr_c{}^2\dot\theta_c)\\ &\qquad+\epsilon r_cJ_{a\theta}\Big]+\epsilon\dot r_c\partial^2V_a/\partial r\partial\theta\\ &\qquad-[r_c\dot\theta_c+\epsilon(r_c\dot\theta_a+r_a\dot\theta_c)]\frac{\partial}{\partial r}\Big[(r_c+\epsilon r_a)\\ &\qquad\times(\partial V_c/\partial r+\epsilon r_a\partial^2V_c/\partial r^2+\epsilon\partial V_a/\partial r)\Big]. \end{aligned} \tag{37}$$

Terms independent on ϵ just cancel due to (I.21)

$$4\pi\rho_c r_c+\frac{\partial}{\partial r}(r_c\partial V_c/\partial r)=0, \tag{38}$$

and ϵ terms result in

$$\frac{d}{dt}(\partial V_a/\partial\theta)=-4\pi r_a\frac{\partial}{\partial r_c}(\rho_c r_c^2\dot\theta_c)-4\pi r_c J_{a\theta}$$
$$+\dot r_c\partial^2 V_a/\partial r\partial\theta-r_c\dot\theta_c\frac{\partial}{\partial r}[r_a\partial V_c/\partial r$$
$$+r_c r_a\partial^2 V_c/\partial r^2+r_c\partial V_a/\partial r]$$
$$-[r_c\dot\theta_a+r_a\dot\theta_c]\frac{\partial}{\partial r}(r_c\partial V_c/\partial r), \tag{39}$$

where the last term according to (38) is equal to

$$+4\pi\rho_c r_c(r_c\dot\theta_a+r_a\dot\theta_c).$$

4. TYPE OF ELEMENTARY SOLUTIONS

The new system of Eqs. (32) to (39) is linear with respect to all of the alternating quantities, a condition which enables us to superimpose elementary solutions and to make use of imaginary exponentials. Each alternating quantity is supposed to depend on θ and t in the following way

$$f_a(r,\theta,t)=f_a(r)e^{i(\omega t-n\theta)}. \tag{40}$$

$f_a(r)$ is an imaginary expression including the phase angle factor.

A solution of type (40) represents one elementary solution, and the general solution of any particular problem may involve superposition of such elementary solutions in order to satisfy boundary conditions. One elementary solution corresponds to a sort of wave rotating about the filament with angular velocity ω/n. In the example shown in Fig. 2, the potential distribution on the anodic cylinder should be represented by Eq. (2). This result will be obtained by the superposition of two solutions $+n$ and $-n$ of type (40), provided these two solutions have the same amplitude factor f_a for $r=b$. These two $\pm n$ solutions will, however, depend on r in different ways so that the superposition will yield a potential (2) only on the cylinder $r=b$. This will be discussed later on.

An elementary solution (40) must be studied for

$$\omega>0, \quad n \text{ positive or negative.} \tag{41}$$

One must remember, however, that a simultaneous change of the signs on ω and n does not affect the exponential in formula (40). Hence

ω, n and $-\omega, -n$ should yield the same results;

$\omega, -n$ and $-\omega, n$ should also be equivalent. Every elementary solution must satisfy the boundary conditions on the filament

$$V_a(a)=0, \quad \partial V/\partial r=0, \quad \text{for} \quad r=a. \tag{42}$$

From Eq. (40) one readily gets

$$\partial/\partial t=i\omega, \quad \partial/\partial\theta=-in. \tag{43}$$

Our equation system contains derivatives d/dt taken along the path of one electron, as expressed in Eq. (24). On the other hand, making use of Eq. (31), we have reduced any quantity f, observed at the point where an electron is located in the unperturbed motion, to a function of the coordinates r_c, θ_c defining the position of the same electron in the unperturbed motion.[2] The result is that in order to follow the motion of the perturbed electron, we only need $r_c\theta_c$ to describe an unperturbed trajectory; this yields

$$d/dt=\partial/\partial t+\dot r_c\partial/\partial r_c+\dot\theta_c\partial/\partial\theta$$
$$=i(\omega-n\dot\theta_c)+\dot r_c\partial/\partial r_c. \tag{44}$$

Calculations appear to be very complicated in the general case, so we make some simplifying assumptions:

$$\begin{aligned}&\text{A. very small filament} && a=0,\\ &\text{B. magnetron in the critical state} && I_c=0.\end{aligned} \tag{45}$$

Conditions A and B were discussed in "Magnetron I," Section 3, in which we found that the

[2] Referring to Eqs. (29) and (31), one should notice that they correspond to the use of Lagrange's definitions in hydrodynamics. The same problem could be discussed on a different basis with Euler's definitions. In (29) we compare the position of one particular electron in the unperturbed motion with the position of the *same* electron in the perturbed motion. Euler's method consists in comparing a certain electron located at r, θ (velocities v_r, v_θ) in the unperturbed motion with a *different* electron which, in the perturbed motion happens to come to the same position r, θ, but with different velocities $v_r+\epsilon u_r$, $v_\theta+\epsilon u_\theta$. Euler's method seems to be the one chosen by Blewett and Ramo [Phys. Rev. **57**, 635 (1940)]. With such definitions Eq. (31) must be cancelled, while Eq. (44) should be completed with additional terms because following the motion of one unperturbed electron means comparing different perturbed electrons.

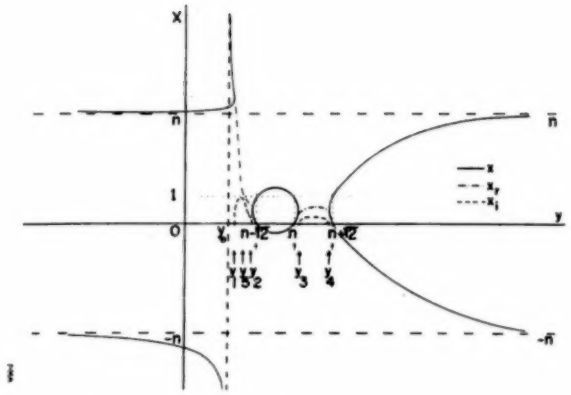

FIG. 3. The roots of Eq. (56).

electrons build a cloud with constant space charge density ρ_0 and rotating about the filament with a constant angular velocity ω_H.

$$\rho_0 = m\omega_H^2/2\pi e, \quad \dot{\theta}_c = \omega_H, \quad \dot{r}_c = 0. \tag{46}$$

Hence Eq. (44) reduces to

$$d/dt = i\alpha, \quad \alpha = \omega - n\omega_H. \tag{47}$$

These simple relations must be introduced into the general equations of Section 3. The problem to be discussed here is very similar to the one treated in "Magnetron I," Section 6. There we had to discuss the role which some damping terms should play in a more complete theory, and the same remarks apply here. The use of Eqs. (43) and (47) is equivalent to taking account only of forced vibrations and neglecting proper vibrations of the electronic system, as such proper vibrations must be damped and practically disappear after a short time.

Equation (34) yields

$$\left[-\alpha^2+\omega_H^2+\frac{e}{m}\partial^2 V_c/\partial r^2\right] r_a = -\frac{e}{m}\partial V_a/\partial r. \tag{48}$$

V_c is given by Eq. (I.23)

$$V_c = V_0 = -\frac{m}{2e}\omega_H^2 r^2. \tag{49}$$

Hence

$$r_a = (e/m\alpha^2)\partial V_a/\partial r. \tag{50}$$

Turning now to Eq. (35), one finds

$$\dot{\theta}_a = en\,V_a/mr_c^2\alpha. \tag{51}$$

By using (49) and (36) the following relation is obtained:

$$2\frac{m}{e}\alpha\omega_H^2 r_a r_c - \omega r_c \partial V_a/\partial r = -i4\pi r_c J_{ar}, \tag{52}$$

while Eq. (32) results in

$$\frac{\partial}{\partial r}(rJ_{ar}) = inJ_{a\theta}. \tag{53}$$

Equations (50) and (52) give

$$J_{ar} = (i/4\pi)\partial V_a/\partial r(2\omega_H^2/\alpha - \omega). \tag{54}$$

Equation (39) may now be greatly simplified by using (47) and (53):

$$\begin{aligned} n\alpha V_a = &-4\pi r_a \frac{\partial}{\partial r_c}(m\omega_H^3 r_c^2/2\pi e) \\ &+(4\pi i/n) r_c \frac{\partial}{\partial r_c}(r_c J_{ar}) \\ &-r_c\omega_H \frac{\partial}{\partial r_c}\left[-\frac{2m}{e}\omega_H^2 r_a r_c + r_c \partial V_a/\partial r\right] \\ &+2\frac{m}{e}\omega_H^2 r_c(r_c\dot{\theta}_a + r_a\omega_H). \end{aligned} \tag{55}$$

Referring now to (50), (51), and (54), one finds a homogeneous differential equation for V_a:

$$\begin{aligned} &Ar\frac{\partial}{\partial r}\frac{\partial V_a}{\partial r} + Br\frac{\partial V_a}{\partial r} + CV_a = 0, \\ &A = \frac{1}{n}(2\omega_H^2/\alpha - \omega) + \omega_H(1 - 2\omega_H^2/\alpha^2), \\ &B = 2\omega_H^3/\alpha^2, \\ &C = n(\alpha - 2\omega_H^2/\alpha). \end{aligned} \tag{56}$$

Let us introduce a variable $y = \omega/\omega_H$, $\alpha = \omega_H(y-n)$ and new coefficients

$$\begin{aligned} A' &= (y-n)^2 A/\omega_H = -2 - \zeta/n, \\ B' &= (y-n)^2 B/\omega_H = 2, \\ C' &= (y-n)^2 C/\omega_H = n\zeta, \\ \zeta &= (y-n)^3 - 2(y-n). \end{aligned}$$

A solution may be found by taking

$$\begin{aligned} V_a &= Kr^x, \\ A'x^2 + B'x + C' &= 0. \end{aligned} \tag{57}$$

We thus obtain two solutions:

$$\left.\begin{matrix} x_1 \\ x_2 \end{matrix}\right) = -\frac{B'}{2A'} \pm \frac{1}{2A'}(B'^2 - 4A'C')^{\frac{1}{2}}. \qquad (58)$$

It should be immediately noticed that A', B', and C' are functions of y and n, so that the solutions x_1, x_2 will depend only upon these two variables. Furthermore we should remember the conditions (42) stating that V_a and $\partial V_a/\partial r$ have to be zero on the filament. This results in the necessity of choosing the root with a real part greater than one.

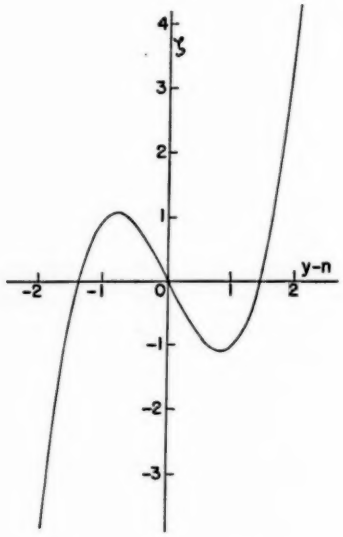

FIG. 4. ζ as a function of $y-n$.

$$\mathbf{Re}(x) \geqslant 1. \qquad (59)$$

For each elementary solution (57) in V_a we shall obtain the corresponding current densities from Eqs. (53) and (54).

$$\begin{aligned} V_a &= Kr^x, \\ J_{ar} &= ixV_a/4\pi r[2\omega_H{}^2/(\omega - n\omega_H) - \omega], \\ J_{a\theta} &= -\frac{i}{n}\frac{\partial}{\partial r}(rJ_{ar}) \\ &= (x^2 V_a/4\pi nr)[2\omega_H{}^2/(\omega - n\omega_H) - \omega]. \end{aligned} \qquad (60)$$

5. DISCUSSION OF THE RESULTS

A discussion of the practical results must be based on a numerical calculation of the two roots x_1 and x_2 of Eq. (56). These roots, x_1 and x_2, must be calculated as functions of $y=\omega/\omega_H$ for different values of n. The solutions corresponding to $+\omega$ and $\pm n$ may also be obtained with $+n$ and $\pm\omega$ according to a remark on Eq. (41). Figure 3 shows a typical graph of x as a function of y as found for $n=2, 3, \cdots$. The case $n=1$ is exceptional. Figure 3 is self-explanatory and shows the behavior of the roots as functions of y. There are two regions, y_1y_2 and y_3y_4, which give imaginary solutions $x=x_r \pm ix_i$. Curves representing x and $x_r x_i$ have been drawn separately. The limits of these regions are given by

$$\begin{aligned} \tfrac{1}{4}B'^2 - A'C' &= 1 + \zeta(\zeta + 2n) = 0, \\ \zeta &= -n \pm (n^2 - 1)^{\frac{1}{2}}. \end{aligned} \qquad (61)$$

Inside these regions of imaginary solutions we are interested in defining the point y_5 for which $x_r = 1$:

$$x_r = -B'/2A' = 1/(2 + \zeta/n) = 1, \quad \zeta = -n.$$

Other points of interest are y_0, where $A'=0$ ($\zeta=-2n$) and the points $\zeta=0$ ($y=n$ or $n\pm\sqrt{2}$) where the x roots are 1 and 0. All these solutions are easily obtained by the use of Fig. 4 relating ζ to $y-n$. The case $n=1$ is exceptional since the regions y_1y_2 and y_3y_4 both disappear and the x roots are always real, one of them being 1 for any y value (Fig. 5).

We now wish to discuss these results in relation to condition (59). The following cases are to be distinguished:

I. Two real roots less than 1. None of these roots can be used for our problem. This occurs for

$$y_2 < y < n - \sqrt{2}, \quad n < y < y_3, \quad y_4 < y < n + \sqrt{2}. \qquad (62)$$

II. Two real roots, one greater and the other

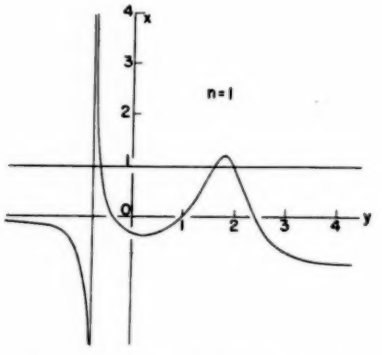

FIG. 5. Roots of Eq. 56 for $n=1$.

less than 1. The first root can be used. This occurs for

$$y<y_0, \quad n-\sqrt{2}<y<n, \quad n+\sqrt{2}<y.$$

III. Two real roots greater than 1, both yielding possible solutions. This occurs for

$$y_0<y<y_1.$$

IV. Two imaginary roots with $x_r<1$. No useful root. This occurs for

$$y_5<y<y_2, \quad y_3<y<y_4.$$

V. Two imaginary roots with $x_r>1$, yielding two possible solutions. This occurs for

$$y_1<y<y_5.$$

These results are summarized on Fig. 6, which shows the distribution of the different regions corresponding to cases I, II, III, IV, and V in the y, n plane. Curves have been drawn considering n as a continuous variable but the results have physical meaning only for integral values of n. In addition to the previously defined curves, the curve corresponding to $x=n-2$ is also plotted. This is interesting in view of the approximation introduced in Section 2, neglecting the additional field E'. (See Section 7.)

In case II we obtain one possible solution (57) and there will be no difficulty in solving completely our problem. We shall prove that the magnetron operated under such conditions behaves like a pure imaginary impedance and should be unable to sustain oscillations.

In cases III and V we obtain two distinct solutions, yielding a potential

$$V_a=K_1r^{x_1}+K_2r^{x_2}. \tag{63}$$

This leaves an arbitrary constant, K_1/K_2 for instance, which we are unable to determine. It is thus impossible to draw any precise conclusions in these cases. This difficulty seems to be connected with the simplifying assumption made in Section 4 [Eq. (45.A)] about the filament having a radius zero. A special discussion of a magnetron with finite filament radius should be made to answer the question.

In cases I or IV no solution is obtained. Both roots are smaller than 1, which means that condition (59) cannot be fulfilled. If we try any one of the roots, we obtain an infinite oscillating electric field $-\partial V/\partial r$ on the filament ($r=0$). Instead of a magnetron working far from saturation and showing small oscillations around its steady conditions, we obtain large oscillations where the current emitted by the filament is zero (half of the time) or the saturation current for the other half periods. This shows that cases I and IV should represent the conditions under which a magnetron is able to oscillate and to

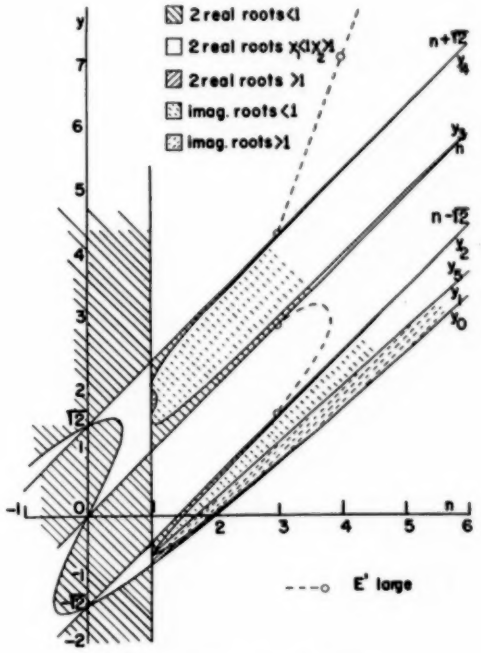

FIG. 6. Summary of results.

sustain high frequency oscillations in an outer circuit. The frequency is given by the corresponding y values:

$$\begin{aligned} y_5<y<n-\sqrt{2}, \\ n<y<n+\sqrt{2}. \end{aligned} \tag{64}$$

We must now see how to build up the complete solution for the potential distribution inside a magnetron with $2n$ anodes, operated at the frequency $\omega=y\omega_H$. According to the remarks at the beginning of Section 4 this complete solution will result from the superposition of elementary solutions corresponding to n and $-n$. Let us first suppose the corresponding roots x_+ and x_- both to be real and greater than 1 (case II).

$$V_a(r, \theta, t)=K_+r^{x_+}e^{i(\omega t-n\theta)}+K_-r^{x_-}e^{i(\omega t+n\theta)}, \tag{65}$$

where the K_+ and K_- constants must be adjusted so as to reproduce, for $r=b$, the assumed potential distribution (2) on the anodes

$$V_a(b, \theta, t) = V_a(b)e^{i\omega t} \sin n\theta. \tag{66}$$

This gives

$$K_+ = -\frac{1}{2i}V_a(b)b^{-x_+}, \quad K_- = \frac{1}{2i}V_a(b)b^{-x_-},$$

and

$$V_a(r, \theta, t) = \frac{1}{2i}V_a(b)e^{i\omega t} \times\left(-\left(\frac{r}{b}\right)^{x_+}e^{-in\theta}+\left(\frac{r}{b}\right)^{x_-}e^{in\theta}\right), \tag{67}$$

which gives the complete potential distribution inside the magnetron.

6. INTERNAL RESISTANCE OF THE MAGNETRON

Having obtained the distribution of potential in the magnetron, we are now in a position to compute the current densities and to calculate the current reaching the anodes. This might involve some difficulties when the anodes are narrow and far apart from each other, but if the magnetron is built with wide anodes and small intervals between them ($\alpha \gg \beta$), we may assume that each anode collects all the current flowing radially throughout an angle π/n. Thus the total current flowing to the first anode will be

$$I_{1r} = \epsilon\int_0^{\pi/n} J_{ar}r\,d\theta, \quad r=b, \tag{68}$$

but there are n anodes (numbers $1, 3, \cdots, 2n-1$) connected in parallel and the total current is n times greater

$$I_{ar} = \epsilon n\int_0^{\pi/n} J_{ar}r\,d\theta. \tag{69}$$

J_{ar} will consist of two terms corresponding to $\pm n$, each of which is related to the corresponding voltage term by Eq. (60). Let us first consider the case of two real roots x_+ and x_- with a potential (67). The relation (60) has to be applied separately on the two terms of (67) which gives

$$J_{ar} = (V_a(b)/8\pi r)e^{i\omega t} \times\left[-x_+(r/b)^{x_+}\left(\frac{2\omega_H{}^2}{\omega-n\omega_H}-\omega\right)e^{-in\theta} +x_-(r/b)^{x_-}\left(\frac{2\omega_H{}^2}{\omega+n\omega_H}-\omega\right)e^{in\theta}\right]. \tag{70}$$

Now

$$\int_0^{\pi/n} e^{\pm in\theta}d\theta = \pm 2i/n. \tag{71}$$

Making $r=b$, and using (69) to (71), we obtain

$$I_{ar} = \epsilon\frac{i}{4\pi}V_a(b)e^{i\omega t}\left[x_+\left(\frac{2\omega_H{}^2}{\omega-n\omega_H}-\omega\right) +x_-\left(\frac{2\omega_H{}^2}{\omega+n\omega_H}-\omega\right)\right]. \tag{72}$$

And according to Eq. (2), the potential of the odd anodes is

$$U_a e^{i\omega t} = \epsilon V_a(b)\frac{\pi n\beta}{8\sin(n\beta/2)}e^{i\omega t} \approx \epsilon\frac{\pi}{4}V_a(b)e^{i\omega t}. \quad \beta \ll \alpha. \tag{73}$$

In addition to radial currents, we have found that there are also angular components of the current density inside the magnetron. Thus we may have to add a correction term representing the current flowing to the edges of the anode; this would be something like

$$I_{a\theta} = \epsilon n[J_{a\theta}(\theta=0) - J_{a\theta}(\theta=\pi/n)]\delta r, \quad \text{for} \quad r=b, \tag{74}$$

δr representing the apparent thickness of the electrode and the n factor taking care of the fact that there are n anodes connected in parallel. The edges of the first anode correspond to $\theta=0$ and π/n. $J_{a\theta}$ is known from Eq. (60) which must be applied separately to each elementary V_a solution, yielding for each solution an equation of the form

$$J_{a\theta} = -\frac{i}{n}\frac{\partial}{\partial r}(rJ_{ar}) = \frac{x^2}{4\pi nr}\left(\frac{2\omega_H{}^2}{\omega-n\omega_H}-\omega\right)V_a(r, \theta, t).$$

Hence, for the superposition of the $\pm n$ solutions,

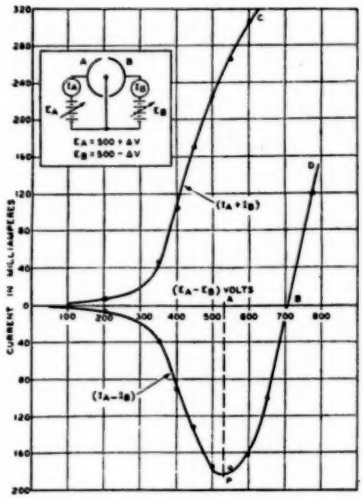

FIG. 7. Static characteristics of a two-segment magnetron.

as given by (67)

$$J_{a\theta}=\frac{V_a(b)e^{i\omega t}}{8\pi ir}\times\left[-\frac{x_+^2}{n}\left(\frac{2\omega_H^2}{\omega-n\omega_H}-\omega\right)\left(\frac{r}{b}\right)^{x_+}e^{-in\theta}-\frac{x_-^2}{n}\left(\frac{2\omega_H^2}{\omega+n\omega_H}-\omega\right)\left(\frac{r}{b}\right)^{x_-}e^{in\theta}\right]. \quad (75)$$

Exponentials are 1 for $\theta=0$ and -1 for $\theta=\pi/n$ so that the two terms in (74) are equal and one obtains

$$I_{a\theta}=\frac{\epsilon i}{4\pi b}V_a(b)e^{i\omega t}\left\langle x_+^2\left(\frac{2\omega_H^2}{\omega-n\omega_H}-\omega\right)+x_-^2\left(\frac{2\omega_H^2}{\omega+n\omega_H}-\omega\right)\right\rangle\delta r. \quad (76)$$

x_+ and x_- are of the order of magnitude of n, so that the additional contribution is of the order

$$I_{a\theta}\approx I_{ar}n\frac{\delta r}{b}, \quad (76a)$$

and will probably be small if the apparent thickness of the anodes is small. The important fact is that it comes out with the same phase angle as I_{ar} when both roots x_+ and x_- are real (case II). In such cases the currents I_{ar} and $I_{a\theta}$ retain pure imaginary amplitudes, while the potential keeps a real amplitude (73). This means that magnetrons operated under such conditions are equivalent to pure impedances without any (either positive or negative) resistance and seem to be unable to sustain oscillations in an outer circuit.

It should be noticed that in the present paper the currents have been written with a sign convention opposite to the usual one in circuit theory. Hence the internal impedance Z_a of the split anode magnetron should be defined as

$$Z_a=\frac{-U_ae^{i\omega t}}{I_{ar}}=i\pi^2\left[x_+\left(\frac{2\omega_H^2}{\omega-n\omega_H}-\omega\right)+x_-\left(\frac{2\omega_H^2}{\omega+n}-\omega\right)\right]^{-1} \quad (77)$$

from Eqs. (72) and (73). This impedance is observed in the devices shown on Fig. 1 or Fig. 7.

7. VALIDITY OF THE ASSUMPTION MADE IN SECTION 2, NEGLECTING THE ADDITIONAL FIELD E'

As noticed in Section 2, just after Eq. (18), the assumption has been made that the additional electric field E', induced by the alternating magnetic fields, could be neglected. It is now possible to compute the order of magnitude of this E' field, which is determined by Eq. (20). Because the $e^{i(\omega t-n\theta)}$ factor appears in this field, as in all alternating quantities, Eq. (20) reads

$$\frac{1}{r}\frac{\partial}{\partial r}r\frac{\partial}{\partial r}rE_r'-\frac{n^2}{r}E_r'=4\pi\mu_0 i\omega r J_r, \quad (78)$$

where J_r is the sum of terms (60) corresponding to each elementary term r^z in V_a, as may be seen from Eqs. (67) and (70). We may, for instance, write (70) this way

$$J_{ar}=J_{ar}(+n)+J_{ar}(-n),$$

$$J_{ar}(\pm n)=\mp\frac{V_a(b)}{8\pi r}e^{i(\omega t\mp n\theta)}\times\left(\frac{r}{b}\right)^{x(\pm n)}x(\pm n)\omega_H\left(\frac{2}{y\mp n}-y\right). \quad (79)$$

And our Eq. (78) will read

$$E_r'=E_r'(+n)+E_r'(-n),$$

$$\frac{1}{r}\frac{\partial}{\partial r}r\frac{\partial}{\partial r}rE_r'(+n)-\frac{n^2}{r}E_r'(+n)=4\pi\mu_0 i\omega r J_{ar}(+n). \tag{80}$$

The solution is obvious since J_{ar} depends upon r by r^{x-1}.

$$E_r'(+n)=\frac{4\pi i\mu_0\omega r^2 J_{ar}(+n)}{(x(+n)+2)^2-n^2}=\frac{8\pi^2 i}{c}\frac{r}{\lambda}\frac{rJ_{ar}(+n)}{(x(+n)+2)^2-n^2}, \tag{81}$$

as $\mu_0=c^{-2}$ and $\omega/c=2\pi/\lambda$. This shows that the additional field E' is very small because of the factor $(1/c)(r/\lambda)$, so long as the dimensions of the magnetron are small compared with the wave-length, which corresponds to statement (19). The only case for trouble would be when one of the roots x should come near to $\pm n-2$, a condition to be discussed in a moment.

The additional potential V' on the anode $r=b$ corresponding to E_r' can be computed. It should be reminded that r^2J_{ar} depends on r as r^{x+1}. This gives

$$V'=V'(+n)+V'(-n),$$

$$V'(+n)=-\int_0^b E_r'(+n)dr=-\frac{8\pi^2 i b^3 J_{ar}(+n)}{c\lambda(x_++2)[(x_++2)^2-n^2]}. \tag{82}$$

This must be calculated for the middle of the first anode, i.e., for $r=b$, $\theta=\pi/2n$. Formula (72) may be written

$$I_{ar}=\epsilon 2b[J_{ar}(+n)+J_{ar}(-n)], \tag{83}$$

for $r=b$, $\theta=\pi/2n$, while

$$\epsilon V'=-\epsilon\frac{8\pi^2 i}{c\lambda}b^2\left[\frac{J_{ar}(+n)}{(x_++2)[(x_++2)^2-n^2]}+\frac{J_{ar}(-n)}{(x_-+2)[(x_-+2)^2-n^2]}\right],\quad r=b,\ \theta=\pi/2n. \tag{84}$$

This shows that the additional voltage V' is out of phase with the current (i factor) and very small except for the cases

$$x=\pm n-2. \tag{85}$$

An order of magnitude can be obtained, if one remembers that the x values are of the order of n. This gives

$$\epsilon V'\approx-\frac{i\pi^2 b^2}{c\lambda(n+2)(n+1)}I_{ar}. \tag{86}$$

The addition of a voltage $\epsilon V'$ to the voltage $\epsilon V_a(b)$ already assumed on the anodes is equivalent to adding a series impedance $Z'=-\epsilon V'/I_{ar}$, the order of magnitude of which would thus be

$$Z'=i\frac{\pi^2 b^2}{c\lambda(n+2)(n+1)}. \tag{87}$$

Let us take, for instance, $b=\frac{1}{10}\lambda$ and $\lambda=1$ cm which will be a very unfavorable situation.

$$Z'=i\frac{0.3\pi^2}{(n+2)(n+1)},$$

which is of the order of magnitude of a fraction of an ohm, a very small quantity when compared to the thousands of ohms which electron tubes yield as internal resistance.

Let us now discuss the conditions (85) for which the additional electric field takes a really important part. A glance at Fig. 3 shows that this condition can be fulfilled only for $x(+n)$, between $y=n-\sqrt{2}$ and n (where x_+ is slightly above 1) or above $y=n+\sqrt{2}$. The first case is for $n=3$, $x=1$, $y=3-\sqrt{2}$, 3, $3+\sqrt{2}$; then $n=4$, etc. These points are plotted on Fig. 6. They all lie in the region where magnetrons have been proved to yield pure imaginary internal impedance and to be unfit for sustaining oscillations.

It thus appears legitimate to neglect the role played by the additional field E' induced by alternating internal magnetic fields.

8. CONCLUSIONS

The results of this study are summarized in Fig. 6 which shows the type of solutions obtained in different regions of the y, n plane. These results will perhaps be easier to understand for practical applications if we notice that Larmor's angular velocity ω_H is proportional to the

magnetic field, which means

$$\omega_H = 0.884\ 10^7 H, \quad H \text{ in Gauss}$$
$$y = \omega/\omega_H = 2\pi c/\lambda\omega_H = 21310/\lambda H. \quad \lambda \text{ in cm} \quad (88)$$

This enables a comparison with experimental results, which are usually given in terms of λH corresponding to different types of oscillations.

On the map drawn in Fig. 6, the different regions corresponding to the cases I to V defined in Section 6 [Eq. (62)] have been represented. The physical meaning of the various cases seems to be:

I and IV. Large oscillations.

$$y_b < y < n - \sqrt{2}, \quad n < y < n + \sqrt{2}. \quad (64)$$

II. No oscillations, the magnetron being equivalent to a pure imaginary impedance.

III and V. The solution still contains an arbitrary constant; probably no oscillations. The different regions corresponding to these cases I to V are neatly divided for magnetrons corresponding to $n = 2, 3, 4 \cdots$ (number of anodes $2n = 4, 6, 8 \cdots$); one always finds two different regions, defined by conditions (64), where oscillations could possibly take place.

For the usual split-anode magnetron ($n = 1$; 2 anodes) it is hard to foresee the conditions of oscillations, as the whole diagram changes just on the line $n = 1$. These very typical circumstances should make this magnetron very sensitive to all sorts of perturbations such as increase in the diameter of the filament, effect of large oscillations, etc. Experimental values on the usual split-anode magnetron are found in a paper by G. R. Kilgore,[3] with an attempt at theoretical explanation, which unfortunately does not take account of space charge effects, and therefore remains far away from actual conditions in magnetrons. Figure 7 is a reproduction of Kilgore's Fig. 3, showing the static characteristic for a split-anode magnetron. This means $\omega = 0$, $y = 0$. The magnetic field applied was 1.5 times the critical field. The average anode potential was 500 volts, and variations as large as ± 400 volts (giving $E_A - E_B = 800$ volts) were applied. This means very large perturbations, for which our theory would certainly be only a rough first approximation. It appears from the curves that the negative resistance is zero for small ΔV and reaches a maximum of about -1500 ohms for $\Delta V = 400$ volts. Efficiencies of magnetrons operated under different conditions are given by Kilgore on page 372 and can be summarized as follows ($H = 1.5 H_c$, H_c critical field):

Efficiency	10%	20%	30%	40%	50%	
$\lambda H 10^{-4}$	5.45	6.7	8.1	9.8	12	(82)
$y = \omega/\omega_H$.	0.39	0.32	0.265	0.218	0.178.	

If these y values are taken with a negative sign, they lie just between the horizontal n axis and the line $y = n - \sqrt{2}$. Another type of oscillation has been found on split-anode magnetrons with λH values around 12,000, which gives

$$y \approx 1.8.$$

This value of y seems to correspond to the upper band of our diagram, as it lies between 1 and $1 + \sqrt{2}$.

A further prediction of the theory concerns the possibility for a magnetron of type n to work as magnetrons of types $3n$, $5n$, $\cdots$ but with lower efficiency.

Magnetrons $n = 3$ (6 anodes) should behave differently, as the perturbation by the oscillating magnetic field is especially large in that case.

[3] G. R. Kilgore, Proc. I. R. E. (August, 1936). Reprinted by RCA in *Radio at Ultra-High Frequencies* (1940), p. 360.

Letters to the Editor

PROMPT publication of brief reports of important discoveries in physics may be secured by addressing them to this department. The closing date for this department is the third of the month. Because of the late closing date for the section no proof can be shown to authors. The Board of Editors does not hold itself responsible for the opinions expressed by the correspondents. Communications should not in general exceed 600 words in length.

On the Decay of Slow Mesons

M. D. DE SOUZA SANTOS
Departamento de Physica, Universidade de São Paulo, Brasil
June 20, 1942

IN order to measure accurately the mean life of slow mesons, an experiment was designed to measure their decay curve. The disintegration electron intensity was measured at different time intervals, after the mesons came to rest, through the use of a variable time delay coincidence set.[1]

The counter arrangement used is illustrated in Fig. 1.

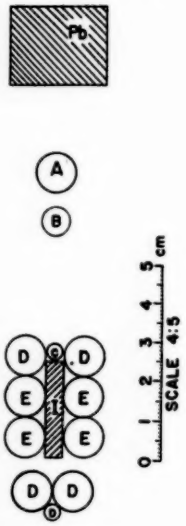

FIG. 1. Counter arrangement.

Counters (A, B, C) are connected to a threefold coincidence system with a coincidence time $T''=2\times10^{-6}$ sec. The counters D are connected to a double channel mixer system[2] and are in anticoincidence with the vertical telescope (A, B, C).[3] The counters E are connected to a double channel mixer system and the coincidences between the pulses from (A, B, C), delayed by a time interval $T\pm T'$, and the pulses from E are measured for different values of T. T' is a constant of the apparatus (coincidence time of the second mixer: $T'=1.2\times10^{-7}$ sec.).

The spurious coincidences are due mainly to showers produced either in the lead block above the counters, which absorbs the soft component, or to knock on showers produced in the iron block I. Both phenomena are eliminated by the anticoincidence counters D. Besides, since the pulses from (A, B, C) are delayed by a time interval $T\pm T'$, relatively to those from counters E, the chance coincidences can be shown to be about 10^{-4} of the observed frequency (the true coincident phenomena such as showers being eliminated by the time delay system).

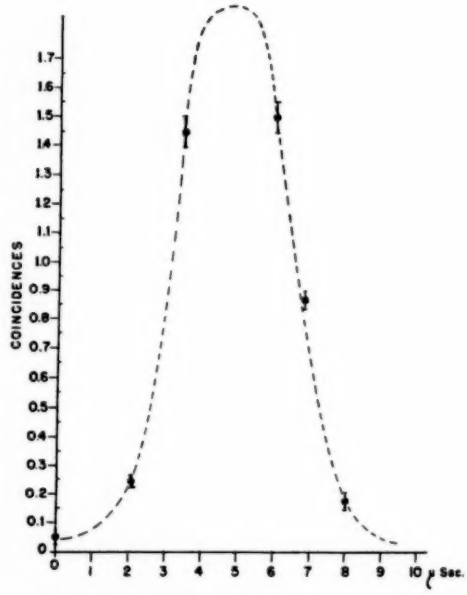

FIG. 2. Coincidences for different time delays.

When $T\lesssim T'$, the observed frequency corresponds both to the decay of mesons which occurred in I and to the scattered mesons, but for $T>T'$ the observed frequency corresponds to the number of mesons disintegrated between $T-T'$ and $T+T'$.

In an experiment such as this one, the results obtained can only be accepted provided that the breakdown time[4] of the counters used is smaller than the coincidence time used; that characteristic can only be obtained through the use of a multivibrator circuit[5] and fast alcohol counters with a discharge started by a Penning effect. In this way, the time lags observed are smaller than the coincidence time used. The obtained efficiency of both apparatus and counters was nearly 100 percent and a complete account of the experimental set used together with the apparatus used to measure small time intervals will be published elsewhere.

The preliminary results obtained are illustrated in Fig. 2 and it is seen that the shape of the curve resembles that of a Gauss distribution around $T_0=5\times10^{-6}$ sec. the curve being symmetrical about the axis $t=5\times10^{-6}$ sec. which was considered as a measure of the "life" of the meson at rest.

The important result to be emphasized here is that the shape of the curve is altogether different from what one would expect from an analogy with the laws of disintegration of radioactive substances. If the time distribution of

the decayed mesons would be the same as observed for, say, beta-rays, the shape of the decay curve would be an exponential one.[6] We can therefore conclude that the laws responsible for both beta-ray phenomena are altogether different, and that the law of disintegration of mesons at rest is different from that of beta-rays.

A complete account of the experiment together with new results that are being obtained will be published elsewhere.

It is a pleasure to thank the British Council for the award of a Research Scholarship which has made possible the construction of the apparatus used and to Professors G. Wataghin and G. Occhialini for many helpful discussions.

[1] Prior to the author's measurements, the only coincidence experiments on the detection of delayed electrons were those of Montgomery, Ramsey, Cowie, and Montgomery, with negative results, and the experiments of Rasetti, with a similar geometrical arrangement, but with an altogether different experimental technique.
[2] M. D. de Souza Santos, An. Acad. Bras. Sci. (in press).
[3] G. Occhialini and M. D. de Sousa Santos, *Symposium on Cosmic Rays in Rio de Janeiro (1941)* to be published shortly.
[4] That is, the time interval between the moment in which an ionizing particle passes through the counter and the first electron avalanche reaches the wire.
[5] M. D. de Souza Santos, An. Acad. Bras. Sci. **12**, 183 (1940).
[6] A. Moraes, An. Acad. Bras. Sci. (in the press).

Temperature Diffuse Diffraction Maxima and Crystal Perfection

DONALD S. TEAGUE
Department of Physics, Stanford University, Stanford University, California
July 31, 1942

THE non-Laue x-ray diffraction maxima called by Raman "modified," and by Zachariasen and others "diffuse" have been observed by many investigators, using a continually growing list of crystals. Existing differences of opinion as to the detailed nature of these effects can be reconciled only on the basis of additional and quantitative observations. For these purposes no observation is more critical than the observation of the angle of deviation of the diffraction maximum. The mere existence of a maximum of a monochromatic line off of coincidence with the Laue spot of the continuum proves nothing. Measurement of the intensity or breadth of the line maximum may assist in classifying the maximum as something other than a Laue or Bragg reflection, though the test is rarely decisive because the theory of the width and intensity of the latter in an imperfect crystal specimen is impossibly complex, and because the maximum is often a mixture of ordinary and temperature diffuse effects. On the other hand, an angle of deviation varying with the angle of incidence is rather decisively indicative of a non-Laue maximum. Demonstration of a deviation which is constant with angle of incidence removes a crystal from consideration in any discussion of temperature diffuse reflection, since it indicates a structure so imperfect that the diffuse reflection, if any, is swamped by the ordinary reflection from misaligned blocks.

A study of six crystalline substances has been conducted with a photographic spectrograph in an attempt to determine the variation of the angle of deviation of Mo $K\alpha$ with angle of incidence. More than 200 exposures were made with the crystal faces inclined to a well-collimated incident beam at angles near the Bragg angle. The results are given in Table I. The order in which the crystals are

TABLE I. Variation of angle of deviation of Mo $K\alpha$. A = reflecting planes used. B = range of angles of incidence over which line reflections (Mo $K\alpha_1$ or α_2) were observed. C = Δ deviation angle/Δ incidence angle observed. D = Δ deviation angle/Δ incidence angle, theoretical.* E = character of reflected lines.

Crystal	A	B	C	D	E
Iron	100(?)	largest	—	—	broad, unsharp
Zinc blende	110 1	>4°	Appr. zero	—	fairly sharp
Barite	100	54′	$K\alpha_1$ 0.00469	0.022	sharp
			$K\alpha_2$ 0.0203	.024	
Calcite	100	17′	$K\alpha_1$ 0.26	.0295	sharp
			$K\alpha_2$ 0.218	.028	
Rochelle salt	?	6′	$K\alpha_1$ 1.95(approx.)	.0266	sharp
			$K\alpha_2$ 2.4(approx.)	.0264	
Quartz	110	negligible	—	—	

* S. Siegel and W. H. Zachariasen, Phys. Rev. **57**, 795 (1940).

listed is the order of increasing structural perfection.[1] Apparently neither very perfect nor very imperfect crystals are favorable to studies of the angular shift of the reflected maximum, though the reasons differ in the two cases. With imperfect crystals the situation is as stated in the first paragraph; with a crystal as perfect as the quartz sample the reflection had an observable intensity only at or extremely near the Bragg angle of incidence and no systematic trend could be established even though five-hour exposures were used in an attempt to extend the range of the observations. With the crystals of intermediate perfection there is a qualitative confirmation of theory as shown in columns C and D but a satisfactory quantitative agreement occurs only in the case of barite. The tendency of the observed shift to exceed the theoretical, observed with calcite, has been noted before.[2] One might be inclined to regard it as an instrumental effect except that it does not appear with all crystals.

[1] R. M. Bozorth and F. E. Haworth, Phys. Rev. **45** 821 (1934). Additional crystals have been arranged from evidence obtained in connection with the research herein described.
[2] P. Kirkpatrick Phys. Rev. **59**, 452 (1941).

The Spectrum of Chlorine I

J. B. GREEN AND J. T. LYNN
Mendenhall Laboratory of Physics, Ohio State University, Columbus, Ohio
July 14, 1942

MEASUREMENTS on the Zeeman effect in the spectrum of Cl I in the region λλ 3000–9200 have resulted in the identification of several new levels and some lines not listed by Kiess[1] as well as classification of many lines listed in his tables.

The g values and g sums for a few configurations have been determined and show sharing of g sums for the $3s^23p^44p$ and $3s^23p^45p$. The discrepancies in the g sums can be practically completely accounted for on the basis of the overlapping of the $4p(^1D)$ and $5p(^3P)$ parts of these configurations.

A complete report will be published later.

[1] Kiess, Bur. Stand. J. Research **10**, 827 (1933).

Meson Theory and the Magnetic Moments of Protons and Neutrons

H. Fröhlich
H. H. Wills Physical Laboratory, University of Bristol, England
July 27, 1942

IN various recent papers in this Journal[1] it was shown that an analysis of cosmic-ray data leads to the suggestion that the spin of cosmic-ray mesons is zero, and that they are described by a pseudoscalar field. The question now arises whether all mesons follow such a pseudoscalar theory, or whether there are also mesons with spin $1\hbar$ (described by a vector field) which would have escaped detection in cosmic rays under the assumption that their lifetime is much shorter than that of pseudoscalar mesons. Such a combined theory was in fact proposed by Møller and Rosenfeld[2] in order to escape theoretical difficulties which are met in a pure pseudoscalar or vector theory. In this letter I should like to forward an argument in favor of the Møller-Rosenfeld theory. Some time ago it was shown that on the basis of the vector theory a qualitative understanding of the anomalous magnetic moments of protons and of neutrons could be reached.[3] I have now carried out an analogous calculation for the pseudoscalar theory[4] and found that there are no contributions to the anomalous magnetic moments. A pure pseudoscalar meson theory, therefore, would not allow an understanding of the anomalous magnetic moments, whereas the Møller-Rosenfeld theory does so and at the same time remains in agreement with cosmic-ray experiments. It may be hoped that further experiments, especially a measurement of the dependence of proper lifetime on height, would yield the required existence of two lifetimes.

[1] R. F. Christy and S. Kusaka, Phys. Rev. **59**, 405 and 414 (1941); J. R. Oppenheimer, Phys. Rev. **59**, 462 (1941); J. R. Oppenheimer and J. Schwinger, Phys. Rev. **60**, 150 (1941).
[2] Møller and Rosenfeld, Math. Phys. Comm. Acad. Sci. Copenhagen, **17**, 8 (1940); Rozental, Phys. Rev. **60**, 612 (1941).
[3] Fröhlich, Heitler, and Kemmer, Proc. Roy. Soc. **166**, 154 (1938).
[4] In the course of the calculations it turned out to be wrong to neglect in the matrix elements the recoil of the proton (neutron) as was done previously. In the vector theory this changes only the numerical factor, but it is of great importance in the pesudoscalar theory.